

Semialgebraic Convex Bodies

Von der Fakultät für Mathematik und Informatik
der Universität Leipzig
angenommene

D I S S E R T A T I O N

zur Erlangung des akademischen Grades

DOCTOR RERUM NATURALIUM
(Dr.rer.nat.)

im Fachgebiet

Mathematik

vorgelegt

von M.Sc. Chiara Meroni
geboren am 22.01.1996 in Gorizia (Italien)

Contents

Introduction	4
1. Background	6
1.1. Basics of convex geometry	6
1.1.1. Face structure	7
1.1.2. Duality in convex geometry	9
1.1.3. Functions and convex bodies	12
1.2. Varieties and convex bodies	13
1.2.1. The algebraic boundary	17
1.2.2. More dualities	19
2. Zonoids	23
2.1. Zonoids and their problems	24
2.1.1. Discotopes	26
2.1.2. The faces of a zonoid	27
2.2. The geometry of discotopes	28
2.2.1. Joins of quadrics	29
2.2.2. Exposed points of the discotope	32
2.2.3. Two-dimensional discs	35
2.2.4. Conclusions	42
3. Constructions with convex bodies	44
3.1. Fiber convex bodies	45
3.1.1. Puffed polytopes	50
3.1.2. Curved convex bodies	53
3.1.3. Fiber zonoids	56
3.1.4. Conclusions	60
3.2. Intersection bodies of polytopes	60
3.2.1. The role of the origin	64
3.2.2. Algebraic boundary and degree bound	65
3.2.3. The cube	70
3.2.4. Conclusions	73

4. Convex hulls	74
4.1. Surfaces in fourspace	74
4.2. Curves and volumes	74
5. Convex bodies in applications: quantum physics	75
5.1. Introduction	76
5.1.1. Background from physics	76
5.1.2. A view from mathematics	78
5.1.3. Short review of previous work	80
5.2. Description of the correlation body	81
5.2.1. Boundary, faces, and extreme points	85
5.2.2. Semialgebraic description	88
5.3. Description of the dual body	91
5.3.1. The duality transform	91
5.3.2. The normal cycle	95
5.3.3. Support function	97
5.4. Geometric aspects of quantum key distribution	98
5.5. Proofs	100
5.5.1. Proof of Theorem 1	100
5.5.2. Self-duality	106
5.5.3. Further boundary properties	107
5.6. Conclusions	111

Introduction

Convex Geometry has been classically studied from an analytical point of view. To convex sets, one can associate appropriate functions and measures, study regularity and inequalities, in the interplay between functional analysis, harmonic analysis and probability. On the other hand, polyhedra are also naturally connected to combinatorics, linear algebra and linear programming. This has been the starting point for the development of the field of Convex Algebraic Geometry, which focuses mainly on semidefinite optimization, dealing for instance with spectrahedra and sums of squares.

This work aims to taking a further step toward the connection between the two communities of convex geometry and algebraic geometry. The underlying theme is indeed to approach the study of convex bodies using tools from real and complex algebraic geometry. For this to be meaningful, one should dive into the realm of semialgebraic convex bodies, which are convex compact subsets of a Euclidean space defined by a boolean combination of polynomial inequalities. One of the main characters that will guide us throughout the text is the algebraic boundary of a convex body. It is defined to be the Zariski closure of the topological boundary, i.e., it is the smallest complex algebraic variety that contains the topological boundary. This procedure allows us to associate a variety to a convex body, and thereby to study and get information about the latter via algebraic geometry.

One of the centerpieces of the thesis is visualization. The author's intuition in mathematics frequently derives from examples and drawings. These are thus the methods that are used here to introduce new notions and objects; they will hopefully help the reader in the comprehension and make the thesis more enjoyable. In order to compute examples, we rely on mathematical software, mainly **Macaulay2**, **Mathematica**, **Julia** and **SageMath**.

The next chapters are structured as follows. In Chapter 1 we introduce basic concepts from convex geometry and fix some notation. Some recurring examples will be used to present concretely all the new notions. Afterwards, we will transition from a more analytical point of view to an algebraic approach. This will require the discussion of some fundamental tools in complex and real algebraic geometry. Here we will then define the algebraic boundary of a convex body and examine its properties. These will be the bare bones of the thesis.

Chapter 2 focuses on particular convex bodies, called zonoids. We give their definition and enumerate their peculiar properties and questions. The beauty and the strength of problems regarding zonoids is that they can be studied from many different perspectives. Classically, mathematicians took the advantage of measure theory; more recently, probabilistic methods have been exploit. We approach them here using algebraic geometry. For this purpose, we restrict to the family of discotopes, strictly contained in the set of all semialgebraic zonoids. The goal is to characterize their algebraic boundary, in the spirit

of the Zonoid Problem. This chapter is based on [GM21].

In Chapter 3 we deal with two constructions with convex bodies. Fiber bodies are a generalization of the classical notion of fiber polytopes. They are a Minkowski integral of the fibers of a convex body with respect to a certain projection. We analyse basic properties, such as strict convexity, and then dig deeper in the case of three specific classes of convex bodies. One of the examples computed in this section establishes that semialgebraicity is not preserved by the construction of the fiber body. The second half of the chapter is devoted to intersection bodies. They are connected to the volume of hyperplane sections of a convex body. Popular among the community of convex geometry, intersection bodies still lack of an actual geometric comprehension. We prove here that the intersection body of a polytope is semialgebraic. We compute its algebraic boundary, and give upper bounds for the degree of such a variety. The two sections of this chapter are strongly based on [MM21] and [BBMS22] respectively.

Chapter 4 concerns convex hulls. Understanding the boundary of a convex hull is a hard task in general. However, algebraic geometry provides formulas for the algebraic boundary of the convex hull of a variety. We specify them in the case of surfaces in fourspace. In particular, we list the components that contribute to the boundary and their degrees, for Del Pezzo and Bordiga surfaces. In the last section of the chapter, we give formulas for the volume of the convex hull of curves, under certain hypotheses, that are not necessarily varieties. This shows how algebraic methods can be used also to study convex bodies that are not semialgebraic.

Finally, Chapter 5 presents an application in the world of quantum physics. One of the fundamental objects of this theory is the set of quantum correlations, which is a semialgebraic convex body. We meticulously study it. We provide the support function, classify all its boundary points, and prove that up to an affine transformation it is self-dual. The understanding of the correlation body has concrete applications for instance in the field of quantum cryptography. This chapter is strongly based on [LMS⁺21].

Chapter 1

Background

In this chapter we will start by introducing basic notions in convex geometry, that will be useful in later chapters. For extended discussions and proofs we refer to Schneider's book [Sch13] and Barvinok's book [Bar02]. The second section is devoted to review relevant definitions and results regarding semialgebraic convex bodies, based mainly on [Sin15]. We will also recall some machineries from real, complex and projective algebraic geometry.

1.1. Basics of convex geometry

To start talking about convex geometry, we shall introduce the notion of convex set. Throughout the thesis we will always work in a Euclidean space, therefore we give all the definitions in this setting, even though some would make sense also in more generality. A set $A \subset \mathbb{R}^d$ is said to be *convex* if for every pair of points $x, y \in A$ the whole segment between them is contained in A . More precisely, given two points $x, y \in \mathbb{R}^d$ the segment between them is the set of all their convex combinations, namely

$$[x, y] = \{\alpha x + (1 - \alpha)y \mid \alpha \in [0, 1]\}.$$

The *dimension* of a convex set A is meant to be its dimension as topological space. Equivalently, it is the (vector space) dimension of the affine span of A . When $0 \in A$ in particular, $\dim A = \dim \langle A \rangle$, where $\langle \cdot \rangle$ denotes the linear span. We will focus here on a specific class of convex sets.

Definition 1.1.1. A set $K \subset \mathbb{R}^d$ is called a *convex body* if it is a convex compact non-empty set. We denote the family of convex bodies of \mathbb{R}^d by $\mathcal{K}(\mathbb{R}^d)$.

The intersection of convex sets is convex; the intersection of convex bodies is a convex body. Convexity is a very geometric, visual, intuitive condition and it is indeed easy to construct examples or counterexamples of convex sets and convex bodies. A ball is a convex body, a circle is not convex, a halfspace is convex but not a convex body. In \mathbb{R} a set is convex if and only if it is a line segment. Since not every set is convex, we need an operation to 'convexify': this is the *convex hull*. The convex hull of $A \subset \mathbb{R}^d$ is the smallest convex set containing A , or alternatively it is the set of all convex combinations of points of A ; in formula

$$\text{conv } A = \left\{ \alpha_1 x_1 + \dots + \alpha_n x_n \mid x_1, \dots, x_n \in A, \alpha_1, \dots, \alpha_n \in [0, 1], \sum_{i=1}^n \alpha_i = 1 \right\}.$$

In particular, if $A \subset \mathbb{R}^d$ is compact, then $\text{conv } A$ is a convex body. An important family of convex bodies can be defined using the notion of convex hull.

Definition 1.1.2. A *polytope* is the convex hull of finitely many points.

Polytopes appear in an extraordinary number of mathematical areas and have applications that go in many directions, from optimization, to life sciences, to physics (we will have a glimpse of this in Chapter 5). This should suggest that the literature on polytopes is huge and here we will just introduce few basic concepts that are relevant for later chapters. For an accurate introduction on this subject, proofs and exercises, we refer to Ziegler's book [Zie12]. Another object, intimately related to polytopes is the following.

Definition 1.1.3. Let $a_1, \dots, a_n \in \mathbb{R}^d$ and $b_1, \dots, b_n \in \mathbb{R}$. The set

$$\left\{ x \in \mathbb{R}^d \mid \langle a_i, x \rangle \geq b_i \text{ for all } i = 1, \dots, n \right\},$$

where $\langle \cdot, \cdot \rangle$ is the standard scalar product on \mathbb{R}^d , is a *polyhedron*.

Polyhedra are intersections of halfspaces, hence they are convex. The following is known as Weyl-Minkowski's Theorem, also called the 'Main theorem for polytopes' by Ziegler.

Theorem 1.1.4. A subset $P \subset \mathbb{R}^d$ is a polytope if and only if it is a bounded polyhedron.

This result provides two equivalent, dual (in a sense that will be made precise later) characterizations of a polytope. Definition 1.1.2 is called the *v*-representation of a polytope (the name will be clear later), whereas its description as a bounded polyhedron is the *h*-representation, since we are intersecting halfspaces defined by the hyperplanes. It is very useful to work with both definitions for proving statements. There are also other equivalent characterizations of a polytope, see [Zie12, Theorem 2.15]. The family of polytopes is closed with respect to many operations: the intersection of two polytopes is a polytope, the projection of a polytope is a polytope, the convex hull of polytopes is a polytope. There are other important operations allowed on $\mathcal{K}(\mathbb{R}^d)$:

- dilation: $\lambda K = \{\lambda x \mid x \in K\}$, for $\lambda \geq 0$, $K \in \mathcal{K}(\mathbb{R}^d)$,
- Minkowski sum: $K_1 + K_2 = \{x_1 + x_2 \mid x_i \in K_i \text{ for } i = 1, 2\}$, for $K_1, K_2 \in \mathcal{K}(\mathbb{R}^d)$.

The family of polytopes is closed with respect to these operations too. Combining them, we can turn the set of convex bodies into a metric space. One possible way is to use the *Hausdorff metric*. Given two convex bodies $K_1, K_2 \in \mathcal{K}(\mathbb{R}^d)$, define their Hausdorff distance to be

$$\text{dist}_H(K_1, K_2) = \min\{\lambda \mid K_1 \subset K_2 + \lambda B^d \text{ and } K_2 \subset K_1 + \lambda B^d\}$$

where B^d is the unit d -dimensional ball. This is in fact a metric and $(\mathcal{K}(\mathbb{R}^d), \text{dist}_H)$ is a complete metric space [Sch13, Theorems 1.8.3, 1.8.6]. We are now allowed to talk about density and limits, and whenever we will discuss a metric property of a convex body, even if not specified, we will always refer to the Hausdorff metric. A first remark is that polytopes are dense in $\mathcal{K}(\mathbb{R}^d)$. Therefore, given any convex body $K \subset \mathbb{R}^d$ and given $\varepsilon > 0$ there exists a polytope $P \subset \mathbb{R}^d$ such that $\text{dist}_H(K, P) \leq \varepsilon$ [Sch13, Theorem 1.8.16].

1.1.1. Face structure

What do people study about convex bodies? One of the (many!) possible answers is: the boundary. It is also one of the main focus points of this thesis. If $A \subset \mathbb{R}^d$, we denote its *topological boundary* by ∂A . We want to establish a systematic way to describe the boundary of a convex body. This can be done for instance via the notion of faces.

Definition 1.1.5. A convex subset $F \subset K$ of a convex body is a *face* if $x, y \in K$ and $\frac{x+y}{2} \in F$ implies $x, y \in F$. If $F = \{x\}$, it is called *extreme point*; if $\dim F = 1$, it is called *edge*; if $\dim F = \dim K - 1$, it is called *facet*.

In particular, a point $x \in K$ is extreme if for every convex combination $x = \alpha y + (1-\alpha)z$ with $y, z \in K$, $\alpha \in [0, 1]$, then $y = z = x$. The union of all the faces of a convex body is its topological boundary. If all the boundary points are extreme points, then we say that K is *strictly convex*. In this case there are no segments contained in ∂K , or equivalently ∂K is a manifold with strictly positive curvature at all points. We can refine the notion of face as follows. Let $\langle \cdot, \cdot \rangle$ be the standard scalar product of \mathbb{R}^d ; we use it throughout the whole thesis to identify the Euclidean space and its dual. Nevertheless, we will try to be consistent with the notation, using x, y, z, \dots for the original space and u, v, w, \dots for the dual.

Definition 1.1.6. Let $K \in \mathcal{K}(\mathbb{R}^d)$ and let $u \in \mathbb{R}^d$. The *face of K exposed by u* is

$$K^u = \{x \in K \mid \langle u, x \rangle \geq \langle u, y \rangle \text{ for all } y \in K\}.$$

We will also say that K^u is the face of K exposed by u . If a point $\{x\}$ is an exposed face of K , it is called *exposed point*.

Such a vector $u \in \mathbb{R}^d$ corresponds, via the scalar product, to a linear functional $u \in (\mathbb{R}^d)^*$, that with abuse of notation we denote again by u . In this language, K^u is the set of points of K where the linear functional u attains its maximum over K . Geometrically, an exposed face arises as the intersection of K with a *separating* (or supporting) *hyperplane*: it is a hyperplane H such that K is contained in one of the two (closed) halfspaces identified by H , and satisfying $H \cap K \neq \emptyset$. Such a hyperplane is parallel to u^\perp , the orthogonal complement of u . Notice that an exposed face is a face, but a face need not to be exposed. Polytopes are a special case: all faces are exposed and every face is the convex hull of finitely many points, hence a polytope again. The fallout is that polytopes have finitely many faces, that we can store in the *f-vector* (f_0, \dots, f_{d-1}) . The $f_i(P)$ is the number of i -th dimensional faces of P .

In general, we will denote the set of extreme points of a convex body K by $\text{Ext}(K)$ and the set of its exposed points by $\text{Exp}(K)$. The set of extreme points contains the set of exposed points, but it is not much bigger: every extreme point is a limit (in the Euclidean topology) of exposed points [Sch13, Theorem 1.4.7].

Example 1.1.7. Consider the convex body in Figure 1.1, namely

$$K = \text{conv} \left\{ \{(x \pm 1)^2 + y^2 = 1\} \cup \{(0, -2)\} \right\}.$$

The four points $(\pm 1, 1), (\pm \frac{8}{5}, -\frac{4}{5})$ are extreme but not exposed. They belong to one of the facets exposed by the vectors $(0, 1), (\pm 3, -4)$. The set of exposed points is the union of two (open) arcs and a point, whereas the extreme points are

$$\text{Ext}(K) = \text{Exp}(K) \cup \left\{ (\pm 1, 1), \left(\pm \frac{8}{5}, -\frac{4}{5} \right) \right\}.$$

K is not strictly convex since there are three segments contained in the boundary: they are the facets of K . \blacklozenge

In a way, the extreme points contain all the information regarding a convex body. This is made precise by a result obtained by Krein and Milman, proved in more generality in [KM40], which is also known as Minkowski's Theorem.

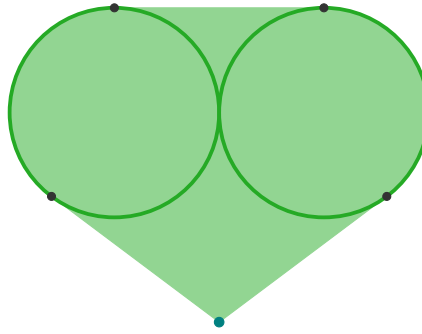


Figure 1.1: The convex hull of two circles and a point. The four black dots are extreme, non-exposed points.

Theorem 1.1.8. Let $K \in \mathcal{K}(\mathbb{R}^d)$. Then K is the convex hull of the set of its extreme points. In formula, $K = \text{conv}(\text{Ext}(K))$.

Note that taking the convex hull of the extreme points is the best we can do: for every subset $A \subsetneq \text{Ext}(K)$ we have that $\text{conv } A \subsetneq K$.

The counterparts of the faces of a convex body are the normal cones. A convex cone is a set $C \subset \mathbb{R}^d$ such that if $x \in C$ then $\lambda x \in C$ for all $\lambda \geq 0$. In particular, a cone is unbounded, hence it is not a convex body. Also in this case, we can turn any set A into a cone by considering its *conic hull* $\text{co } A$, which is defined to be the smallest convex cone containing A .

Given a point $x \in K$, the *normal cone* to $x \in K$ is the convex cone

$$\mathsf{N}_K(x) = \left\{ u \in \mathbb{R}^d \mid \langle u, x \rangle \geq \langle u, y \rangle \text{ for all } y \in K \right\}.$$

This is the set of all vectors that expose a face of K containing x , so it also makes sense to consider the normal cone $\mathsf{N}_K(F)$ to a face F of K . The correspondence $F \mapsto \mathsf{N}_K(F)$ is an inclusion-reversing map. By the linearity of the scalar product, normal cones are convex cones, but their dimension can vary.

Definition 1.1.9. Let $K \in \mathcal{K}(\mathbb{R}^d)$ be a full dimensional convex body. An extreme point $x \in \partial K$ is a *vertex* if $\dim \mathsf{N}_K(x) > 1$.

If the convex body is a polytope $P \subset \mathbb{R}^d$, the normal cone to a face F has dimension $d - \dim F$, so all the extreme points are vertices. This justifies the letter ‘*v*’ in the *v*-representation of Definition 1.1.2. In this case, the union of all normal cones is a complete fan [Zie12, Definition 7.1], called the *normal fan* of P .

In Example 1.1.7 the normal cone at $x = (0, -2)$ is the two-dimensional set

$$\mathsf{N}_K(x) = \text{co} \left\{ \left(\pm \frac{8}{5}, -\frac{4}{5} \right) \right\},$$

hence x is a vertex of K . At all the other points of ∂K the normal cone is a ray. Notice that the two vectors $(\pm \frac{8}{5}, -\frac{4}{5})$ already appeared in our example, and it is not a coincidence. In order to comprehend such a structure we should define an object that encodes information about K , its normal cones and its exposed faces.

1.1.2. Duality in convex geometry

In this section we introduce the first constructions with convex bodies, a theme that will come back in Section 3. The general philosophy consists in manipulating a convex body K

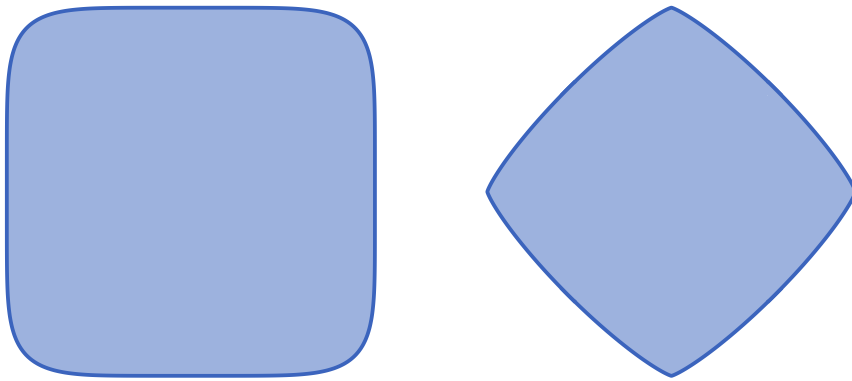


Figure 1.2: Left: the L^6 unit ball. Right: the $L^{\frac{6}{5}}$ unit ball.

in order to create a new object (another convex body for instance) and study the relations among the former and the latter.

Definition 1.1.10. Let $K \in \mathcal{K}(\mathbb{R}^d)$. The *dual* (or polar) convex body of K is

$$K^\circ = \left\{ u \in \mathbb{R}^d \mid \langle u, x \rangle \leq 1 \text{ for all } x \in K \right\}.$$

Formally, the dual body would live in the dual space $(\mathbb{R}^d)^*$ that we are identifying with \mathbb{R}^d . Note that in the literature there are different definitions of the dual body: here we are using the convention with *outer* normal vectors. Directly from the definition, one can prove that this duality is an inclusion-reversing operation on convex bodies and that it almost commutes with linear transformations: given $g \in \mathrm{GL}(\mathbb{R}^d)$ we have that $(g \cdot K)^\circ = g^{-t} \cdot K^\circ$. Another immediate observation is that K° is always a convex set that contains the origin. This leads to the Bidual (or Bipolar) Theorem.

Theorem 1.1.11. Let $K \in \mathcal{K}(\mathbb{R}^d)$ such that $0 \in K$. Then $K^{\circ\circ} = K$.

More in general $K^{\circ\circ} = \mathrm{conv}(K \cup 0)$. We will usually use the expression ‘dual body’ instead of ‘polar’ in order to emphasize that there is a duality relation. Moreover, this object is linked to other notions of duality, as we will discuss in Section 1.2. The following example gives us a glimpse of that.

Example 1.1.12. Let $K \subset \mathbb{R}^d$ be the L^p unit ball of \mathbb{R}^d . It is a convex body. Using Hölder’s inequality one can prove that its dual body is the L^q unit ball, where $\frac{1}{p} + \frac{1}{q} = 1$. Figure 1.2 shows the case $d = 2$, $p = 6$, $q = \frac{6}{5}$. ◆

The polytopal case is again special: the dual body of a polytope is a polytope itself. In particular, the v -representation of P becomes the h -representation of P° , and conversely. We highlight this with an example.

Example 1.1.13. Let $P = [-1, 1]^4$ be the four-dimensional cube centred at the origin. Its dual polytope is

$$P^\circ = \left\{ u \in \mathbb{R}^d \mid \langle u, v \rangle \leq 1 \text{ for all vertices } v \in P \right\}.$$

The vertices of P° are the eight points $(\pm 1, 0, 0, 0), (0, \pm 1, 0, 0), (0, 0, \pm 1, 0), (0, 0, 0, \pm 1)$, which are exactly the vectors that give the linear inequalities in the definition of P (i.e., they are the a_i ’s of Definition 1.1.3). ◆

The construction of the dual convex body induces an analogous notion on faces. Let F be a face of K ; define its *dual face* F° to be the set of linear functionals that attain their maximum over K at F . In the nice case in which the origin lies in the interior of K , one has

$$F^\circ = \left\{ u \in \mathbb{R}^d \mid \langle u, x \rangle = 1 \text{ for all } x \in F \right\}.$$

The dual face is always an exposed face by definition, and we can also recover all the exposed faces in this way. We make it precise by the following statement: a version of biduality for faces.

Corollary 1.1.14. Let $K \in \mathcal{K}(\mathbb{R}^d)$ with $0 \in K$. Let F be an exposed face of K . Then $F^{\circ\circ} = F$.

When the convex body is a polytope P , all faces are exposed and the dual face to F is just the intersection of $N_P(F)$ with the hyperplane $\langle u, x \rangle = 1$. Hence, we always have that

$$\dim F + \dim F^\circ = d - 1. \quad (1.1.1)$$

In particular, vertices of P correspond to facets of P° , edges of P correspond to faces of P° of dimension $d - 2$, and so on. We can translate this observation in terms of the f -vector: $f_i(P) = f_{d-1-i}(P^\circ)$ for a full dimensional polytope $P \subset \mathbb{R}^d$. Equation (1.1.1) does not hold for more general convex bodies. For instance, consider the L^6 unit ball displayed in Figure 1.2, left. Since it is strictly convex, all the points in its boundary are faces. In this case, all faces are actually exposed and they are always exposed by a unique vector. So we have that $\dim F + \dim F^\circ = 0 < 1$ for every face.

The normal cycle. The definition of the polar suggests to look at the *incidence relation* between points $x \in K$ and $u \in K^\circ$ for which the inequality $\langle u, x \rangle \leq 1$ is tight. The resulting set is called normal cycle.

Definition 1.1.15. Let $K \in \mathcal{K}(\mathbb{R}^d)$ with the origin in its interior. The *normal cycle* of K is defined as

$$N(K) = \{ (x, u) \in \partial K \times \partial K^\circ \mid \langle x, u \rangle = 1 \}.$$

This integrates K and K° into a single structure, but it is useful far beyond this role. Fixing x to range over a face $F \subset \partial K$ leaves u to range over the exposed face F° of K° .

Let us look at the two extreme cases of convex sets: first, we have strictly convex sets with smooth boundary, whose only faces are exposed points. Here, $N(K)$ is the graph of a homeomorphic identification of ∂K with ∂K° . If on the other hand K is a polytope, although the normal cycle is far from being a convex set, for every k -dimensional face F , the set $F \times F^\circ \subset N(K)$ is a polytope of dimension $k + (d - k - 1) = d - 1$.

Example 1.1.16. Consider the four-dimensional cube $P = [-1, 1]^4$ from Example 1.1.3 and its dual polytope P° . Their f -vectors are $(16, 32, 24, 8)$ and $(8, 24, 32, 16)$ respectively. The common (up to relabelling the coordinates) normal cycle $N(P) = N(P^\circ)$ is a $(d - 1)$ -dimensional submanifold of \mathbb{R}^{2d} and it consists of 80 strata (this word will be made precise later, for now just think of them as pieces, building blocks), one for each of the $16 + 32 + 24 + 8$ pairs (F, F°) , where $F \subset \partial P$ and $F^\circ \subset \partial P^\circ$ are faces of complement dimension. For instance, if $\dim(F) = 1$ then F° is a triangle and $F \times F^\circ$ is a triangular prism. ◆

The power of the normal cycle lies in the uniform treatment covering the whole range of convex bodies from polytopes to smooth. Indeed, for any compact convex d -dimensional set K containing the origin in its interior, $N(K)$ is always a $(d - 1)$ -dimensional (Lipschitz

Legendrian) submanifold of \mathbb{R}^{2d} [Fu14]. Moreover, the map $K \mapsto \mathbf{N}(K)$ is continuous in the Hausdorff metric for sets. This makes the normal cycle a remarkably stable structure under approximations either by smooth manifolds or by polytopes.

The normal cycle plays the role of the normal bundle for more general geometric objects. It was defined by Federer [Fed59] for sets of positive reach. These include convex bodies but also much crazier sets. It is an important tool from geometric measure theory, used for defining curvature measures [Win82, Zäh86]. This is related to the classic result of Steiner, who noted that the volume of the smooth approximation to a body, which one gets as the union of all balls of small radius r centered on the body, is a polynomial in r , whose coefficients relate to curvature of different dimensionality. On the other hand, stable polyhedral approximations are needed in visualization, computer graphics and computational anatomy (see [CSM03, RG17, SLC⁺19]). Recently, the normal cycle has also emerged as a key player in convex algebraic geometry [CKLS19a, PSW21] as we will see in Section 1.2.

1.1.3. Functions and convex bodies

One of the reasons why polytopes are popular is that they have finite descriptions, as we highlighted for instance with the v and the h -representations. As soon as one moves away from polytopes, these finiteness properties are not true any more. Therefore, one needs to find other efficient ways to describe a convex body. This can be done using functions (for details see [Sch13, Section 1.7]).

Definition 1.1.17. The *support function* of a convex body K is $h_K : \mathbb{R}^d \rightarrow \mathbb{R}$ such that

$$h_K(u) = \max \{ \langle u, x \rangle \mid x \in K \}. \quad (1.1.2)$$

As the name suggests, it is related to the supporting hyperplanes of K . In particular, the value of $h_K(u)$ is the (signed) distance to the origin of the supporting hyperplane with outer normal vector u . This implies that $\langle u, x \rangle \leq h_K(u)$ for every $x \in K$. We also get an alternative description of the exposed faces of K :

$$K^u = \{x \in K \mid \langle u, x \rangle = h_K(u)\}.$$

Playing with the definition, one finds out that the support function is sublinear, i.e., $h_K(\lambda u) = \lambda h_K(u)$ for all $\lambda \geq 0$, and $h_K(u+v) \leq h_K(u) + h_K(v)$. In fact, all sublinear functions are support functions, as stated in the following, which is [Sch13, Theorem 1.7.1].

Theorem 1.1.18. Let $h : \mathbb{R}^d \rightarrow \mathbb{R}$ be a sublinear function. Then there exists a unique convex body $K \in \mathcal{K}(\mathbb{R}^d)$ such that $h_k = h$.

Therefore, a convex body is uniquely identified by its support function. Endowing the space of convex bodies with the Hausdorff metric, we can think of the support function as $h : \mathcal{K}(\mathbb{R}^d) \times \mathbb{R}^d \rightarrow \mathbb{R}$ and it is a continuous function in both arguments [Sch13, Lemma 1.8.12]. Also, we can use it to express the Hausdorff distance between two convex bodies [Sch13, Lemma 1.8.14]:

$$\text{dist}_H(K_1, K_2) = \sup_{u \in S^{d-1}} |h_{K_1}(u) - h_{K_2}(u)|.$$

We summarize further properties of the support function in the following proposition.

Proposition 1.1.19. Let $K_1, K_2 \in \mathcal{K}(\mathbb{R}^d)$ with their respective support functions h_{K_1}, h_{K_2} . Then

- (i) $h_{\lambda K_1} = \lambda h_{K_1}$;
- (ii) $h_{K_1+K_2} = h_{K_1} + h_{K_2}$;
- (iii) If $T : \mathbb{R}^d \rightarrow \mathbb{R}^k$ is a linear map then $h_{TK} = h_K \circ T^t$;
- (iv) h_K is differentiable at $u \in \mathbb{R}^d$ if and only if the point x realizing the maximum in (1.1.2) is unique. In that case $x = K^u = \nabla h_K(u)$, where ∇h_K denotes the gradient of h_K .

Recognizing a convex body from its support function is not always easy, but there are some cases in which it is possible. The convex body K is a polytope if and only if h_K is piecewise linear; in particular, $h_K(\cdot) = \langle \cdot, x \rangle$ if and only if $K = \{x\}$. The support function of the ball of radius r centred at the origin is $h_{rB^d}(u) = r\|u\|$.

Another function that will be useful later in Section 3.2 is the radial function.

Definition 1.1.20. Let $K \in \mathcal{K}(\mathbb{R}^d)$ containing the origin. Its *radial function* is $\rho_K : \mathbb{R}^d \rightarrow \mathbb{R}$ such that

$$\rho_K(x) = \max\{\lambda \geq 0 \mid \lambda x \in K\}. \quad (1.1.3)$$

Radial functions are actually meaningful for a larger class of sets: the starshaped sets. A set $A \subset \mathbb{R}^d$ is *starshaped* if there exists $x_0 \in A$ such that for all $x \in K$ we have $[x_0, x] \subset A$. Convex sets are starshaped with respect to any of their points. We assume from now on, when talking about starshaped sets, that they are starshaped with respect to the origin, i.e., $x_0 = 0$. Then, compact starshaped sets have an associated radial function as defined in (1.1.3). This function satisfies $\rho_K(\lambda x) = \frac{1}{\lambda}\rho_K(x)$ for all $\lambda > 0$, hence it is enough to define it on the unit sphere. Given the radial function ρ , we can recover the associated starshaped set A and its topological boundary (when the origin lies in the interior of A):

$$A = \left\{ x \in \mathbb{R}^d \mid \rho(x) \geq 1 \right\}, \quad \partial A = \left\{ x \in \mathbb{R}^d \mid \rho(x) = 1 \right\}.$$

Let K be a convex body with the origin in its interior. Its support and radial functions are related to each other via duality, namely

$$h_K(u) = \frac{1}{\rho_{K^\circ}(u)}, \quad \rho_K(u) = \frac{1}{h_{K^\circ}(u)}.$$

As a consequence, we can describe the boundary of the dual body K° as the set of points $x \in \mathbb{R}^d$ such that $h_K(u) = 1$.

1.2. Varieties and convex bodies

We begin this section by introducing some relevant concepts from semialgebraic geometry. The main reference for the theory is [BCR13].

A subset $A \subset \mathbb{R}^d$ is a *basic closed* (respectively open) *semialgebraic set* if it can be written as

$$A = \left\{ x \in \mathbb{R}^d \mid f_1(x) \geq 0, \dots, f_n(x) \geq 0 \right\}$$

(respectively $A = \left\{ x \in \mathbb{R}^d \mid f_1(x) > 0, \dots, f_n(x) > 0 \right\}$)

for some polynomials $f_1, \dots, f_n \in \mathbb{R}[x_1, \dots, x_d]$. Basic closed (respectively open) semialgebraic sets are closed (respectively open) in the Euclidean topology of \mathbb{R}^d .

Definition 1.2.1. A *semialgebraic* set $A \subset \mathbb{R}^d$ is a finite boolean combination of basic (closed or open) semialgebraic sets.

By a finite boolean combination we mean finitely many unions, intersections and complements. Semialgebraic sets satisfy many nice properties; at the core of most of their proofs there is the fact that semialgebraic sets are stable under projections [BCR13, Theorem 2.2.1].

Theorem 1.2.2. Let $A \subset \mathbb{R}^{d+1}$ be a semialgebraic set and consider the projection $\pi : \mathbb{R}^{d+1} \rightarrow \mathbb{R}^d$ onto the first d coordinates. Then $\pi(A)$ is a semialgebraic set.

The first consequences of this result are that the interior $\text{int } A$ and the Euclidean closure $\text{cl } A$ of a semialgebraic set A are semialgebraic. Hence, the topological boundary of a semialgebraic set is semialgebraic.

It might be convenient sometimes to translate the notion of semialgebraic sets into the language of logic. It allows to define the analogous of semialgebraic sets for more general real closed fields. In this context, a semialgebraic set is described via a quantifier free first-order formula. A (slightly stronger) version of the projection theorem in this setting is known as the Quantifier Elimination Theorem. Since the thesis focuses only on semialgebraic subsets of Euclidean spaces, we will not expand on the general case, but the curious reader can find the details in [BCR13, Chapter 5].

Having a definition of a property of a set, often leads to the introduction of an analogous property of functions, via their graph.

Definition 1.2.3. A map $f : \mathbb{R}^d \rightarrow \mathbb{R}^k$ is a *semialgebraic function* if $\text{graph}(f) \subset \mathbb{R}^d \times \mathbb{R}^k$ is a semialgebraic set.

By the projection theorem, the image of a semialgebraic set under a semialgebraic function is a semialgebraic set. Moreover, semialgebraic functions are stable under composition and inverse. Polynomials are semialgebraic functions, but also wilder maps as the square root or the absolute value are.

Another useful consequence of the projection theorem, which provides a stratification of a semialgebraic set, is the Cylindrical Algebraic Decomposition, often abbreviated as CAD. It follows from this technical result [BCR13, Theorem 2.3.1].

Theorem 1.2.4. Let $f_1, \dots, f_n \in \mathbb{R}[x, y] = \mathbb{R}[x_1, \dots, x_d, y]$ be polynomials in $d+1$ variables. Then, there exists a partition

$$\mathbb{R}^d = S_1 \cup \dots \cup S_k$$

of \mathbb{R}^d into a finite number of semialgebraic sets S_1, \dots, S_k and for all $i = 1, \dots, k$ there are finitely many continuous semialgebraic functions $\xi_{i,1} < \dots < \xi_{i,\ell_i} : S_i \rightarrow \mathbb{R}$ with the following properties:

- (i) for every $x \in S_i$, the set $\{\xi_{i,1}, \dots, \xi_{i,\ell_i}\}$ coincides with the set of roots of those polynomials $f_j(x, y)$ that are not identically zero at x ;
- (ii) the polynomials f_1, \dots, f_n have constant sign on each $\text{graph}(\xi_{i,j})$ and on every band $\{(x, y) \in \mathbb{R}^{d+1} \mid \xi_{i,j}(x) < y < \xi_{i,j+1}(x)\}$, where $j = 0, \dots, \ell_{i+1}$ with the convention that $\xi_{i,0} = -\infty$ and $\xi_{i,\ell_{i+1}} = +\infty$.

Then, given a semialgebraic set $A \subset \mathbb{R}^{d+1}$ we say that a cylindrical algebraic decomposition of A , with respect to the projection $\pi : \mathbb{R}^{d+1} \rightarrow \mathbb{R}^d$, is a partition of \mathbb{R}^d as in Theorem 1.2.4 such that A can be written as a union of graphs and bands.

Corollary 1.2.5. Every semialgebraic set admits a CAD.

Iterating this process with subsequent projections $\mathbb{R}^{d+1} \rightarrow \mathbb{R}^d \rightarrow \dots \rightarrow \mathbb{R}$ gives a *stratification* of a semialgebraic set $A \subset \mathbb{R}^{d+1}$. We can in fact write A as a disjoint union of semialgebraic sets S_i , called (*open*) *strata*, that are semialgebraically homeomorphic to the unit ball B^n for some $n \geq 0$ [BCR13, Theorem 2.3.6]. One can refine such a stratification adding different requirements: for instance it is possible to find a decomposition such that the closure of each stratum is a union of strata. Clearly, this construction is very much non-unique: it depends on the projections and on the choices of the semialgebraic functions. Since the content of the theorem above is quite technical, we illustrate a CAD in the following example.

Example 1.2.6. Let K be the set from Example 1.1.7. This is a semialgebraic subset of \mathbb{R}^2 since we can write it as the set of points $(x, y) \in \mathbb{R}^2$ such that

$$(x - 1)^2 + y^2 \leq 1 \quad \text{or} \quad (x + 1)^2 + y^2 \leq 1 \quad \text{or} \\ \{y \leq 1, 4y \geq 3x - 10, 4y \geq -3x - 10, y \leq 3x + 4, y \leq -3x + 4\}.$$

Consider the projection onto the y axis. It induces a CAD of K as $S_1 \cup \dots \cup S_{10}$ where the strata are

$$\begin{aligned} S_1 &= \{(0, -2)\}, \\ S_2 &= \{(x, y) \in \mathbb{R}^2 \mid y \in (-2, -\frac{4}{5}), 3x = -4y - 10\}, \\ S_3 &= \{(x, y) \in \mathbb{R}^2 \mid y \in (-2, -\frac{4}{5}), -4y - 10 < 3x < 4y + 10\}, \\ S_4 &= \{(x, y) \in \mathbb{R}^2 \mid y \in (-2, -\frac{4}{5}), 3x = 4y + 10\}, \\ S_5 &= \{(x, y) \in \mathbb{R}^2 \mid y \in (-\frac{4}{5}, 1), x = -\sqrt{1 - y^2} - 1\}, \\ S_6 &= \{(x, y) \in \mathbb{R}^2 \mid y \in (-\frac{4}{5}, 1), -\sqrt{1 - y^2} - 1 < x < \sqrt{1 - y^2} + 1\}, \\ S_7 &= \{(x, y) \in \mathbb{R}^2 \mid y \in (-\frac{4}{5}, 1), x = \sqrt{1 - y^2} + 1\}, \\ S_8 &= \{(-1, 1)\}, \\ S_9 &= \{(x, 1) \in \mathbb{R}^2 \mid -1 < x < 1\}, \\ S_{10} &= \{(1, 1)\}. \end{aligned}$$

◆

Now that we know what a semialgebraic set is, we are ready to define the main characters of this thesis: semialgebraic convex bodies.

Definition 1.2.7. A set $K \subset \mathbb{R}^d$ is a *semialgebraic convex body* if it is a semialgebraic set and a convex body.

Examples are polytopes, since they arise as they intersection of finitely many half-spaces, but also more ‘curved’ objects such as those shown in Figures 1.1 and 1.2. We collect in the following proposition some basic properties of semialgebraic convex bodies that highlight the good behaviour of semialgebraicity with respect to the notions in convexity that we introduced in Section 1.1.

Proposition 1.2.8. Let $K \in \mathcal{K}(\mathbb{R}^d)$, then the following are equivalent:

- (i) K is semialgebraic;
- (ii) the support function h_K is a semialgebraic function;

- (iii) the radial function ρ_K is a semialgebraic function;
- (iv) any face $F \subset K$ is a semialgebraic convex body;
- (v) the set of extreme points $\text{Ext}(K)$ is a semialgebraic set;
- (vi) assuming that $0 \in \text{int } K$, the dual body K° is a semialgebraic convex body;

Moreover, the Minkowski sum of two semialgebraic convex bodies is a semialgebraic convex body, and the convex hull of a compact semialgebraic set is a semialgebraic convex body.

Proof. All the statements are a direct consequence of quantifier elimination, since all these objects can be written as first-order formulae over \mathbb{R} . \square

Thus, the family of semialgebraic convex bodies is closed with respect to many fundamental operations and constructions in convex geometry. Not all convex bodies are semialgebraic. For instance, the set

$$K = \text{conv}\{(x, y) \in \mathbb{R}^2 \mid x \in [0, 1], y = e^x\}$$

cannot be written as a finite boolean combination of polynomial inequalities. However, if we restrict to the class of semialgebraic convex bodies, it is possible to generalize some of the nice properties of polytopes and recover their finiteness. Indeed, by definition we have a finite description of a semialgebraic convex body. We will see later that one can partition (a dense subset of) the boundary of K into finitely many open sets, that resemble the faces of a polytope.

Spectrahedra. There are many ways in which one can generalize polytopes. A natural option, that goes in the direction of optimization, is the following. Let us begin by rewriting the definition of polytopes in a slightly different way:

$$P = \left\{ x \in \mathbb{R}^d \mid M_0 + M_1 x_1 + \dots + M_d x_d \succcurlyeq 0 \right\}$$

where the M_i 's are $n \times n$ diagonal matrices and $\succcurlyeq 0$ means positive semidefinite. A symmetric matrix $M \in \mathbb{R}^{n \times n}$ is positive semidefinite if $x^T M x \geq 0$ for every $x \in \mathbb{R}^n$, and the set of symmetric positive semidefinite $n \times n$ matrices is a convex cone that we will denote by \mathcal{S}_+^n . From this point of view, a polytope is a particular linear cut of this cone.

Definition 1.2.9. A *spectrahedron* $K \subset \mathbb{R}^d$ is the intersection of \mathcal{S}_+^n with an affine linear space, embedded in \mathbb{R}^d , namely

$$K = \left\{ x \in \mathbb{R}^d \mid M_0 + M_1 x_1 + \dots + M_d x_d \succcurlyeq 0 \right\}$$

for some $M_i \in \mathcal{S}_+^n$.

If linear programming optimizes linear functionals over polytopes, semidefinite programming does it over spectrahedra. This was the starting point for the investigation of these objects, from the point of view of convex optimization. The condition that a matrix with linear polynomial entries is positive semidefinite, is the intersection of finitely many polynomials inequalities, hence spectrahedra are basic closed semialgebraic convex sets. Just like polytopes, all the faces of a spectrahedron are exposed. However, they do not behave as well as polytopes: the class of spectrahedra is not closed under projection and duality. To solve this problem, one needs to consider the larger family of spectrahedral shadows [Sch18c], i.e. images of spectrahedra under projections.

Example 1.2.10. A classical non-trivial example of a spectrahedron is the *elliptope* [LP95]

$$K = \left\{ (x, y, z) \in \mathbb{R}^3 \mid \begin{bmatrix} 1 & x & y \\ x & 1 & z \\ y & z & 1 \end{bmatrix} \succcurlyeq 0 \right\}. \quad (1.2.1)$$

The boundary ∂K consists of six edges and a surface of extreme points. Among the extreme points we find four vertices, namely $(1, 1, 1), (1, -1, -1), (-1, 1, -1), (-1, -1, 1)$; the edges of ∂K are the line segments connecting the vertices. ♦

Spectrahedra are connected also to the broad theories of hyperbolic polynomials and sums of squares.

1.2.1. The algebraic boundary

The goal of this section is to do a transition from geometry to algebra: we start with a convex body, and we associate to it a complex algebraic variety. Prior to this, we recall few notions from algebraic geometry, to fix the notation. For a friendly introduction to the subject, we refer to [MS21a]; for more details, see [CLO15].

A (affine) *variety* is the set of common zeros of some polynomials: given $f_1, \dots, f_n \in \mathbb{C}[x_1, \dots, x_d]$ the associated variety is

$$\mathcal{V}(f_1, \dots, f_n) = \{x \in \mathbb{C}^d \mid f_1(x) = \dots = f_n(x) = 0\}.$$

The set of zeros does not change if we consider instead of the polynomials, the ideal they generate. Let $I = (f_1, \dots, f_n)$, then $\mathcal{V}(I) = \mathcal{V}(f_1, \dots, f_n)$. When the ideal I can be generated by one (non-constant) polynomial, we say that $\mathcal{V}(I) = \mathcal{V}(f)$ is a *hypersurface*. A variety is called *irreducible* if it cannot be written as a union of proper subvarieties, i.e.

$$\mathcal{V}(I) = \mathcal{V}(J_1) \cup \mathcal{V}(J_2) \Rightarrow \mathcal{V}(I) = \mathcal{V}(J_1) \text{ or } \mathcal{V}(I) = \mathcal{V}(J_2).$$

If a polynomial f is irreducible, the hypersurface $\mathcal{V}(f)$ is irreducible itself. If f is not irreducible, we can factorize it into irreducible factors as $f(x) = f_1(x) \cdot \dots \cdot f_n(x)$ and the varieties $\mathcal{V}(f_i)$ are the *irreducible components* of $\mathcal{V}(f)$. In terms of ideals, a variety $\mathcal{V}(I)$ being irreducible corresponds to I being prime. The analogue of the factorization of a polynomial, is given here by the *primary decomposition* of the ideal I .

Varieties form a basis of closed sets for a topology, called the *Zariski topology*. Since we will be interested later in the Real story, we will often consider just varieties defined by polynomials with real coefficients; they define the \mathbb{R} -Zariski topology. It is much coarser than the Euclidean topology. We will denote by \overline{A} the closure of the set A with respect to the (\mathbb{R})-Zariski topology. In this setting, we can make sense of a word very much appreciated by algebraic geometers: generic. Something is said to be generic, or to hold for the generic element of \mathbb{C}^d if it is not true for points in a subset which is closed with respect to the Zariski topology.

Two important invariants of varieties are their dimension (or codimension) and degree. Consider the variety $\mathcal{V}(I) \subset \mathbb{C}^d$ and some generic hyperplanes H_i . There exists a well defined k such that $\mathcal{V}(I) \cap H_1 \cap \dots \cap H_k$ is a finite number of points. Informally, such a k is the *codimension* of $\mathcal{V}(I)$, $d - k$ is its *dimension* and the cardinality of $\mathcal{V}(I) \cap H_1 \cap \dots \cap H_k$ is its *degree*.

Definition 1.2.11. The *algebraic boundary* of $K \in \mathcal{K}(\mathbb{R}^d)$, denoted by $\partial_a K \subset \mathbb{C}^d$, is the closure of the topological boundary with respect to the (\mathbb{R})-Zariski topology. In other words, it is the smallest variety containing ∂K .

This definition provides the connection between convex geometry and algebraic geometry. We have a convex body K , a concrete geometrical object, and we associate to it a variety $\partial_a K$ and thus an ideal. Now we can use tools from commutative algebra, real and complex algebraic geometry, to study such a variety (its dimension, degree, equations), in order to get information about K itself. For instance we can deduce whether K is a semialgebraic convex body from its algebraic boundary. The following is [Sin15, Proposition 2.9].

Theorem 1.2.12. Let $K \in \mathcal{K}(\mathbb{R}^d)$ be full dimensional. Then K is a semialgebraic convex body if and only if its algebraic boundary $\partial_a K$ is a hypersurface.

If K is not semialgebraic, then $\partial_a K = \mathbb{R}^d$ hence it is not interesting. To avoid heavy notation, we will use the same symbol for the algebraic boundary and its real part: when we refer to the real part, we will simply write $\partial_a K \subset \mathbb{R}^d$. Let us go back to the examples that we encountered so far and comment on the various algebraic boundaries. For a polytope P the algebraic boundary $\partial_a P$ is a union of finitely many hyperplanes, the ones that define its facets. Hence, it is a reducible variety with degree equal to $f_{d-1}(P)$. The algebraic boundary of the convex body K from Example 1.1.7 has five irreducible components, two quadrics and three lines:

$$\begin{aligned}\partial_a K = & \mathcal{V}((x+1)^2 + y^2 - 1) \cup \mathcal{V}((x-1)^2 + y^2 - 1) \\ & \cup \mathcal{V}(y-1) \cup \mathcal{V}(3x-4y-10) \cup \mathcal{V}(3x+4y+10).\end{aligned}$$

On the other hand, Example 1.1.12 illustrates a semialgebraic convex body whose algebraic boundary is irreducible: $\partial_a K = \mathcal{V}(x^6 + y^6 - 1)$. Its dual body is semialgebraic by point (vi) of Proposition 1.2.8. Its algebraic boundary is an irreducible variety of degree 30:

$$\begin{aligned}& \mathcal{V}(x^{30} + 5x^{24}y^6 + 10x^{18}y^{12} + 10x^{12}y^{18} + 5x^6y^{24} + y^{30} - 5x^{24} \\ & + 605x^{18}y^6 - 1905x^{12}y^{12} + 605x^6y^{18} - 5y^{24} + 10x^{18} + 1905x^{12}y^6 \\ & + 1905x^6y^{12} + 10y^{18} - 10x^{12} + 605x^6y^6 - 10y^{12} + 5x^6 + 5y^6 - 1).\end{aligned}$$

We can write both K and K° as the locus where the associated polynomial is less or equal than zero. This is not always the case, even for convex bodies with irreducible algebraic boundary. Indeed, let us move to Example 1.2.10. The algebraic boundary of the ellipope is the zero locus of the cubic polynomial

$$f = 2xyz - x^2 - y^2 - z^2 + 1 \tag{1.2.2}$$

and the points of the ellipope satisfy $f \geq 0$. However, not all $(x, y, z) \in \mathbb{R}^3$ such that $f(x, y, z) \geq 0$ belong to the ellipope; in fact, the locus where f is non-negative includes also four unbounded ‘ears’, as shown in Figure 1.3. For spectrahedra there is in fact a general rule for computing the algebraic boundary: it is the zero locus of the determinant of the defining matrix. For instance (1.2.2) is the determinant of the matrix that appears in (1.2.1).

Remark 1.2.13. The algebraic boundary does not determine the convex body. Let $K \subset \mathbb{R}^d$ be a full dimensional semialgebraic convex body. Then the real part of $\partial_a K$ cuts the space into finitely many regions: the connected components of $\mathbb{R}^d \setminus \partial_a K$. The convex body K is thus the union of some of these components, but in general there can be multiple choices. For example, let

$$\partial_a K = \mathcal{V}(x^2 + y^2 - 1) \cup \mathcal{V}(x) \subset \mathbb{C}^2.$$

Then there are two possible choices for K : it is either the half unit ball with $x \geq 0$ or the half unit ball with $x \leq 0$.

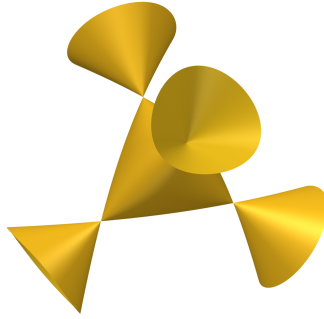


Figure 1.3: The real part of the algebraic boundary of the ellotope.

1.2.2. More dualities

We now go back to the notion of dual body and we analyse it from the point of view of the algebraic boundary. The results that we present here appear in [Sin14, Sin15], with particular emphasis on the relation between the boundary of K and K° . For computational aspects and a comparison of different notions of duality in convex geometry, algebraic geometry and optimization, see [RS10].

The transition from convex geometry to algebraic geometry is marked by some crucial steps:

1. Convex geometry: a convex body;
2. Real algebraic geometry: a *semialgebraic* convex body;
3. Complex algebraic geometry: the algebraic boundary;
4. Projective geometry: the algebraic boundary in terms of dual varieties.

The present section will be devoted to the inspection of point 4. We start by introducing dual varieties. Recall that the complex projective space \mathbb{P}^d is the quotient \mathbb{C}^{d+1}/\sim , where $x \sim y$ if and only if there exists $\lambda \neq 0$ such that $x = \lambda y$. We denote a point in projective space by $[x_0, \dots, x_d] \in \mathbb{P}^d$. Here one can define *projective varieties* to be the zero locus of *homogeneous* polynomials, that are precisely those polynomials whose zero locus is preserved by \sim . We can move between affine and projective varieties by homogenizing or dehomogenizing polynomials and ideals. As for affine varieties, we have the notion of Zariski topology in \mathbb{P}^d and irreducibility, smoothness, dimension and degree of a projective variety. For rigorous definitions and results we refer to [CLO15, Chapter 8].

Let $X \subset \mathbb{P}^d$ be a variety and denote by X_{reg} the subset of smooth points of X . A point $u \in (\mathbb{P}^d)^*$ is said to be *tangent* to X at $x \in X_{\text{reg}}$ if the associated hyperplane $u^\perp \subset \mathbb{P}^d$ contains $T_x X$, the embedded tangent space to X at x .

Definition 1.2.14. The *conormal variety* of X , denoted $\mathbf{CN}(X)$, is the Zariski closure of the set

$$\{(x, u) \in \mathbb{P}^d \times (\mathbb{P}^d)^* \mid x \in X_{\text{reg}}, T_x X \subset u^\perp\}.$$

If X is irreducible, then $\mathbf{CN}(X)$ is irreducible as well and has dimension $d - 1$. Informally, the conormal variety is the Zariski closure of the conormal bundle, by looking at the projection of \mathbf{CN} onto the first factor. On the other hand, the projection π_2 onto the second factor gives the dual variety.

Definition 1.2.15. Let $X \subset \mathbb{P}^d$ be a projective variety. Its *dual variety* X^* is the Zariski closure of the set of hyperplanes tangent to X . In formula, $X^* = \overline{\pi_2(\mathbf{CN}(X))} \subset (\mathbb{P}^d)^*$.

We collect some useful properties of dual varieties in the following proposition.

Proposition 1.2.16. Let $X \subset \mathbb{P}^d$ be a projective variety. Then

- (i) $\dim X^* \leq d - 1$;
- (ii) if X is a smooth hypersurface of degree δ , then $\deg X^* = \delta(\delta - 1)^{d-1}$;
- (iii) biduality: if X is irreducible, then $X^{**} = X$.

Remark 1.2.17. Throughout the thesis, we will usually talk about the dual variety of an affine variety $\mathcal{V}(I) \subset \mathbb{C}^d$. With this terminology we mean the following. Consider first the projective closure X of $\mathcal{V}(I)$, that is, the projective variety associated to the homogenization of I . We do this by identifying \mathbb{C}^d with the affine chart $\{[x_0, \dots, x_d] \in \mathbb{P}^d \mid x_0 = 1\}$. Then, compute the dual variety $X^* \subset (\mathbb{P}^d)^*$ and restrict it back to $\{x_0 = -1\}$. This is an affine variety $\mathcal{V}(I)^*$ that we will call the dual variety to $\mathcal{V}(I)$. The minus sign in the chart of the dual space is a consequence of the convention that we chose, to use outer normal vectors for the dual body.

Going back to convexity, we want to understand how the notions of dual convex body and dual variety combine. In order to deal with dual convex bodies, we make the assumption that $0 \in \text{int } K$ in the rest of the section. Krein-Milman Theorem 1.1.8 essentially says that, among boundary points, ‘it is enough’ to look at the extreme points of a convex body. In analogy, the next results will show that extreme points are sufficient also to describe the algebraic boundary. Denote by $\text{Ext}_a K$ the Zariski closure of the extreme points of the convex body K . Contrary to the algebraic boundary, this variety is not always a hypersurface, but it is a subvariety of $\partial_a K$. The following result is the affine version of [Sin15, Proposition 3.1, Theorem 3.3, Corollary 3.5].

Theorem 1.2.18. Let $K \in \mathcal{K}(\mathbb{R}^d)$ be full dimensional with the origin in its interior. Then

$$(\text{Ext}_a K)^* \subset \partial_a K^\circ \quad \text{and} \quad (\partial_a K)^* \subset \text{Ext}_a K^\circ.$$

Moreover, $(\partial_a K)^* = \text{Ext}_a K^\circ$.

For polytopes, $(\partial_a P)^*$ is a union of finitely many points, namely the vertices of P° . Also the opposite is true: $(\text{Ext}_a P^\circ)^* = \text{vertices}(P^\circ)^* = \partial_a P$, so we can recover the algebraic boundary of P . Similarly, consider the convex body K from Example 1.1.12. In this case $\text{Ext}_a K = \partial_a K = (\partial_a K^\circ)^* = (\text{Ext}_a K^\circ)^*$. So in general, we would like to apply a biduality argument to the equation in Theorem 1.2.18. Unfortunately, this cannot be done, since the algebraic boundary is not always irreducible. The variety $(\text{Ext}_a K^\circ)^*$ might miss some component of $\partial_a K$, as shown in the following example.

Example 1.2.19. Let K be the convex body from Example 1.1.7, displayed in Figure 1.1. Its dual body K° is shown in Figure 1.4. Its algebraic boundary is the union of three irreducible components:

$$\mathcal{V}(-y^2 + 2x + 1), \quad \mathcal{V}(-y^2 - 2x + 1), \quad \mathcal{V}(-2y - 1).$$

The Zariski closure of the extreme points of K° is the union of the two parabolas only. Hence $(\text{Ext}_a K^\circ)^* = \mathcal{V}((x \pm 1)^2 + y^2 - 1) \subsetneq \partial_a K$. \blacklozenge

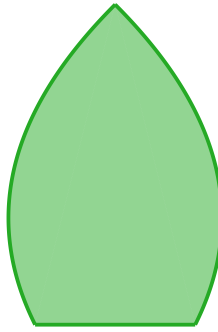


Figure 1.4: The convex body K° from Example 1.2.19. It is the dual body of K from Example 1.1.7, Figure 1.1.

Patches. We have seen in Section 1.1 that polytopes have always finitely many faces. They can be recorded via the f -vector, and give rise to many interesting problems in combinatorics. As soon as one leaves the family of polytopes, convex bodies have infinitely many faces. However, in the case of a semialgebraic convex body K , we can group together some of the faces in finitely many *patches*, to mimic the f -vector and describe ∂K as the union of finitely many pieces. In order for the patches to have ‘nice’ properties, the definition is unfortunately quite technical. It first appeared in [CKLS19a] and it was then exemplified in detail in [PSW21].

Given a projective variety $X \subset \mathbb{P}^d$, let the *biregular locus* of its conormal variety be the open submanifold

$$\mathbf{CN}_{\text{bireg}}(X) = \left\{ (x, u) \in \mathbb{P}^d \times (\mathbb{P}^d)^* \mid x \in X_{\text{reg}}, u \in (X^*)_{\text{reg}} \right\}.$$

There are two natural projections $\pi_1 : \mathbf{CN}_{\text{bireg}}(X) \rightarrow \mathbb{P}^d$ and $\pi_2 : \mathbf{CN}_{\text{bireg}}(X) \rightarrow (\mathbb{P}^d)^*$. By [PSW21, Theorem 1.7], if $0 \in \text{int } K$, the normal cycle $\mathbf{N}(K)$ is a compact semialgebraic set of pure dimension $d - 1$. We can (and will) here view it as a subset of $\mathbb{P}^d \times (\mathbb{P}^d)^*$, via the embedding of $\mathbb{R}^d \subset \mathbb{C}^d$ in \mathbb{P}^d as in Remark 1.2.17.

Definition 1.2.20. Let $K \in \mathcal{K}(\mathbb{R}^d)$ be full dimensional with the origin in its interior and denote by $X \subset \mathbb{P}^d$ the projective closure of $\partial_a K$. Let Y be an irreducible component of X . A *patch* of K (over Y) is a connected component of the semialgebraic subset of $\mathbf{N}(K) \cap \mathbf{CN}_{\text{bireg}}(Y) \subset \mathbb{P}^d \times (\mathbb{P}^d)^*$ consisting of pairs (x, u) such that x is not contained in any irreducible component of X other than Y .

A *closed patch* $\text{cl}(\mathsf{P})$ is intended to be the Euclidean closure of a patch P of K . Following [PSW21], we will denote the family of patches of K as $\mathscr{P}(K)$. This is a finite set. The assumptions in Definition 1.2.20 are essential to avoid pathological cases, as pointed out via many examples in [PSW21]. The following results are the affine versions of [PSW21, Lemma 2.11, Theorem 2.15].

Lemma 1.2.21. Let $K \in \mathcal{K}(\mathbb{R}^d)$ be full dimensional with the origin in its interior, then

$$\partial K = \bigcup_{\mathsf{P} \in \mathscr{P}(K)} \pi_1(\text{cl}(\mathsf{P})).$$

Theorem 1.2.22. Let $K \in \mathcal{K}(\mathbb{R}^d)$ be full dimensional with the origin in its interior and let P be a patch of K over an irreducible component Y of the projective closure of $\partial_a K$. Then

- (i) P is of pure projective dimension $d - 1$;
- (ii) $\pi_1(P)$ is open in ∂K and of pure projective dimension $d - 1$;
- (iii) $\pi_2(P)$ is an open semialgebraic subset of the real points of Y_{reg}^* . In particular it is of pure dimension $\dim Y^*$;
- (iv) given $u \in K^\circ$, let H be the hyperplane supporting K with outer normal u . Then the dimension of the face K^u is $d - \dim Y^*$, for all $u \in \pi_2(P)$. Furthermore, $\pi_1(P) \cap H$ is Zariski dense in K^u , for all $u \in \pi_2(P)$;
- (v) in the situation of (iv), the union of $\pi_1(P) \cap H$ over all patches P of K over Y is dense in K^u in the Euclidean topology.

Besides technicalities, the message is that the patches cover the topological boundary ∂K and that the faces of K that are grouped in the same patch have the same dimension. Moreover, the faces belonging to the same (closed) patch satisfy some continuity in the Hausdorff topology [PSW21, Lemma 2.19].

Example 1.2.23. We go back again to Example 1.1.7 and analyse the patches of K . The set $\mathcal{P}(K)$ consists of five patches: two open arcs

$$\begin{aligned} P_1 &= \left\{ (x, y) \in (-2, -1) \times \left(-\frac{4}{5}, 1 \right) \mid (x + 1)^2 + y^2 = 1 \right\}, \\ P_2 &= \left\{ (x, y) \in (1, 2) \times \left(-\frac{4}{5}, 1 \right) \mid (x - 1)^2 + y^2 = 1 \right\}, \end{aligned}$$

and three open line segments

$$\begin{aligned} P_3 &= \left\{ (x, y) \in (-1, 1) \times \{1\} \right\}, \\ P_4 &= \left\{ (x, y) \in \left(-\frac{8}{5}, 0 \right) \times \left(-2, -\frac{4}{5} \right) \mid 3x + 4y + 10 = 0 \right\}, \\ P_5 &= \left\{ (x, y) \in \left(0, \frac{8}{5} \right) \times \left(-2, -\frac{4}{5} \right) \mid 3x - 4y - 10 = 0 \right\}. \end{aligned}$$

Thus, there are two patches of 0-dimensional faces and three patches of 1-dimensional faces. They cover ∂K except for five points: the intersection points of two irreducible components of the algebraic boundary, excluded from the patches by definition. As predicted, we can recover the whole topological boundary by taking the closure of the P_i 's. \blacklozenge

Chapter 2

Zonoids

Zonoids are limits, in the Hausdorff metric, of zonotopes [Bol69]. The latter are finite Minkowski sums of line segments. They are relatively well-understood: for instance, it is known that a polytope is a zonotope if and only if all its 2-dimensional faces are (translates of) centrally symmetric polygons [Bol69,Sch70]. This lies in the context of the *Zonoid Problem*, introduced in [Bol71], but already appearing in [Bla23]: this problem consists in determining whether a given convex body is a zonoid. These special convex sets play an important role in convex geometry, measure theory, functional analysis and random geometry [Bol69,SW83,Vit91,GW93]. More recently, connections to enumerative geometry and real intersection theory were drawn [BL16], which led to the introduction of the zonoid algebra in [BBLM22] as a probabilistic version of cohomology. A simple geometric characterization of zonoids seems hopeless, and in full generality even the decidability of the Zonoid Problem is not understood. Restricting to the subclass of semialgebraic convex bodies would potentially make the problem easier. For instance, in the algebraic setting, the rigidity of the Zariski topology implies that global properties can be checked locally.

Discotopes form a special subclass of semialgebraic zonoids, discussed in [GM21]. They were introduced in [AS16] for the combinatorial study of matroids associated to subspace arrangements. They appeared in the context of convex geometry in [MM21], which will be analysed in Section 3.1. Discotopes are a first possible generalization of zonotopes, still amenable to be studied with tools from algebra, geometry and combinatorics. They are finite Minkowski sums of higher dimensional discs: from this point of view, zonotopes correspond to the special case of 1-dimensional discs.

We introduce zonoids in Section 2.1, exploit some basic properties and characterizations to connect them to measure theory and probability. Section 2.1.1 presents the formal definition of discotopes. We then focus on the facial structure of zonoids and in particular discotopes, in Section 2.1.2. Section 2.2 focuses on the algebraic boundary of discotopes. We introduce a particular subvariety \mathcal{S} of their algebraic boundary, central in the rest of the chapter. Section 2.2.1 provides a full characterization of \mathcal{S} in a special range. Section 2.2.2 describes its role in the geometry of the exposed points of the discotope. In Section 2.2.3, we study discotopes that are Minkowski sums of 2-dimensional discs; we prove that in this case \mathcal{S} is an irreducible hypersurface and provide an upper bound for its degree. As a by-product of this result, we prove that certain non-generic linear sections of the classical determinantal variety are irreducible and of the expected dimension. We conclude the section with an important example, the dice, which presents peculiar birational properties. Finally, in Section 2.2.4, we propose some open problems and conjectures: in particular, Conjecture 2.2.22 predicts that the variety \mathcal{S} is irreducible under minimal assumptions.

2.1. Zonoids and their problems

One of the operations that we can use on the space of convex bodies is the Minkowski sum. We thus fix some points $z_{1,1}, z_{1,2}, \dots, z_{n,1}, z_{n,2} \in \mathbb{R}^d$ and consider

$$Z = \sum_{i=1}^n [z_{i,1}, z_{i,2}].$$

This object, namely the Minkowski sum of finitely many line segments, is called *zonotope*. If $z_{i,1} = -z_{i,2}$ for all i , then Z is said to be *centered*, and given any zonotope we can always translate it to make it centered. Since we are interested in the geometry of such a convex body, we can restrict to study centered zonotopes. Therefore, from now on, we will drop the word ‘centered’ for simplicity. Zonotopes are in particular polytopes that satisfy $Z = -Z$, i.e. they are *centrally symmetric* polytopes centered at the origin. There is in fact a neat procedure to check if a given polytope is a zonotope.

Theorem 2.1.1. A polytope P is a zonotope if and only if all the two-dimensional faces of P are centrally symmetric polytopes.

For instance, all two-dimensional centrally symmetric polytopes are zonotopes. This is not true in higher dimension: the octahedron $P \subset \mathbb{R}^3$ is centrally symmetric, but its two-dimensional faces are triangles. Hence it is not a zonotope.

Definition 2.1.2. A *zonoid* is a limit, in the Hausdorff topology, of zonotopes.

We can interpret zonoids as an infinite Minkowski sum of line segments, or as those convex bodies that can be approximated by zonotopes. In particular, zonoids are centrally symmetric convex bodies. In order for a zonoid to be a polytope, it must be a zonotope. Regarding operations and constructions that we introduced in the first chapter, the family of zonoids is closed under Minkowski sum and scalar multiplication. On the other hand, the dual body of a zonoid is not necessarily a zonoid.

Example 2.1.3. Let $P = [-1, 1]^4$ be the four-dimensional cube centered at the origin. Let P° be its dual polytope, as in Example 1.1.13. The cube P is a zonotope, indeed

$$\begin{aligned} P = & [(-1, 0, 0, 0), (1, 0, 0, 0)] + [(0, -1, 0, 0), (0, 1, 0, 0)] \\ & + [(0, 0, -1, 0), (0, 0, 1, 0)] + [(0, 0, 0, -1), (0, 0, 0, 1)]. \end{aligned}$$

On the other hand, all the 32 two-dimensional faces of P° are triangles, hence they are not centrally symmetric, hence P° is not a zonotope. ◆

Example of zonoids that are not polytopes are the unit ball in \mathbb{R}^d and L^p balls in \mathbb{R}^2 and also in \mathbb{R}^d when $d \geq 3$ and $2 \leq p \leq \infty$ [Bol69, Theorem 6.6]. However, not all zonoids are semialgebraic, as we will see in Example 3.1.35.

Remark 2.1.4. In definition 2.1.2, it is not necessary that the zonotopes are centered. With this condition we actually obtain centered zonoids. Otherwise, we would get more general convex bodies, that up to translation are centered zonoids. As for the case of zonotopes, since we are interested in the geometry of these objects, that does not depend on translations, we will reduce to the family of centered zonoids, and we will drop the word ‘centered’ for simplicity.

Central in the literature on zonoids is the study of the following inclusion:

$$\{ \text{zonoids} \} \subset \{ \text{centrally symmetric convex bodies} \}.$$

This inclusion becomes an equality in \mathbb{R}^2 , but it is a strict inclusion in \mathbb{R}^d for $d > 2$. More precisely, zonoids are nowhere dense in the set of centrally symmetric convex bodies, since having a triangular face is enough for not being a zonoid. So a natural question arises:

How to recognize a zonoid?

More precisely, given a centrally symmetric convex body, how can we check whether it is a zonoid or not? Theorem 2.1.1 gives the answer to the question in the case when the given convex body is a polytope. In the general case, this question is known as the *Zonoid Problem*. It is a very hard problem for many reasons. As shown in [Wei77], being a zonoid is not a local property. Indeed, for every convex body K , and every point p of its boundary ∂K , there exists a zonoid whose support function coincides with the support function of K in a neighborhood of p . Moreover, in [Wei82], it was shown that being a zonoid is not a property characterized by projections: there exist convex bodies which are not zonoids but such that all their projections are zonoids. Also restricting to smaller subclasses of zonoids is not a big improvement: the zonoid problem is open even in the simplest non-trivial case of semialgebraic convex bodies in \mathbb{R}^3 , see e.g. [Stu21, Problem 12]. However, a positive result is given in [LM22], where the authors prove the tameness of a particular class of semialgebraic zonoids. More precisely, they study the set of zonoids defined by $\{p(x) \geq 0\}$ as a subset of the set of convex bodies with an analogous definition, where p is a polynomial of a given degree and number of unknowns. [LM22, Theorem 1] states that this family of zonoids is definable over a certain o-minimal structure.

If geometrically we do not really know what zonoids look like, from a more analytic point of view there are some ways to characterize zonoids. These identify their support functions. We outline two possible directions here, one connected to measures in the sphere and the other with a probabilistic flavour.

Theorem 2.1.5. Let $K \in \mathcal{K}(\mathbb{R}^d)$. It is a zonoid if and only if its support function can be written as

$$h_K(u) = \int_{S^{d-1}} |\langle u, x \rangle| d\rho(x)$$

where ρ is an even measure on S^{d-1} .

By a measure on the sphere we mean a real-valued σ -additive nonnegative function on the σ -algebra of Borel sets of the sphere. It is even if it is invariant under reflections with respect to the origin. In the setting of Theorem 2.1.5, which is [Sch13, Theorem 3.5.3], ρ is sometimes called the *generating measure* of K . It can be also proved that there is a one to one correspondence between convex bodies and their generating measures [Sch13, Theorem 3.5.4]. For instance, the generating measure of a zonotope is concentrated in finitely many points. At the opposite side, a constant ρ is the generating function of a ball.

Richard Vitale on the other hand in [Vit91] characterizes zonoids using random vectors. Let $X \in \mathbb{R}^d$ be a random vector and assume that the expectation $\mathbb{E}\|X\|$ is finite, then the function

$$\frac{1}{2}\mathbb{E}|\langle u, X \rangle| \tag{2.1.1}$$

is well defined, with values in \mathbb{R} , and sublinear. The following is [Vit91, Theorem 3.1].

Theorem 2.1.6. A convex body $K \in \mathcal{K}(\mathbb{R}^d)$ is a zonoid if and only if there exists a random vector $X \in \mathbb{R}^d$ with $\mathbb{E}\|X\| < \infty$ such that $h_K(u)$ is given by (2.1.1).

We will sometimes call such a zonoid the *Vitale zonoid* associated to the random vector X , and denote it by $K(X)$. It is easy to see that different random vectors are associated to the same zonoid. Indeed, let λ be a random variable with $\mathbb{E}|\lambda| = 1$. Then

$K(X) = K(\lambda X)$, provided that λ and X are independent [BBLM22, Lemma 2.7]. For the zonotope $Z = \sum_{i=1}^n [-z_i, z_i]$, consider the random vector X that takes value nz_i with probability $1/n$; then $K(X) = Z$. In the case in which X is a centered Gaussian vector, $K(X)$ is a ball. For details we refer to [BBLM22]. In that work the authors introduce the *zonoid algebra* via the definition of the wedge product of zonoids. This allows to generalize Vitale's formula for the expectation of the absolute value of the determinant of a random matrix, in terms of mixed volumes. As the authors point out, the fact that the characterization given by Theorem 2.1.6 is not one to one is not a disadvantage, but a feature.

2.1.1. Discotopes

Since semialgebraic zonoids are already complicated, we restrict now to a subclass of objects called *discotopes*. If a zonotope is a Minkowski sum of one-dimensional discs, a discotope is the Minkowski sum of discs, with no requirements on their dimension. This allows to generalize the well understood family of zonotopes in a way that preserves some combinatorial properties.

Fix $n, d \in \mathbb{N}$, $n \leq d$, and let $\mathcal{B} := \{b_1, \dots, b_n\}$ be a set of linearly independent vectors of \mathbb{R}^d . Denote by $A_{\mathcal{B}} : \mathbb{R}^n \rightarrow \mathbb{R}^d$ the linear map mapping the i -th standard basis element e_i of \mathbb{R}^n to b_i . The *generalized disc* $D_{\mathcal{B}}$ is the image of the unit ball B^n via $A_{\mathcal{B}}$. Throughout this chapter, generalized discs are simply called discs.

The topological boundary $\partial D_{\mathcal{B}}$ is a real algebraic hypersurface in the linear span $\langle \mathcal{B} \rangle$: its ideal is defined by $d - n$ linear forms determining $\langle \mathcal{B} \rangle$ and a single inhomogeneous quadric $q_{\mathcal{B}} - 1$, where $q_{\mathcal{B}}$ is the quadratic form associated to the matrix $(A_{\mathcal{B}})(A_{\mathcal{B}})^T$. In particular, generalized discs are semialgebraic sets.

Remark 2.1.7. For every d and every choice of \mathcal{B} , the generalized disc $D_{\mathcal{B}}$ is a zonoid. This is immediate from the fact that linear images of zonoids are zonoids [Bol69, Lemma 1.4]. In particular for $d = 1$, generalized discs are all the compact segments centered at the origin; for higher d , generalized discs are ellipsoids centered at the origin.

Definition 2.1.8. Given the generalized discs $D_{\mathcal{B}_1}, \dots, D_{\mathcal{B}_N}$ in \mathbb{R}^d , the *discotope* $\mathcal{D}_{\mathfrak{B}}$ associated to $\mathfrak{B} = \{\mathcal{B}_j \mid j = 1, \dots, N\}$ is their Minkowski sum

$$\mathcal{D}_{\mathfrak{B}} = D_{\mathcal{B}_1} + \dots + D_{\mathcal{B}_N}.$$

Write $D_i := D_{\mathcal{B}_i}$ if no confusion arises. Let N_m be the number of discs of dimension m among D_1, \dots, D_N . The *type* of the discotope $\mathcal{D}_{\mathfrak{B}}$ is the integer vector $\mathbf{N} = (N_1, \dots, N_d) \in \mathbb{N}^d$. Note that $N = \sum N_m$.

Usually, we will be interested in the case where the sets \mathcal{B}_j are chosen generically. More precisely, we say that a property holds for the *generic discotope* of type \mathbf{N} if the sets \mathfrak{B} for which it does not hold form a proper Zariski closed subset of the set of all possible bases.

In the case $\mathbf{N} = (N, 0, \dots, 0)$, all the generalized discs are segments centered at the origin: the associated discotope is a zonotope centered at the origin [Zie12, Section 7.3]. The case $\mathbf{N} = (0, N, 0)$ of discotopes in \mathbb{R}^3 was studied in [MM21] in the context of fiber convex bodies, as we will see in Section 3.1. In [AS16], discs of higher dimensions were considered, suitably rescaled so that their volume is normalized.

Discotopes can be realized as the image of the addition map restricted to the product

of the discs. More precisely, define Σ to be the (complex) *addition map*

$$\begin{aligned}\Sigma : (\mathbb{C}^d)^N &\rightarrow \mathbb{C}^d \\ (\xi_j)_{j=1,\dots,N} &\mapsto \sum \xi_j.\end{aligned}$$

Then, the discotope \mathcal{D} associated to \mathfrak{B} is the image of $\prod_j D_j \subseteq (\mathbb{R}^d)^N$ under Σ . In particular, the projection theorem for semialgebraic sets, Theorem 1.2.2, guarantees that \mathcal{D} is semialgebraic.

Since Minkowski sums of zonoids are zonoids, every discotope is a zonoid. In particular, discotopes form a class of semialgebraic zonoids and one may wonder whether all semialgebraic zonoids arise in this way. This is not the case. An example of a semialgebraic zonoid which is not a discotope is the unit ball of the L^4 -norm $\{x_1^4 + x_2^4 \leq 1\}$ in \mathbb{R}^2 : indeed, there is no discotope in \mathbb{R}^2 whose boundary is an irreducible curve of degree 4, see Remark 2.2.18.

We point out that a discotope is full dimensional if and only if $\sum_j \langle \mathcal{B}_j \rangle = \mathbb{R}^d$. In particular, a necessary condition for this to happen is that $\sum_1^d m N_m \geq d$. For a generic discotope this condition is also sufficient. We always assume that \mathcal{D} is full dimensional: this is not restrictive as one can always restrict the analysis to the linear span $H = \sum_j \langle \mathcal{B}_j \rangle = \langle \mathcal{D} \rangle$.

2.1.2. The faces of a zonoid

In the case of zonoids, as Bolker points out [Bol69], there is a nice recipe to construct a face. Indeed, given a zonoid K every proper face $F \subset K$ is a zonoid of lower dimension which is a summand of K , i.e., there exists another zonoid K' such that $K = K' + F$.

We can examine this relation in more details for discotopes. Consider the discotope $\mathcal{D} = D_1 + \dots + D_N$. For every disc D_j , let $C_j = S^{d-1} \cap \langle D_j \rangle^\perp$, that is the unit sphere of dimension $d - \dim D_j - 1$ consisting of directions orthogonal to D_j . Let $\mathcal{U} = S^{d-1} \setminus \left(\bigcup_j C_j \right)$, which is Zariski open in S^{d-1} . If $u \in \mathcal{U}$, then for every disc D_j the face D_j^u exposed by u is a single point.

As a consequence, if $u \in \mathcal{U}$, then the face of the discotope \mathcal{D}^u consists of a single point. To see this, let $p = \sum \xi_j \in \mathcal{D}^u$ be a point of the face exposed by u . Then

$$h_{\mathcal{D}}(u) = \langle u, p \rangle = \sum_j \langle u, \xi_j \rangle > \sum_j \langle u, \tilde{\xi}_j \rangle$$

for any other $\tilde{\xi}_j \in D_j$. Therefore $\mathcal{D}^u = \{p\}$ and hence p is an exposed point of \mathcal{D} .

On the other hand if $u \notin \mathcal{U}$, let $J \subseteq \{1, \dots, N\}$ be the maximal subset of indices such that $u \in \bigcap_{j \in J} C_j$; then u^\perp contains $\sum_{j \in J} \langle \mathcal{B}_j \rangle$. In this case the face of \mathcal{D} exposed by u is (a properly translated copy of) a smaller discotope \mathcal{D}' , given by the Minkowski sum of the discs D_j for $j \in J$. In general, the exposed faces of \mathcal{D} of dimension k are given by

$$\sum_{j \in J} D_j + \sum_{i \notin J} \{p_i\}$$

where $p_i \in \partial D_i$ are suitable points and J is such that $\dim(\sum_{j \in J} \langle \mathcal{B}_j \rangle) = k$.

Remark 2.1.9. A discotope \mathcal{D} of type $\mathbf{N} = (N_1, \dots, N_d)$ is the Minkowski sum of a zonotope \mathcal{Z} given by N_1 segments and a discotope \mathcal{D}' of type $(0, N_2, \dots, N_d)$:

$$\mathcal{D} = \mathcal{Z} + \mathcal{D}'.$$

Since the convex hull of a Minkowski sum equals the Minkowski sum of convex hulls, the discotope \mathcal{D} is the convex hull of copies of \mathcal{D}' placed at the vertices of \mathcal{Z} . As a consequence, many of the geometric properties of \mathcal{D} only depend on analogous properties of \mathcal{D}' . For instance, the algebraic study of extreme points of \mathcal{D} can be reduced to the one of extreme points of \mathcal{D}' . This can be visualized in the following example.

Example 2.1.10. Let D_1, D_2, D_3 be the discs in \mathbb{R}^3 defined by

$$\begin{aligned} D_1 &= \{(x_1, x_2, x_3) : x_3 = 0, -1 \leq x_1 = x_2 \leq 1\}, \\ D_2 &= \{(x_1, x_2, x_3) : x_1 = 0, x_2^2 + x_3^2 \leq 1\}, \\ D_3 &= \{(x_1, x_2, x_3) : x_2 = 0, x_1^2 + x_3^2 \leq 1\}. \end{aligned}$$

Consider the associated discotope $\mathcal{D} = D_1 + D_2 + D_3$, shown in Figure 2.1, left. Faces of dimension 0, 1 and 2 are represented in red, green and blue, respectively. The red points are exposed and arise as $\xi_1 + \xi_2 + \xi_3$, for certain $\xi_i \in \partial D_i$. Every green segment arises as $D_1 + \xi_2 + \xi_3$, for certain $\xi_i \in \partial D_i$. The four blue discs (only two of which are visible) come in pairs: two are obtained as $\xi_1 + D_2 + \xi_3$ and the other two as $\xi_1 + \xi_2 + D_3$, for certain $\xi_i \in \partial D_i$. As observed in Remark 2.1.9, $\mathcal{D} = \mathcal{Z} + \mathcal{D}'$ where $\mathcal{Z} = D_1$ is a zonotope

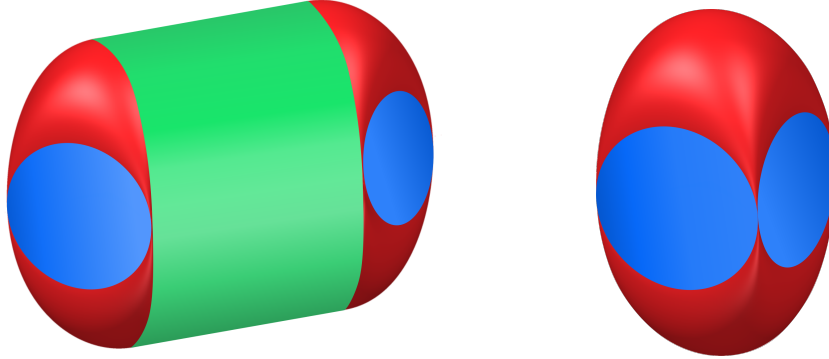


Figure 2.1: Left: a discotope of type $\mathbf{N} = (1, 2, 0)$. Right: a discotope of type $\mathbf{N} = (0, 2, 0)$. Faces of dimension 0 are in red, faces of dimension 1 are in green and faces of dimension 2 are in blue.

and $\mathcal{D}' = D_2 + D_3$ is a discotope with $N_1 = 0$, shown in Figure 2.1, right. The algebraic boundary $\partial_a \mathcal{D}'$ consists of five irreducible components: four planes and the quartic surface

$$\mathcal{S} = \mathcal{V}(x_1^4 - 2x_1^2x_2^2 + x_2^4 + 2x_1^2x_3^2 + 2x_2^2x_3^2 + x_3^4 - 4x_3^2).$$

The latter is the Zariski closure of the set of extreme points of \mathcal{D}' , namely $\text{Ext}_a \mathcal{D}'$. Instead, $\text{Ext}_a \mathcal{D}$ is the union of two copies of \mathcal{S} , translated by the extrema of the segment D_1 , i.e., the vectors $\pm(1, 1, 0)$. \blacklozenge

2.2. The geometry of discotopes

In this section, we investigate the algebraic boundary of discotopes. In order to do that, we introduce a complex algebraic variety associated to a discotope, called its purely nonlinear part, which will be the main object of study in the rest of the chapter.

Definition 2.2.1. Let $\mathcal{D}^\partial = \Sigma(\prod_j \partial D_j) \subseteq \mathcal{D}$. The *purely nonlinear part* of \mathcal{D} is

$$\mathcal{S} = \overline{\mathcal{D}^\partial \cap \partial \mathcal{D}},$$

the Zariski closure of $\mathcal{D}^\partial \cap \partial\mathcal{D}$ in \mathbb{C}^d .

By definition if $p \in \text{Ext } \mathcal{D}$, then $p \in \mathcal{S}$. Therefore, by the Krein–Milman Theorem [Bar02, Section II.3], we have $\mathcal{D} = \text{conv}(\mathcal{S} \cap \partial\mathcal{D})$.

In particular, \mathcal{S} carries all the information regarding the extreme points of \mathcal{D} . In general, the variety \mathcal{S} may have several irreducible components, possibly of different dimension. In fact, it is a priori not clear whether \mathcal{S} coincides with $\text{Ext}_a \mathcal{D}$. We will prove some results in this direction in Section 2.2.2. In particular, Corollary 2.2.11 guarantees that when the discs are chosen generically, \mathcal{S} has dimension $d - 1$ (possibly with lower dimensional components) in \mathbb{C}^d if and only if the following non-degeneracy condition holds:

$$\sum_{m=1}^d (m-1)N_m \geq d-1. \quad (2.2.1)$$

Notice that this condition implies the non-degeneracy condition $\sum_1^d mN_m \geq d$ for the discotope, and it is immediately satisfied if $N_d \geq 1$.

Remark 2.2.2. In the special case of discotopes of type $\mathbf{N} = (0, \dots, 0, N)$, all the boundary points of \mathcal{D} are exposed and therefore \mathcal{S} coincides with $\text{Ext}_a \mathcal{D}$. Further, $\partial\mathcal{D}$ is smooth (see, e.g., [BJ17]), which guarantees that \mathcal{S} is irreducible: indeed, if it was reducible, any two irreducible components would intersect on $\partial\mathcal{D}$, in contradiction with its smoothness. Figure 2.2 shows a discotope \mathcal{D} obtained as the sum of three ellipses in \mathbb{R}^2 . The topological boundary $\partial\mathcal{D}$ is smooth and coincides with one of the connected components of the real locus of $\partial_a \mathcal{D}$. These properties are further discussed in Section 2.2.3.

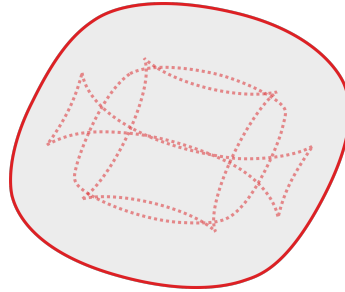


Figure 2.2: A discotope of type $\mathbf{N} = (0, 3)$. Its algebraic boundary is an irreducible curve of degree 24. The dashed curves represent the real points of the algebraic boundary that are not part of the topological boundary of \mathcal{D} .

2.2.1. Joins of quadrics

If (2.2.1) holds with the reverse inequality, then we characterize the purely nonlinear part \mathcal{S} as an affine version of the geometric join of the quadrics $\partial_a D_i$. The theory is developed classically in the projective setting, see, e.g., [Rus16, Chapter 1] and [FOV99]. In this section we translate some of these projective notions to the affine space and apply them to \mathcal{S} .

Given two (complex) projective varieties $X, Y \subseteq \mathbb{P}^d$, their join is the projective variety $J(X, Y) = \{p \in \langle x, y \rangle : x \in X, y \in Y\}$. We are concerned with the properties of the join summarized in the following lemma, which is a consequence of [Har92, Example 18.17].

Lemma 2.2.3. Let $X, Y \subseteq \mathbb{P}^d$ be irreducible varieties. Then $J(X, Y)$ is irreducible. If $X \cap Y = \emptyset$ then $\dim J(X, Y) = \dim X + \dim Y + 1$. Furthermore, if $\dim X + \dim Y + 1 < d$, then $\deg(J(X, Y)) = \deg(X) \deg(Y)$.

We prove an affine version of Lemma 2.2.3, which will be useful to prove Theorem 2.2.5 below. Regard the affine space \mathbb{C}^d as an affine open subset of \mathbb{P}^d : for an affine variety $X \subseteq \mathbb{C}^d$, write $\mathbb{X} \subseteq \mathbb{P}^d$ for its projective closure and $X_\infty = \mathbb{X} \setminus X$ for its *hyperplane cut at infinity*. Given two affine varieties $X, Y \subseteq \mathbb{C}^d$, we say that X, Y do not intersect at infinity if $X_\infty \cap Y_\infty = \emptyset$. For two varieties $X, Y \subseteq \mathbb{C}^d$, write $\Sigma(X \times Y) = \overline{X + Y}$ for the Zariski closure of their Minkowski sum: this can be regarded as an affine version of the geometric join.

Proposition 2.2.4. Let $X, Y \subseteq \mathbb{C}^d$ be irreducible affine varieties, not intersecting at infinity and such that $\dim X + \dim Y < d$. Then $\Sigma(X \times Y)$ is irreducible, $\dim \Sigma(X \times Y) = \dim X + \dim Y$ and $\deg \Sigma(X \times Y) = \deg(X) \deg(Y)$.

Proof. The variety $\Sigma(X \times Y)$ is the closure of the image of the addition map $\Sigma : X \times Y \rightarrow \mathbb{C}^d$ defined by $\Sigma(x, y) = x + y$. Since X, Y are irreducible, $\Sigma(X \times Y)$ is irreducible as well.

Let Z, Z' be two 1-dimensional vector spaces and consider $\mathbb{P}^{d+1} = \mathbb{P}(\mathbb{C}^d \oplus Z \oplus Z')$ with homogeneous coordinates x_1, \dots, x_d, z, z' . Reembed X, Y in \mathbb{P}^{d+1} as follows:

$$\begin{array}{ll} X & \rightarrow \mathbb{P}^{d+1} \\ x & \mapsto (x, 1, 0), \end{array} \quad \begin{array}{ll} Y & \rightarrow \mathbb{P}^{d+1} \\ y & \mapsto (y, 0, 1); \end{array}$$

denote by \mathbb{X}, \mathbb{Y} the closures (in the Zariski topology of \mathbb{P}^{d+1}) of the two images.

Observe that \mathbb{X}, \mathbb{Y} are disjoint. Indeed, if $p \in \mathbb{X} \cap \mathbb{Y}$, then in coordinates one has $z(p) = z'(p) = 0$; hence p belongs to the intersection $X_\infty \cap Y_\infty$ of the two hyperplane cuts at infinity, which is empty by hypothesis. Therefore $\mathbb{X} \cap \mathbb{Y} = \emptyset$. By Lemma 2.2.3, $J(\mathbb{X}, \mathbb{Y})$ is irreducible, with $\dim J(\mathbb{X}, \mathbb{Y}) = \dim \mathbb{X} + \dim \mathbb{Y} + 1$. Moreover, since $\dim \mathbb{X} + \dim \mathbb{Y} + 1 < d + 1$, we obtain $\deg J(\mathbb{X}, \mathbb{Y}) = \deg(\mathbb{X}) \deg(\mathbb{Y})$.

Now, one can check explicitly in coordinates that

$$\Sigma(X \times Y) = J(\mathbb{X}, \mathbb{Y}) \cap \{z = z' \neq 0\};$$

in other words, $\Sigma(X \times Y)$ is an affine chart of the hyperplane section $\{z = z'\}$ of $J(\mathbb{X}, \mathbb{Y})$. Note that $J(\mathbb{X}, \mathbb{Y}) \cap \{z = z'\}$ is irreducible. To see this, observe that in the affine chart $\{z \neq 0\}$ it coincides with $\Sigma(X \times Y)$ which is irreducible; therefore other irreducible components would be supported at $z = z' = 0$. However, there is no line $L = \langle x, y \rangle$ with $x \in \mathbb{X}$ and $y \in \mathbb{Y}$ such that $L \cap \{z = z' = 0\} \neq \emptyset$, unless $x \in X_\infty$ or $y \in Y_\infty$. This shows that $J(\mathbb{X}, \mathbb{Y}) \cap \{z = z' = 0\} = J(X_\infty, Y_\infty)$. Since

$$\dim J(X_\infty, Y_\infty) \leq \dim X_\infty + \dim Y_\infty + 1 = \dim J(\mathbb{X}, \mathbb{Y}) - 2,$$

$J(X_\infty, Y_\infty)$ is not an irreducible component of a hyperplane section of $J(\mathbb{X}, \mathbb{Y})$. This proves that $J(\mathbb{X}, \mathbb{Y}) \cap \{z = z'\}$ is irreducible, hence its affine chart on $\{z = z' \neq 0\}$ is irreducible as well. We conclude

$$\begin{aligned} \dim \Sigma(X \times Y) &= \dim J(\mathbb{X}, \mathbb{Y}) - 1 = \dim X + \dim Y, \\ \deg \Sigma(X \times Y) &= \deg J(\mathbb{X}, \mathbb{Y}) = \deg(X) \deg(Y). \end{aligned}$$

□

Applying Proposition 2.2.4 iteratively to the boundaries of the discs defining the discotope, we obtain the following result.

Theorem 2.2.5. Let $\mathbf{N} = (0, N_2, \dots, N_d) \subseteq \mathbb{N}^d$ be such that $\sum_{m=1}^d (m-1)N_m \leq d-1$. Let \mathcal{D} be a generic discotope in \mathbb{R}^d of type \mathbf{N} . Then \mathcal{S} is irreducible of degree 2^N , where $N = \sum N_m$.

Proof. Let D_1, \dots, D_N be the discs defining the discotope and let $d_i = \dim \langle D_i \rangle$; in particular $\dim \partial_a D_i = d_i - 1$. For $n = 1, \dots, N$, let

$$X_n = \Sigma \left(\prod_{i=1}^n \partial_a D_i \right).$$

First notice $X_N = \mathcal{S}$. The inclusion $\mathcal{S} \subseteq X_N$ is clear by the definition of \mathcal{S} . For the other inclusion, we show that there is a (real) Euclidean open subset $U \subseteq \prod \partial D_i$ such that $\Sigma(U) \subseteq \mathcal{S}$; passing to the Zariski closure we obtain the equality. Let $\xi = (\xi_1, \dots, \xi_N) \in \prod \partial D_i$, and for every i write $T_{\xi_i} \partial D_i$ for the (real) tangent space at ξ_i ; note $\dim T_{\xi_i} \partial D_i = d_i - 1$, hence $\langle T_{\xi_i} \partial D_i : i = 1, \dots, N \rangle$ is a proper linear subspace of \mathbb{R}^d . Let $u \in \mathbb{R}^d$ be a unit vector such that the hyperplane u^\perp contains $\langle T_{\xi_i} \partial D_i : i = 1, \dots, N \rangle$. Up to replacing ξ_i with $-\xi_i$, assume $\langle u, \xi_i \rangle \geq 0$. Let $p = \Sigma(\xi) = \xi_1 + \dots + \xi_N$. By definition $p \in X_N$; moreover $p \in \partial \mathcal{D}$, because

$$\langle u, p \rangle = \sum_{i=1}^N \langle u, \xi_i \rangle \geq \sum_{i=1}^N \langle u, \tilde{\xi}_i \rangle = \langle u, \tilde{p} \rangle$$

for any other point $\tilde{p} = \tilde{\xi}_1 + \dots + \tilde{\xi}_N$ of \mathcal{D} . This shows that p belongs to the face of \mathcal{D} exposed by u , and in particular to the boundary of \mathcal{D} . Therefore $p \in \mathcal{S}$. We conclude that $X_N = \mathcal{S}$.

Next, we show that for every n , X_{n-1} and $\partial_a D_n$ have no intersection at infinity, for a generic choice of the discs. Having empty intersection at infinity is an open condition on the parameter space of the embeddings of the discs; hence, in order to show that there is no intersection at infinity for a generic choice of embeddings, it suffices to exhibit a choice for which this property is verified.

By assumption, $\sum_1^N (d_i - 1) \leq d - 1$; let $\delta = \max\{0, (\sum_1^N d_i) - d\}$ and notice $\delta \leq N - 1$. Then, one can choose the embeddings of D_1, \dots, D_N so that the following properties hold:

- if $n = 1, \dots, \delta + 1$, then $\dim(\langle D_1, \dots, D_{n-1} \rangle \cap \langle D_n \rangle) = \dim(\langle D_{n-1} \rangle \cap \langle D_n \rangle) = 1$,
- if $n = \delta + 2, \dots, N$, then $\langle D_1, \dots, D_{n-1} \rangle \cap \langle D_n \rangle = 0$.

With this choice of embeddings, we show that for every n , X_{n-1} and $\partial_a D_n$ have no intersection at infinity. Write $X_{n-1, \infty}$ and $\partial_a D_{n, \infty}$ for the two components at infinity; they are subvarieties of $\mathbb{P}(\langle D_1, \dots, D_n \rangle)$. Their intersection is a subvariety of $\mathbb{P}(\langle D_1, \dots, D_{n-1} \rangle) \cap \mathbb{P}(\langle D_n \rangle) = \mathbb{P}(\langle D_{n-1} \rangle \cap \langle D_n \rangle)$. If $n \leq \delta + 1$, $\mathbb{P}(\langle D_{n-1} \rangle \cap \langle D_n \rangle)$ is a single point, and such point does not belong to $\partial_a D_{n, \infty}$; if $n \geq \delta + 2$, then $\mathbb{P}(\langle D_{n-1} \rangle \cap \langle D_n \rangle)$ is empty. This proves the claim.

To conclude, we use induction on n to show that $\dim X_n = \sum_{i=1}^n (d_i - 1)$ and $\deg X_n = 2^n$. The statement is clear for $n = 1$. Assume $n \geq 2$. We have $X_n = \Sigma(X_{n-1} \times \partial_a D_n)$. Since X_{n-1} and $\partial_a D_n$ do not intersect at infinity, Proposition 2.2.4 applies, hence

$$\begin{aligned} \dim X_n &= \dim X_{n-1} + \dim \partial_a D_n = \sum_{i=1}^{n-1} (d_i - 1) + (d_n - 1) = \sum_{i=1}^n (d_i - 1), \\ \deg X_n &= \deg X_{n-1} \cdot \deg \partial_a D_n = 2^{n-1} \cdot 2 = 2^n. \end{aligned}$$

For $n = N$, we obtain the desired result for \mathcal{S} . □

Example 2.2.6. Consider the following discs in \mathbb{R}^6 :

$$\begin{aligned} D_1 &= \{(x_1, \dots, x_6) : x_3 = x_4 = x_5 = x_6 = 0, x_1^2 + x_2^2 \leq 1\}, \\ D_2 &= \{(x_1, \dots, x_6) : x_1 = x_2 = x_5 = x_6 = 0, x_3^2 + x_4^2 \leq 1\}, \\ D_3 &= \{(x_1, \dots, x_6) : x_1 - x_3 = x_2 = x_4 = 0, (x_1 + x_3)^2 + x_5^2 + x_6^2 \leq 1\}. \end{aligned}$$

Let $\mathcal{D} = D_1 + D_2 + D_3$. This discotope is full dimensional but the condition (2.2.1) holds with reverse inequality: indeed, $1 + 1 + 2 < 5$. Thus, by Theorem 2.2.5, $\mathcal{S} = \overline{\partial_a D_1 + \partial_a D_2 + \partial_a D_3}$ is irreducible, of codimension 2 and degree 8. Its ideal is generated by one cubic and three quartic polynomials:

$$\begin{aligned} &4x_1^2x_3 + 4x_2^2x_3 - 4x_1x_3^2 - 4x_1x_4^2 + x_1x_5^2 - x_3x_5^2 + x_1x_6^2 - x_3x_6^2 + 3x_1 - 3x_3, \\ &16x_3^4 + 32x_3^2x_4^2 + 16x_4^4 + 8x_3^2x_5^2 - 8x_4^2x_5^2 + x_5^4 + 8x_3^2x_6^2 - 8x_4^2x_6^2 + 2x_5^2x_6^2 + x_6^4 - 40x_3^2 - 24x_4^2 + 6x_5^2 + 6x_6^2 + 9, \\ &16x_1^4 + 32x_1^2x_2^2 + 16x_2^4 + 8x_1^2x_5^2 - 8x_2^2x_5^2 + x_5^4 + 8x_1^2x_6^2 - 8x_2^2x_6^2 + 2x_5^2x_6^2 + x_6^4 - 40x_1^2 - 24x_2^2 + 6x_5^2 + 6x_6^2 + 9, \\ &16x_1^2x_3^2 + 16x_2^2x_3^2 + 16x_1^2x_4^2 + 16x_2^2x_4^2 - 4x_1^2x_5^2 - 4x_2^2x_5^2 - 4x_3^2x_5^2 - 4x_4^2x_5^2 - 4x_1^2x_6^2 - 4x_2^2x_6^2 - 4x_3^2x_6^2 - 4x_4^2x_6^2 + \\ &x_5^4 + 2x_5^2x_6^2 + x_6^4 + 16x_1x_3x_5^2 + 16x_1x_3x_6^2 - 12x_1^2 - 12x_2^2 - 16x_1x_3 - 12x_3^2 - 12x_4^2 + 6x_5^2 + 6x_6^2 + 9. \end{aligned}$$

◆

2.2.2. Exposed points of the discotope

In the rest of the chapter, we assume that (2.2.1) is satisfied. Recall that all extreme points of \mathcal{D} , hence all its exposed points, are contained in \mathcal{S} . In this section, we prove that they form a full dimensional subset of the boundary of the discotope; in particular, at least one irreducible component of \mathcal{S} of dimension $d - 1$ is the Zariski closure of a subset of exposed points. Further, we prove that exposed points are generically exposed by a unique vector in S^{d-1} . First, we give a general result which will be useful in the following.

Lemma 2.2.7. Let K_1, \dots, K_N be convex bodies in \mathbb{R}^d . Consider a point $p = p_1 + \dots + p_N \in \partial K$ where K is the Minkowski sum of the K_i 's, and assume that p_i is a smooth point of ∂K_i for every $i = 1, \dots, N$. Fix $u \in S^{d-1}$. Then $T_{p_i} \partial K_i \subseteq u^\perp$ for every i if and only if p belongs to the face of K exposed by u .

Proof. Assume $T_{p_i} \partial K_i \subseteq u^\perp$ for every i for some $u \in S^{d-1}$. Then one of these vectors u satisfies $p_i \in K_i^u$ for every i . As a consequence, $p \in K^u$. Conversely, let $p \in K^u$. Therefore, $h_K(u) = \langle p, u \rangle = \sum_{i=1}^N \langle p_i, u \rangle$ and for every i and for every $\tilde{p}_i \in D_i$,

$$\langle p_i, u \rangle \geq \langle \tilde{p}_i, u \rangle.$$

Hence $h_{D_i}(u) = \langle p_i, u \rangle$. There are two possible situations: either $u \perp \langle D_i \rangle$, or p_i is exposed by u . In both cases it is clear that $T_{p_i} \partial K_i \subseteq u^\perp$. □

Proposition 2.2.8. Let $\Sigma : \prod \partial_a D_i \rightarrow \mathbb{C}^d$ be the restriction of the addition map to the algebraic boundaries of N generic discs. Assume that (2.2.1) holds with strict inequality. Then

$$\Sigma^{-1}(\mathcal{S}) \subseteq \text{crit}(\Sigma).$$

Here $\text{crit}(\Sigma)$ denotes the critical locus, that is the variety of points $\xi \in \prod \partial_a D_i$ where the differential $d_\xi \Sigma$ does not have full rank.

Proof. Since (2.2.1) holds with strict inequality, for a generic $\xi \in \prod \partial_a D_i$ the differential $d_\xi \Sigma$ is surjective. By density, it is enough to check that $d_\xi \Sigma$ is not surjective at the real points of $\Sigma^{-1}(\mathcal{S})$. For every $\xi \in \prod \partial D_i$, the image of the differential $d_\xi \Sigma$ is the sum $T_{\xi_1} \partial D_1 + \dots + T_{\xi_N} \partial D_N$. If $\Sigma(\xi)$ belongs to the face \mathcal{D}^u , then by Lemma 2.2.7 $T_{\xi_i} \partial D_i \subseteq u^\perp$ for every i . In particular the differential is not surjective, hence ξ is a critical point of Σ . Passing to the Zariski closure, we obtain $\Sigma^{-1}(\mathcal{S}) \subseteq \text{crit}(\Sigma)$. \square

The next result identifies a region of $\partial \mathcal{D}$ of points exposed by a unique vector of S^{d-1} .

Lemma 2.2.9. Let \mathcal{D} be a generic discotope such that condition (2.2.1) is satisfied. Let $p \in \mathcal{D}^\partial \cap \partial \mathcal{D}$. The following are equivalent:

- there exists a unique $u \in S^{d-1}$ such that $p \in \mathcal{D}^u$;
- $p = \sum_{i=1}^N \xi_i$ for some $\xi_i \in \partial D_i$ such that $\text{codim} \left(\sum_{i=1}^N T_{\xi_i} \partial D_i \right) = 1$.

Let Ω be the set of points that satisfy either (hence both) these conditions; then Ω is non-empty and Euclidean open in $\mathcal{D}^\partial \cap \partial \mathcal{D}$.

Proof. The equivalence of the two conditions follows from Lemma 2.2.7. To show that Ω is non-empty, we construct a point in the following way. Consider $u \in \mathcal{U}$ and let $p = \sum_{i=1}^N \xi_i = \mathcal{D}^u$. For the sake of notation, write $T_{\xi_i} = T_{\xi_i} \partial D_i$. Suppose that $L_\xi = T_{\xi_1} + \dots + T_{\xi_N}$ is a subspace of codimension $c \geq 2$. Since $u \in \mathcal{U}$, for every i we have $\langle D_i \rangle \not\subseteq L_\xi$. Condition (2.2.1) implies that, up to relabeling, $T_{\xi_1} \cap (T_{\xi_2} + \dots + T_{\xi_N}) = L' \neq \{0\}$. Let L'' be a complement of L' in T_{ξ_1} , so that

$$L' + L'' = T_{\xi_1} \quad \text{and} \quad L' \cap L'' = \{0\}.$$

Consider the set of points $\tilde{\xi}_1 \in \partial D_1$ such that $T_{\tilde{\xi}_1} \supseteq L''$ and let $\tilde{\xi} = (\tilde{\xi}_1, \xi_2, \dots, \xi_N)$. For a generic choice of such $\tilde{\xi}_1$ there exists $\tilde{u} \in \mathcal{U}$ such that $L_{\tilde{\xi}} \subseteq \tilde{u}^\perp$. Therefore the point $\tilde{p} = \tilde{\xi}_1 + \xi_2 + \dots + \xi_N$ is an exposed point of \mathcal{D} . Moreover, if $\tilde{\xi}_1 \neq \pm \xi_1$ then $\text{codim } L_{\tilde{\xi}} \leq c-1$. Repeating this argument one constructs a point ξ such that $\text{codim}(T_{\xi_1} + \dots + T_{\xi_N}) = 1$. The condition that this codimension is 1 is Zariski open, hence Ω is Euclidean open in $\mathcal{D}^\partial \cap \partial \mathcal{D}$. \square

Recall from Proposition 1.1.19, point (iv), that the support function is differentiable at $u \in S^{d-1}$ if and only if the face K^u is a unique point; this point coincides with $\nabla h_K(u)$. In particular, $h_{\mathcal{D}}$ is differentiable at all points of \mathcal{U} . This will be useful in the next result, to prove that the set of exposed points of \mathcal{D} is full dimensional in its boundary.

Proposition 2.2.10. In the hypotheses of Lemma 2.2.9, there exists an open dense subset \mathcal{U}' of \mathcal{U} such that $\nabla h_{\mathcal{D}}|_{\mathcal{U}'}$ is one to one.

Proof. Fix $u \in \mathcal{U}$ and denote by p_u the point of the discotope exposed by u . Let $\xi_i \in \partial D_i$ be the unique point of the i -th disc such that $h_{D_i}(u) = \langle \xi_i, u \rangle$; then $p_u = \sum_{i=1}^N \xi_i$. The tangent space $T_{\xi_i} \partial D_i = u^\perp \cap \langle D_i \rangle$ is a $(\dim D_i - 1)$ -dimensional subspace of u^\perp . Because of the non-degeneracy condition (2.2.1), there exists a Euclidean open and dense subset \mathcal{U}' of \mathcal{U} such that for all $u \in \mathcal{U}'$

$$\sum_{i=1}^N T_{\xi_i} \partial D_i = u^\perp. \tag{2.2.2}$$

If $u \in \mathcal{U}'$ then the support function of the discotope is smooth in a neighborhood of u , because $h_{\mathcal{D}}(u) = \sum h_{D_i}(u)$ and the h_{D_i} 's are smooth in a neighborhood of u . Hence we have the following map

$$\begin{aligned}\nabla h_{\mathcal{D}}|_{\mathcal{U}'} : \mathcal{U}' &\rightarrow \partial \mathcal{D} \\ u &\mapsto \nabla h_{\mathcal{D}}(u) = p_u.\end{aligned}$$

Its image lies inside Ω because of (2.2.2). Since these are exactly the points exposed by only one direction, $\nabla h_{\mathcal{D}}|_{\mathcal{U}'}$ is one to one. \square

From Proposition 2.2.10, we see that $\nabla h_{\mathcal{D}}(\mathcal{U}')$ is a set of exposed points which is open in $\partial \mathcal{D}$; in particular it has dimension $d - 1$. Moreover, $\nabla h_{\mathcal{D}}$ defines a diffeomorphism between \mathcal{U}' and its image, therefore $\nabla h_{\mathcal{D}}(\mathcal{U}')$ consists of smooth points of $\partial_a \mathcal{D}$. A consequence of this is that the Zariski closure of the exposed points (or equivalently of the extreme points) contains at least one irreducible component of \mathcal{S} of dimension $d - 1$. This leads to the following result.

Corollary 2.2.11. Let \mathcal{D} be a generic discotope such that the non-degeneracy condition (2.2.1) holds. Then \mathcal{S} has at least one irreducible component of dimension $d - 1$ and this is an irreducible component of the algebraic boundary $\partial_a \mathcal{D}$.

In general, it is not clear whether \mathcal{S} has multiple irreducible components, possibly even of different dimension. Indeed, the set $\mathcal{D}^{\partial} = \Sigma(\prod_j \partial D_j)$, introduced in Definition 2.2.1, may intersect positive dimensional faces of \mathcal{D} . This might produce lower dimensional components of \mathcal{S} . However, we expect this not to be the case, as stated in Conjecture 2.2.22.

We conclude this section pointing out that in general some boundary points of \mathcal{D} can be vertices, i.e., exposed by more than one vector (see Definition 1.1.9). These can be identified by the following condition. Set $L_i = \langle D_i \rangle$, so that L_1, \dots, L_N are N generic linear subspaces of \mathbb{R}^d . Consider the hyperplanes $H = u^\perp \subseteq \mathbb{R}^d$ for $u \in \mathcal{U}$; hence $\dim(H \cap L_i) = \dim L_i - 1$ for every i . A point $p = \mathcal{D}^u$ is a vertex if and only if H satisfies

$$\dim((H \cap L_1) + \dots + (H \cap L_N)) \leq d - 2. \quad (2.2.3)$$

Indeed, when (2.2.3) holds, there exists a linear subspace V of dimension at least one such that $H = (H \cap L_1) + \dots + (H \cap L_N) + V$. By perturbing V we obtain a family of hyperplanes that expose the point p . The condition (2.2.3) can be formulated in terms of a degeneracy property of an associated polymatroid, but a full characterization seems difficult in general. We point out that such a configuration of linear spaces is connected to objects that are relevant in coding theory. If the dimension in (2.2.3) is $d - 1$ for all hyperplanes H , the set $\{L_1, \dots, L_N\}$ is called a *hyperplane generating set* (see [FS14] for a study of the case where $\dim L_i = 2$ for all i). They have been used in [DGMP11], where they are called ‘strong generating sets’, to construct saturating sets in a field extension, which correspond geometrically to covering codes. In [ABN22], the authors call them ‘cutting blocking sets’ and prove that they correspond to minimal linear codes, i.e., those codes whose codewords are all minimal with respect to the inclusion of their supports.

Example 2.2.12. In the case $N = 2$, vertices always occur. Let $d_1 = \dim D_1$, $d_2 = \dim D_2$. By the non-degeneracy condition (2.2.1), $d_1 + d_2 \geq d + 1$. Let $L_i = \langle D_i \rangle$; by genericity

$\dim(L_1 \cap L_2) = d_1 + d_2 - d$. For a hyperplane H such that $\dim(L_i \cap H) = d_i - 1$, we have

$$\begin{aligned} \dim((L_1 \cap H) + (L_2 + H)) &= \\ (d_1 - 1) + (d_2 - 1) - \dim(L_1 \cap L_2 \cap H) &= \begin{cases} d - 2 & \text{if } L_1 \cap L_2 \subseteq H, \\ d - 1 & \text{otherwise.} \end{cases} \end{aligned}$$

Therefore, a point $p \in \mathcal{D}$ exposed by a hyperplane H such that $L_1 \cap L_2 \not\subseteq H$, is exposed only by such hyperplane. On the other hand, if p is exposed by a hyperplane H with $L_1 \cap L_2 \subseteq H$, then there is a cone of hyperplanes \tilde{H} with $L_1 \cap L_2 \subseteq \tilde{H}$ exposing p as well. The case $d = 3$, $d_1 = d_2 = 2$ is shown in Figure 2.1, right. This discotope \mathcal{D}' is defined in Example 2.1.10; in this case $L_1 \cap L_2$ is the vertical x_3 -axis. The plane $\{x_3 = 0\}$ is partitioned into four 2-dimensional cones and every u in the interior of the same cone exposes the same point. These four vertices are the pairwise intersection of two adjacent blue discs. \blacklozenge

2.2.3. Two-dimensional discs

In this section, we consider discotopes $\mathcal{D} \subseteq \mathbb{R}^d$ of type $(0, N, 0, \dots, 0) \in \mathbb{N}^d$, that are realized as sum of 2-dimensional discs, as in Figure 2.3. If $N \leq d - 1$, the variety \mathcal{S} is

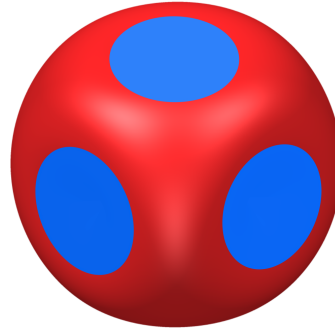


Figure 2.3: The dice, a discotope of type $(0, 3, 0)$.

described by Theorem 2.2.5. Thus assume that $N \geq d - 1$, which ensures that $\dim \mathcal{S} = d - 1$. We will prove that the purely nonlinear part \mathcal{S} is irreducible, hence it is the Zariski closure of the extreme points of \mathcal{D} . In addition, we will provide an upper bound for the degree of this component of the algebraic boundary.

Theorem 2.2.13. Let \mathcal{D} be a generic discotope of type $(0, N, 0, \dots, 0)$ in \mathbb{R}^d , with $N \geq d - 1$. Let \mathcal{S} be the purely nonlinear part of \mathcal{D} . Then \mathcal{S} is irreducible, and coincides with $\text{Ext}_a \mathcal{D}$. Moreover,

$$\deg(\mathcal{S}) \leq 2^N \cdot \binom{N}{d-1}.$$

Let D_1, \dots, D_N be 2-dimensional discs in \mathbb{R}^d in general position. For every $j = 1, \dots, N$, consider the (complexification of the) embedding $A_j : \mathbb{C}^2 \rightarrow \mathbb{C}^d$ defining the generalized disc D_j ; let $\mathcal{B}_j = \{b_1^{(j)}, b_2^{(j)}\}$ be the associated basis of the image of A_j . Then, the product $\prod_{j=1}^N \partial_a D_j$ is the image of the restriction of $A = A_1 \times \dots \times A_N$ to $\prod\{c_j^2 + s_j^2 = 1\} \subseteq (\mathbb{C}^2)^N$. Here (c_j, s_j) are the coordinates on the j -th copy of \mathbb{C}^2 . Consider the addition map

$$\Sigma : \partial_a D_1 \times \dots \times \partial_a D_N \rightarrow \mathbb{C}^d.$$

The critical locus of the restriction of $\Sigma \circ A$ is the variety defined by the ideal

$$I = \Delta + (c_1^2 + s_1^2 - 1, \dots, c_N^2 + s_N^2 - 1) \subseteq \mathbb{C}[c_1, s_1, \dots, c_N, s_N] \quad (2.2.4)$$

where Δ is the ideal of the $d \times d$ minors of the $N \times d$ matrix

$$M = \begin{pmatrix} b_2^{(1)} c_1 - b_1^{(1)} s_1 \\ \vdots \\ b_2^{(N)} c_N - b_1^{(N)} s_N \end{pmatrix}.$$

This is the (transpose of the) matrix representing the differential of the restriction of $\Sigma \circ A$. Since A is a linear embedding, $\text{crit } \Sigma$ is irreducible if and only if $\text{crit}(\Sigma \circ A)$ is irreducible, and their degrees coincide.

We will prove the irreducibility of $\text{crit } \Sigma$ and compute its degree by first studying the variety $\mathcal{V}(\Delta)$. We show that it is irreducible and that its degree coincides with the one of the classical determinantal variety of $N \times d$ matrices of submaximal rank. This is a consequence of Lemma 2.2.15, which provides a more general result on special linear sections of the determinantal variety. This topic is object of classical study, see [Eis88], [Eis05, Section 6B]. However, those results rely on a specific condition, called 1-genericity, which is not satisfied in our setting.

We state the following version of Bertini's Theorem for projective varieties, which can be obtained from [Jou80, Theorem 6.3] applied to the special case of quasi-projective varieties.

Lemma 2.2.14. Let X be an irreducible projective variety. Let \mathcal{L} be a line bundle on X defining a map $\Phi : X \dashrightarrow \mathbb{P}^{h_0(\mathcal{L})-1}$ such that $\dim \Phi(X) \geq s+1$. Let $D_1, \dots, D_s \in |\mathcal{L}|$ be generic elements of the linear system defined by \mathcal{L} . Let $Y = D_1 \cap \dots \cap D_s$ and let B be the base locus of \mathcal{L} . Then $\overline{Y \setminus B}$ is irreducible of codimension s in X .

Proof. The proof follows from [Jou80, Theorem 6.3 (4)] applied to the quasi-projective variety $\tilde{X} = X \setminus B$ and the morphism $\Phi|_{\tilde{X}}$. \square

Informally, this result guarantees that the intersection of generic divisors is irreducible and of the expected codimension outside of the base locus of the line bundle. We use Lemma 2.2.14 to prove that certain non-generic linear sections of the classical determinantal variety are irreducible and of the expected dimension. Let $\text{Mat}_{n \times m}$ denote the (complex) vector space of $n \times m$ matrices and let

$$\mathcal{M}_r^{n \times m} = \{A \in \mathbb{P}\text{Mat}_{n \times m} : \text{rank}(A) \leq r\}$$

be the r -th determinantal variety. Use coordinates x_{ij} on $\text{Mat}_{n \times m}$, where x_{ij} is the entry at row i and column j .

Lemma 2.2.15. Let $m, n, r \geq 2$ be integers with $r < m, n$. Let s be an integer $1 \leq s < r$. For $i = 1, \dots, n$, let $\ell_1^{(i)}, \dots, \ell_s^{(i)}$ be generic linear forms on $\text{Mat}_{n \times m}$ only involving the variables $\{x_{ij} : j = 1, \dots, m\}$ of the i -th row. Let

$$\mathcal{Y}_r^{n \times m} = \mathcal{M}_r^{n \times m} \cap \left\{ A \in \mathbb{P}\text{Mat}_{n \times m} : \ell_p^{(i)}(A) = 0 \text{ for } i = 1, \dots, n, p = 1, \dots, s \right\}.$$

Then $\mathcal{Y}_r^{n \times m}$ is irreducible and of codimension ns in $\mathcal{M}_r^{n \times m}$.

Proof. For $i = 1, \dots, n$, let

$$\Gamma_i = \{A \in \mathbb{P}\text{Mat}_{n \times m} : a_{ij} = 0 \text{ for all } j = 1, \dots, m\}$$

be the linear subspace of matrices having zero i -th row. Let $\Gamma = \bigcup_{i=1}^n \Gamma_i$. For $t = 0, \dots, n$, let

$$\mathcal{Y}^{(t)} = \mathcal{M}_r^{n \times m} \cap \left\{ A \in \mathbb{P}\text{Mat}_{n \times m} : \ell_p^{(i)}(A) = 0 \text{ for } i = 1, \dots, t, p = 1, \dots, s \right\};$$

we have $\mathcal{M}_r^{n \times m} = \mathcal{Y}^{(0)} \supseteq \mathcal{Y}^{(1)} \supseteq \dots \supseteq \mathcal{Y}^{(n)} = \mathcal{Y}_r^{n \times m}$.

Let $\Phi_i : \mathbb{P}\text{Mat}_{n \times m} \dashrightarrow \mathbb{P}^{m-1}$ be the projection on the i -th row; Φ_i is a rational map, whose indeterminacy locus is Γ_i . Let $\mathcal{L}_i = \Phi_i^*\mathcal{O}(1)$ be the pullback of the hyperplane bundle on \mathbb{P}^{m-1} : global sections of \mathcal{L}_i are linear forms only involving the variables of the i -th row; in particular the base locus of \mathcal{L}_i is exactly Γ_i . For a fixed n , we use induction on t to show that $\mathcal{Y}^{(t)}$ is irreducible up to components contained in Γ , in the sense that $\mathcal{Y}^{(t)} \setminus \Gamma$ is irreducible.

If $t = 0$, then $\mathcal{Y}^{(t)} = \mathcal{M}_r^{n \times m}$ is irreducible. If $t \geq 1$, then $\mathcal{Y}^{(t)}$ is the intersection of s divisors $D_1, \dots, D_s \in |\mathcal{L}_i|_{\mathcal{Y}^{(t-1)}}|$ on $\mathcal{Y}^{(t-1)}$, where $D_p = \{\ell_p^{(t)} = 0\}$ and $\mathcal{L}_i|_{\mathcal{Y}^{(t-1)}}$ is the restriction of \mathcal{L}_i to $\mathcal{Y}^{(t-1)}$. By the induction hypothesis, $\mathcal{Y}^{(t-1)}$ is a union of irreducible components, only one of which is not contained in Γ . In order to apply Lemma 2.2.14, we need $\dim \Phi_t(\mathcal{Y}^{(t-1)}) \geq s+1$. In fact we show that $\Phi_t(\mathcal{Y}^{(t-1)}) = \mathbb{P}^{m-1}$.

If $t \leq r$, this is clear because for every choice of the first t rows, the corresponding matrix can be completed to a rank r matrix. If $t > r$, notice that every r -dimensional subspace $E \subset \mathbb{C}^m$ can be realized as the span of the first $t-1$ rows of a matrix in $\mathcal{Y}^{(t-1)}$. Since $s < r$, for every $i = 1, \dots, t-1$ the intersection of E with the subspace of \mathbb{C}^m cut out by the linear forms $\ell_1^{(i)}, \dots, \ell_s^{(i)}$ is non-trivial. Consider the matrix $A \in \mathcal{Y}^{(t-1)}$ whose i -th row is a generic element of this intersection for $i < t$, and suitably completed to a rank r matrix. By the genericity of the linear forms the span of the first $t-1$ rows of A is exactly E . Fix now $v \in \mathbb{C}^m$ and let E be an r -dimensional subspace containing v . The associated matrix A constructed above can be chosen so that the t -th row coincides with v . In this way, $\Phi_t(A) = v$ and $\dim \Phi_t(\mathcal{Y}^{(t-1)}) = m-1 \geq s+1$ follows.

Therefore, Lemma 2.2.14 applies and we obtain that $\mathcal{Y}^{(t)}$ is irreducible up to components contained in the base locus of \mathcal{L}_i , that is $\Gamma_i \subseteq \Gamma$. This proves the desired property for $\mathcal{Y}^{(t)}$ and, in particular, shows that $\mathcal{Y}_r^{n \times m}$ is irreducible up to components contained in Γ . For every t , let $Y^{(t)}$ be the component of $\mathcal{Y}^{(t)}$ not contained in Γ . In particular, $Y^{(t)}$ is not contained in the base locus of $\mathcal{L}_i|_{Y^{(t-1)}}$; therefore, by Lemma 2.2.14, it has the expected codimension. This provides $\text{codim}_{\mathcal{M}_r^{n \times m}}(Y^{(t)}) = ts$.

Finally, we prove that in fact $\mathcal{Y}_r^{n \times m}$ does not have components contained in Γ , thus it is irreducible. This is proved by induction on n . The base case of the induction is $n = r$. In this case $\mathcal{M}_r^{n \times m}$ is the whole space $\mathbb{P}\text{Mat}_{r \times m}$ and $\mathcal{Y}_r^{n \times m}$ is the transverse intersection of ns linear spaces. Therefore it is irreducible.

Let $n > r$. Suppose by contradiction that $\mathcal{Y}_r^{n \times m}$ has at least one component, denoted by C , contained in Γ . Then $C \subseteq \Gamma_i$ for some i ; without loss of generality, suppose $i = n$. Identify $\text{Mat}_{(n-1) \times m}$ with the subspace of $\text{Mat}_{n \times m}$ having the n -th row equal to 0. Under this identification, the component C is contained in $\mathcal{Y}_r^{(n-1) \times m}$, so $\dim C \leq \dim \mathcal{Y}_r^{(n-1) \times m}$. By the induction hypothesis, $\mathcal{Y}_r^{(n-1) \times m}$ is irreducible, so it coincides with its only component not contained in Γ and in particular it has the expected codimension in $\mathcal{M}_r^{(n-1) \times m}$. We obtain

$$\begin{aligned} \dim C &\leq \dim \mathcal{Y}_r^{(n-1) \times m} = \dim \mathcal{M}_r^{(n-1) \times m} - (n-1)s \\ &= r((n-1) + m - r) - (n-1)s \\ &= r(n+m-r) - ns - (r-s) = \dim \mathcal{M}_r^{n \times m} - ns - (r-s). \end{aligned}$$

This implies $\text{codim}_{\mathcal{M}_r^{n \times m}}(C) > ns$ in contradiction with the fact that $\mathcal{Y}_r^{n \times m}$ is cut out by ns equations in $\mathcal{M}_r^{n \times m}$. We conclude that $\mathcal{Y}_r^{n \times m}$ has no components contained in Γ ; thus it is irreducible. \square

Remark 2.2.16. In Lemma 2.2.15, it is not necessary to have the same number of linear relations on every row. The same argument applies if, on the i -th row, one has s_i linear relations, with $s_i < r$ for every i . Then $\mathcal{Y}_r^{n \times m}$ is irreducible and of codimension $\sum s_i$ in $\mathcal{M}_r^{n \times m}$.

Lemma 2.2.15 shows that linear sections of the determinantal variety only involving a single row are *generic enough* in the sense that they preserve irreducibility and have the expected dimension. We apply Lemma 2.2.15 to the variety $\mathcal{V}(\Delta)$: in this case $r = d - 1$ and $s = d - 2$.

Proposition 2.2.17. The variety $\text{crit}(\Sigma)$ is irreducible, of dimension $d - 1$, and degree $2^N \binom{N}{d-1}$.

Proof. Since $A = A_1 \times \dots \times A_N$ is a linear embedding, it suffices to prove the statement for $\text{crit}(\Sigma \circ A)$, that is the variety defined by the ideal I in (2.2.4). By Lemma 2.2.15, the variety $\mathcal{V}(\Delta) \subseteq \mathbb{C}^2 \times \dots \times \mathbb{C}^2$ is irreducible of dimension $N + d - 1$. Consider its closure in $\mathbb{P}^2 \times \dots \times \mathbb{P}^2$, where the j -th copy of \mathbb{P}^2 has homogeneous coordinates $[c_j, s_j, z_j]$. For every $j = 1, \dots, N$, the polynomial $c_j^2 + s_j^2 - 1$ on \mathbb{C}^2 defines a homogeneous quadric $\{c_j^2 + s_j^2 - z_j^2 = 0\}$ on \mathbb{P}^2 . This gives a generic element of $|\mathcal{O}_{\mathbb{P}^2}(2)|$, which pulls back to a generic element $Q_j \in |\mathcal{O}_{(\mathbb{P}^2)^N}(0, \dots, 0, 2, 0, \dots, 0)|$. Recursively applying Lemma 2.2.14, for every j we have that $\mathcal{V}(\Delta) \cap Q_1 \cap \dots \cap Q_j$ is irreducible of dimension $N - j + d - 1$. For $j = N$, we obtain the irreducibility of $\mathcal{V}(\Delta) \cap Q_1 \cap \dots \cap Q_N$.

As a consequence, $\text{crit}(\Sigma \circ A) = \mathcal{V}(I)$ is irreducible of dimension $d - 1$. In particular, the intersection of the determinantal variety $\mathcal{V}(\Delta)$ with the quadrics is dimensionally transverse. Moreover, $\mathcal{V}(\Delta)$ is arithmetically Cohen-Macaulay, see e.g. [ACGH85, Chapter 2]. Therefore [EH16, Corollary 2.5] guarantees

$$\deg(\text{crit}(\Sigma \circ A)) = \deg(\mathcal{V}(\Delta)) \cdot \prod_{i=1}^N \deg(\partial_a D_i) = \binom{N}{d-1} \cdot 2^N.$$

\square

Proof of Theorem 2.2.13. The irreducibility of $\text{crit}(\Sigma)$ implies the irreducibility of its image under the addition map Σ , that is the purely nonlinear part \mathcal{S} . By the linearity of Σ , we obtain an upper bound on the degree of \mathcal{S} :

$$\deg(\mathcal{S}) \leq 2^N \cdot \binom{N}{d-1}.$$

From the discussion in Section 2.2.2, the set of extreme points of \mathcal{D} is contained in \mathcal{S} and contains a Zariski dense subset of (at least) one of the components of \mathcal{S} . By irreducibility, we conclude. \square

We end this section with some observations in the case of discotopes of type $\mathbf{N} = (0, N)$ in \mathbb{R}^2 . In this case $\partial_a \mathcal{D} = \mathcal{S}$, which is an irreducible curve of degree $2^N \cdot N$. The real points of $\text{crit} \Sigma$ come naturally in 2^{N-1} connected components, described as follows. Given a line $\ell \subseteq \mathbb{R}^2$ through the origin, there are exactly two points $\pm p_i$ on each ellipse ∂D_i such that $T_{\pm p_i} \partial D_i$ is parallel to ℓ . The choice of these signs (up to a global sign) determines locally a

parametrization of the real points of $\text{crit } \Sigma$, which has 2^{N-1} connected components. After the projection to \mathbb{R}^2 , many components of the real points of $\text{crit } \Sigma$ can be mapped to the same connected component of the real points of \mathcal{S} . This can be visualized in the example in Figure 2.2, where the red curve \mathcal{S} is union of $2^2 = 4$ subsets homeomorphic to circles: these are the images of the 4 connected components of $\text{crit } \Sigma$. Exactly one of them is the topological boundary of \mathcal{D} .

Furthermore the degree of the map $\Sigma : \text{crit}(\Sigma) \rightarrow \mathcal{S}$ is odd. By a density argument, this can be computed considering the fiber over a generic point $p \in \partial\mathcal{D}$. This contains a single real point (ξ_1, \dots, ξ_N) where $\xi_j \in \partial D_j$ is the unique point exposed by the vector $u \in S^1$ which exposes p ; the non-real points of $\Sigma^{-1}(p)$ come in pairs of complex conjugates, therefore there is an even number of them. We conclude that the fiber $\Sigma^{-1}(p)$ consists of an odd number of points, hence the degree of Σ is odd.

Remark 2.2.18. In the case $d = 2$ the degree of the critical locus of Σ is $2^N \cdot N$ and the degree of the map $\Sigma : \text{crit } \Sigma \rightarrow \mathcal{S}$ is odd. Write $N = 2^\kappa \cdot M$, with M odd. Then $\deg(\mathcal{S})$ is necessarily an odd multiple of $2^N \cdot 2^\kappa$. A consequence of this is that the unit ball of the L^4 -norm $\{x_1^4 + x_2^4 \leq 1\}$ is not a discotope. If it was a discotope, it would be of type $(0, N)$ for some $N \geq 2$. But this discussion shows that no curve of degree 4 is the boundary of a discotope of type $(0, N)$ in \mathbb{R}^2 .

Example 2.2.19 (The dice). We provide an extended analysis of the algebro-geometric features of the surface $\mathcal{S} \subseteq \mathbb{C}^3$ for a specific discotope of type $\mathbf{N} = (0, 3, 0)$. Notice that, up to changing coordinates, the generic case of a discotope of type $\mathbf{N} = (0, 3, 0)$ can be reduced to the case where the three generalized discs of interest lie in the three coordinate hyperplanes. We further restrict to the case of three unit discs:

$$\begin{aligned} D_1 &= \{(x_1, x_2, x_3) : x_1 = 0; x_2^2 + x_3^2 \leq 1\}, \\ D_2 &= \{(x_1, x_2, x_3) : x_2 = 0; x_1^2 + x_3^2 \leq 1\}, \\ D_3 &= \{(x_1, x_2, x_3) : x_3 = 0; x_1^2 + x_2^2 \leq 1\}. \end{aligned}$$

Let $\mathcal{D} \subseteq \mathbb{R}^3$ be the resulting discotope shown in Figure 2.3, that we call *dice*, and let $\mathcal{S} \subseteq \mathbb{C}^3$ be its purely nonlinear part. By a direct computation, or by Theorem 2.2.13, \mathcal{S} is an irreducible surface of degree 24. Its defining polynomial $F_{\mathcal{S}}$ is

$$x_1^{24} + 4x_1^{22}x_2^2 + 2x_1^{20}x_2^4 + \dots + 728x_3^4 - 160x_1^2 - 160x_2^2 - 160x_3^2 + 16,$$

which is made of $91 + 78 + 66 + 55 + 45 + 36 + 28 + 21 + 15 + 10 + 6 + 3 + 1 = 455$ monomials, here distinguished by their degree. Because of the symmetries of the problem, all the monomials appearing in $F_{\mathcal{S}}$ are squares. Since \mathcal{S} is the image of a polynomial map, $F_{\mathcal{S}}$ can be computed via elimination theory [CLO15, Section 4.4, Theorem 3]. More precisely, consider the ideal

$$J = I + \left((x_1, x_2, x_3) - \sum_{i=1}^3 b_1^{(i)} c_i + b_2^{(i)} s_i \right) \subset \mathbb{C}[x_i, c_i, s_i : i = 1, 2, 3]$$

where $b_1^{(1)} = b_2^{(3)} = (0, 1, 0)$, $b_1^{(2)} = b_2^{(1)} = (0, 0, 1)$, $b_1^{(3)} = b_2^{(2)} = (1, 0, 0)$ and I is the ideal in (2.2.4). Then $F_{\mathcal{S}}$ is the unique (up to scaling) generator of $J \cap \mathbb{C}[x_1, x_2, x_3]$ and it can be computed using a computer algebra software, e.g., *Macaulay2* [GS].

One can verify that the surface \mathcal{S} is singular in codimension 1. The singular locus is highly reducible and has degree 294. Our next goal is to construct a desingularization of \mathcal{S} . Consider the rational parametrization of the (complex) circle $\psi : t \mapsto (\frac{1-t^2}{1+t^2}, \frac{2t}{1-t^2})$. Let

$\Sigma \circ (\psi_1 \times \psi_2 \times \psi_3)$ be the composition of the addition map with the parameterization of the three circles $\partial_a D_i$; explicitly

$$\begin{array}{ccc} \mathbb{C} \times \mathbb{C} \times \mathbb{C} & \xrightarrow{\psi_1 \times \psi_2 \times \psi_3} & \mathbb{C}^3 \\ (t_1, t_2, t_3) & \mapsto & \left(\left(\begin{array}{c} 0 \\ \frac{1-t_1^2}{1+t_1^2} \\ \frac{2t_1}{1+t_1^2} \end{array} \right), \left(\begin{array}{c} \frac{2t_2}{1+t_2^2} \\ 0 \\ \frac{1-t_2^2}{1+t_2^2} \end{array} \right), \left(\begin{array}{c} \frac{1-t_3^2}{1+t_3^2} \\ \frac{2t_3}{1+t_3^2} \\ 0 \end{array} \right) \right) \\ & & \left(\left(\begin{array}{c} x_1 \\ x_2 \\ x_3 \end{array} \right), \left(\begin{array}{c} y_1 \\ y_2 \\ y_3 \end{array} \right), \left(\begin{array}{c} z_1 \\ z_2 \\ z_3 \end{array} \right) \right) \mapsto \left(\begin{array}{c} x_1 + y_1 + z_1 \\ x_2 + y_2 + z_2 \\ x_3 + y_3 + z_3 \end{array} \right). \end{array}$$

The differential of the composition is given by

$$M(t_1, t_2, t_3) = \begin{pmatrix} 0 & \frac{1-t_2^2}{1+t_2^2} & \frac{-2t_3}{1-t_3^2} \\ \frac{-2t_1}{1+t_1^2} & 0 & \frac{1-t_3^2}{1+t_3^2} \\ \frac{1-t_1^2}{1+t_1^2} & \frac{-2t_2}{1+t_2^2} & 0 \end{pmatrix}$$

so that the critical locus is the hypersurface in \mathbb{C}^3 determined by the vanishing of

$$\det(M(t_1, t_2, t_3)) = \frac{1}{(1+t_1^2)(1+t_2^2)(1+t_3^2)} [(1-t_1^2)(1-t_2^2)(1-t_3^2) - 8t_1t_2t_3]. \quad (2.2.5)$$

The map $\Sigma \circ (\psi_1 \times \psi_2 \times \psi_3)$ extends to a regular map $\phi : \mathbb{P}^1 \times \mathbb{P}^1 \times \mathbb{P}^1 \rightarrow \mathbb{P}^3$; from (2.2.5), we obtain that the critical locus of this extension is the surface $\tilde{\mathcal{S}}$ of multidegree $(2, 2, 2)$ defined by the equation

$$(u_1^2 - t_1^2)(u_2^2 - t_2^2)(u_3^2 - t_3^2) - 8u_1u_2u_3t_1t_2t_3 = 0,$$

where $[u_i, t_i]$ are homogeneous coordinates on the i -th copy of \mathbb{P}^1 .

Theorem 2.2.20. The surface $\tilde{\mathcal{S}}$ is a smooth K3 surface. The map ϕ is a birational equivalence between $\tilde{\mathcal{S}}$ and \mathcal{S} . In particular $\tilde{\mathcal{S}}$ is a desingularization of \mathcal{S} .

Proof. The smoothness and the irreducibility of $\tilde{\mathcal{S}}$ are verified by a direct calculation. It is a classical fact that a smooth divisor of multidegree $(2, 2, 2)$ in $\mathbb{P}^1 \times \mathbb{P}^1 \times \mathbb{P}^1$ is a K3 surface. For completeness, we give an explicit proof. Let $\mathcal{O}_{\tilde{\mathcal{S}}}$ and $K_{\tilde{\mathcal{S}}}$ be the structure and the canonical sheaves of $\tilde{\mathcal{S}}$, respectively. We verify the two conditions $K_{\tilde{\mathcal{S}}} \simeq \mathcal{O}_{\tilde{\mathcal{S}}}$ and $h^1(\mathcal{O}_{\tilde{\mathcal{S}}}) = 0$, characterizing a K3 surface.

First, we prove $K_{\tilde{\mathcal{S}}} \simeq \mathcal{O}_{\tilde{\mathcal{S}}}$. This follows from the classical adjunction formula, see, e.g., [EH16, Proposition 1.33]. Since $\tilde{\mathcal{S}}$ is a smooth divisor of multidegree $(2, 2, 2)$, we have

$$K_{\tilde{\mathcal{S}}} = (K_{\mathbb{P}^1 \times \mathbb{P}^1 \times \mathbb{P}^1}(2, 2, 2))|_{\tilde{\mathcal{S}}} = (\mathcal{O}_{\mathbb{P}^1 \times \mathbb{P}^1 \times \mathbb{P}^1}(-2, -2, -2) \otimes \mathcal{O}_{\mathbb{P}^1 \times \mathbb{P}^1 \times \mathbb{P}^1}(2, 2, 2))|_{\tilde{\mathcal{S}}} = \mathcal{O}_{\tilde{\mathcal{S}}}.$$

In order to show $h^1(\mathcal{O}_{\tilde{\mathcal{S}}}) = 0$, consider the restriction exact sequence of $\tilde{\mathcal{S}}$:

$$0 \rightarrow \mathcal{I}_{\tilde{\mathcal{S}}} \rightarrow \mathcal{O}_{\mathbb{P}^1 \times \mathbb{P}^1 \times \mathbb{P}^1} \rightarrow \mathcal{O}_{\tilde{\mathcal{S}}} \rightarrow 0.$$

Since $\tilde{\mathcal{S}}$ is a smooth divisor of multidegree $(2, 2, 2)$, we have $\mathcal{I}_{\tilde{\mathcal{S}}} \simeq \mathcal{O}_{\mathbb{P}^1 \times \mathbb{P}^1 \times \mathbb{P}^1}(-2, -2, -2)$; passing to the long exact sequence in cohomology, we have

$$\cdots \rightarrow H^1(\mathcal{O}_{\mathbb{P}^1 \times \mathbb{P}^1 \times \mathbb{P}^1}) \rightarrow H^1(\mathcal{O}_{\tilde{\mathcal{S}}}) \rightarrow H^2(\mathcal{O}_{\mathbb{P}^1 \times \mathbb{P}^1 \times \mathbb{P}^1}(-2, -2, -2)) \rightarrow \cdots$$

By Künneth's formula, $h^1(\mathcal{O}_{\mathbb{P}^1 \times \mathbb{P}^1 \times \mathbb{P}^1}) = 0$. Since $\mathcal{O}_{\mathbb{P}^1 \times \mathbb{P}^1 \times \mathbb{P}^1}(-2, -2, -2) = K_{\mathbb{P}^1 \times \mathbb{P}^1 \times \mathbb{P}^1}$, by Serre duality we obtain $h^2(\mathcal{O}_{\mathbb{P}^1 \times \mathbb{P}^1 \times \mathbb{P}^1}(-2, -2, -2)) = h^1(\mathcal{O}_{\mathbb{P}^1 \times \mathbb{P}^1 \times \mathbb{P}^1}) = 0$. We conclude $h^1(\mathcal{O}_{\tilde{\mathcal{S}}}) = 0$. This shows that $\tilde{\mathcal{S}}$ is a K3 surface.

It remains to show that $\phi : \tilde{\mathcal{S}} \rightarrow \mathcal{S}$ is a birational equivalence. This follows again by a direct calculation and by linearity of the addition map. Indeed, the set of critical points of the addition map $\Sigma : \partial_a D_1 \times \partial_a D_2 \times \partial_a D_3 \rightarrow \mathbb{C}^3$ is clearly birational to $\tilde{\mathcal{S}}$. Moreover, Theorem 2.2.13 implies that this set, regarded as a subvariety of $\mathbb{C}^9 = \mathbb{C}^3 \times \mathbb{C}^3 \times \mathbb{C}^3$, is a surface of degree 24. Since $\Sigma : \mathbb{C}^9 \rightarrow \mathbb{C}^3$ is linear, the degree of the image of (the birational copy of) $\tilde{\mathcal{S}}$ is at most 24; moreover, if equality holds, then Σ is generically one-to-one [Mum95, Theorem 5.11] and it defines a birational equivalence between the critical locus and its image. Since $\deg(\mathcal{S}) = 24$, we conclude. \square

The subdivision of \mathbb{R}^3 into its eight orthants induces a subdivision of the boundary of the dice, hence of $\text{Ext } \mathcal{D} = \mathcal{S} \cap \partial \mathcal{D}$. Each of these eight regions can be parametrized by the corresponding arcs on two of the three ∂D_i 's.

Let $p \in \mathcal{S} \cap \partial \mathcal{D}$ be written as $p = \xi_1 + \xi_2 + \xi_3$, with $\xi_i \in \partial D_i$. We parametrize the boundaries of the discs via angles $\theta_1, \theta_2, \theta_3$ as follows:

$$\begin{aligned}\partial D_1 &= \{(0, 0, 1) \cos \theta_1 + (0, 1, 0) \sin \theta_1 : \theta_1 \in [0, 2\pi]\}, \\ \partial D_2 &= \{(1, 0, 0) \cos \theta_2 + (0, 0, 1) \sin \theta_2 : \theta_2 \in [0, 2\pi]\}, \\ \partial D_3 &= \{(0, 1, 0) \cos \theta_3 + (1, 0, 0) \sin \theta_3 : \theta_3 \in [0, 2\pi]\}.\end{aligned}$$

Then the coordinates of ξ_3 can be expressed as algebraic functions of the coordinates of ξ_1 and ξ_2 . More precisely, from the equation of the determinant (2.2.5), we deduce

$$\begin{aligned}\cos \theta_3 &= \pm \frac{|\sin \theta_1 \sin \theta_2|}{\sqrt{\cos^2 \theta_1 \cos^2 \theta_2 + \sin^2 \theta_1 \sin^2 \theta_2}}, \\ \sin \theta_3 &= \pm \frac{|\cos \theta_1 \cos \theta_2|}{\sqrt{\cos^2 \theta_1 \cos^2 \theta_2 + \sin^2 \theta_1 \sin^2 \theta_2}}.\end{aligned}\tag{2.2.6}$$

If $(\theta_1, \theta_2) = (k\frac{\pi}{2}, (k+1)\frac{\pi}{2}) \times (l\frac{\pi}{2}, (l+1)\frac{\pi}{2})$, there are exactly two possible choices of the signs in (2.2.6) such that $\xi_1 + \xi_2 + \xi_3 \in \mathcal{S}$. This subdivides the real points of \mathcal{S} into $32 = 4 \cdot 4 \cdot 2$ regions. Exactly eight of these regions cover $\mathcal{S} \cap \partial \mathcal{D}$ and they are identified by the condition that ξ_1, ξ_2, ξ_3 belong to the same (closed) orthant. \blacklozenge

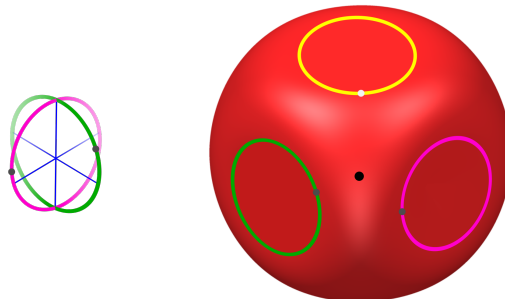


Figure 2.4: Parametrization of $\mathcal{S} \cap \partial \mathcal{D}$ with two of the three circles. Given a pair of generic (grey) points on the pink and green circle, there is a unique (white) point on the yellow circle, such that their sum is an extreme exposed point of \mathcal{D} (black).

2.2.4. Conclusions

We summarize our main results concerning the purely nonlinear part of a generic discotope.

- \mathcal{S} coincides with $\text{Ext}_a \mathcal{D}$ for the following types:

- ▶ $\mathbf{N} = (0, N, 0, \dots, 0)$ with $N \geq d - 1$;
- ▶ $\mathbf{N} = (0, \dots, 0, N)$.

- \mathcal{S} is irreducible in the following cases:

- ▶ when (2.2.1) holds with the reverse inequality, in which case $\deg(\mathcal{S}) = 2^N$;
- ▶ $\mathbf{N} = (0, N, 0, \dots, 0)$ with $N \geq d - 1$, in which case $\deg(\mathcal{S}) \leq 2^N \cdot \binom{N}{d-1}$;
- ▶ $\mathbf{N} = (0, \dots, 0, N)$.

In this section, we discuss some open problems, and observations directed toward future work. A first question one should address regards an analogue of Theorem 2.2.13 when discs of dimension higher than two are involved. We present an example to explain some of the difficulties.

Example 2.2.21. Let $D_1 = \{x_4 = 0, x_1^2 + x_2^2 + x_3^2 = 1\}$, $D_2 = \{x_1 = 0, x_2^2 + x_3^2 + x_4^2 = 1\}$ be two 3-discs in \mathbb{R}^4 and let $\mathcal{D} = D_1 + D_2$. This discotope is full dimensional and $\dim \mathcal{S} = 3$. The ideal of the critical locus of the addition map can be computed via a determinantal method similar to the one discussed in Section 2.2.3. We obtain the equation of \mathcal{S} ,

$$x_1^4 + 2x_1^2x_2^2 + x_2^4 + 2x_1^2x_3^2 + 2x_2^2x_3^2 + x_3^4 - 2x_1^2x_4^2 + 2x_2^2x_4^2 + 2x_3^2x_4^2 + x_4^4 - 4x_2^2 - 4x_3^2 = 0,$$

which is irreducible of degree 4. The boundary $\partial\mathcal{D}$ contains translates of the 3-dimensional discs: two translated copies of D_1 at $x_4 = \pm 1$ and two translated copies of D_2 at $x_1 = \pm 1$. The four points of their pairwise intersections are the only vertices: these points are $(1, 0, 0, 1), (-1, 0, 0, 1), (-1, 0, 0, -1), (1, 0, 0, -1)$ and they are, respectively, exposed by the cones

$$\begin{aligned} C_1 &= \{x_2 = x_3 = 0, x_1 > 0, x_4 > 0\}, \\ C_2 &= \{x_2 = x_3 = 0, x_1 < 0, x_4 > 0\}, \\ C_3 &= \{x_2 = x_3 = 0, x_1 < 0, x_4 < 0\}, \\ C_4 &= \{x_2 = x_3 = 0, x_1 > 0, x_4 < 0\}. \end{aligned}$$

Notice that for every i and for every $u \in C_i$, the hyperplane u^\perp contains $\langle D_1 \rangle \cap \langle D_2 \rangle$, as observed in Example 2.2.12. ◆

We point out that the determinantal method mentioned above to obtain the equation of \mathcal{S} is not as straightforward as in the case of 2-dimensional discs. Implicitly, this method relies on a parametrization of the tangent bundle of the product $\partial_a D_1 \times \dots \times \partial_a D_N$, in order to impose that the differential of the addition map has submaximal rank. For higher dimensional spheres this parametrization cannot be global since their tangent bundles are not trivial, unlike the case of the circle. Nevertheless, in the cases where it can be computed explicitly, the hypersurface \mathcal{S} is irreducible, hence it coincides with $\text{Ext}_a \mathcal{D}$. We propose the following:

Conjecture 2.2.22. Let \mathcal{D} be a generic discotope of type $(0, N_2, \dots, N_d)$. Then \mathcal{S} is irreducible.

Theorem 2.2.5 proves the conjecture if (2.2.1) holds with the reverse inequality. Remark 2.2.2 proves the statement in the case $(0, \dots, 0, N)$, and Theorem 2.2.13 in the case $(0, N, 0, \dots, 0)$. In general, we expect the critical locus of Σ to be already irreducible, and the addition map Σ to be a birational equivalence between $\text{crit } \Sigma$ and \mathcal{S} . Were this true, in the case of 2-dimensional discs, the upper bound in Theorem 2.2.13 would be an equality. For higher dimensional discs, even under the assumption that the critical locus is irreducible, computing its degree is non-trivial and it would be interesting to address it via the classical Giambelli-Thom-Porteous construction, applied to the product of the tangent bundles of the spheres $\partial_a D_i$.

The geometric features highlighted in this work can be used as necessary conditions for a convex body to be a discotope: for instance, there are restrictions for the degrees of $\text{Ext}_a \mathcal{D}$. An important future step would be to understand a characterization of discotopes among zonoids or more generally among convex bodies, in the spirit of the zonoid problem. We identify two problems in this direction.

Problem 2.2.23. Let $K \subseteq \mathbb{R}^d$ be a convex body and $D \subseteq \mathbb{R}^d$ be an n -dimensional (generalized) disc. Determine whether D is a Minkowski summand of K , in the sense that there exists a convex body $K' \subseteq \mathbb{R}^d$ such that $K = K' + D$.

Problem 2.2.23 is understood in the case where D is a disc of dimension 1, i.e. a segment [Bol69, Lemma 3.4]. We state the next problem in a probabilistic language.

Problem 2.2.24. Characterize the set of random vectors of \mathbb{R}^d whose associated Vitale zonoid is a full dimensional discotope in \mathbb{R}^d .

Finally, we expect discotopes not to be spectrahedra, except possibly for small special cases, for instance when $N = 1$. However, they are *spectrahedral shadows* [Sch18b] since they are defined as Minkowski sums of spectrahedra. We already observed that \mathcal{D} is the convex hull of the semialgebraic set $\mathcal{S} \cap \partial\mathcal{D}$. We propose the following conjecture, which is verified in the cases that we can compute explicitly.

Conjecture 2.2.25. The discotope \mathcal{D} is the convex hull of the real points of \mathcal{S} .

This would provide examples of real algebraic varieties whose convex hull is a spectrahedral shadow. This topic has been studied for instance in [Sch18a, RS10] and is related to the Helton–Nie conjecture [HN10]. Such questions draw connections between discotopes and the world of convex algebraic geometry, optimization and semidefinite programming.

Chapter 3

Constructions with convex bodies

Many areas of convex geometry investigate objects that are defined starting from a convex body. The goal is to describe relations between the original set and the new one. We consider here two particular constructions: fiber convex bodies and intersection bodies.

If K is a convex body in \mathbb{R}^{n+m} and $\pi : \mathbb{R}^{n+m} \rightarrow V$ is the orthogonal projection onto a subspace $V \subset \mathbb{R}^{n+m}$ of dimension n , the fiber body of K with respect to π is the *average* of the fibers of K under this projection:

$$\Sigma_\pi K = \int_{\pi(K)} (K \cap \pi^{-1}(x)) dx. \quad (3.0.1)$$

This expression is known as a Minkowski integral, and it will be made rigorous in Proposition 3.1.6.

Such a notion was introduced for polytopes by Billera and Sturmfels in [BS92]. It has been investigated in many different contexts, from combinatorics such as in [ADRS00] to algebraic geometry and even tropical geometry in the direction of polynomial systems [EK08, Est08, SY08]. Notably, recent studies concern the particular case of monotone path polytopes [BL21].

We focus here on the fiber bodies of convex bodies that are not polytopes. This construction was introduced and studied by Esterov in [Est08]. We state some general properties and then devote three subsections to the analysis of the fiber body of three particular classes of convex bodies.

Section 3.1.1 concerns the *puffed polytopes*, the affine version of the derivative cones, linked to the theory of hyperbolic polynomials. They are convex bodies that are obtained from polytopes by taking the ‘derivative’ of their algebraic boundary (see Definition 3.1.12). Propositions 3.1.17, 3.1.18 and 3.1.19 describe the strict convexity of the fiber body of a puffed polytope. As a concrete example we study the case of the ellotope and a particular projection.

In Section 3.1.2 we investigate the class of curved convex bodies. Namely, we consider convex bodies whose boundary is a C^2 hypersurface with a strictly positive curvature. In that case Theorem 3.1.24 gives an explicit formula for the support function of $\Sigma_\pi K$, directly in terms of the support function of K . This is an improvement of equation (3.1.2) which involves the support function of the fibers of K . We give an example in which the support function of the fiber body is easily computed using Theorem 3.1.24.

Finally, we go back to the case of zonoids. We prove that the fiber body of a zonoid is a zonoid, and give an explicit formula to compute it in Theorem 3.1.31. We then exhibit an example of a discotope, the dice, that has a fiber body which is not semialgebraic.

Hence, semialgebraicity is not preserved by the operation of computing the fiber body.

Section 3.2 focuses on intersection bodies of polytopes, from the perspective of real algebraic geometry. Originally, intersection bodies were defined by Lutwak [Lut88] in the context of convex geometry. In view of the notion of $(d-1)$ -dimensional cross-section measures and the related concepts of associated bodies (such as intersection bodies, cross-section bodies, and projection bodies), intersection bodies play an essential role in geometric tomography (see [Gar06, Chapter 8] and [Mar94, Section 2.3]). In particular, we mention here the Busemann-Petty problem which asks if one can compare the volumes of two convex bodies by comparing the volumes of their sections [Gar94a, Gar94b, GKS99, Kol98, Zha99b]. Moreover, Ludwig showed that the unique non-trivial $GL(\mathbb{R}^d)$ -covariant star-body-valued valuation on convex polytopes corresponds to taking the intersection body of the dual polytope [Lud06]. Due to such results, the knowledge on properties of intersection bodies interestingly contributes also to the (still not systematized) theory of starshaped sets, see [HHMM20, Section 17].

We study here intersection bodies of polytopes from a geometric and algebraic perspective. It is known that in \mathbb{R}^2 , the intersection body of a centrally symmetric polytope centered at the origin is the same polytope rotated by $\pi/2$ and dilated by a factor of 2 (see e.g. [Gar06, Theorem 8.1.4]). Moreover, if K is a full-dimensional convex body in \mathbb{R}^d centered at the origin, then so is its intersection body [Gar06, Chapter 8.1]. But what do these objects look like in general? In \mathbb{R}^d , with $d \geq 3$, they cannot be polytopes [Cam99, Zha99a] and they may not even be convex. In fact, for every convex body K , there exists a translate of K such that its intersection body is not convex [Gar06, Theorem 8.1.8]. This happens because of the important role played by the origin in this construction.

Our main contribution is Theorem 3.2.9, which states that the intersection body of a polytope is a semialgebraic set. The proof relies on two key facts. First, the volume of a polytope can be computed using determinants. Second, the combinatorial type of the intersection of a polytope with a hyperplane is fixed for each region of a certain central hyperplane arrangement. We first prove the semialgebraicity of the intersection body of polytopes containing the origin, and we generalize the result to arbitrary polytopes in Section 3.2.1. An implementation is available at <https://mathrepo.mis.mpg.de/intersection-bodies>. In Section 3.2.2, we describe the algebraic boundary of the intersection body, which is a hypersurface consisting of several irreducible components, each corresponding to a region of the aforementioned hyperplane arrangement. Theorem 3.2.14 gives a bound on the degree of the irreducible components. Section 3.2.3 focuses on the intersection body of the d -cube centered at the origin.

3.1. Fiber convex bodies

Consider the Euclidean vector space \mathbb{R}^{n+m} endowed with the standard Euclidean structure and let $V \subset \mathbb{R}^{n+m}$ be a subspace of dimension n . Denote by W its orthogonal complement, such that $\mathbb{R}^{n+m} = V \oplus W$. Let $\pi : \mathbb{R}^{n+m} \rightarrow V$ be the orthogonal projection onto V . We continue to canonically identify the Euclidean space with its dual.

If $K \in \mathcal{K}(\mathbb{R}^{n+m})$ we write K_x for the orthogonal projection onto W of the fiber of $\pi|_K$ over x , namely

$$K_x := \{y \in W \mid (x, y) \in K\}.$$

Definition 3.1.1. A map $\gamma : \pi(K) \rightarrow W$ such that for all $x \in \pi(K)$, $\gamma(x) \in K_x$ is called

a *section* of π . When there is no ambiguity on the map π we will simply say that γ is a *section*.

Using this notion we are able to define our object of study. Notice that the word *measurable* is always intended with respect to the Borelians.

Definition 3.1.2. The *fiber body* of K with respect to the projection π is the convex body

$$\Sigma_\pi K := \left\{ \int_{\pi(K)} \gamma(x) dx \mid \gamma : \pi(K) \rightarrow W \text{ measurable section} \right\} \in \mathcal{K}(W).$$

Here dx denotes the integration with respect to the n -dimensional Lebesgue measure on V . We say that a section γ *represents* $y \in \Sigma_\pi K$ if $y = \int_{\pi(K)} \gamma(x) dx$.

Remark 3.1.3. Note that, with this definition, if $\pi(K)$ is of dimension $< n$, then its fiber body is $\Sigma_\pi K = \{0\}$.

The notion of fiber bodies, that can be found for example in [Est08] under the name *Minkowski integral*, extends the classical construction of fiber polytopes [BS92], up to a constant. Here, we choose to omit the normalization $\frac{1}{\text{vol}(\pi(K))}$ in front of the integral used by Billera and Sturmfels in order to make apparent the *degree* of the map Σ_π seen in (3.1.1). This degree becomes clear with the notion of *mixed fiber body*, see [Est08, Theorem 1.2].

Proposition 3.1.4. For any $\lambda \in \mathbb{R}$ we have $\Sigma_\pi(\lambda K) = \lambda |\lambda|^n \Sigma_\pi K$. In particular if $\lambda \geq 0$

$$\Sigma_\pi(\lambda K) = \lambda^{n+1} \Sigma_\pi K. \quad (3.1.1)$$

Proof. If $\lambda = 0$ it is clear that the fiber body of $\{0\}$ is $\{0\}$. Suppose now that $\lambda \neq 0$ and let $\gamma : \pi(K) \rightarrow W$ be a section. We can define another section $\tilde{\gamma} : \pi(\lambda K) \rightarrow W$ by $\tilde{\gamma}(x) := \lambda \gamma\left(\frac{x}{\lambda}\right)$. Using the change of variables $y = x/\lambda$, we get that

$$\int_{\lambda\pi(K)} \tilde{\gamma}(x) dx = \lambda |\lambda|^n \int_{\pi(K)} \gamma(y) dy.$$

This proves that $\Sigma_\pi \lambda K \subseteq \lambda |\lambda|^n \Sigma_\pi K$. Repeating the same argument for λ^{-1} instead of λ , the other inclusion follows. \square

Corollary 3.1.5. If K is centrally symmetric then so is $\Sigma_\pi K$.

Proof. Apply the previous proposition with $\lambda = -1$ to get $\Sigma_\pi((-1)K) = (-1)\Sigma_\pi K$. If K is centrally symmetric with respect to the origin, then $(-1)K = K$ and the result follows. The general case is obtained by a translation. \square

As a consequence of the definition, it is possible to deduce a formula for the support function of the fiber body. This is the rigorous version of equation (3.0.1).

Proposition 3.1.6. For any $u \in W$ we have

$$h_{\Sigma_\pi K}(u) = \int_{\pi(K)} h_{K_x}(u) dx. \quad (3.1.2)$$

Proof. By definition

$$h_{\Sigma_\pi K}(u) = \sup \left\{ \int_{\pi(K)} \langle u, \gamma(x) \rangle dx \mid \gamma \text{ measurable section} \right\} \leq \int_{\pi(K)} h_{K_x}(u) dx.$$

To obtain the equality, it is enough to show that there exists a measurable section $\gamma_u : \pi(K) \rightarrow W$ with the following property: for all $x \in \pi(K)$ the point $\gamma_u(x)$ maximizes the linear form $\langle u, \cdot \rangle$ on K_x . In other words for all $x \in \pi(K)$, $\langle u, \gamma_u(x) \rangle = h_{K_x}(u)$. This is due to [Aum65, Proposition 2.1]. \square

A similar result can be shown for the exposed faces of the fiber body. Recall that K^u denotes the face of K exposed by the vector u . Moreover, if $\mathcal{U} = \{u_1, \dots, u_k\}$ is an ordered family of vectors of \mathbb{R}^{n+m} , we write

$$K^{\mathcal{U}} := (\cdots (K^{u_1})^{u_2} \cdots)^{u_k}.$$

We show that the exposed face of the fiber body is, in some sense, the fiber body of the exposed faces.

Lemma 3.1.7. Let $\mathcal{U} = \{u_1, \dots, u_k\}$ be a an ordered family of linearly independent vectors of W , take $y \in \Sigma_{\pi} K$ and let $\gamma : \pi(K) \rightarrow W$ be a section that represents y . Then $y \in (\Sigma_{\pi} K)^{\mathcal{U}}$ if and only if $\gamma(x) \in (K_x)^{\mathcal{U}}$ for almost all $x \in \pi(K)$. In particular we have that

$$(\Sigma_{\pi} K)^{\mathcal{U}} = \left\{ \int_{\pi(K)} \gamma(x) dx \mid \gamma \text{ section such that } \gamma(x) \in (K_x)^{\mathcal{U}} \text{ for all } x \right\}. \quad (3.1.3)$$

Proof. Suppose first that $\mathcal{U} = \{u\}$. Assume that $\gamma(x)$ is not in $(K_x)^u$ for all x in a set of non-zero measure $\mathcal{O} \subset \pi(K)$. Then there exists a measurable function $\xi : \pi(K) \rightarrow W$ with $\langle u, \xi \rangle \geq 0$ and $\langle u, \xi(x) \rangle > 0$ for all $x \in \mathcal{O}$, such that $\tilde{\gamma} := \gamma + \xi$ is a section (for example you can take $\tilde{\gamma}(x)$ to be the nearest point on K_x of $\gamma(x) + u$). Let $\tilde{y} := \int_{\pi(K)} \tilde{\gamma}$. Then $\langle u, \tilde{y} \rangle = \langle u, y \rangle + \int_{\pi(K)} \langle u, \xi \rangle > \langle u, y \rangle$. Thus y does not belong to the face $(\Sigma_{\pi} K)^u$.

Suppose now that y is not in the face $(\Sigma_{\pi} K)^{\mathcal{U}}$. Then there exists $\tilde{y} \in \Sigma_{\pi} K$ such that $\langle u, \tilde{y} \rangle > \langle u, y \rangle$. Let $\tilde{\gamma}$ be a section that represents \tilde{y} . It follows that $\int_{\pi(K)} \langle u, \tilde{\gamma} \rangle > \int_{\pi(K)} \langle u, \gamma \rangle$. This implies the existence of a set $\mathcal{O} \subset \pi(K)$ of non-zero measure where $\langle u, \tilde{\gamma}(x) \rangle > \langle u, \gamma(x) \rangle$ for all $x \in \mathcal{O}$. Thus for all $x \in \mathcal{O}$, $\gamma(x)$ does not belong to the face $(K_x)^u$.

In the case $\mathcal{U} = \{u_1, \dots, u_{k+1}\}$ we can apply inductively the same argument. Replace $\Sigma_{\pi} K$ by $(\Sigma_{\pi} K)^{\{u_1, \dots, u_k\}}$ and u by u_{k+1} , and use the representation of $(\Sigma_{\pi} K)^{\{u_1, \dots, u_k\}}$ given by (3.1.3). \square

Using the same strategy of Proposition 3.1.6 we can deduce that for every $u, v \in W$,

$$h_{(\Sigma_{\pi} K)^u}(v) = \int_{\pi(K)} h_{(K_x)^u}(v) dx. \quad (3.1.4)$$

The fiber body behaves well under the action of $\mathrm{GL}(V) \oplus \mathrm{GL}(W)$ as a subgroup of $\mathrm{GL}(\mathbb{R}^{n+m})$.

Proposition 3.1.8. Let $g_n \in \mathrm{GL}(V)$, $g_m \in \mathrm{GL}(W)$ and $K \in \mathcal{K}(\mathbb{R}^{n+m})$. Then

$$\Sigma_{\pi}((g_n \oplus g_m)(K)) = |\det(g_n)| \cdot g_m(\Sigma_{\pi} K).$$

Proof. This is a quite straightforward consequence of the definitions. After observing that

$$((g_n \oplus g_m)(K))_x = g_m(K_{g_n^{-1}(x)})$$

and $\pi((g_n \oplus g_m)(K)) = g_n \pi(K)$, use equation (3.1.2) with the change of variables $x \mapsto g_n^{-1}x$. By Proposition 1.1.19-(iii) we have $h_{g_m K_x}(u) = h_{K_x}(g_m^t u)$, so the thesis follows. \square

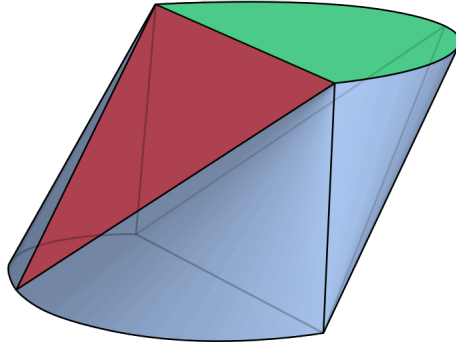


Figure 3.1: The convex body of Example 3.1.9. In its boundary there are 2 green half discs, 2 red triangles and 4 blue cones.

Regularity of the sections. By definition, a point y of the fiber body $\Sigma_\pi K$ is the integral $y = \int_{\pi(K)} \gamma(x)dx$ of a *measurable* section γ . Thus γ can be modified on a set of measure zero without changing the point y , i.e. y only depends on the L^1 class of γ . It is natural to ask what our favourite representative in this L^1 class will be and how regular can it be. In the case where K is a polytope, γ can always be chosen continuous. However if K is not a polytope and if y belongs to the boundary of $\Sigma_\pi K$, a continuous representative may not exist. This is due to the fact that in general the map $x \mapsto K_x$ is only upper semicontinuous, see [Kho12, Section 6].

Example 3.1.9. Consider the function $f : S^1 \rightarrow \mathbb{R}$ such that

$$f(x, y) = \begin{cases} 0 & x < 0 \\ 1 & x \geq 0 \end{cases}$$

and let $K := \text{conv}(\text{graph}(f)) \subset \mathbb{R}^3$, displayed in Figure 3.1. This is a semialgebraic convex body, whose boundary may be subdivided in 8 patches: two half-discs lying on the planes $\{z = 0\}$ and $\{z = 1\}$, two triangles with vertices $(-1, 0, 0), (0, \pm 1, 1)$ and $(1, 0, 1), (0, \pm 1, 0)$ respectively, four cones with vertices $(0, \pm 1, 0), (0, \pm 1, 1)$. Let $\pi : \mathbb{R}^3 \rightarrow \mathbb{R}$ be the projection on the first coordinate $\pi(x, y, z) = x$. Then the point $p \in \Sigma_\pi K \subset \mathbb{R}^2$ maximizing the linear form associated to $(y, z) = (1, 0)$ must have only non-continuous sections. This can be proved using the representation of a face given by (3.1.3). \blacklozenge

We prove that most of the points of the fiber body have a continuous representative.

Proposition 3.1.10. Let $K \in \mathcal{K}(\mathbb{R}^{n+m})$ and let $\Sigma_\pi K$ be its fiber body. The set of its points that can be represented by a continuous section is convex and dense. In particular, all interior points of $\Sigma_\pi K$ can be represented by a continuous section.

Proof. Consider the set

$$C = \left\{ \int_{\pi(K)} \gamma(x)dx \mid \gamma : \pi(K) \rightarrow K \text{ continuous section} \right\}$$

that is clearly contained in the fiber body $\Sigma_\pi K$. It is convex: take $a, b \in C$ represented by continuous sections $\alpha, \beta : \pi(K) \rightarrow K$ respectively. Then any convex combination can be written as $c = ta + (1 - t)b = \int_{\pi(K)} (t\alpha(x) + (1 - t)\beta(x))dx$. Since $t\alpha + (1 - t)\beta$ is a continuous section for any $t \in [0, 1]$, C is convex.

We now need to prove that the set C is also dense in $\Sigma_\pi K$. Let γ be a measurable section; by definition it is a measurable function $\gamma : \pi(K) \rightarrow W$, such that $\gamma(x) \in K_x$ for

all $x \in \pi(K)$. For every $\varepsilon > 0$ there exists a continuous function $g : \pi(K) \rightarrow W$ with $\|\gamma - g\|_{L^1} < \varepsilon$; this is not necessarily a section of K , since a priori $g(x)$ can be outside K_x . Hence, define $\tilde{\gamma} : \pi(K) \rightarrow W$ such that

$$\tilde{\gamma}(x) = p(K_x, g(x))$$

where $p(A, a)$ is the nearest point map at a with respect to the convex set A . By [Sch13, Lemma 1.8.11] $\tilde{\gamma}$ is continuous and by definition $\text{graph}(\tilde{\gamma}) \subset K$. Therefore $\int_{\pi(K)} \tilde{\gamma} \in C$. Moreover,

$$\|\gamma - \tilde{\gamma}\|_{L^1} \leq \|\gamma - g\|_{L^1} < \varepsilon$$

hence the density is proved. As a consequence we get that $\text{int } \Sigma_\pi K \subseteq C \subseteq \Sigma_\pi K$ so all the interior points of the fiber body have a continuous representative. \square

To our knowledge, the minimal regularity of the sections needed to represent all points is not known.

Strict convexity. In the case where K^u consists of only one point we say that K is *strictly convex in direction u* . If convex body is strictly convex in every direction, then it is strictly convex. We now investigate this property for fiber bodies.

Proposition 3.1.11. Let $K \in \mathcal{K}(\mathbb{R}^{n+m})$ and let us fix a vector $u \in W$. The following are equivalent:

- (i) $\Sigma_\pi K$ is strictly convex in direction u ;
- (ii) almost all the fibers K_x are strictly convex in direction u .

Proof. By Proposition 1.1.19-(iv), a convex body is strictly convex in direction u if and only if its support function is C^1 at u . Therefore, if almost all the fibers K_x are strictly convex in u then, the convex body being compact, the support function $h_{\Sigma_\pi K}(u) = \int_{\pi(K)} h_{K_x}(u) dx$ is C^1 at u , i.e., the fiber body is strictly convex in that direction.

Now suppose that $\Sigma_\pi K$ is strictly convex in direction u , i.e. $(\Sigma_\pi K)^u$ consists of just one point y . This means that the support function of this face is linear and it is given by $\langle y, \cdot \rangle$. We now prove that the support function of K_x^u is linear for almost all x , and this will conclude the proof. Equation (3.1.4) implies that

$$h_{(\Sigma_\pi K)^u} = \int_{\pi(K)} h_{K_x^u} dx = \langle y, \cdot \rangle.$$

For any two vectors v_1, v_2 , we have

$$\langle y, v_1 + v_2 \rangle = \int_{\pi(K)} h_{K_x^u}(v_1 + v_2) dx \leq \int_{\pi(K)} h_{K_x^u}(v_1) dx + \int_{\pi(K)} h_{K_x^u}(v_2) dx = \langle y, v_1 \rangle + \langle y, v_2 \rangle$$

thus the inequality in the middle must be an equality. But since $h_{K_x^u}(v_1 + v_2) \leq h_{K_x^u}(v_1) + h_{K_x^u}(v_2)$, we get that this is an equality for almost all x , i.e. the support function of K_x^u is linear for almost every $x \in \pi(K)$. Therefore almost all the fibers are strictly convex. \square

Example 3.1.20 provides a convex body, the ellipope K , and a projection π such that the fiber body $\Sigma_\pi K$ is strictly convex, but the two fibers $K_{\pm 1}$ are segments, hence not strictly convex.

3.1.1. Puffed polytopes

In this section we introduce a particular class of convex bodies arising from polytopes. A known concept in the context of hyperbolic polynomials and hyperbolicity cones is that of the *derivative cone*; see [Ren06] or [San13]. Since we are dealing with compact objects, we will repeat the same construction in affine coordinates, i.e. for polytopes instead of polyhedral cones.

Let P be a full dimensional polytope in \mathbb{R}^d , containing the origin, with N facets given by affine equations $l_1(x_1, \dots, x_d) = a_1, \dots, l_N(x_1, \dots, x_d) = a_N$. Consider the polynomial

$$p(x_1, \dots, x_d) = \prod_{i=1}^N (l_i(x_1, \dots, x_d) - a_i). \quad (3.1.5)$$

Its zero locus is the algebraic boundary of P . Consider the homogenization of p , that is $\tilde{p}(x_1, \dots, x_d, w) = \prod_{i=1}^N (l_i(x_1, \dots, x_d) - a_i w)$. It is the algebraic boundary of a polyhedral cone and it is hyperbolic with respect to the direction $(0, \dots, 0, 1) \in \mathbb{R}^{d+1}$. Then for all $i < N$ the polynomial

$$\left(\frac{\partial^i}{\partial w^i} \tilde{p} \right) (x_1, \dots, x_d, 1) \quad (3.1.6)$$

is the algebraic boundary of a convex set containing the origin, see [San13].

Definition 3.1.12. Let Z_i be the zero locus of (3.1.6) in \mathbb{R}^d . The i -th puffed P is the closure of the connected component of the origin in $\mathbb{R}^d \setminus Z_i$. We denote it by $\text{puff}_i(P)$.

In particular the puffed polytopes are always spectrahedra [Brä14, Corollary 1.3]. As the name suggests, the puffed polytopes $\text{puff}_i(P)$ are fat, inflated versions of the polytope P and in fact contain P . On the other hand, despite the definition involves a derivation, the operation of ‘taking the puffed’ does not behave as a derivative. In particular, it does not commute with the Minkowski sum, that is, in general for polytopes P_1, P_2 :

$$\text{puff}_1(P_1 + P_2) \neq \text{puff}_1(P_1) + \text{puff}_1(P_2).$$

To show this with, we build a counterexample in dimension $N = 2$.

Example 3.1.13. Let us consider two squares in \mathbb{R}^2 , namely $P_1 = \text{conv}\{(\pm 1, \pm 1)\}$ and $P_2 = \text{conv}\{(0, \pm 1), (\pm 1, 0)\}$. The first puffed square is a ball with radius half of the diagonal, so $\text{puff}_1(P_1)$ has radius $\sqrt{2}$ and $\text{puff}_1(P_2)$ has radius 1. Therefore $\text{puff}_1(P_1) + \text{puff}_1(P_2)$ is a ball centered at the origin of radius $1 + \sqrt{2}$. On the other hand $P_1 + P_2$ is an octagon. Its associated polynomial in (3.1.5) is

$$p(x, y) = ((x + y)^2 - 9)((x - y)^2 - 9)(x^2 - 4)(y^2 - 4).$$

Via the procedure explained above we obtain the boundary of this puffed octagon as the zero locus of the following irreducible polynomial

$$2x^6 + 7x^4y^2 + 7x^2y^4 + 2y^6 - 88x^4 - 193x^2y^2 - 88y^4 + 918x^2 + 918y^2 - 2592.$$

This is a curve with three real connected components, shown in violet in Figure 3.2. The puffed octagon is not a ball, hence $\text{puff}_1(P_1) + \text{puff}_1(P_2) \neq \text{puff}_1(P_1 + P_2)$. \blacklozenge

Strict convexity of the puffed polytopes. Our aim is to study the strict convexity of the fiber body of a puffed polytope. In order to do so, we shall at first say something more about the boundary structure of a puffed polytope itself. In particular, we will see

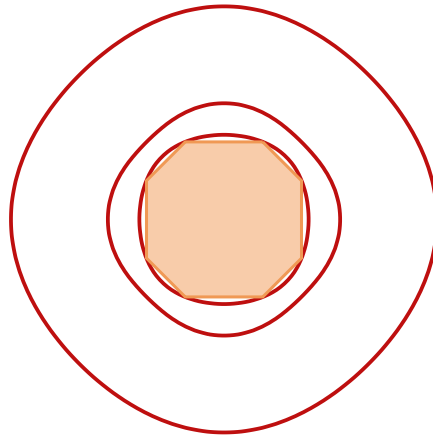


Figure 3.2: The octagon, orange; the algebraic boundary of its puffed octagon, red.

that the appropriate quantity to consider is the *multiplicity* of the faces, that is, their multiplicity as zeroes of the polynomial defining the algebraic boundary. Indeed, a face $F \subset P$ will be part of the boundary of $\text{puff}_i(P)$ for all i less or equal than the multiplicity of F .

Lemma 3.1.14. Let $P \subset \mathbb{R}^d$ be a full dimensional polytope. Then all faces F of P of dimension $k < d - i$, are contained in the boundary of $\text{puff}_i(P)$.

Proof. Let F be a k -face of P ; it is contained in the zero set of the polynomial (3.1.5). Moreover F arises as the intersection of at least $d - k$ facets, thus its points are zeros of multiplicity at least $d - k$. Hence, if $d - k > i$ the face F is still in the zero set of (3.1.6), i.e. it belongs to the boundary of $\text{puff}_i(P)$. \square

The other direction is not always true: there may be k -faces of P , with $k \geq d - i$, whose points are zeros of (3.1.6) of multiplicity higher than i , and hence faces of $\text{puff}_i(P)$. However, there are two cases in which this is not possible.

Lemma 3.1.15. Let $P \subset \mathbb{R}^d$ be a full dimensional polytope.

- $i = 1$: the flat faces of $\text{puff}_1(P)$ are exactly the faces of dimension $k < d - 1$;
- $i = 2$: the flat faces of $\text{puff}_2(P)$ are exactly the faces of dimension $k < d - 2$.

Proof. The first point is clear because the facets are the only zeroes of multiplicity one. The second point follows from the so called ‘diamond property’ of polytopes [Zie12]. \square

Remark 3.1.16. By [Ren06, Proposition 24] we deduce that the flat faces of a puffed polytope must be faces of the polytope itself. The remaining points in the boundary of $\text{puff}_i(P)$ are exposed points.

Using this result we can deduce conditions for the strict convexity of the fiber body of a puffed polytope.

Proposition 3.1.17 (Fiber 1st puffed polytope). Let $P \subset \mathbb{R}^{n+m}$ be a full dimensional polytope, $n \geq 1$, $m \geq 2$, and take any projection $\pi : \mathbb{R}^{n+m} \rightarrow \mathbb{R}^n$. The fiber puffed polytope $\Sigma_\pi(\text{puff}_1(P))$ is strictly convex if and only if $m = 2$.

Proof. By Lemma 3.1.15, the flat faces in the boundary of $\text{puff}_1(P)$ are the faces of P of dimension $k < n + m - 1$. Suppose first that $m > 2$ and let F be a $(n + m - 2)$ -face of P . Take a point p in the relative interior of F and let $x_p := \pi(p)$. Then the dimension of $F \cap \pi^{-1}(x_p)$ is at least $m - 2 \geq 1$; we can also assume without loss of generality that

$$1 \leq \dim(F \cap \pi^{-1}(x_p)) < n + m - 2. \quad (3.1.7)$$

Furthermore there is a whole neighborhood U of x_p such that condition (3.1.7) holds, so for every $x \in U$ the convex body $(\text{puff}_1(P))_x$ is not strictly convex. By Proposition 3.1.11 then $\Sigma_\pi(\text{puff}_1(P))$ is not strictly convex. Suppose now that $m = 2$ and fix a flat face F of $\text{puff}_1(P)$. Its dimension is less or equal than n , so $(F \cap \pi^{-1}(x_p))$ is either one point or a face of positive dimension. In the latter case $\dim \pi(F) \leq n - 1$, i.e. it is a set of measure zero in $\pi(\text{puff}_1(P))$. Because there are only finitely many flat faces, we can conclude that almost all the fibers are strictly convex and thus by Proposition 3.1.11, $\Sigma_\pi(\text{puff}_1(P))$ is strictly convex. \square

A similar result holds for the second fiber puffed polytope, using Lemma 3.1.15.

Proposition 3.1.18 (Fiber 2nd puffed polytope). Let $P \subset \mathbb{R}^{n+m}$ be a full dimensional polytope, $n \geq 1$, $m \geq 2$, and take any projection $\pi : \mathbb{R}^{n+m} \rightarrow \mathbb{R}^n$. The fiber puffed polytope $\Sigma_\pi(\text{puff}_2(P))$ is strictly convex if and only if $m \leq 3$, i.e. $m = 2$ or 3 .

Proof. We can use the previous strategy again. If $m > 3$, there always exists a face of $\text{puff}_2(P)$ of dimension $n + m - 3$ whose non-empty intersection with fibers of π has dimension at least 1 and strictly less than $n + m - 3$. In this case we get a non strictly convex fiber body. On the other hand, when $m = 2$ or 3 the intersection of the fibers and the flat faces has positive dimension only on a measure zero subset of \mathbb{R}^n , hence almost all the fibers are strictly convex and the thesis follows. \square

Can we generalize this result for the i -th puffed polytope? In general no, and the reason is precisely that a k -face may be contained in more than $(n + m - k)$ facets, when $k < n + m - 2$. Those polytopes P for which this does not happen are called *simple polytopes*. Thus, with the same proof as above we obtain the following.

Proposition 3.1.19 (Fiber i -th puffed simple polytope). Let $P \subset \mathbb{R}^{n+m}$ be a full dimensional simple polytope, $n \geq 1$, $m \geq 2$, and take any projection $\pi : \mathbb{R}^{n+m} \rightarrow \mathbb{R}^n$. The fiber puffed polytope $\Sigma_\pi(\text{puff}_i(P))$ is strictly convex if and only if $m \leq i + 1$.

In the case where P is not simple, one has to take into account the multiplicity of each face of dimension $k \geq n + m - i$, in order to understand if they are or not part of the boundary of $\text{puff}_i(P)$.

Example 3.1.20. Let P be the tetrahedron in \mathbb{R}^3 realized as

$$\text{conv}\{(1, 1, 1), (1, -1, -1), (-1, 1, -1), (-1, -1, 1)\}.$$

The first puffed tetrahedron (for the rest of the paragraph we will omit the term ‘first’) is the ellipotope K from Example 1.2.10. Let π be the projection on the first coordinate: $\pi(x, y, z) = x$. The fibers of the ellipotope at x for $x \in (-1, 1)$ are the ellipses defined by

$$K_x = \left\{ (y, z) \mid \left(\frac{y - xz}{\sqrt{1 - x^2}} \right)^2 + z^2 \leq 1 \right\}.$$

Introducing the matrix

$$M_x := \begin{pmatrix} \frac{1}{\sqrt{1-x^2}} & \frac{-x}{\sqrt{1-x^2}} \\ 0 & 1 \end{pmatrix}$$

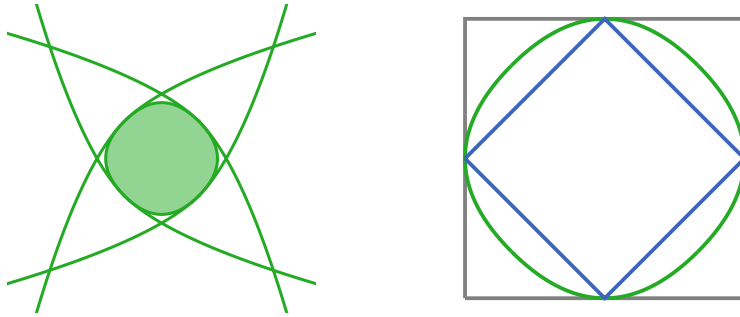


Figure 3.3: Left: the four green parabolas meet in the four black points on the boundary of the fiber elliptope, that lie on the diagonals $y = z$ and $y = -z$. Right: sandwiched fiber bodies. The blue rhombus is the fiber tetrahedron $\Sigma_\pi P$; the green convex body is the fiber elliptope $\Sigma_\pi K$; the grey square is the fiber cube $\Sigma_\pi([-1, 1]^3)$.

it turns out that $K_x = \{(y, z) \mid \|M_x(y, z)\|^2 \leq 1\} = (M_x)^{-1}B^2$, where B^2 is the unit 2-disc. We obtain

$$h_{K_x}(u, v) = h_{B^2}\left((M_x)^{-t}(u, v)\right) = \|(M_x)^{-t}(u, v)\| = \sqrt{u^2 + v^2 + 2xuv}.$$

By (3.1.2) we need to compute the integral of h_{K_x} between $x = -1$ and $x = 1$ to obtain the support function of the fiber body of the ellipope. We get

$$h_{\Sigma_\pi K}(u, v) = \frac{1}{3uv}(|u + v|^3 - |u - v|^3).$$

Hence the fiber body is semialgebraic and its algebraic boundary is the zero set of the four parabolas $3y^2 + 8z - 16$, $3y^2 - 8z - 16$, $8y + 3z^2 - 16$, $8y - 3z^2 + 16$, displayed in Figure 3.3, left.

As anticipated in Proposition 3.1.17 the fiber elliptope is strictly convex. Notice that the ellipope is naturally sandwiched between two polytopes: the tetrahedron P and the cube $[-1, 1]^3$. Therefore, as a natural consequence of the definition, the same chain of inclusions works also for their fiber bodies:

$$\Sigma_\pi P \subset \Sigma_\pi K \subset \Sigma_\pi([-1, 1]^3)$$

as shown in Figure 3.3, right. ♦

Remark 3.1.21. From this example it is clear that the operation of ‘taking the fiber body’ does not commute with the operation of ‘taking the puffed polytope’. In fact the puffed polytope of the blue square in Figure 3.3, right, is not the green convex body bounded by the four parabolas: it is the disc $y^2 + z^2 \leq 4$.

3.1.2. Curved convex bodies

In this section we are interested in the case where the boundary of the convex body K is highly regular. We prove Theorem 3.1.24 which is a formula to compute the support function of the fiber body directly in terms of the support function of K , without having to compute those of the fibers.

Definition 3.1.22. We say that a convex body K is *curved* if its support function h_K is C^2 and the gradient ∇h_K restricted to the sphere is a C^1 diffeomorphism with the boundary of K .

In that case K is full dimensional, strictly convex, and its boundary is a C^2 hypersurface. Such convex bodies are treated in [Sch13, Section 2.5], where they are said to be ‘of class C_+^2 ’. If $K \in \mathcal{K}(\mathbb{R}^{n+m})$ is a curved convex body and $v \in S^{n+m-1}$, then the differential $d_v \nabla h_K$ is a symmetric positive definite automorphism of v^\perp . The following gives an expression for the exposed points of the fiber body. This is to be compared with the case of polytopes which is given in [EK08, Lemma 11].

Lemma 3.1.23. If K is a curved convex body and $u \in W$ with $\|u\| = 1$, then

$$\nabla h_{\Sigma_\pi K}(u) = \int_V \nabla h_K(u + \xi) \cdot J_{\psi_u}(\xi) \, d\xi$$

where $\psi_u : V \rightarrow V$ is given by $\psi_u(\xi) = (\pi \circ \nabla h_K)(u + \xi)$ and $J_{\psi_u}(\xi)$ denotes its Jacobian (i.e. the determinant of its differential) at the point ξ .

Proof. From (3.1.3) we have that $\nabla h_{\Sigma_\pi K}(u) = \int_{\pi(K)} \gamma_u(x) dx$, where $\gamma_u(x) = \nabla h_{K_x}(u)$. Assume that $x = \psi_u(\xi)$, as defined in the statement, is a change of variables. We get $\gamma_u(x) = (\gamma_u \circ \pi \circ \nabla h_K)(u + \xi) = \nabla h_K(u + \xi)$ and the result follows.

It remains to prove that it is indeed a change of variables. Note that $\nabla h_K(u + \xi) = \nabla h_K(v)$ where $v = \frac{u+\xi}{\|u+\xi\|} \in S^{n+m-1}$. The differential of the map $\xi \mapsto v$ maps V to $(V + \mathbb{R}u) \cap v^\perp$. Moreover ∇h_K restricted to the sphere is a C^1 diffeomorphism by assumption. Thus it only remains to prove that its differential $d_v \nabla h_K$ sends $(V + \mathbb{R}u) \cap v^\perp$ to a subspace that does not intersect $\ker(\pi|_{v^\perp})$. To see this, note that $\ker(\pi|_{v^\perp})^\perp = (V + \mathbb{R}u) \cap v^\perp$. Moreover $\langle w, d_v \nabla h_K \cdot w \rangle = 0$ if and only if $w = 0$. Thus, if $w \in \ker(\pi|_{v^\perp})^\perp$ and $w \neq 0$, then $\pi(d_v \nabla h_K \cdot w) \neq 0$. Putting everything together, this proves that $d_\xi \psi_u$ has no kernel, which is what we wanted. \square

As a direct consequence we derive a formula for the support function.

Theorem 3.1.24. Let $K \in \mathcal{K}(\mathbb{R}^{n+m})$ be a curved convex body. Then the support function of its fiber body is

$$h_{\Sigma_\pi K}(u) = \int_V \langle u, \nabla h_K(u + \xi) \rangle \cdot J_{\psi_u}(\xi) \, d\xi \quad (3.1.8)$$

for all $u \in W$, where $\psi_u : V \rightarrow V$ is given by $\psi_u(\xi) = (\pi \circ \nabla h_K)(u + \xi)$ and $J_{\psi_u}(\xi)$ denotes its Jacobian at the point ξ .

Proof. Apply the previous lemma to $h_{\Sigma_\pi K}(u) = \langle u, \nabla h_{\Sigma_\pi K}(u) \rangle$. \square

Assume that the support function h_K is *algebraic*, i.e. it is a root of some polynomial equation. Then the integrand in Lemma 3.1.23 and in Theorem 3.1.24 is also algebraic. Indeed, it is simply $\nabla h_K(u + \xi)$ times the Jacobian of ψ_u , which is a composition of algebraic functions. We can generalize this concept in the direction of D -modules (see [Zei90], or [SS19] for a text with a view towards applied nonlinear algebra). One can define what it means for a D -ideal of the Weyl algebra D to be *holonomic*. Then a function is holonomic if its annihilator, a D -ideal, is holonomic. Intuitively, this means that such a function satisfies a system of linear homogeneous differential equations with polynomial coefficients, plus a suitable dimension condition. Holonomicity can be seen as a generalization of algebraicity which is closed under integration. We say that a convex body K is *holonomic* if its support function h_K is holonomic. In this setting, the fiber body satisfies the following property.

Corollary 3.1.25. If K is a curved holonomic convex body, then its fiber body is again holonomic.

Proof. We prove that the integrand in Theorem 3.1.24 is a holonomic function of u and ξ . Then the result follows from the fact that the integral of a holonomic function is holonomic [SS19, Proposition 2.11]. If h_K is holonomic then $\nabla h_K(u + \xi)$ is a holonomic function of u and ξ , as well as its scalar product with u . It remains to prove that the Jacobian of ψ_u is holonomic. But ψ_u is the projection of a holonomic function and thus holonomic, so the result follows. \square

Example 3.1.26. In [Sch13, note 6 of Section 3.5] Schneider exhibits an example of a one parameter family of semialgebraic centrally symmetric convex bodies that are not zonoids. Their support function is polynomial when restricted to the sphere. We will show how in that case Theorem 3.1.24 makes the computation of the fiber body relatively easy.

Schneider's polynomial body is the convex body $K_\alpha \in \mathcal{K}(\mathbb{R}^3)$ whose support function is given by

$$h_{K_\alpha}(u) = \|u\| \left(1 + \frac{\alpha}{2} \left(\frac{3(u_3)^2}{\|u\|^2} - 1 \right) \right)$$

for $\alpha \in [-8/20, -5/20]$. Let $\pi := \langle e_1, \cdot \rangle : \mathbb{R} \oplus \mathbb{R}^2 \rightarrow \mathbb{R}$ be the projection onto the first coordinate. We want to apply Theorem 3.1.24 to compute the support function of $\Sigma_\pi K_\alpha$. For the gradient we obtain:

$$\nabla h_{K_\alpha}(u) = \frac{1}{2\|u\|^3} \begin{pmatrix} -u_1 ((u_1)^2(\alpha - 2) + (u_2)^2(\alpha - 2) + 2(u_3)^2(2\alpha - 1)) \\ -u_2 ((u_1)^2(\alpha - 2) + (u_2)^2(\alpha - 2) + 2(u_3)^2(2\alpha - 1)) \\ \frac{u_3}{\|u\|^2} ((u_1)^2(5\alpha + 2) + (u_2)^2(5\alpha + 2) + 2(u_3)^2(2\alpha + 1)) \end{pmatrix}.$$

For $u = (0, u_2, u_3)$, the Jacobian is $J_{\psi_u}(t) = \frac{d}{dt} (\pi \circ \nabla h_{K_\alpha}(t, u_2, u_3))$, which gives

$$J_{\psi_u}(t) = \frac{t^2(-(u_2)^2(\alpha - 2) + (u_3)^2(5\alpha + 2)) - \|u\|^2((u_2)^2(\alpha - 2) + 2(u_3)^2(2\alpha - 1))}{2(t^2 + \|u\|^2)^{\frac{5}{2}}}.$$

Substituting in (3.1.8), we integrate $\langle u, \nabla h_{K_\alpha}(t, u_2, u_3) \rangle \cdot J_{\psi_u}(t)$ and get the support function of the fiber body (see Figure 3.4) which is again polynomial: $h_{\Sigma_\pi K_\alpha}(u)$ equals

$$\frac{\pi}{64\|u\|^3} \left(8(\alpha - 2)(u_2)^4 - 8(\alpha^2 + 2\alpha - 8)(u_2)^2(u_3)^2 + (-25\alpha^2 + 16\alpha + 32)(u_3)^4 \right).$$

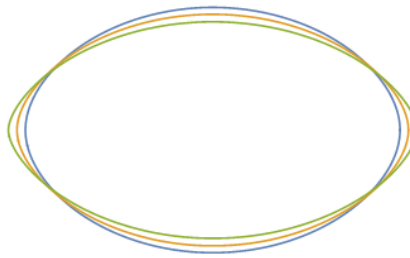


Figure 3.4: The fiber bodies of Schneider's polynomial bodies for $\alpha = -i/20$ with $i = 5, 6$ and 7



3.1.3. Fiber zonoids

We now show that the fiber body of a zonoid is a zonoid and give a formula to compute it in Theorem 3.1.31. Let us first introduce some of the tools used by Esterov in [Est08]. For any $u \in W$ let $T_u = \mathbf{1}_V \oplus \langle u, \cdot \rangle : V \oplus W \rightarrow V \oplus \mathbb{R}$.

Definition 3.1.27. Let $C \in \mathcal{K}(V \oplus \mathbb{R})$ and let π be the orthogonal projection onto V . The *shadow volume* $V_+(C)$ of C is defined to be the integral of the maximal function on $\pi(C) \subset V$ such that its graph is contained in C , i.e.

$$V_+(C) = \int_{\pi(C)} \varphi(x) dx,$$

where $\varphi(x) = \sup \{t \mid (x, t) \in C\}$. In particular if $(-1)C = C$, then the shadow volume is $V_+(C) = \frac{1}{2} \text{vol}_{n+1}(C)$.

The shadow volume can then be used to express the support function of the fiber body.

Lemma 3.1.28. For $u \in W$ and $K \in \mathcal{K}(\mathbb{R}^{n+m})$, we have

$$h_{\Sigma_\pi K}(u) = V_+(T_u(K)).$$

In particular, if $(-1)K = K$

$$h_{\Sigma_\pi K}(u) = \frac{1}{2} \text{vol}_{n+1}(T_u(K)). \quad (3.1.9)$$

Proof. We also denote by $\pi : V \oplus \mathbb{R} \rightarrow V$ the projection onto V . The shadow volume is the integral on $\pi(T_u(K)) = \pi(K)$ of the function $\varphi(x) = \sup \{t \mid (x, t) \in T_u(K)\} = \sup \{\langle u, y \rangle \mid (x, y) \in K\} = h_{K_x}(u)$. Thus the result follows from Proposition 3.1.6. \square

Remark 3.1.29. Note that if $m = 2$ then T_u is the projection onto the hyperplane spanned by V and u . In that case (3.1.9) is the formula for the support function of the *projection body* ΠK of K at gu , where g is a rotation by $\pi/2$ in W , see [Sch13, Section 10.9]. In that case, $\Sigma_\pi K$ is the projection of ΠK onto W rotated by $\pi/2$.

We will show that the mixed fiber body of zonoids comes from a multilinear map defined directly on the vector spaces.

Definition 3.1.30. We define the following (completely skew-symmetric) multilinear map:

$$\begin{aligned} F_\pi : (V \oplus W)^{n+1} &\rightarrow W \\ ((x_1, y_1), \dots, (x_{n+1}, y_{n+1})) &\mapsto \frac{1}{(n+1)!} \sum_{i=1}^{n+1} (-1)^{n+1-i} (x_1 \wedge \dots \wedge \hat{x}_i \wedge \dots \wedge x_{n+1}) y_i \end{aligned}$$

where $x_1 \wedge \dots \wedge \hat{x}_i \wedge \dots \wedge x_{n+1}$ denotes the determinant of the chosen vectors, omitting x_i .

We are now able to prove the main result of this section, here stated in the probabilistic language of Vitale zonoids, as in Theorem 2.1.6.

Theorem 3.1.31. The fiber body of a zonoid is a zonoid. Moreover, if $X \in \mathbb{R}^{n+m}$ is a random vector such that $\mathbb{E}\|X\| < \infty$ and $K = K(X)$ is the associated Vitale zonoid, then

$$\Sigma_\pi K = K(F_\pi(X_1, \dots, X_{n+1}))$$

where $X_1, \dots, X_{n+1} \in \mathbb{R}^{n+m}$ are i.i.d. copies of X . In other words, the support function of the fiber body $\Sigma_\pi K$ is given for all $u \in W$ by

$$h_{\Sigma_\pi K}(u) = \frac{1}{2} \mathbb{E} |\langle u, Y \rangle| \quad (3.1.10)$$

where $Y \in W$ is the random vector defined by $Y = F_\pi(X_1, \dots, X_{n+1})$.

Proof. Denote $K = K(X)$ and let $u \in W$. Note that by (2.1.1) and Proposition 1.1.19-(iii), $T_u(K) = K(T_u(X_1))$. Thus by (3.1.9) and [Vit91, Theorem 3.2] we get

$$h_{\Sigma_\pi K}(u) = \frac{1}{2} \text{vol}(K(T_u(X))) = \frac{1}{2} \frac{1}{(n+1)!} \mathbb{E} |T_u(X_1) \wedge \dots \wedge T_u(X_{n+1})| \quad (3.1.11)$$

where $X_1, \dots, X_{n+1} \in \mathbb{R}^{n+m}$ are iid copies of X . Let us write $X_i := (\alpha_i, \beta_i)$ with $\alpha_i \in V$ and $\beta_i \in W$. Then

$$\begin{aligned} |T_u(X_1) \wedge \dots \wedge T_u(X_{n+1})| &= |(\alpha_1, \langle u, \beta_1 \rangle) \wedge \dots \wedge (\alpha_{n+1}, \langle u, \beta_{n+1} \rangle)| \\ &= \left| \sum_{i=1}^{n+1} (-1)^{n+1-i} (\alpha_1 \wedge \dots \wedge \widehat{\alpha_i} \wedge \dots \wedge \alpha_{n+1}) \langle u, \beta_i \rangle \right| \\ &= |\langle u, (n+1)! F_\pi((\alpha_1, \beta_1), \dots, (\alpha_{n+1}, \beta_{n+1})) \rangle|. \end{aligned}$$

Reintroducing this in (3.1.11), we obtain (3.1.10). \square

This allows to generalize [BS92, Theorem 4.1] for all zonotopes.

Corollary 3.1.32. Given $z_1, \dots, z_N \in \mathbb{R}^{n+m}$, the fiber body of the zonotope $\sum_{i=1}^N [-z_i, z_i]$ is the zonotope given by

$$\Sigma_\pi \left(\sum_{i=1}^N [-z_i, z_i] \right) = (n+1)! \sum_{1 \leq i_1 < \dots < i_{n+1} \leq N} [-F_\pi(z_{i_1}, \dots, z_{i_{n+1}}), F_\pi(z_{i_1}, \dots, z_{i_{n+1}})]. \quad (3.1.12)$$

Proof. We apply Theorem 3.1.31 to the discrete random vector X , that is equal to Nz_i with probability $1/N$ for all $i = 1, \dots, N$. In this case one can check from (2.1.1) that the Vitale zonoid $K(X)$ is precisely the zonotope $\sum_{i=1}^N [-z_i, z_i]$, and the result follows from (3.1.10). \square

An implementation of formula (3.1.12) for OSCAR 0.8.2-DEV [OSC22] and SageMath 9.2 [Sag21] is available at <https://mathrepo.mis.mpg.de/FiberZonotopes>.

Esterov shows in [Est08] that the map $\Sigma_\pi : \mathcal{K}(\mathbb{R}^{n+m}) \rightarrow \mathcal{K}(W)$ comes from another map, which is (Minkowski) multilinear in each variable: the so called *mixed fiber body*. The following is [Est08, Theorem 1.2].

Proposition 3.1.33. There is a unique symmetric multilinear map

$$\text{M}\Sigma_\pi : \left(\mathcal{K}(\mathbb{R}^{n+m}) \right)^{n+1} \rightarrow \mathcal{K}(W)$$

such that for all $K \in \mathcal{K}(\mathbb{R}^{n+m})$, $\text{M}\Sigma_\pi(K, \dots, K) = \Sigma_\pi(K)$.

Once its existence is proved, one can see that the mixed fiber body $\text{M}\Sigma_\pi(K_1, \dots, K_{n+1})$ is the coefficient of $t_1 \dots t_{n+1}$ in the expansion of $\Sigma_\pi(t_1 K_1 + \dots + t_{n+1} K_{n+1})$, up to a factor of $(n+1)!$. Using this *polarization formula*, one can deduce from Theorem 3.1.31 a similar statement for the mixed fiber body of zonoids.

Proposition 3.1.34. The mixed fiber body of zonoids is a zonoid. Moreover, if the random vectors $X_1, \dots, X_{n+1} \in \mathbb{R}^{n+m}$ are independent (not necessarily identically distributed) and such that $\mathbb{E}\|X_i\|$ is finite, and if $K_i = K(X_i)$ are the associated Vitale zonoids, then

$$\text{M}\Sigma_\pi(K_1, \dots, K_{n+1}) = K(F_\pi(X_1, \dots, X_{n+1})).$$

Proof. Let us show the case of $n + 1 = 2$ variables. The general case is done in a similar way. Let $\tilde{X} := 2t_1\alpha X_1 + 2t_2(1-\alpha)X_2$ where α is a Bernoulli random variable of parameter $1/2$ independent of X_1 and X_2 . Using (2.1.1), one can check that $K(\tilde{X}) = t_1K_1 + t_2K_2$. Now let Y_1 (respectively Y_2) be an i.i.d. copy of X_1 (respectively X_2) independent of all the other variables. Define $\tilde{Y} := 2t_1\beta Y_1 + 2t_2(1-\beta)Y_2$ where β is a Bernoulli random variable of parameter $1/2$ independent of all the other variables. By Theorem 3.1.31 we have that $\Sigma_\pi(t_1K_1 + t_2K_2) = K(F_\pi(\tilde{X}, \tilde{Y}))$. By (2.1.1), using the independence assumptions, it can be deduced that for all $t_1, t_2 \geq 0$

$$h_{K(F_\pi(\tilde{X}, \tilde{Y}))} = t_1^2 h_{\Sigma_\pi K_1} + t_2^2 h_{\Sigma_\pi K_2} + t_1 t_2 (h_{K(F_\pi(X_1, Y_2))} + h_{K(F_\pi(Y_1, X_2))}).$$

The claim follows from the fact that $K(F_\pi(X_1, Y_2)) = K(F_\pi(Y_1, X_2)) = K(F_\pi(X_1, X_2))$. \square

Example 3.1.35. Consider the dice \mathcal{D} from Example 2.2.19. Its boundary consists of 7 patches: 6 two-dimensional discs of radius 1, lying in the center of the facets of the cube $[-2, 2]^3$, and an irreducible surface.

Let $\pi := \langle e_1, \cdot \rangle : \mathbb{R} \oplus \mathbb{R}^2 \rightarrow \mathbb{R}$. Even in this simple example the fibers of the dice under this projection can be tricky to describe. However, using the formula for zonoids one can compute explicitly the fiber body (see Figure 3.5) as explained in the next proposition. \blacklozenge

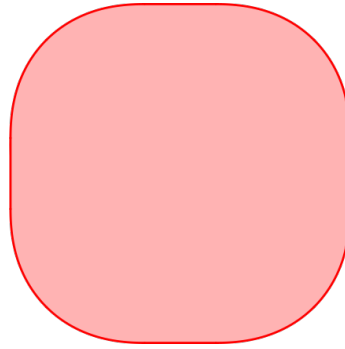


Figure 3.5: The fiber body of the dice.

Proposition 3.1.36. In the setting of Example 3.1.35, with respect to the projection π , the fiber body of the dice \mathcal{D} is

$$\Sigma_\pi(\mathcal{D}) = D_1 + \frac{\pi}{4} \left([(0, -1, 0), (0, 1, 0)] + [(0, 0, -1), (0, 0, 1)] \right) + \frac{1}{2} \Lambda$$

where Λ is the convex body whose support function is given by

$$h_\Lambda(u_2, u_3) = \frac{1}{2} \int_0^\pi \sqrt{\cos(\theta)^2 (u_2)^2 + \sin(\theta)^2 (u_3)^2} d\theta.$$

Proof. First of all let us note that by expanding the mixed fiber body $\text{M}\Sigma_\pi(\mathcal{D}, \mathcal{D})$ we have

$$\Sigma_\pi(\mathcal{D}) = \Sigma_\pi(D_1) + \Sigma_\pi(D_2) + \Sigma_\pi(D_3) + 2(\text{M}\Sigma_\pi(D_1, D_2) + \text{M}\Sigma_\pi(D_1, D_3) + \text{M}\Sigma_\pi(D_2, D_3)).$$

Using the notation introduced for discotopes, given a generalized disc $D_{\{b_1, b_2\}}$, define the random vector $\sigma(\theta) := (\cos(\theta)b_1 + \sin(\theta)b_2)$ with $\theta \in [0, 2\pi]$ uniformly distributed. Then we have

$$D_{\{b_1, b_2\}} = \pi \cdot K(\sigma(\theta)) \quad (3.1.13)$$

In other words we can write the support function as

$$h_{\{b_1, b_2\}}(u) = \sqrt{\langle u, b_1 \rangle^2 + \langle u, b_2 \rangle^2} = \frac{\pi}{2} \mathbb{E}|\langle u, \sigma(\theta) \rangle|. \quad (3.1.14)$$

Let $\sigma_1(\theta) := (0, \cos(\theta), \sin(\theta))$, $\sigma_2(\theta) := (\cos(\theta), 0, \sin(\theta))$ and $\sigma_3(\theta) := (\cos(\theta), \sin(\theta), 0)$ in such a way that $h_{D_i}(u) = \frac{\pi}{2} \mathbb{E}|\langle u, \sigma_i(\theta) \rangle|$. We then want to use Theorem 3.1.31 and Proposition 3.1.34 to compute all the summands of the expansion of $\Sigma_\pi(\mathcal{D})$.

Using (3.1.13), we have that $M\Sigma_\pi(D_i, D_j) = \pi^2 K(F_\pi(\sigma_i(\theta), \sigma_j(\phi)))$ with $\theta, \phi \in [0, 2\pi]$ uniform and independent. In our case, $F_\pi(x, y) = (x_1y_2 - y_1x_2, x_1y_3 - y_1x_3)/2$. We obtain

$$\begin{aligned} F_\pi(\sigma_1(\theta), \sigma_1(\phi)) &= 0, \\ F_\pi(\sigma_2(\theta), \sigma_2(\phi)) &= \frac{1}{2}(0, \sin(\phi - \theta)), \quad F_\pi(\sigma_3(\theta), \sigma_3(\phi)) = \frac{1}{2}(\sin(\phi - \theta), 0), \\ F_\pi(\sigma_1(\theta), \sigma_2(\phi)) &= -\frac{\cos(\phi)}{2}(\cos(\theta), \sin(\theta)), \quad F_\pi(\sigma_1(\theta), \sigma_3(\phi)) = -\frac{\cos(\phi)}{2}(\cos(\theta), \sin(\theta)), \\ F_\pi(\sigma_2(\theta), \sigma_3(\phi)) &= \frac{1}{2}(\cos(\theta)\sin(\phi), \sin(\theta)\cos(\phi)). \end{aligned}$$

Computing the support function $h_{\pi^2 K(F_\pi(\sigma_i(\theta), \sigma_j(\phi)))} = \frac{\pi^2}{2} \mathbb{E}|\langle u, F_\pi(\sigma_i(\theta), \sigma_j(\phi)) \rangle|$ and using that $\mathbb{E}|\cos(\phi)| = 2/\pi$, we get

$$\begin{aligned} \Sigma_\pi(D_1) &= 0, \quad \Sigma_\pi(D_2) = \frac{\pi}{4} [(0, -1, 0), (0, 1, 0)], \quad \Sigma_\pi(D_3) = \frac{\pi}{4} [(0, 0, -1), (0, 0, 1)], \\ M\Sigma_\pi(D_1, D_2) &= M\Sigma_\pi(D_1, D_3) = \frac{1}{4} D_1 \end{aligned}$$

It only remains to compute $M\Sigma_\pi(D_2, D_3)$. We have

$$h_{M\Sigma_\pi(D_2, D_3)}(u) = \frac{\pi^2}{8} \mathbb{E}|\langle u, F_\pi(\sigma_2(\theta), \sigma_3(\phi)) \rangle| = \frac{\pi^2}{16} \mathbb{E}|u_2 \cos(\theta) \sin(\phi) + u_3 \sin(\theta) \cos(\phi)|.$$

We use then the independence of θ and ϕ and (3.1.14) to find

$$h_{M\Sigma_\pi(D_2, D_3)}(u) = \frac{\pi}{8} \mathbb{E} \sqrt{\cos(\theta)^2 (u_2)^2 + \sin(\theta)^2 (u_3)^2} = \frac{1}{4} h_\Lambda(u)$$

Putting back together everything we obtain the result. \square

Remark 3.1.37. It is worth noticing that the convex body Λ also appears, up to a multiple, in [BL16, Section 5.1] where it is called $D(2)$, with no apparent link to fiber bodies. In the case where $u_2 \neq 0$ we have

$$h_\Lambda(u) = |u_2| E \left(\sqrt{1 - \left(\frac{u_3}{u_2} \right)^2} \right)$$

where $E(s) = \int_0^{\pi/2} \sqrt{1 - s^2 \sin(\theta)^2} d\theta$ is the complete elliptic integral of the second kind. This function is not semialgebraic thus the example of the dice shows that the fiber body of a semialgebraic convex body is not necessarily semialgebraic. However, E is holonomic. This suggests that the curved assumption in Corollary 3.1.25 may not be needed.

3.1.4. Conclusions

Add conclusions and further research directions.

3.2. Intersection bodies of polytopes

If for fiber bodies it was natural to look at the support function, here we are going to deal with the radial function. Regarding the notation, in this section only we will use ‘ x ’ for a point in \mathbb{R}^d and ‘ u ’ for a point in S^{d-1} (and not for the dual space, as usual).

Definition 3.2.1. Let K be a convex body in \mathbb{R}^d . Its *intersection body* is the starshaped set IK with radial function (restricted to the sphere)

$$\rho_{IK}(u) = \text{vol}_{d-1}(K \cap u^\perp)$$

for $u \in S^{d-1}$, where vol_i is the i -dimensional Euclidean volume, for $i \leq d$.

We focus here on the study of intersection bodies of polytopes, and begin our investigation by considering polytopes which contain the origin. If the origin belongs to the interior of the polytope P , then ρ_P is continuous and hence ρ_{IP} is also continuous [Gar06]. Otherwise we may have some points of discontinuity which correspond to unit vectors u such that u^\perp contains a facet of P ; there are finitely many such directions. The intersection body is well defined, but there may arise subtleties when dealing with the boundary. However, we will see later (in Remark 3.2.10) that for our purposes everything works out.

Example 3.2.2. We will use the cube as an ongoing example to illustrate the key concepts. Let P be the 3-dimensional cube $[-1, 1]^3 \subseteq \mathbb{R}^3$. If we intersect P with hyperplanes $(x, y, z)^\perp$, for $(x, y, z) \in \mathbb{R}^3$, we can observe that there are two possible combinatorial types (for the definition see [Zie12, Section 2.2]) for $P \cap (x, y, z)^\perp$: it is either a parallelogram or a hexagon, as displayed in Figure 3.6. There are finitely many regions of \mathbb{R}^3 for which the

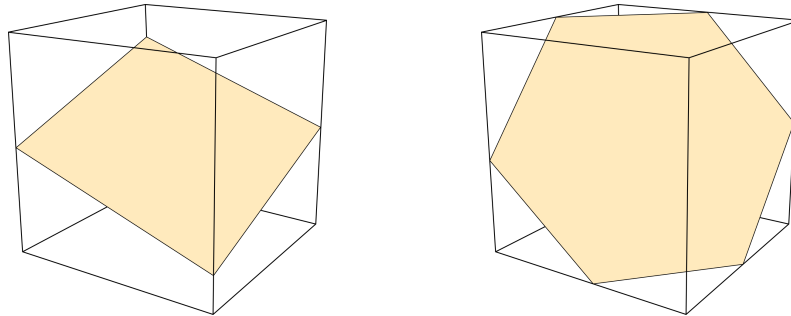


Figure 3.6: The two combinatorial types of hyperplane sections of the 3-cube.

combinatorial type stays the same (as stated more precisely in Lemma 3.2.3). Using this we can parameterize the area of the parallelogram or hexagon with respect to the vector (x, y, z) to construct the radial function of IP . Indeed, as will be shown in the proof of Theorem 3.2.5, this can be equivalently written to provide a semialgebraic description of the intersection body. In particular, if the intersection $P \cap (x, y, z)^\perp$ is a square, then the radial function in a neighborhood of (x, y, z) will be a constant term over a coordinate variable, e.g. $\frac{4}{z}$. On the other hand, when the intersection is a hexagon, the radial function is a degree two polynomial over xyz . The intersection body is convex as promised by the theory and displayed in Figure 3.9, left. We continue with this analysis in Example 3.2.11. ♦

Lemma 3.2.3. Let P be a full-dimensional polytope in \mathbb{R}^d . Then there exists a central hyperplane arrangement \mathcal{H} in \mathbb{R}^d whose maximal open chambers C 's satisfy the following property. For all $x \in C$, the hyperplane x^\perp intersects a fixed set of edges of P and the polytopes $Q = P \cap x^\perp$ are of the same combinatorial type.

Proof. Let $x \in \mathbb{R}^d \setminus \{0\}$ and consider $Q = P \cap x^\perp$. The vertices of Q are the points of intersection of x^\perp with the edges of P . Perturbing x continuously, the intersecting edges (and thus the combinatorial type) remain the same, unless the hyperplane x^\perp passes through a vertex v of P . This happens if and only if $\langle x, v \rangle = 0$ and thus the set of normal vectors of such hyperplanes is given by $v^\perp = \{x \in \mathbb{R}^d \mid \langle x, v \rangle = 0\}$. Taking the union over all vertices yields the central hyperplane arrangement

$$\mathcal{H} = \{v^\perp \mid v \text{ is a vertex of } P \text{ and } v \text{ is not the origin}\}.$$

Then each open region C of $\mathbb{R}^d \setminus \mathcal{H}$ is a convex cone. C contains points x such that x^\perp intersects a fixed set of edges of P . \square

The proof of Lemma 3.2.3 implies that the number of regions we are interested in is the number of chambers of the central hyperplane arrangement \mathcal{H} . Denote by m the cardinality of the set $\{v \text{ is a vertex of } P\}/\sim$, where $v \sim w$ if $v = \pm w$. There is an upper bound for the number of chambers of \mathcal{H} :

$$\sum_{j=0}^d \binom{m}{j}$$

which is the number of chambers of a generic arrangement [Sta07, Prop. 2.4].

Remark 3.2.4. We note that there are several ways to view the hyperplane arrangement \mathcal{H} in Lemma 3.2.3. For example, since the vertices of P are the normal vectors to the facets of the dual polytope P° , we can describe \mathcal{H} as the collection of linear hyperplanes which are parallel to facets of P° . We also note that \mathcal{H} induces a fan Σ , which is the normal fan of a zonotope whose edge directions are orthogonal to the hyperplanes of \mathcal{H} :

$$Z(P) = \sum_{v \text{ is a vertex of } P} [-v, v].$$

We will call this object the *zonotope associated to P* . As will be clarified later in Remark 3.2.17, the dual body of $Z(P)$ plays an important role in the visualization and the combinatorics of the intersection body IP .

Theorem 3.2.5. Let $P \subseteq \mathbb{R}^d$ be a full-dimensional polytope containing the origin. Then IP , the intersection body of P , is semialgebraic.

Proof. Fix a region $U = C \cap S^{d-1}$ for an open cone C from Lemma 3.2.3. For every $u \in U$ the hyperplane u^\perp intersects P in the same set of edges. Let v be a vertex of $Q = P \cap u^\perp$. Then there is an edge $[a, b]$ of P such that $v = [a, b] \cap u^\perp$. This implies that $v = \lambda a + (1 - \lambda)b$ for some $\lambda \in (0, 1)$ and $\langle v, u \rangle = 0$. From this we get that

$$\lambda = \frac{\langle b, u \rangle}{\langle b - a, u \rangle}$$

which implies that

$$v = \frac{\langle b, u \rangle}{\langle b - a, u \rangle}(a - b) + b = \frac{\langle b, u \rangle a - \langle a, u \rangle b}{\langle b - a, u \rangle}.$$

In this way we express v as a function of u (for fixed a and b). Let v_1, \dots, v_n be the vertices of Q and let $[a_i, b_i]$ be the corresponding edges of P .

We now consider the following triangulation of Q : first, triangulate each facet of Q that does not contain the origin, without adding new vertices (this can always be done, e.g., by a regular subdivision using a generic lifting function, see [LRS10, Prop. 2.2.4]). For each $(d-2)$ -dimensional simplex Δ in this triangulation, consider the $(d-1)$ -dimensional simplex $\text{conv}(\Delta, 0)$ with the origin. These constitute a triangulation $T = \{\Delta_j : j \in J\}$ of Q , in which the origin is a vertex of every simplex.

Restricting to U , the radial function of the intersection body IP in direction u is the volume of Q , and hence given by

$$\rho_{IP}(u) = \text{vol}(Q) = \sum_{j \in J} \text{vol}(\Delta_j).$$

We can thus compute $\rho_{IP}(u)$ as

$$\rho_{IP}(u) = \sum_{j \in J} \frac{1}{(d-1)!} |\det(M_j(u))|,$$

where

$$M_j(u) = \begin{bmatrix} v_{i_1}(u) \\ v_{i_2}(u) \\ \vdots \\ v_{i_{d-1}}(u) \\ u \end{bmatrix} = \begin{bmatrix} \frac{\langle b_{i_1}, u \rangle a_{i_1} - \langle a_{i_1}, u \rangle b_{i_1}}{\langle b_{i_1} - a_{i_1}, u \rangle} \\ \vdots \\ \frac{\langle b_{i_{d-1}}, u \rangle a_{i_{d-1}} - \langle a_{i_{d-1}}, u \rangle b_{i_{d-1}}}{\langle b_{i_{d-1}} - a_{i_{d-1}}, u \rangle} \\ u \end{bmatrix}$$

and the row vectors $\{v_{i_1}, v_{i_2}, \dots, v_{i_{d-1}}\}$ (along with the origin) are vertices of the simplex Δ_j of the triangulation. Therefore, we obtain an expression $\rho_{IP}(u) = \frac{p(u)}{q(u)}$ for some polynomials $p, q \in \mathbb{R}[u_1, \dots, u_d]$ without common factors, for $u \in U$. With the same procedure applied to all regions $U_i = C_i \cap S^{d-1}$, for C_i as in Lemma 3.2.3, we obtain an expression for $\rho|_{S^{d-1}}$ that is continuous and piecewise a quotient of two polynomials p_i, q_i . It follows from the definition of the radial function that

$$IP = \left\{ x \in \mathbb{R}^d \mid \rho_{IP}(x) \geq 1 \right\} = \left\{ x \in \mathbb{R}^d \mid \frac{1}{\|x\|} \rho_{IP}\left(\frac{x}{\|x\|}\right) \geq 1 \right\}.$$

Notice that for every $j \in J$ we have the following equality:

$$\det\left(M_j\left(\frac{x}{\|x\|}\right)\right) = \det\begin{bmatrix} v_{i_1}\left(\frac{x}{\|x\|}\right) \\ \vdots \\ v_{i_{d-1}}\left(\frac{x}{\|x\|}\right) \\ \frac{x}{\|x\|} \end{bmatrix} = \det\begin{bmatrix} v_{i_1}(x) \\ \vdots \\ v_{i_{d-1}}(x) \\ \frac{x}{\|x\|} \end{bmatrix} = \frac{1}{\|x\|} \det(M_j(x))$$

and therefore, if $\frac{x}{\|x\|} \in U$,

$$\rho_{IP}\left(\frac{x}{\|x\|}\right) = \sum_{j \in J} \frac{1}{(d-1)!} \left| \det\left(M_j\left(\frac{x}{\|x\|}\right)\right) \right| = \frac{1}{\|x\|} \sum_{j \in J} \frac{1}{(d-1)!} |\det(M_j(x))| = \frac{p(x)}{\|x\| q(x)}.$$

By Proposition 1.2.8, since the radial function is a semialgebraic map, the intersection body is also semialgebraic. More explicitly, let I be the set of indices i such that $\rho_{IP}|_{U_i} \neq 0$.

Then we can write the intersection body as

$$\begin{aligned} IP &= \bigcup_{i \in I} \left\{ x \in \overline{C}_i \mid \frac{1}{\|x\|^2} \cdot \frac{p_i(x)}{q_i(x)} \geq 1 \right\} \\ &= \bigcup_{i \in I} \left\{ x \in \overline{C}_i \mid \|x\|^2 q_i(x) - p_i(x) \leq 0 \right\}. \end{aligned}$$

This expression gives a semialgebraic description of IP . \square

Example 3.2.6. Let P be the regular icosahedron in \mathbb{R}^3 , whose 12 vertices are all the even permutations of $(0, \pm\frac{1}{2}, \pm(\frac{1}{4}\sqrt{5} + \frac{1}{4}))$. The associated hyperplane arrangement has $32 = 12 + 20$ chambers. The first type of chambers is spanned by five rays and the radial function of IP is given by a quotient of a quartic and a quintic, defined over $\mathbb{Q}(\sqrt{5})$. In the remaining twenty chambers ρ_{IP} is a quintic over a sextic, again with coefficients in $\mathbb{Q}(\sqrt{5})$. This intersection body is the convex set shown in Figure 3.7. We will continue

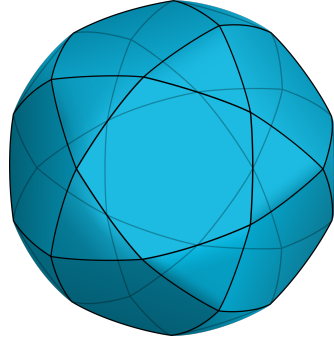


Figure 3.7: The intersection body of the icosahedron.

the analysis of IP in Example 3.2.18. \diamond

The theory of intersection bodies assures that the intersection body of a centrally symmetric convex body is again a centrally symmetric convex body, as it happens in Examples 3.2.2 and 3.2.6. On the other hand, given any polytope P (indeed this holds more generally for any convex body) there exists a translation of P such that IP is not convex. This is the content of the next example.

Example 3.2.7. Let P be the cube $[-1, 1]^3 + (1, 1, 1)$, so that the origin is a vertex of P . The hyperplane arrangement associated to P divides the space in 32 chambers. In two of them the radial function is 0. In six regions the radial function has the following shape (up to permutation of the coordinates and sign):

$$\rho(x, y, z) = \frac{4}{z}.$$

There are then $18 = 6 + 12$ regions in which the radial function looks like

$$\rho(x, y, z) = \frac{2x}{yz} \quad \text{or} \quad \rho(x, y, z) = \frac{2(x + 2z)}{yz}.$$

In the remaining six regions we have functions such as

$$\rho(x, y, z) = \frac{2(x^2 + 2xy + y^2 + 2xz + z^2)}{xyz}.$$

Figure 3.8 shows two different points of view of IP , which is in particular not convex. \diamond

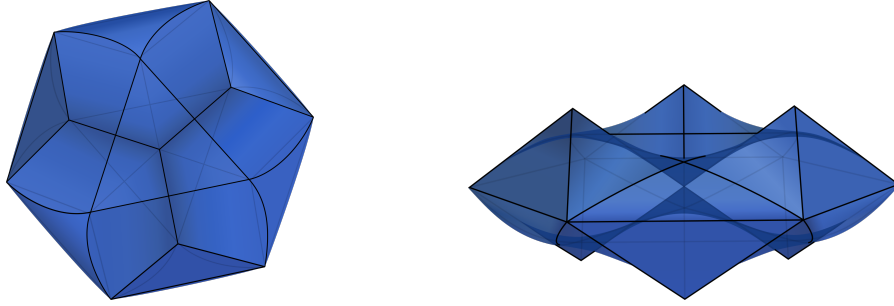


Figure 3.8: The intersection body of the cube in Example 3.2.7 from two different points of view.

3.2.1. The role of the origin

The proof of Theorem 3.2.5 relies on the fact that the origin is in the polytope. However, if the origin is not contained in P , we can still find a semialgebraic description of IP by adjusting how we compute the volume of $P \cap u^\perp$. The remainder of this section will be dedicated to proving this.

Lemma 3.2.8. Let $P \subset \mathbb{R}^d$ be a full-dimensional polytope, and let \mathcal{F} be the set of its facets. Let p be a point outside of P . For each face $F \in \mathcal{F}$, let \hat{F} denote the set $\text{conv}(F \cup \{p\})$. Then the following equality holds:

$$\text{vol}(P) = \sum_{F \in \mathcal{F}} \text{sgn}(F) \text{vol}(\hat{F})$$

where $\text{sgn}(F)$ is 1 if P and p belong to the same halfspace defined by F , and -1 otherwise.

Proof. Let $\hat{P} = \text{conv}(P \cup \{p\})$ and denote by \mathcal{F}_p^+ the set of facets F of P for which the halfspace defined by F containing P also contains p , possibly on its boundary. Let $\mathcal{F}_p^- = \mathcal{F} \setminus \mathcal{F}_p^+$.

First we will show that $\hat{P} = \bigcup_{F \in \mathcal{F}_p^+} \hat{F}$. The inclusion $\bigcup_{F \in \mathcal{F}_p^+} \hat{F} \subseteq \hat{P}$ follows immediately from convexity. To see the opposite direction, let $q \in \hat{P}$ and consider r to be the ray starting at p and going through q . Either r intersects P only along its boundary, or there are some intersection points also in the interior of P . In the first case $r \cap P \subset F$ and so $q \in \hat{F}$ for some face F , that by convexity must be in \mathcal{F}_p^+ . On the other hand, if the ray r intersects the interior of the polytope P , denote by a the farthest among the intersection points:

$$\|a - p\| = \max\{\|\alpha - p\| \mid \alpha \in P \cap r\}.$$

Let F_a be a facet containing a . Then, q is contained in the convex hull of $F_a \cup \{p\}$, that is \hat{F}_a . From the definition of a it follows that the halfspace defined by F_a containing p must also contain P , so $F_a \in \mathcal{F}_p^+$ and our statement holds.

Next, we will show that $\bigcup_{F \in \mathcal{F}_p^-} \hat{F} = \overline{\hat{P} \setminus P}$. The pyramid \hat{F} is contained in the closed halfspace defined by F which contains p . By the definition of \mathcal{F}_p^- this halfspace does not contain P , thus $\hat{F} \cap P = F$. Also, $\hat{F} \subseteq \hat{P}$ so we have that $\hat{F} \subseteq \overline{\hat{P} \setminus P}$ and hence $\bigcup_{F \in \mathcal{F}_p^-} \hat{F} \subseteq \overline{\hat{P} \setminus P}$. Conversely, let $q \in \overline{\hat{P} \setminus P}$. If $q = p$ we are done, so assume $q \neq p$. Then, $q = \lambda p + (1 - \lambda)b$ for some $b \in P$, $\lambda \in [0, 1]$. Let a be the point at which the segment from p to b first intersects the boundary of P , i.e.

$$\|a - p\| = \min\{\|\alpha - p\| \mid \alpha \in P, \alpha = tp + (1 - t)b \text{ for } t \in [0, 1]\}.$$

Then by construction there exists a facet $F_a \in \mathcal{F}_p^-$ containing a , such that $q \in \hat{F}_a$. Thus

$$\text{vol}(\bigcup_{F \in \mathcal{F}_p^+} \hat{F}) = \text{vol}(\hat{P}) = \text{vol}(\hat{P} \setminus P) + \text{vol}(P) = \text{vol}(\bigcup_{F \in \mathcal{F}_p^-} \hat{F}) + \text{vol}(P).$$

If $F_1 \neq F_2$ and $F_1, F_2 \in \mathcal{F}_p^+$ or $F_1, F_2 \in \mathcal{F}_p^-$, then the volume of $\hat{F}_1 \cap \hat{F}_2$ is zero, therefore

$$\sum_{F \in \mathcal{F}_p^+} \text{vol}(\hat{F}) = \sum_{F \in \mathcal{F}_p^-} \text{vol}(\hat{F}) + \text{vol}(P)$$

and the claim follows. \square

Theorem 3.2.9. Let $P \subset \mathbb{R}^d$ be a full-dimensional polytope. Then IP , the intersection body of P , is semialgebraic.

Proof. What remains to be shown is that IP is semialgebraic in the case when the origin is not contained in P , and hence it is not contained in any of its sections $Q = P \cap u^\perp$. From Lemma 3.2.8, with $p = 0 \in \mathbb{R}^d$ we have that

$$\text{vol}(Q) = \sum_{F \text{ facet of } Q} \text{sgn}(F) \text{vol}(\hat{F})$$

where \hat{F} is the convex hull of F and the origin. Let $T_F = \{\Delta_j : j \in J_F\}$ be a triangulation of F . We can calculate as in the proof of Theorem 3.2.5

$$\text{vol}(\hat{F}) = \sum_{j \in J_F} \frac{1}{(d-1)!} |\det M_j|$$

where M_j is the matrix whose rows are the vertices of the simplex $\Delta_j \in T_F$ and u . We then follow the remainder of the proof of Theorem 3.2.5 to see that the intersection body is semialgebraic. \square

The proofs from Theorems 3.2.5 and 3.2.9 lead to an algorithm to compute the radial function of the intersection body of a polytope. This algorithm has as input the polytope P and as output a list of pairs $\{C, \rho|_C\}$ where C is a chamber of the hyperplane arrangement associated to P and $\rho|_C$ is the radial function of IP in C . An implementation of these algorithms for SageMath 9.2 [Sag21] and Oscar 0.7.1-DEV [OSC22] is available at <https://mathrepo.mis.mpg.de/intersection-bodies>.

3.2.2. Algebraic boundary and degree bound

Knowing the radial function of a convex body K implies knowing its boundary. In fact, when $0 \in \text{int } K$ then $x \in \partial K$ if and only if $\rho_K(x) = 1$ (see Remark 3.2.10 for the other cases). Therefore, using the same notation as in the proof of Theorem 3.2.5, we can observe that the algebraic boundary of the intersection body of a polytope is contained in the union of the varieties $\mathcal{V}(\|x\|^2 q_i(x) - p_i(x))$. Indeed, we actually know more: as will be proven in Proposition 3.2.13, the p_i 's are divisible by the polynomial $\|x\|^2$, and hence

$$\partial_a IP = \bigcup_{i \in I} \mathcal{V}\left(q_i(x) - \frac{p_i(x)}{\|x\|^2}\right)$$

because of the assumption made in the proof of Theorem 3.2.5 that p_i, q_i do not have common components. That is, these are exactly the irreducible components of the boundary of IP .

Remark 3.2.10. As anticipated above, there may be difficulties when computing the boundary of IP in the case where the origin is not in the interior of the polytope P . In particular, x is a discontinuity point of the radial function of IP if and only if x^\perp contains a facet of P . Therefore ρ_{IP} has discontinuity points if and only if the origin lies in the union of the affine linear spans of the facets of P . In this case, there are finitely many rays where the radial function is discontinuous and they belong to $\mathbb{R}^d \setminus (\cup_{i \in I} C_i)$, i.e. to the hyperplane arrangement \mathcal{H} . If $d = 2$, these rays disconnect the space, and this implies that we loose part of the (algebraic) boundary of IP : to the set $\{x \in \mathbb{R}^d \mid \rho_{IP}(x) = 1\}$ we need to add segments from the origin to the boundary points in the direction of these rays. However, in higher dimensions the discontinuity rays do not disconnect \mathbb{R}^d so $\{x \in \mathbb{R}^d \mid \rho_{IP}(x) = 1\}$ approaches the region where the radial function is zero continuously except for these finitely many directions. Therefore there are no extra components of $\partial_a IP$ for $d > 2$.

Example 3.2.11 (Continuation of Example 3.2.2, Figure 3.9, left). Starting from the radial function of the intersection body of the 3-cube P , we can recover the equations of its algebraic boundary. The Euclidean boundary of this convex body is divided in 14 patches. Among them, 6 arise as the intersection of a convex cone spanned by 4 rays with a hyperplane: they constitute facets of IP . For example the facet exposed by the vector $(1, 0, 0)$ is the intersection of $z = 4$ with the convex cone

$$\overline{C}_1 = \text{co}\{(1, 0, 1), (-1, 0, 1), (0, 1, 1), (0, -1, 1)\}.$$

In other words, the variety $\mathcal{V}(z - 4)$ is one of the irreducible components of $\partial_a IP$. The remaining 8 patches are spanned by 3 rays each, and the polynomial that defines the boundary of IP is a cubic, such as

$$2xyz - 2x^2 - 4xy - 2y^2 - 4xz + 4yz - 2z^2$$

in the region

$$\overline{C}_2 = \text{co}\{(0, 1, 1), (-1, 1, 0), (-1, 0, 1)\}.$$

These cubics are in fact, up to a change of coordinates, the algebraic boundary of an ellotope. Hence $\partial_a IP$ is the union of 14 irreducible components, six of degree 1 and eight of degree 3. \blacklozenge

Remark 3.2.12. It is tempting to think that each region of Lemma 3.2.3 corresponds to a patch, as in Definition 1.2.20. Indeed, this happens for the centered 3-cube in Example 3.2.11. On the other hand, if $P = [-1, 1]^3 + (0, 0, 1)$ there are 4 regions that define the same patch of the algebraic boundary of IP . Therefore there is, unfortunately, no one-to-one correspondence between regions and patches.

Proposition 3.2.13. Using the notation of Lemma 3.2.3 and Theorem 3.2.9, consider a chamber C of \mathcal{H} and let $Q = P \cap u^\perp$ for some $u \in U = C \cap S^{d-1}$. Then the polynomial $\|x\|^2 = x_1^2 + \dots + x_d^2$ divides $p(x)$ and

$$\deg \left(q(x) - \frac{p(x)}{\|x\|^2} \right) \leq f_0(Q).$$

Proof. For the fixed region C , let T be a triangulation of Q with simplices indexed by J . Then the volume of Q is given by

$$\frac{p(x)}{q(x)} = \frac{1}{(d-1)!} \sum_{j \in J} |\det(M_j(x))|$$

where M_j is the matrix as in the proof of Theorem 3.2.5. Notice that for each $M = M_j$, we can rewrite the determinant to factor out a denominator (we also write for simplicity $\Delta = \Delta_j$):

$$\begin{aligned} \det(M(x)) &= \sum_{\sigma \in S_d} \operatorname{sgn}(\sigma) \prod_{i=1}^d M_{i\sigma(i)} \\ &= \sum_{\sigma \in S_d} \operatorname{sgn}(\sigma) x_{\sigma(d)} \prod_{i=1}^{d-1} \frac{\langle b_i, u \rangle a_{i\sigma(i)} - \langle a_i, u \rangle b_{i\sigma(i)}}{\langle b_i - a_i, u \rangle} \\ &= \prod_{i=1}^{d-1} \frac{1}{\langle b_i - a_i, u \rangle} \sum_{\sigma \in S_d} \operatorname{sgn}(\sigma) x_{\sigma(d)} \prod_{i=1}^{d-1} (\langle b_i, u \rangle a_{i\sigma(i)} - \langle a_i, u \rangle b_{i\sigma(i)}) \\ &= \left(\prod_{\substack{v_i \in \Delta \\ \text{vertex}}} \frac{1}{\langle b_i - a_i, x \rangle} \right) \cdot \det(\hat{M}(x)) \end{aligned}$$

where

$$\hat{M}(x) = \begin{bmatrix} & & \vdots & \\ \langle b_i, x \rangle a_i - \langle a_i, x \rangle b_i & & & \\ & & \vdots & \\ & & & x \end{bmatrix}$$

and the determinant of $\hat{M}(x)$ is a polynomial of degree d in the x_i 's. Note that if we multiply $\hat{M}(x) \cdot x$ we obtain the vector $(0, \dots, 0, x_1^2 + \dots + x_d^2)$. Hence if $x_1^2 + \dots + x_d^2 = 0$, then $\hat{M}(x) \cdot x = 0$, i.e. the kernel of $\hat{M}(x)$ is non-trivial and thus $\det \hat{M}(x) = 0$. This implies the containment of the complex varieties $\mathcal{V}(\|x\|^2) \subseteq \mathcal{V}(\det \hat{M}(x))$ and therefore the polynomial $x_1^2 + \dots + x_d^2$ divides the polynomial $\det \hat{M}(x)$. When we sum over all the simplices in the triangulation T we obtain that

$$\begin{aligned} q(x) &= (d-1)! \left(\prod_{\substack{v_i \in \Delta_j \\ \text{vertex}}} \frac{1}{\langle b_i - a_i, x \rangle} \right) \cdot \left(\prod_{\substack{v_i \notin \Delta_j \\ \text{vertex}}} \frac{1}{\langle b_i - a_i, x \rangle} \right) \\ &= \prod_{\substack{v_i \in Q \\ \text{vertex}}} \frac{1}{\langle b_i - a_i, x \rangle} \end{aligned}$$

and

$$p(x) = \sum_{j \in J} \left(|\det(\hat{M}_j(x))| \cdot \prod_{\substack{v_i \notin \Delta_j \\ \text{vertex}}} \frac{1}{\langle b_i - a_i, x \rangle} \right).$$

Hence $\deg q \leq f_0(Q)$ and $\deg p \leq f_0(Q) + 1$, so the claim follows. \square

Notice that generically, meaning for the generic choice of the vertices of P , the bound in Proposition 3.2.13 is attained, because p and q will not have common factors.

Theorem 3.2.14. Let $P \subset \mathbb{R}^d$ be a full-dimensional polytope with $f_1(P)$ edges. Then the degrees of the irreducible components of $\partial_a IP$ are bounded from above by

$$f_1(P) - (d-1).$$

Proof. We want to prove that $f_0(Q) \leq f_1(P) - (d-1)$, for every $Q = P \cap u^\perp$, $u \in S^{d-1} \setminus \mathcal{H}$. By definition, every vertex of Q is a point lying on an edge of P , so trivially $f_0(Q) \leq f_1(P)$. We want to argue now that it is impossible to intersect more than $f_1(P) - (d-1)$ edges of P with our hyperplane $H = u^\perp$. If the origin is one of the vertices of P , then all the edges that have the origin as a vertex give rise only to one vertex of Q : the origin itself. There are at least d such edges, because P is full-dimensional, and so $f_0(Q) \leq f_1(P) - (d-1)$.

Suppose now that the origin is not a vertex of P , then H does not contain vertices of P . It divides \mathbb{R}^d in two half spaces H_+ and H_- , and so it divides the vertices of P in two families of k vertices in H_+ and ℓ vertices in H_- . Either k or ℓ are equal to 1, or they are both greater than one. In the first case let us assume without loss of generality that $k = 1$, i.e. there is only one vertex v_+ in H_+ . Then pick one vector v_- in H_- : because P is a full-dimensional polytope, there are at least d edges of P with v_- as a vertex. Only one of them may connect v_- to v_+ and therefore the other $d-1$ edges must lie in H_- . This gives $f_0(Q) \leq f_1(P) - (d-1)$.

On the other hand, let us assume that $k, \ell \geq 2$. Then there is at least one edge in H_+ and one edge in H_- . If $d = 3$ these are the $d-1$ edges that do not intersect the hyperplane. For $d > 3$ we proceed as follows. Suppose that H intersects a facet F of P . Then it cannot intersect all the facets of F , otherwise we would get $F \subset H$ which contradicts the fact that H does not intersect vertices of P . So there exists a ridge F' of P that does not intersect the hyperplane; it has dimension $d-2 \geq 2$ and therefore it has at least $d-1$ edges. Hence

$$f_0(Q) \leq f_1(P) - (d-1).$$

□

Corollary 3.2.15. In the hypotheses of Theorem 3.2.14, if P is centrally symmetric and centered at the origin, then we can improve the bound with

$$\frac{1}{2} (f_1(P) - (d-1)).$$

Proof. We already know that for each chamber C_i from Lemma 3.2.3, the degree of the corresponding irreducible component is bounded by the degree of the polynomial q_i . This follows from the construction of p_i and q_i in the proof of Theorem 3.2.5. Specifically, the determinant which gives p_i/q_i comes with the product of $d-1$ rational functions, with linear numerators and denominators, and one linear term. Thus $\deg p_i = \deg q_i + 1$ which implies that $\deg \frac{p_i}{\|x\|^2} < \deg q_i$. By definition these polynomials q_i 's are obtained as the least common multiple of objects with shape

$$\prod_{\substack{v_k \in \Delta_j \\ \text{vertex}}} \frac{1}{\langle b_k - a_k, x \rangle}.$$

If P is centrally symmetric, so is Q , and therefore we have a vertex belonging to the edge $[a_k, b_k]$ and also a vertex belonging to the edge $[-a_k, -b_k]$. When computing the least common multiple, these two vertices produce the same factor, up to a sign, and therefore they count as the same linear factor of q_i . Hence, for every i

$$\deg q_i(x) \leq \frac{f_0(Q)}{2} \leq \frac{1}{2} (f_1(P) - (d-1)).$$

□

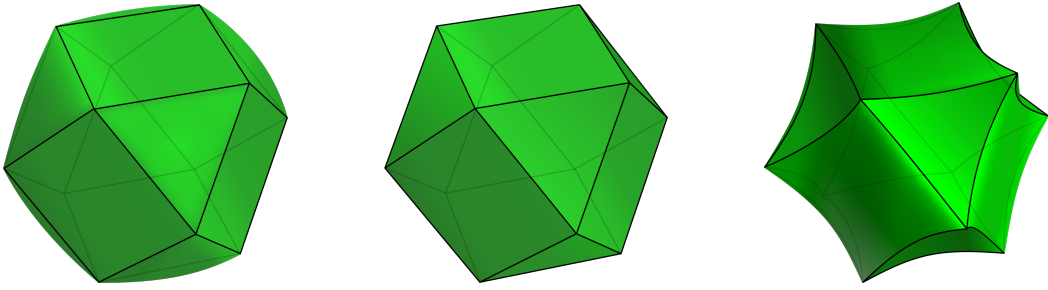


Figure 3.9: Left: the intersection body of the cube in Example 3.2.11. Right: the intersection body of the tetrahedron in Example 3.2.16. Center: the dual body of the zonotope $Z(P)$ associated to both the cube and the tetrahedron. Such a polytope reveals the structure of the boundary divided into regions of these two intersection bodies.

Example 3.2.16. Let $P = \text{conv}\{(-1, -1, -1), (-1, 1, 1), (1, -1, 1), (1, 1, -1)\}$ be a tetrahedron in \mathbb{R}^3 . The associated hyperplane arrangement coincides with the one associated to the cube in Example 3.2.11, so it has 14 chambers that come in two families. The first one consists of cones spanned by four rays, such as \overline{C}_1 (see Example 3.2.11). The polynomial that defines the boundary of IP in this region is a quartic, namely

$$q_2(x, y, z) - \frac{p_2(x, y, z)}{\|(x, y, z)\|^2} = (x + z)(x - z)(y + z)(y - z) - 2(x^2 + y^2 - z^2)z.$$

On the other hand the cones of the second family are spanned by three rays: here the section of P is a triangle and the equation of the boundary if IP is a cubic. An example is the cone \overline{C}_2 with the polynomial

$$q_1(x, y, z) - \frac{p_1(x, y, z)}{\|(x, y, z)\|^2} = (x - y)(x - z)(y + z) + (x - y - z)^2.$$

Note that this region furnishes an example in which the bounds given in Proposition 3.2.13 and Theorem 3.2.14 are attained. \blacklozenge

Remark 3.2.17. Remark 3.2.4, together with Proposition 3.2.13, implies that the structure of the irreducible components of the algebraic boundary of IP is strongly connected with the face lattice of the dual of the zonotope $Z(P)$. More precisely, in the generic case, the lattice of intersection of the irreducible components of $\partial_a IP$ is isomorphic to the face lattice of the dual polytope $Z(P)^\circ$. Thus, a classification of ‘combinatorial types’ of such intersection bodies is analogous to the classification of zonotopes / hyperplane arrangements. It is however worth noting, that the same zonotope can be associated to two polytopes P_1 and P_2 which are not combinatorially equivalent. One example of this instance is a pair of polytopes such that $P_1 = \text{conv}(v_1, \dots, v_n)$ and $P_2 = \text{conv}(\pm v_1, \dots, \pm v_n)$, as can be seen in Figure 3.9 for the cube and the tetrahedron. To have a better overview over the structure of the boundary of IP , one strategy is to use the Schlegel diagram [Zie12, Chapter 5] of $Z(P)^\circ$. We label each maximal cell by the degree of the polynomial that defines the corresponding irreducible component of $\partial_a IP$, as can be seen in Figures 3.10, 3.11.

Example 3.2.18 (Continuation of Example 3.2.6, Figure 3.7). Let P be the regular icosahedron. In the 12 regions which are spanned by five rays, the polynomial that defines the

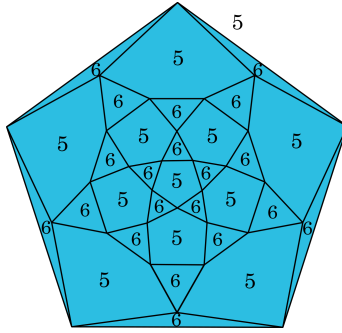


Figure 3.10: The Schlegel diagram of $Z(P)^\circ$, in the case where P is the icosahedron from Example 3.2.18. The labels represent the degrees of the polynomials of $\partial_a IP$.

boundary of IP has degree 5 and it looks like

$$\begin{aligned} & ((\sqrt{5}x + \sqrt{5}y - x + y)^2 - 4z^2)((\sqrt{5}x + x + 2y)^2 - (\sqrt{5}z - z)^2)y + \\ & 8\sqrt{5}x^3y + 68\sqrt{5}x^2y^2 + 72\sqrt{5}xy^3 + 20\sqrt{5}y^4 - 40\sqrt{5}xyz^2 - 20\sqrt{5}y^2z^2 + 4\sqrt{5}z^4 + \\ & 8x^3y + 164x^2y^2 + 168xy^3 + 44y^4 - 8x^2z^2 - 72xyz^2 - 44y^2z^2 + 12z^4. \end{aligned}$$

In the other 20 regions spanned by three rays, ∂IP is the zero set of a sextic polynomial with the following shape

$$\begin{aligned} & ((\sqrt{5}x + x + 2y)^2 - (\sqrt{5}z - z)^2)((\sqrt{5}y - 2x - y)^2 - (\sqrt{5}z - z)^2)xy + 20\sqrt{5}x^4y - \\ & 20\sqrt{5}x^2y^3 - 4\sqrt{5}xy^4 + 4\sqrt{5}y^5 - 4\sqrt{5}x^3z^2 - 60\sqrt{5}x^2yz^2 - 12\sqrt{5}xy^2z^2 + 12\sqrt{5}xz^4 + 44x^4y - \\ & 8x^3y^2 - 44x^2y^3 + 12xy^4 + 12y^5 - 12x^3z^2 - 156x^2yz^2 - 60xy^2z^2 - 8y^3z^2 + 28xz^4. \end{aligned}$$

We visualize the structure of these pieces using the Schlegel diagram in Figure 3.10, where the numbers correspond to the degree of the polynomials, as explained in Remark 3.2.17. ♦

Using this technique we are then able to visualize the boundary of intersection bodies of 4-dimensional polytopes via the Schlegel diagram of $Z(P)^\circ$.

Example 3.2.19. Let $P = \text{conv}\{(1, 1, 0, 0), (0, 1, 0, 0), (0, -1, 0, 0), (0, 0, -1, 0), (0, 0, 0, -1)\}$. The boundary of its intersection body IP is subdivided in 16 regions. In four of them the equation is given by a polynomial of degree 3, whereas in the remaining twelve regions the polynomial has degree 5. In Figure 3.11 we show the Schlegel diagram of

$$Z(P)^\circ = \text{conv}\{\pm(1/2, -1/2, 0, 0), \pm(1, 0, 0, 0), \pm(0, 0, 1, 0), \pm(0, 0, 0, 1)\}$$

with a number associated to each maximal cell which represents the degree of the polynomial in the corresponding region of ∂IP . ♦

3.2.3. The cube

In this section we study the intersection body of the d -dimensional cube $C^{(d)} = [-1, 1]^d$, with a special emphasis on the linear components of its algebraic boundary.

Proposition 3.2.20. The algebraic boundary of the intersection body of the d -dimensional cube $C^{(d)}$ has at least $2d$ linear components. These components correspond to the $2d$ open regions from Lemma 3.2.3 which contain the standard basis vectors and their negatives.

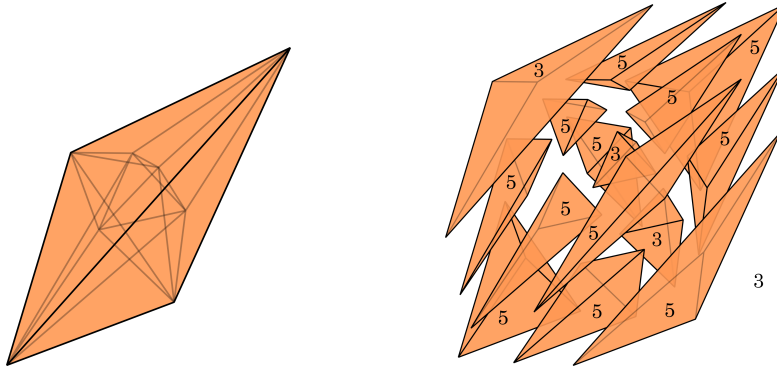


Figure 3.11: The Schlegel diagram of $Z(P)^\circ$ from Example 3.2.19. There are four cells whose corresponding polynomial in $\partial_a IP$ has degree 3, including the outer facet; the others correspond to polynomials of degree 5.

Proof. We show the claim for the first standard basis vector e_1 . The argument for the other vectors $\pm e_i, i = 1, \dots, d$ is analogous. Let C be the region from Lemma 3.2.3 which contains e_1 and consider $U = C \cap S^{d-1}$. For any $u \in U$, the polytope $C^{(d)} \cap u^\perp$ is combinatorially equivalent to $C^{(d-1)}$. Hence we can compute the (signed) volume,

$$\text{vol}(C^{(d)} \cap u^\perp) = \det \begin{bmatrix} v^{(1)} - v^{(0)} \\ \vdots \\ v^{(d-1)} - v^{(0)} \\ u \end{bmatrix}$$

where $v^{(0)}$ is an arbitrarily chosen vertex of $C^{(d)} \cap u^\perp$ and the remaining $v^{(i)}$ are vertices of $C^{(d)} \cap u^\perp$ adjacent to $v^{(0)}$. Next, we observe that for any vertex v of $C^{(d)} \cap u^\perp$ which lies on the edge $[a, b]$ of $C^{(d)}$, v is the vector

$$v = \left(-\frac{1}{u_1} \sum_{j=2}^d a_j u_j, a_2, \dots, a_d \right).$$

This follows from the formulation of v in the proof of Theorem 3.2.5 and the fact that $b_1 = -a_1$ and $b_i = a_i$ for $i = 2, \dots, d$. Combining this with the determinant above gives the following expression for the radial function restricted to U :

$$\rho(u) = \frac{1}{u_1} \det \begin{bmatrix} -\sum_{j=2}^d (a_j^{(1)} - a_j^{(0)}) u_j & a_2^{(1)} - a_2^{(0)} & \dots & a_d^{(1)} - a_d^{(0)} \\ -\sum_{j=2}^d (a_j^{(2)} - a_j^{(0)}) u_j & a_2^{(2)} - a_2^{(0)} & \dots & a_d^{(2)} - a_d^{(0)} \\ \vdots & \vdots & & \vdots \\ -\sum_{j=2}^d (a_j^{(d)} - a_j^{(0)}) u_j & a_2^{(d)} - a_2^{(0)} & \dots & a_d^{(d)} - a_d^{(0)} \\ u_1^2 & u_2 & \dots & u_d \end{bmatrix}$$

where we assume the determinant is nonnegative, else we multiply by -1 . Expanding the determinant along the bottom row of the matrix yields

$$\rho(u) = \frac{1}{u_1} \left(u_1^2 \det \begin{bmatrix} a_2^{(1)} - a_2^{(0)} & \dots & a_d^{(1)} - a_d^{(0)} \\ a_2^{(2)} - a_2^{(0)} & \dots & a_d^{(2)} - a_d^{(0)} \\ \vdots & & \vdots \\ a_2^{(d)} - a_2^{(0)} & \dots & a_d^{(d)} - a_d^{(0)} \end{bmatrix} + \gamma(u_2, \dots, u_n) \right).$$

where $\gamma(u_2, \dots, u_d)$ is a polynomial consisting of the quadratic terms in the remaining u_i 's. Note that since γ does not contain the variable u_1 and ρ is divisible by the quadric $u_1^2 + \dots + u_d^2$ by Proposition 3.2.13, it follows that

$$\rho(u) = \frac{u_1^2 + \dots + u_d^2}{u_1} \det \begin{bmatrix} a_2^{(1)} - a_2^{(0)} & \dots & a_d^{(1)} - a_d^{(0)} \\ a_2^{(2)} - a_2^{(0)} & \dots & a_d^{(2)} - a_d^{(0)} \\ \vdots & & \vdots \\ a_2^{(d)} - a_2^{(0)} & \dots & a_d^{(d)} - a_d^{(0)} \end{bmatrix}. \quad (3.2.1)$$

Let A be the $(d-1) \times (d-1)$ -matrix appearing in (3.2.1). Then the irreducible component of the algebraic boundary on the corresponding region C is described by the linear equation $x_1 = |\det A|$. \square

Note that for an arbitrary polytope P of dimension at least 3, the irreducible components of the algebraic boundary $\partial_a IP$ cannot all be linear. It is implied by the fact that in this setting the intersection body of a convex body is not a polytope. It is thus worth noting that the intersection body of the cube has remarkably many linear components. We now investigate the non-linear pieces of $\partial_a IC^{(4)}$.

Example 3.2.21. Let P be the 4-dimensional cube $[-1, 1]^4$ and IP be its intersection body. The associated hyperplane arrangement has $8 + 32 + 64 = 104$ chambers. The first 8 are spanned by 6 rays and the boundary here is linear, i.e. it is a 3-dimensional cube. For example, the linear face exposed by $(w, x, y, z) = (1, 0, 0, 0)$ is cut out by the hyperplane $w = 8$. The second family of chambers is made of cones with 5 extreme rays, where the boundary is defined by a cubic equation with shape

$$3xyz - 3w^2 - 6x^2 - 12xy - 6y^2 - 12xz + 12yz - 6z^2.$$

Finally, a quartic such as

$$\begin{aligned} 4wxyz - w^3 - 3w^2x - 3wx^2 - x^3 - 3w^2y - 6wxy - 3x^2y - 3wy^2 - 3xy^2 \\ - y^3 - 3w^2z - 6wxz - 3x^2z + 18wyz - 6xyz - 3y^2z - 3wz^2 - 3xz^2 - 3yz^2 - z^3 \end{aligned}$$

defines the boundary of the intersection body in the remaining 64 cones spanned by 4 rays. \blacklozenge

Proposition 3.2.20 gives a lower bound on the number of linear components of the algebraic boundary of $IC^{(d)}$. We conjecture that for any $d \in \mathbb{N}$, the algebraic boundary of the intersection body of the d -dimensional cube centered at the origin has exactly $2d$ linear components. Computational results for $d \leq 5$ support this conjecture, as displayed in Table 3.1. It shows the number of irreducible components of $\partial_a IC^{(d)}$ sorted by the degree of the component, for $d = 2, 3, 4, 5$. The first two columns are the dimension of the polytope, and the number of chambers of the respective hyperplane arrangement \mathcal{H} . The third column is the degree bound from Corollary 3.2.15. The remaining columns show the number of regions whose equation in the algebraic boundary have degree \deg , for $\deg = 1, \dots, 5$.

It is worth noting that the highest degree attained in these examples is equal to the dimension of the respective cube. In particular, the degree bound for centrally symmetric polytopes, as given in Corollary 3.2.15 is not attained in any of the cases for $d \geq 3$. Finally, note that the number of regions grows exponentially in d , and thus for $d \geq 3$, the number of non-linear components exceeds the number of linear components.

dimension	# chambers	degree bound	deg = 1	2	3	4	5
2	4	1	4	0	0	0	0
3	14	5	6	0	8	0	0
4	104	14	8	0	32	64	0
5	1882	38	10	0	80	320	1472

Table 3.1: Number of irreducible components of the algebraic boundary of the intersection body of the d -cube, listed by degree.

3.2.4. Conclusions

Add conclusions and further research directions.

Chapter 4

Convex hulls

4.1. Surfaces in fourspace

4.2. Curves and volumes

Chapter 5

Convex bodies in applications: quantum physics

This chapter is dedicated to the study of a specific convex body in \mathbb{R}^4 , which arises from quantum physics. We present here an almost integral version of the paper [LMS⁺21]. It began as a project of T.P.Le and R.F.Werner, aimed at a better understanding of self-testing. T.Ziegler joined as a Masters student. B. Sturmfels and the author of this thesis contributed with the mathematical aspects. The main character of the article is the set of quantum correlations $\mathcal{Q} \subset \mathbb{R}^4$. It is a full-dimensional semialgebraic convex body, sandwiched between two polytopes: $\mathcal{C} \subset \mathcal{Q} \subset \mathcal{N}$. We point out that \mathcal{N} is the polytope P from Example 1.1.13. The presentation below starts with a brief introduction to quantum correlations. This is followed by a mathematical discussion, where the main results are stated, and by a summary of previous work. Section 5.2 offers a more extended description of the correlation body \mathcal{Q} , from basic visualization and overall properties to a detailed classification of boundary points. In Section 5.3 we focus on the dual body and its connection to \mathcal{Q} . We also investigate their common normal cycle. In these descriptive sections we give no proofs. Proofs are collected in Section 5.5. Every statement of a proposition or theorem begins with a clickable pointer such as (\rightarrow Section 5.5) to the subsection containing the proof. An exception to this rule are statements that are clear from the context, and merely summarize a narrative just given. The proof section is organized in logical order, and should be readable from beginning to end without forward references. This order differs from the narrative in Sections 5.2, 5.3, and also from the theorems in Section 5.1.2.

The notation used in this chapter will sometimes differ from the one used in the previous chapters. We decided to leave it as it is in order to avoid conflicts with standard conventions in quantum physics and to keep it as intuitive as possible. We point out here some of the differences. The coordinates of \mathbb{R}^4 will be usually denoted by $(c_{11}, c_{12}, c_{21}, c_{22})$, whereas $(f_{11}, f_{12}, f_{21}, f_{22})$ will denote a point of the dual space $(\mathbb{R}^4)^*$. Angle brackets will be used for the expectation of a random variable, and ‘.’ for the standard Euclidean scalar product. The support function of a convex body K will be represented by ϕ_K ; its extreme points are $\partial_e K$ in what follows. In any case, every new notation will be properly introduced when needed.

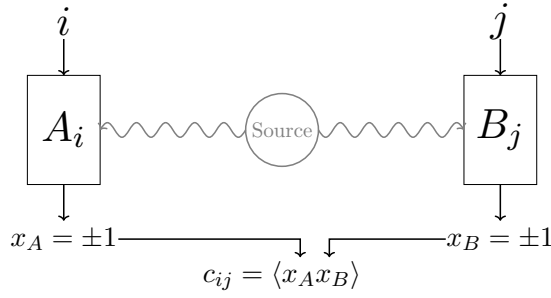


Figure 5.1: A correlation experiment: Alice chooses setting i and Bob setting j . The outcomes of A_i and B_j are ± 1 . One measures the correlation c_{ij} of these outcomes.

5.1. Introduction

The quantum correlation set is a fundamental object in quantum information theory. The key point is that some correlations predicted by quantum theory cannot be modeled within classical probability. In this situation it is natural to ask: where exactly lies the boundary between the classical and the quantum? What other correlations or quantum states exhibit the same features? In a correlation setting, N parties share some quantum state, so that each party can choose from M different measurements, each of which can have K different outcomes. So what exactly is the set of correlation data that can arise from either classical probability or quantum? This is a hard problem even for fairly small N, M, K , as seen on the open problems website [NW⁺, Problems 1,26,27,32,33,34]. The singlet state has the minimal set of parameters $NMK = 222$. Here, characterizations have been known since Tsirelson's seminal work [Tsi87], particularly in the ‘zero-marginals’ case $222|0$, defined by the property that each outcome by itself, without considering the results of other parties, is equidistributed. This is the scenario indicated by the adjective ‘minimal’ in our title. We provide an overview of the literature below in Section 5.1.3. Known results are scattered. The connections between different characterizations are rarely given, the overall structure of the boundary is not analyzed, and no attempts at a full geometric understanding or visualization are made. Moreover, the self-duality of the body seems to have escaped notice altogether. All this will be provided in the present chapter, along with self-contained proofs of all assertions.

5.1.1. Background from physics

In a correlation experiment, several parties carry out measurements on a shared quantum system. We consider $N = 2$ causally disconnected parties, conventionally called Alice and Bob. Each of them chooses from $M = 2$ possible measurements, labeled $i, j = 1, 2$, with $K = 2$ possible outcomes, labeled ± 1 (see Figure 5.1). Thus there are four experiments, labeled by the pairs (i, j) of choices for Alice and Bob. The correlation $c_{ij} \in [-1, 1]$ is the probability of equal outcomes minus that of different outcomes. Equivalently, c_{ij} is the expectation of the product of the outcomes, when these are labeled as ± 1 . The c_{ij} are not sufficient to reconstruct the full statistics. That would give an 8-dimensional convex body, whose coordinates are the marginals for single outcomes, plus one correlation for every pair (i, j) . This count incorporates the no-signalling condition, namely that the marginals do not depend on the setting chosen at the other site. Restricting to the 4-tuples $c = (c_{11}, c_{12}, c_{21}, c_{22})$ corresponds to a *projection* of the 8-dimensional body. We can realize

this projection geometrically by taking the equal weight mixture of the given model with one in which all outcomes are flipped to their negatives. This operation changes the sign of the marginals, but not of the correlations c_{ij} . Therefore, we can alternatively think of the 4-dimensional body as that *section* of the 8-dimensional body, in which the marginals are set equal to zero. This explains why we call our scenario in the 4-dimensional c -space the zero marginals case.

We are interested in the set \mathcal{Q} of correlations $c = (c_{11}, c_{12}, c_{21}, c_{22})$ that are consistent with quantum theory. Quantum systems are described in some separable Hilbert space \mathcal{H} over \mathbb{C} . The source is given by a positive Hermitian operator ρ acting on \mathcal{H} . It satisfies $\text{tr}(\rho) = 1$ and is called the *density operator*. The measurements are characterized by Hermitian operators A_1, A_2, B_1, B_2 on \mathcal{H} that satisfy the hypotheses

$$[A_i, B_j] = 0 \quad \text{and} \quad -\mathbb{1} \leq A_i, B_j \leq \mathbb{1} \quad \text{for } 1 \leq i, j \leq 2. \quad (5.1.1)$$

If $\mathcal{H} = \mathbb{C}^m$ then A_i and B_j are Hermitian $m \times m$ matrices and $\mathbb{1}$ is the identity matrix. Condition (5.1.1) says that A_i commutes with B_j and that the eigenvalues of all these matrices are in $[-1, 1]$. The commutation condition represents the hypothesis that the two parties are causally disconnected, i.e., all measurements by Alice can be executed jointly with those of Bob. In contrast, the commutators $[A_1, A_2]$ and $[B_1, B_2]$ are usually nonzero, i.e., the two measurement choices of each party individually are not commensurate.

The correlations are computed from the operators above by taking traces:

$$c_{ij} = \text{tr}(\rho A_i B_j) \quad \text{for } 1 \leq i, j \leq 2. \quad (5.1.2)$$

The *correlation body* \mathcal{Q} consists of all points c in the cube $[-1, 1]^4$ that admit such a representation.

There is an analogous set \mathcal{C} in classical probability theory, where the A_i and B_j are ± 1 -valued random variables, with joint probability distribution ρ . Writing angle brackets for expectations, the formula is

$$c_{ij} = \langle A_i B_j \rangle \quad \text{for } 1 \leq i, j \leq 2. \quad (5.1.3)$$

The classical set \mathcal{C} consists of all points c in the cube $[-1, 1]^4$ that admit such a representation.

We note that (5.1.3) is the special case of (5.1.2) when all A_i and B_j commute. All matrices can then be taken to be diagonal, and the diagonal entries of ρ form a probability distribution. Hence $\mathcal{C} \subseteq \mathcal{Q}$.

The whole point of our correlation body is that the reverse inclusion is false. A prominent example is

$$c = \frac{1}{\sqrt{2}}(1, 1, 1, -1) \in \mathcal{Q} \setminus \mathcal{C}. \quad (5.1.4)$$

It is easy to build a quantum representation, and this has been realized experimentally to very high precision. So the realizability of this c is a well-confirmed experimental fact. On the other hand, c cannot be classical, because the Clauser-Horne-Shimony-Holt version of John Bell's inequality holds for all $c \in \mathcal{C}$:

$$\text{CHSH}(c) : \quad \frac{1}{2}(c_{11} + c_{12} + c_{21} - c_{22}) \leq 1. \quad (5.1.5)$$

The point c in (5.1.4) is not classical because the left hand side of (5.1.5) equals $\sqrt{2}$, and this exceeds 1. This is a remarkable result, the basis of an experimentum crucis ruling out a whole mode of describing Nature.

The experiments put quantum theory to a sharp test: the value $\sqrt{2}$ is an upper bound for all quantum correlations. If a value significantly larger than $\sqrt{2}$ had been found, then this would refute the quantum way of describing Nature, in just the same way as classical theories are excluded by a violation of Bell's CHSH inequality. This inequality and all linear inequalities bounding \mathcal{Q} are called *Tsirelson inequalities*.

Tsirelson's bound has led to speculations about super-quantum correlations in families of theories ('generalized probabilistic theories'), and to the desire to view the quantum case in a larger context. The only constraint then would be that Alice choosing a measurement device makes no detectable difference for the probabilities of outcomes seen by Bob alone, i.e., without comparing outcomes with Alice. This is the *no signalling set* of correlations, denoted by \mathcal{N} . It satisfies $\mathcal{C} \subset \mathcal{Q} \subset \mathcal{N}$. Since in this paper we ignore marginals seen by only one partner, the remaining constraint is that c lies in the cube, so $\mathcal{N} = [-1, 1]^4$.

When N, M, K are larger than 2, 2, 2, computing optimal bounds for \mathcal{Q} is a hard problem. One source of difficulty is that there are multiple definitions of \mathcal{Q} , depending on how the separation of parties is required to be encoded in a tensor product structure, or just commutativity between Alice and Bob. This is known as Tsirelson's problem [Fri12, JNP⁺11], and was recently resolved in [JNV⁺20]. However, it does not arise in the 222 case. Another source of difficulty is that no bound on the Hilbert space dimension can be assumed. Restricting the dimension to be finite, in general, gives a set that is not closed, so some limiting correlations require infinite dimension [Slo19]. Again this subtlety does not occur in the minimal case. The minimal case considered in this paper is the only one for which a sharp characterization has been achieved. This is the principal reason for undertaking the detailed geometric study that is to follow.

A crucial property for quantum key distribution is that a maximal violation of the CHSH inequality can be achieved in an essentially unique way. Thus, by just verifying such correlations, without any knowledge about the construction of the devices, one can reconstruct ρ, A_i, B_j up to trivial enlargements. This property is called *self-testing*. It implies that any further system will be uncorrelated, so an eavesdropping third party could never learn anything about the data collected by Alice and Bob. We explain the cryptographic background in Section 5.4.

5.1.2. A view from mathematics

The correlation body \mathcal{Q} is compact and convex. Compactness is not obvious but follows from Theorem 5.1.1. For convexity, let $c, \tilde{c} \in \mathcal{Q}$ have realizations (5.1.2) by matrices of size m and \tilde{m} . Any convex combination $\lambda c + (1 - \lambda)\tilde{c}$ is realized by block matrices of size $m + \tilde{m}$, namely $\lambda\rho \oplus (1 - \lambda)\tilde{\rho}$, $A_i \oplus \tilde{A}_i$ and $B_j \oplus \tilde{B}_j$. By contrast, if we were to fix m then compactness is easy to see but convexity generally fails. For instance, fixing $m = 1$, the image under (5.1.2) is the set of 2×2 matrices of rank ≤ 1 with each entry in $[-1, +1]$.

The body \mathcal{Q} lies between two polytopes. First, \mathcal{Q} is contained in the 4-cube $\mathcal{N} = [-1, 1]^4$, which has 16 vertices, 32 edges, 24 ridges and 8 facets. Second, \mathcal{Q} contains the classical set \mathcal{C} , which is also a polytope. Namely, \mathcal{C} is the *demicube*, which is the convex hull of the eight even vertices of \mathcal{N} . The 4-dimensional demicube \mathcal{C} is combinatorially dual to the cube \mathcal{N} (see Example 1.1.13). It coincides with the cross polytope [Zie95, Example 0.4], so it has 8 vertices, 24 edges, 32 ridges and 16 facets. This census of the faces of \mathcal{C} is of direct relevance for our description of the boundary of the convex body \mathcal{Q} , to be given in Proposition 5.2.4.

The correlation body \mathcal{Q} is semialgebraic: it can be described by a Boolean combination

of polynomial inequalities. Here a phenomenon arises that is unfamiliar from polytope theory. It is not sufficient to use a conjunction of polynomial inequalities. In other words, \mathcal{Q} is not a basic semialgebraic set. Moreover, while both polynomials g and h in the description below are needed, only h is determined by \mathcal{Q} , as the unique algebraic description of a part of the boundary, while there is some freedom of choice for g .

A main source of convex semialgebraic sets is the cone of positive semidefinite matrices. Quantum theory is entirely based on this cone. Its states, observables, and channels are all defined in terms of it. In fact, the set \mathcal{Q} arises from a spectrahedron by projection, and it is thus in the class of spectrahedral shadows.

Each of the themes described in the previous paragraphs can be used to characterize the set \mathcal{Q} . This leads to six descriptions that look different at first glance. We summarize these in the following theorem.

Theorem 5.1.1. (\rightarrow Section 5.5.1) The following items describe the same subset \mathcal{Q} in \mathbb{R}^4 :

- (a) The set of quantum correlations c , as defined in Section 5.1.1, i.e., the c_{ij} from (5.1.2) satisfying (5.1.1).
- (b) The convex hull of $\{(\cos \alpha, \cos \beta, \cos \gamma, \cos \delta) \in \mathbb{R}^4 \mid \alpha + \beta + \gamma + \delta \equiv 0 \pmod{2\pi}\}$.
- (c) The image of the demicube \mathcal{C} under the homeomorphism $\mathbf{sin} : \mathcal{N} \rightarrow \mathcal{N}$ mapping c to $\sin(\frac{\pi}{2} c_{ij})_{1 \leq i,j \leq 2}$.
- (d) The semialgebraic set $\{c \in \mathcal{N} \mid g(c) \geq 0 \text{ or } h(c) \geq 0\}$, where

$$\begin{aligned} g(c) &= 2 - (c_{11}^2 + c_{12}^2 + c_{21}^2 + c_{22}^2) + 2c_{11}c_{12}c_{21}c_{22} \\ h(c) &= 4(1 - c_{11}^2)(1 - c_{12}^2)(1 - c_{21}^2)(1 - c_{22}^2) - g(c)^2. \end{aligned}$$

- (e) The spectrahedral shadow consisting of all points $(c_{11}, c_{12}, c_{21}, c_{22}) \in \mathbb{R}^4$ such that

$$C = \begin{pmatrix} 1 & u & c_{11} & c_{12} \\ u & 1 & c_{21} & c_{22} \\ c_{11} & c_{21} & 1 & v \\ c_{12} & c_{22} & v & 1 \end{pmatrix}$$

is positive semidefinite for some choice of $u, v \in \mathbb{R}$.

- (f) The scalar products of pairs of unit vectors a_i, b_j in some Euclidean space: $c_{ij} = a_i \cdot b_j$ for $i, j = 1, 2$.

One way to describe a convex body is by the maxima of all linear functionals. As we discussed in Section 1.1.3, this is the support function, denoted by

$$\phi_{\mathcal{Q}}(f) = \sup\{f \cdot c \mid c \in \mathcal{Q}\}.$$

Here $f \in \mathbb{R}^4$ and ‘ \cdot ’ denotes the scalar product in \mathbb{R}^4 . The following theorem gives an explicit formula.

Theorem 5.1.2. (\rightarrow Section 5.5.3) Consider the following expressions in four variables

$f = (f_{11}, f_{12}, f_{21}, f_{22})$:

$$\begin{aligned} k(f) &= (f_{11}f_{22} - f_{12}f_{21})(f_{11}f_{12} - f_{21}f_{22})(f_{11}f_{21} - f_{12}f_{22}) \\ p(f) &= f_{11}f_{12}f_{21}f_{22} \\ \phi_C(f) &= \max\{|f_{11} + f_{12} + f_{21} + f_{22}|, |f_{11} + f_{12} - f_{21} - f_{22}|, \\ &\quad |f_{11} - f_{12} + f_{21} - f_{22}|, |f_{11} + f_{12} - f_{21} - f_{22}|\} \\ m(f) &= \left(\min_{i,j} |f_{ij}|\right) \left(\sum_{i,j} |f_{ij}|^{-1}\right). \end{aligned}$$

The support function of the correlation body \mathcal{Q} equals

$$\phi_{\mathcal{Q}}(f) = \begin{cases} \sqrt{\frac{k(f)}{p(f)}} & \text{if } p(f) < 0 \text{ and } m(f) > 2, \\ \phi_C(f) & \text{otherwise.} \end{cases} \quad (5.1.8)$$

The case distinction in (5.1.8) is between the ‘classical’ case and the ‘quantum’ case. Indeed, as the notation suggests, the piecewise linear expression ϕ_C in Theorem 5.1.2 is the support function of the cross polytope C . Hence ϕ_C represents inequalities for classical correlations. On the other hand, in first case of (5.1.8), the maximizers are non-classical correlations, and for fixed f the maximizer is unique (see Proposition 5.3.5).

Consider the sequence of inclusions $C \subset \mathcal{Q} \subset \mathcal{N}$ we discussed above. Then we have an analogous chain for the dual bodies: $\mathcal{N}^\circ \subset \mathcal{Q}^\circ \subset C^\circ$. Here C and \mathcal{N}° are cross polytopes, while \mathcal{N} and C° are 4-cubes. However, even stronger statements are true: C is affinely isomorphic to \mathcal{N}° , and \mathcal{N} is affinely isomorphic to C° . Moreover, these isomorphisms extend to the middle term in the inclusion $C \subset \mathcal{Q} \subset \mathcal{N}$, i.e., the correlation body \mathcal{Q} is *self-dual*:

Theorem 5.1.3. (→Section 5.5.2) There is an orthogonal transformation H on \mathbb{R}^4 such that

$$C^\circ = \frac{1}{2}H\mathcal{N}, \quad \mathcal{N}^\circ = \frac{1}{2}HC \quad \text{and} \quad \mathcal{Q}^\circ = \frac{1}{2}H\mathcal{Q}.$$

The proofs of the three theorems are presented in Section 5.5. While proving that they agree, we write $\mathcal{Q}_{(a)}, \mathcal{Q}_{(b)}, \mathcal{Q}_{(c)}, \mathcal{Q}_{(d)}, \mathcal{Q}_{(e)}, \mathcal{Q}_{(f)}$ for the six sets in Theorem 5.1.1. All objects and assertions are explained in detail in Section 5.2. along with lots of additional information. For instance, Proposition 5.2.4 describes the stratification of the boundary of \mathcal{Q} into patches. Readers might start with Figures 5.2, 5.3 and 5.4.

5.1.3. Short review of previous work

The correlation body \mathcal{Q} first came into focus in Tsirelson’s work [Tsi80]. That paper gives no proofs, but some of them were supplied in [Tsi87]. This includes the characterization $\mathcal{Q}_{(a)} = \mathcal{Q}_{(f)}$ in the more general 2M2|0 case ([Tsi80, Theorem 1] = [Tsi87, Theorem 2.1]). Thereby the study of \mathcal{Q} , whose definition also allows infinite dimensional Hilbert spaces, is reduced to a finite dimensional problem. A semialgebraic description for the 222|0 case is given in [Tsi87, Theorem 2.2], along with an expression for the support function [Tsi87, Theorem 2.2]. This is our Theorem 5.1.2. Tsirelson calls these results ‘elementary’ consequences of (f), and does not provide a proof. He also thought about issues not covered in our review, like the full 222 case, multipartite scenarios ($N > 2$) [Tsi87, Section 5], and violations of CHSH inequalities by position and momentum ([Tsi87], see also [KW10]).

The spectrahedral shadow $\mathcal{Q}_{(e)}$ first appeared in Landau's work [Lan88] as a relaxation of the correlation body. That the relaxation is tight follows from Tsirelson's theorem [Tsi80]. Landau also gave a nearly semialgebraic characterization of \mathcal{Q} (see (5.2.6) below), which only misses the semialgebraic standard form by containing a square root. He almost achieved the description (d).

The pushout (c) was found by Masanes [Mas03], who stated that it identifies \mathcal{C} and \mathcal{Q} . He also considered the cosine-parametrized manifold of correlations in (b). The pushout was used implicitly in [NPA08, WWS16], in the form of a characterization of \mathcal{Q} by linear inequalities applied to the inverse pushout. However, it was not pointed out that the linear inequalities just characterize \mathcal{C} . Of course, spectrahedral shadows are used as outer approximants to \mathcal{Q} in the semidefinite hierarchies [DLTW08, NPA08]. This is an important technique for higher NMK, even though one gets the convex body exactly only in the minimal case.

A covering of the set of extreme points $\partial_e \mathcal{Q}$, which results in the cosine parametrization (b) and its analog in the N22|0-case, were found in [WW01], see also [Mas05]. The exact identification of the set of extreme points was found much later in [TVC19, WWS16]. The minimal case is an important example in many applications such as quantum non-locality [BCP⁺14, GKW⁺18], self-testing [ŠB20], and quantum cryptography [SGP⁺20, TSG⁺20].

5.2. Description of the correlation body

The convex body \mathcal{Q} has dimension four. Our aim is to describe it in every detail. Naturally, the geometric description will strain our 3-dimensional intuition. As always, the solution is to build the geometric intuitions (German ‘Anschauung’, visualization) on analytic notions, such as sections, projections, affine submanifolds, extreme points, and faces, which have clear definitions, but also on low-dimensional instances on which intuitions can be grounded. In the case at hand, the dimension gap is not too large, and we will see that some three-dimensional sections faithfully display important features of the four-dimensional body. We will also point out where this becomes too misleading. One general cautionary remark is that extreme points of a section usually fail to be extremal in the higher-dimensional body.

This section is divided into subsections, which are organized by geometric features, from overall properties to the classification of boundary points and their explicit description, to the dual inequalities, and finally the quantum realizations. This is different from the logical ordering in a proof. A complete set of proofs will be given only later in Section 5.5, which is accordingly organized in logical progression.

Gallery. We visualize the 4-dimensional body \mathcal{Q} by showing 3-dimensional sections. Some of these will be at the same time projections. For example, the zero marginal case arises from the full marginal case either by ignoring the marginals (a projection) or by taking the subset with zero marginals (a section by a linear subspace). Such sections/projections often arise by averaging over a symmetry group [VW01].

We begin in Figure 5.2 with correlations that are symmetric under exchanging Alice and Bob, i.e., $c_{12} = c_{21}$. The projection onto this hyperplane is given by the map $(c_{11}, c_{12}, c_{21}, c_{22}) \mapsto (c_{11}, c_{22}, (c_{12} + c_{21})/2)$. The corresponding sections of the polytopes \mathcal{N} and \mathcal{C} are a cube and an octahedron, respectively. The extreme points of the section of \mathcal{C} are not all extremal in four dimensions: The point $(1, 1, 0)$, where two parabolas meet

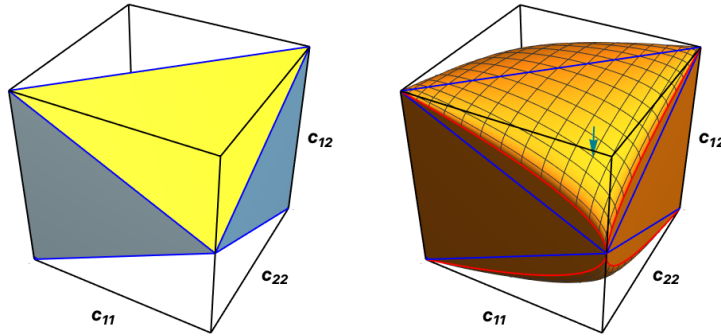


Figure 5.2: The Alice-Bob symmetric subsets of correlations ($c_{12} = c_{21}$), both a projection and a section of their 4-dimensional counterparts. Left: the cube \mathcal{N} with black edges, and the octahedron \mathcal{C} with blue edges. It has two kinds of facets: CHSH-facets (\mathcal{N} -facets (gray). Right: the correlation body \mathcal{Q} . Its boundary consists of a strictly convex surface of exposed extreme points, together with \mathcal{N} -faces extending those of \mathcal{C} , whose boundaries are outlined in red. The arrow points to the CHSH point $c = (1, 1, 1, -1)/\sqrt{2}$.

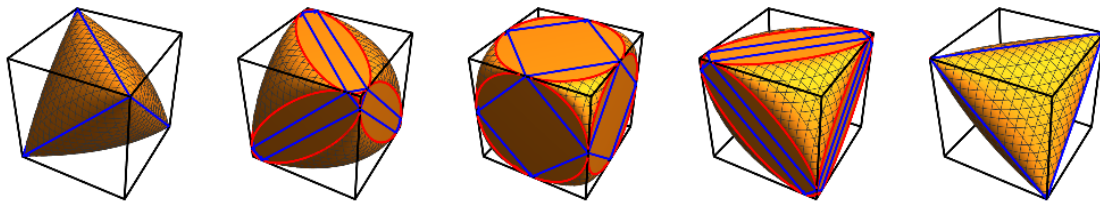


Figure 5.3: Parallel sections $c_{11} = t$ through the body \mathcal{Q} , for $t = -1, -0.8, 0, 0.8, 1$.

in Figure 5.2, has $c_{12} = c_{21} = 0$. It is not extremal in \mathcal{C} . But it is the midpoint between the extreme points $(1, 1, -1, 1)$ and $(1, -1, 1, 1)$ of \mathcal{C} , which lie outside the section shown. The nonlinear boundary in Figure 5.2, right, is a quartic surface, obtained by setting $c_{12} = c_{21}$ in the sextic $h(c)$ and cancelling a factor $(c_{11} - c_{22})^2$. These geometric features have 4-dimensional counterparts, to be described later.

In Figure 5.3 we show the sections parallel to the facets of the cube \mathcal{N} . These are obtained by fixing the value of one coordinate, say c_{11} , at a number t in the interval $[-1, 1]$. This family of pictures gives a full description of \mathcal{Q} . The corresponding projections are non-informative: they are equal to the full 3-cube. The special sections $c_{11} = \pm 1$ are facets of \mathcal{Q} : they are ellipotes (see Example 1.2.10).

Other cutting directions, which can be expected to have an interesting symmetry are sections orthogonal to the main diagonals of \mathcal{N} . Like the vertices, they come in two kinds, either connecting two classical correlations or connecting two PR-boxes. In Figure 5.4 we show, on the left, a cut very close to the hyperplane $c_{11} + c_{12} + c_{21} + c_{22} = 0$, which is orthogonal to the diagonal connecting the classical point $(1, 1, 1, 1)$ and its antipode. On the right in Figure 5.4, we see the cut given by $c_{11} + c_{12} + c_{21} - c_{22} = 0$.

Enclosing and enclosed polytopes. The cube \mathcal{N} consists of the points c such that $-1 \leq c_{ij} \leq 1$. It has $2^4 = 16$ vertices, namely the points in $\{-1, 1\}^4$. The classical distributions are the mixtures of uncorrelated c , i.e., $c_{ij} = a_i b_j$ for some $a_i, b_j \in [-1, 1]$. A classical correlation is extremal when $a_i, b_j = \pm 1$. Hence, the extreme points of \mathcal{C} are

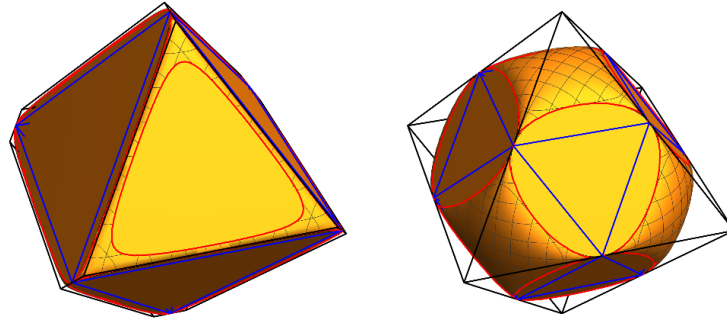


Figure 5.4: Sections through \mathcal{Q} perpendicular to a long diagonal of the cube \mathcal{N} . Left: diagonal connecting two classical correlations. Our cut on is thus slightly off-center, otherwise we would get the full octahedron. Right: diagonal connecting two PR-boxes.

also extreme points of \mathcal{N} , but which? This is decided by a sign: for a classical extreme point we have $c_{11}c_{12}c_{21}c_{22} = a_1^2b_1^2a_2^2b_2^2 = +1$. So the classical extreme points of \mathcal{C} are just the 8 even vertices of \mathcal{N} . The odd vertices are the so-called Popescu-Rohrlich (PR-)box correlations. They have neither classical nor quantum realizations: in (5.1.5) they satisfy $\text{CHSH}(c) = 2$, which clearly exceeds the quantum maximum.

The 16 facets of the demicube \mathcal{C} come in two classes. These are distinguished by how they sit inside the cube \mathcal{N} . A facet in the first class extends to a facet of \mathcal{N} . It is the intersection of \mathcal{C} with a hyperplane like $c_{11} = 1$. There are eight such facets, which we call \mathcal{N} -facets of \mathcal{C} . The more interesting kind is called a *CHSH-facet*, because it saturates a Clauser-Horne-Shimony-Holt inequality (5.1.5). There are eight such inequalities: any odd number of minus signs can multiply the four correlations.

All of this can be seen also in the 3-dimensional cut along the hyperplane $c_{12} = c_{21}$ shown on the left in Figure 5.2. The two polytopes are the intersection of \mathcal{C} and \mathcal{N} with this hyperplane. The CHSH-facets and the \mathcal{N} -facets are marked in different colors. Other slices of \mathcal{C} (blue frame) and \mathcal{N} (black frame) are shown in Figures 5.3 and 5.4. The cut through the origin, orthogonal to the long diagonal connecting classical vertices (approximately as in the left panel in Figure 5.4) has the intersections with \mathcal{N} and \mathcal{C} equal to the same octahedron. Since $\mathcal{C} \subset \mathcal{Q} \subset \mathcal{N}$, this cut also makes our convex body \mathcal{Q} look like a polytope.

Of course, in every cut we see the inclusions $\mathcal{C} \subset \mathcal{Q} \subset \mathcal{N}$. More precisely, the \mathcal{N} -facets of \mathcal{C} extend to facets of \mathcal{Q} , which we also call \mathcal{N} -facets. This is typically a strict extension. The CHSH-facets are no longer faces of \mathcal{Q} . Instead, they become the basis of a bulging part of \mathcal{Q} , above which we find a single vertex of \mathcal{N} . In fact, this is a feature of any body between \mathcal{C} and \mathcal{N} . We record this fact in the following proposition, which helps with keeping track of the parts of \mathcal{Q} .

Proposition 5.2.1. (→Section 5.5.3) Every non-classical correlation $c \in \mathcal{N} \setminus \mathcal{C}$ violates exactly one of the eight CHSH-inequalities.

A feature which will play a major role later, and is characteristic of the minimal case, is the *duality* between the polytopes \mathcal{C} and \mathcal{N} . We saw this in Theorem 5.1.3, and it will be considered in detail in Section 5.3.

Pushout. The connection between the boundary structures of \mathcal{Q} and \mathcal{C} can be raised from a qualitative observation to a precise mathematical statement. There is a natural homeomorphism between the convex bodies. To this end, we define a transformation

$\sin : \mathcal{N} \rightarrow \mathcal{N}$ of the cube, which we call the **pushout** operation:

$$(\sin c)_{ij} = \sin\left(\frac{\pi}{2}c_{ij}\right). \quad (5.2.1)$$

This is the coordinatewise application of a suitably scaled sine function. Since the sine maps the interval $[-\pi/2, \pi/2]$ bijectively and continuously onto $[-1, 1]$, we see that **sin** is bijective, continuous and has a continuous inverse. This is relevant because of the following astonishingly simple characterization of \mathcal{Q} .

Proposition 5.2.2. (\rightarrow Section 5.5.1) $\sin \mathcal{C} = \mathcal{Q}$.

As a connection between convex bodies this is quite strange: the sine is neither convex nor concave on $[-\pi/2, \pi/2]$, so the **sin** transformation applied to a convex set normally does not give a convex set. Moreover, the **sin** function is transcendental but both sets have an algebraic description. So why does this work? What is the general principle? The pushout property is inherited by the sections in Figure 5.2 and by the \mathcal{N} -facets because the hyperplanes $\{c_{12} = c_{21}\}$ and $\{c_{11} = -1\}$ are invariant under **sin**. It also connects \mathcal{C} -sections and \mathcal{Q} -sections in Figure 5.3 when the fixed c_{11} -coordinate is appropriately transformed. The closest we can come to a general principle is related to the fact that the pushout of the tetrahedron is the ellotope. This fact also underlines the cosine parametrization in Proposition 5.2.5. The threefolds of extreme points are parametrized by angles satisfying a linear constraint. A similar connection arises between two families of curves inside the 3-cube, on one hand Lissajous knots, i.e., cosine-parametrized closed rational curves, and, on the other, billiard knots, i.e., closed piecewise linear curves bouncing from the boundaries by specular reflection; see [JP98], [KPS17, Figure 3]. Another feature can be understood from the pushout characterization: at the edges of a polytope extending all the way to the boundary we get a rounded surface with continuous tangents. This is explained in Figure 5.5.

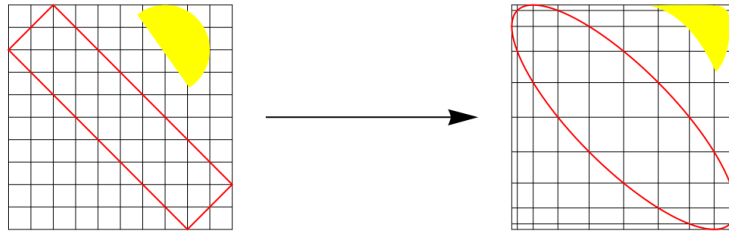


Figure 5.5: The 2-dimensional version of the pushout map in (5.2.1). The rectangle on the left gets mapped to the ellipse on the right. The yellow semicircle shows that convexity is generally not preserved.

Symmetry. The symmetry group of the regular 4-cube $\mathcal{N} = [-1, 1]^4$ is the *hyperoctahedral group* B_4 . This group has order $384 = 2^4 \times 4!$. All of these symmetries are given by rotations and reflections in \mathbb{R}^4 . Each symmetry either preserves the parity of the vertices of \mathcal{N} , or it swaps the eight even vertices and the eight odd vertices. The symmetry group G of the demicube \mathcal{C} is an index two subgroup of B_4 . It consists of symmetries of \mathcal{N} that preserve the parity. It follows from Proposition 5.2.2, and the fact that the pushout map commutes with coordinate permutations and sign changes, that \mathcal{Q} has the same symmetry group G as \mathcal{C} .

Proposition 5.2.3. The common symmetry group of \mathcal{Q} and \mathcal{C} has order 192. It is the semidirect product $G = (\mathbb{Z}/2\mathbb{Z})^3 \rtimes S_4$, where S_4 is the symmetric group on four elements. The first factor swaps labels.

It is noteworthy that this group is larger than one would expect from the definition of \mathcal{Q} . Indeed, some obvious symmetries arise from changing the conventions for describing the correlations: Which party is called Alice, which is Bob? Which outcome is $+1$ or -1 , and which settings get the labels 1 or 2? Changing any of these conventions defines a transformation that clearly leaves each of the correlation sets invariant. The resulting group is visualized in Figure 5.6, and acts on the tuples $(c_{11}, c_{12}, c_{21}, c_{22})$ by sign changes (first row) and permutations (second row) giving only 64 transformations. Not all sign changes can be obtained, only even ones, and the permutations cannot break pairs of diagonally opposing pairs in the square form in which we arranged the c_{ij} . As the additional ‘non-trivial’ transformation needed to generate the group given in Proposition 5.2.3, one can take the swap $(c_{11}, c_{12}, c_{21}, c_{22}) \mapsto (c_{12}, c_{11}, c_{21}, c_{22})$.

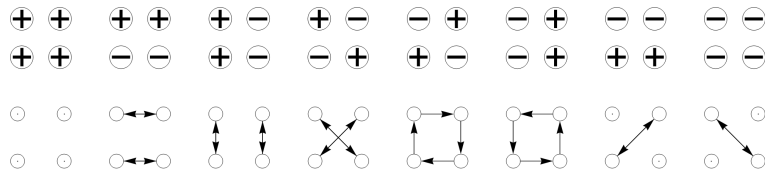


Figure 5.6: Symmetries that preserve the definition of quantum correlations. First row: sign patterns. Second row: permutations arising from a swap of partners or relabeling. The symmetry group G of \mathcal{Q} , as described in Proposition 5.2.3, is larger.

5.2.1. Boundary, faces, and extreme points

Since the pushout is a homeomorphism, it identifies the boundary of \mathcal{Q} with the boundary of \mathcal{C} . The facets of the demicube \mathcal{C} thus provide a partition of the boundary of the correlation body \mathcal{Q} . However, the image of a facet may now become curved, making interior points of the facet extremal in \mathcal{Q} . This happens exactly for the CHSH-facets of \mathcal{C} , as the following proposition shows. We are going to list the interiors of faces because the boundaries already belong to another face. By ‘interior’ we mean the relative interior, i.e., the interior in the affine span of the face. We denote by $\partial_e K$ the extreme points of a convex body K .

Proposition 5.2.4. (\rightarrow Section 5.5.3) The convex body \mathcal{Q} is the disjoint union of the following semialgebraic sets:

(\mathcal{Q}_{cx}) 8 **classical exposed points** $c \in \partial_e \mathcal{C}$.

(\mathcal{Q}_{ce}) 24 **exposed edges**, i.e., the interiors of line segments that connect pairs of classical exposed points.

(\mathcal{Q}_{nx}) 32 surfaces of **non-exposed extreme points**.

Each is the pushout of a triangle in $\partial \mathcal{C}$, which is the intersection of an \mathcal{N} -facet and a CHSH-facet.

(\mathcal{Q}_{qx}) 8 threefolds of **exposed extreme points**.

Each threefold is the curved pushout of the interior of a CHSH-facet of \mathcal{C} , which is a tetrahedron.

(\mathcal{Q}_{ei}) 8 **elliptopes**’ interiors, i.e., the interiors of the facets that arise from \mathcal{N} -facets of \mathcal{C} , as in Figure 5.2.

(\mathcal{Q}_{in}) The interior of \mathcal{Q} .

The stratification of \mathcal{Q} shown in Proposition 5.2.4 mirrors the stratification of the demicube \mathcal{C} into relatively open faces. Indeed, the numbers seen in Proposition 5.2.4 count the faces of various dimension of \mathcal{C} . Namely the f-vector of \mathcal{C} equals $(8, 24, 32, 8+8, 1)$. The Euclidean closures of sets of type (\mathcal{Q}) are said to be *of type* $[\mathcal{Q}]$. Types $[\mathcal{Q}_{\text{qx}}]$ and $[\mathcal{Q}_{\text{ei}}]$ suffice to cover the boundary. Going back to Definition 1.2.20, our body \mathcal{Q} has 16 patches, eight of type $(\mathcal{Q}_{\text{qx}})$ and eight of type $(\mathcal{Q}_{\text{ei}})$.

The difference between the types $(\mathcal{Q}_{\text{qx}})$ and $(\mathcal{Q}_{\text{ei}})$ will be important for what follows. It also relates to the two types of *maximal non-trivial faces* of \mathcal{Q} . The only two types are the singletons in $(\mathcal{Q}_{\text{qx}})$, and the \mathcal{N} -facets $[\mathcal{Q}_{\text{ei}}]$. These maximal faces are also exposed. Exposedness properties will be discussed later in their natural context: duality. An intuitive geometric understanding of the non-exposedness of type $(\mathcal{Q}_{\text{nx}})$ can be gained from considering the pushout mechanism: this converts the junction between a CHSH-facet and an \mathcal{N} -facet of \mathcal{C} to a junction with matching tangents. The prototype for this is shown in Figure 5.5. The red ellipse is tangent to the boundary of the square at the four points of intersection. For $(\mathcal{Q}_{\text{nx}})$ -points the same happens in higher dimension.

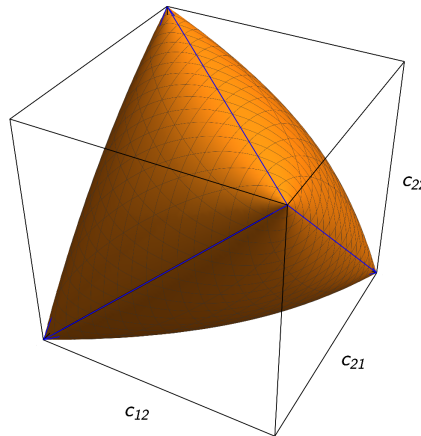


Figure 5.7: Every facet of \mathcal{Q} is an elliptope. Points of type $(\mathcal{Q}_{\text{cx}})$ are vertices of the blue tetrahedron; $(\mathcal{Q}_{\text{ce}})$ gives blue edges, $(\mathcal{Q}_{\text{nx}})$ is the orange surface. Extreme points of the elliptope are not exposed in \mathbb{R}^4 . Type $(\mathcal{Q}_{\text{ei}})$ comprise the interior.

Since the $(\mathcal{Q}_{\text{qx}})$ extreme points will be discussed in more detail later, let us briefly describe the $[\mathcal{Q}_{\text{ei}}]$ facets. These elliptopes are visualized in Figure 5.7, an enlarged version of the first panel in Figure 5.3. Since the pushout map restricts to \mathcal{N} -facets, it is the pushout of the \mathcal{C} -like tetrahedron that forms its skeleton. Indeed, the edges of \mathcal{C} are marked by two of the c_{ij} being ± 1 , and the other two equal up to a sign. This condition is invariant under pushout, so the edges of \mathcal{C} are invariant as sets, but not pointwise fixed, and become exactly the $[\mathcal{Q}_{\text{ce}}]$ -edges of \mathcal{Q} .

How do all these pieces fit together? Once again this is readily answered by looking at the pushout identification of \mathcal{Q} with \mathcal{C} . Consider the bicoloring of the facets of the cross polytope \mathcal{C} . The two colors distinguish CHSH and \mathcal{N} types. Only tetrahedra of different types intersect in a surface, and each surface $[\mathcal{Q}_{\text{nx}}]$ is the intersection of a $[\mathcal{Q}_{\text{qx}}]$ and a $[\mathcal{Q}_{\text{ei}}]$ -set. The triangular surfaces $(\mathcal{Q}_{\text{nx}})$ are thus faithfully portrayed in Figure 5.7. The intersection of two $[\mathcal{Q}_{\text{qx}}]$ -surfaces is lower dimensional: if they are not disjoint opposites, they intersect in a straight edge $[\mathcal{Q}_{\text{ce}}]$.

Curved tetrahedra. Proposition 5.2.4 allows us to turn an affine parametrization of a CHSH-face into a trigonometric parametrization of a curved tetrahedron $(\mathcal{Q}_{\text{qx}})$. For later

purposes, we find cosines a bit more convenient than sines.

Proposition 5.2.5. (\rightarrow Section 5.5.1) The threefolds $(\mathcal{Q}_{\text{qx}})$ of exposed extreme points on \mathcal{Q} are parametrized by

$$\begin{aligned} c = (c_{11}, c_{12}, c_{21}, c_{22}) &= (\cos \alpha, \cos \beta, \cos \gamma, \cos \delta) \quad \text{where} \\ \alpha + \beta + \gamma + \delta &= 0 \pmod{2\pi} \quad \text{and} \\ \Delta = \sin \alpha \cdot \sin \beta \cdot \sin \gamma \cdot \sin \delta &< 0. \end{aligned}$$

The angle parameters can be taken as the triples (α, β, γ) , with $\delta = -(\alpha + \beta + \gamma)$. In this 3-space, the sign of Δ marks a partition into two kinds of subsets: on the one hand, we have the curved tetrahedra with $\Delta < 0$ considered in Proposition 5.2.5. A prototype which contains the CHSH-point $(\pi/4, \pi/4, \pi/4)$ is given by the conditions $\alpha, \beta, \gamma, \alpha + \beta + \gamma \in (0, \pi)$.

On the other hand, consider the angles with $\Delta > 0$. Adding multiples of π to any of α, β, γ (and hence implicitly to δ) corresponds to an even sign change on the c_{ij} , and hence a symmetry of \mathcal{Q} . Therefore, it suffices to consider the cube $(0, \pi)^3$. In this cube only $\sin \delta$ can be negative, so $\Delta > 0$ means $\alpha + \beta + \gamma \in (\pi, 2\pi)$. By taking cosines, these points end up in the interior of \mathcal{Q} . Finally, note that the angle parameters (α, β, γ) with $\Delta = 0$ correspond to further boundary elements from Proposition 5.2.4, as follows. The symmetries also help to reduce each of the classes in the following boundary version of the parametrization to a single case, which is readily checked.

Proposition 5.2.6. (\rightarrow Section 5.5.3) In the cosine parametrization of Proposition 5.2.5, taking $\Delta = 0$ parametrizes further boundary strata of lower dimension. Specifically, we get points of type

$(\mathcal{Q}_{\text{cx}})$ if and only if $\alpha, \beta, \gamma, \delta$ are all multiples of π ,

$(\mathcal{Q}_{\text{ce}})$ if and only if exactly two of these angles are multiples of π , and

$(\mathcal{Q}_{\text{nx}})$ if and only if exactly one of these angles is a multiple of π .

Remark 5.2.7. A special feature of the minimal 222 case is that there exists a parametrized family of quantum models, that realizes all points described in Proposition 5.2.5. Using the notation introduced in Section 5.1.1, we set $m = 4$ and $\mathcal{H} = \mathbb{C}^4$. Algebraically, a quantum state is a positive semidefinite 4×4 matrix ρ with trace 1. For this density operator, we take the rank one matrix with entries $\rho_{\alpha\beta} = \Psi_\alpha \Psi_\beta$, defined by the unit vector

$$\Psi = \left(0, \frac{1}{\sqrt{2}}, -\frac{1}{\sqrt{2}}, 0 \right)^T.$$

The measurements of the two parties are represented by the following real symmetric 4×4 matrices:

$$\begin{aligned} A_1 &= \begin{pmatrix} \cos(\alpha) & 0 & \sin(\alpha) & 0 \\ 0 & \cos(\alpha) & 0 & \sin(\alpha) \\ \sin(\alpha) & 0 & -\cos(\alpha) & 0 \\ 0 & \sin(\alpha) & 0 & -\cos(\alpha) \end{pmatrix}, \quad A_2 = \begin{pmatrix} \cos(\gamma) & 0 & -\sin(\gamma) & 0 \\ 0 & \cos(\gamma) & 0 & -\sin(\gamma) \\ -\sin(\gamma) & 0 & -\cos(\gamma) & 0 \\ 0 & -\sin(\gamma) & 0 & -\cos(\gamma) \end{pmatrix}, \\ B_1 &= \begin{pmatrix} -1 & 0 & 0 & 0 \\ 0 & 1 & 0 & 0 \\ 0 & 0 & -1 & 0 \\ 0 & 0 & 0 & 1 \end{pmatrix}, \quad B_2 = \begin{pmatrix} -\cos(\alpha+\beta) & -\sin(\alpha+\beta) & 0 & 0 \\ -\sin(\alpha+\beta) & \cos(\alpha+\beta) & 0 & 0 \\ 0 & 0 & -\cos(\alpha+\beta) & -\sin(\alpha+\beta) \\ 0 & 0 & -\sin(\alpha+\beta) & \cos(\alpha+\beta) \end{pmatrix}. \end{aligned}$$

These matrices satisfy the hypotheses stated in (5.1.1). Then, the four correlations c_{ij} in (5.1.2) parametrized by $(\alpha, \beta, \gamma, \delta)$ as in Proposition 5.2.5, even without the inequality constraint on Δ , satisfy $c_{ij} = \text{tr}(\rho A_i B_j)$. This is a formal identity, for all $1 \leq i, j \leq 2$, and can be checked using computer algebra, e.g., Macaulay2.

5.2.2. Semialgebraic description

One possibility to decide quickly, for a given $c \in \mathbb{R}^4$, whether $c \in \mathcal{Q}$, is to apply the inverse pushout map, and to check whether the result lies in \mathcal{C} . This involves a transcendental function, and requires the checking of 16 linear inequalities. Here we consider an alternative, which only requires checking the positivity of two polynomials in c . In other words, we will describe our body \mathcal{Q} as a semialgebraic set.

There is a standard method to obtain relevant polynomials from the parametrization given in Proposition 5.2.5. Namely, one represents each angle variable η by the point $(\cos \eta, \sin \eta)$ on the unit circle, i.e., one introduces new variables s_{ij} with $c_{ij}^2 + s_{ij}^2 = 1$, and expresses the constraint on the sum of angles by trigonometrically expanding. Then one eliminates the s_{ij} -variables. Computer algebra systems, such as **Mathematica** or **Macaulay2** [GS] handle such tasks routinely and, in this instance, in no time. The result is the identity $h(c) = 0$ with h the sextic polynomial in (5.2.5) below. But also the condition $\Delta < 0$ has to be transcribed, for which we use the following polynomial g , which on $(\mathcal{Q}_{\text{qx}})$ satisfies $g(c) = \Delta$.

$$g(c) = 2 - (c_{11}^2 + c_{12}^2 + c_{21}^2 + c_{22}^2) + 2c_{11}c_{12}c_{21}c_{22}. \quad (5.2.3)$$

$$h(c) = 4(1 - c_{11}^2)(1 - c_{12}^2)(1 - c_{21}^2)(1 - c_{22}^2) - g(c)^2 \quad (5.2.4)$$

$$\begin{aligned} &= 4(c_{11}c_{22} - c_{12}c_{21})(c_{11}c_{21} - c_{12}c_{22})(c_{11}c_{12} - c_{21}c_{22}) - \\ &\quad - (c_{11} + c_{12} - c_{21} - c_{22})(c_{11} - c_{12} + c_{21} - c_{22})(c_{11} - c_{12} - c_{21} + c_{22})(c_{11} + c_{12} + c_{21} + c_{22}). \end{aligned} \quad (5.2.5)$$

We wrote two formulas for h , because (5.2.4) shows that h is invariant under the full symmetry group in Proposition 5.2.3, and (5.2.5) clarifies that the degree of h is six and not eight, as suggested by (5.2.4). Then we have:

Proposition 5.2.8. (\rightarrow Section 5.5.1) A point c in the cube \mathcal{N} lies in \mathcal{Q} if and only if $h(c) \geq 0$ or $g(c) \geq 0$.

While the polynomial h is an intrinsic feature of \mathcal{Q} , there is some freedom in the choice of g . Indeed h , together with the linear polynomials $1 \pm c_{ij}$, describes the algebraic boundary of \mathcal{Q} . This threefold has unbounded pieces outside the cube \mathcal{N} , but taking its convex hull after the intersection with \mathcal{N} gives exactly \mathcal{Q} . This is visualized in Figure 5.8, left, which shows the surface $\{h(c) = 0\}$ in the 3-space $\{c_{12} - c_{21} = 0\}$. The unbounded pieces arise because the algebraic elimination process works just as well in the complex domain. So the circle $c^2 + s^2 = 1$, as a complex variety, also contains real points with imaginary s , corresponding to angles $\alpha = ir$ or $\alpha = \pi + ir$ with $r \in \mathbb{R}$, and hence $\cos \alpha = \pm \cosh r$ in Proposition 5.2.5.

What is the role of the second polynomial g ? This polynomial is needed to make Proposition 5.2.8 true. Figure 5.8, left, shows the zero set of h , so h is negative on the outside of the yellow surface. This extends well into the cube, where $c \in \mathcal{Q}$, and even $c \in \mathcal{C}$, e.g., near the origin. Hence, ‘ $c \in \mathcal{N}$ and $h(c) \geq 0$ ’ would produce many false negatives. The disjunction with $g(c) \geq 0$ captures the convex hull of the threefold inside the cube \mathcal{N} . The surface defined by g in the hyperplane $\{c_{12} - c_{21} = 0\}$ is shown in Figure 5.8, right. Figure 5.9 is a two-dimensional representation that shows the geometry of the relevant intersections.

We remark that more compact forms than the characterization by two polynomials can be given, if we allow the use of absolute values or roots. Such conditions can be converted to polynomial expressions. However, they typically generate a case distinction, hence some overhead in the logical part of a semialgebraic description. For example, by taking a root in (5.2.4) and combining with Proposition 5.2.8, we can see that $c \in \mathcal{Q}$ is

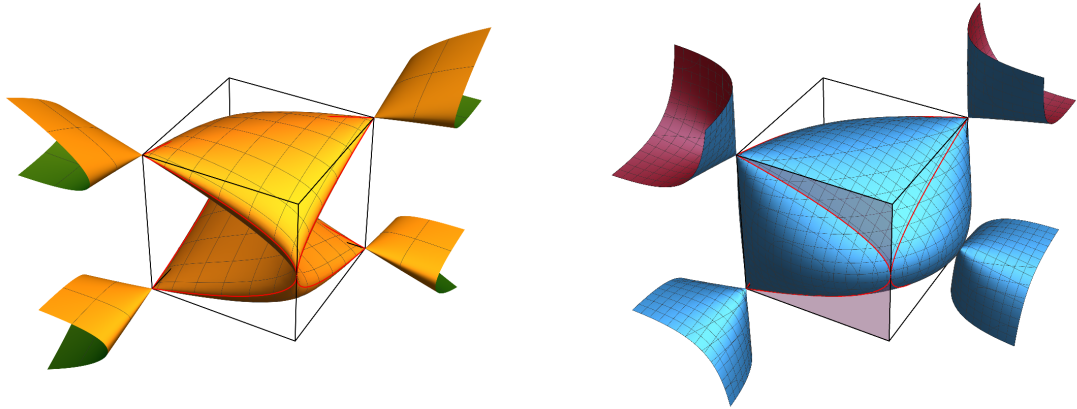


Figure 5.8: Hyperplane $\{c_{12} = c_{21}\}$. Left: the quartic surface $\{(c_{11} - c_{22})^{-2}h = 0\}$. Right: the quartic surface $\{g = 0\}$. The two surfaces intersect transversally in the red parabolas shown in the boundary of the cube.

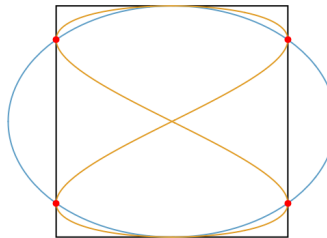


Figure 5.9: A slice that illustrates how the two surfaces in Figure 5.8 intersect. The convex hull of the orange curve represents \mathcal{Q} . The disjunction $h(c) \geq 0$ or $g(c) \geq 0$ describes \mathcal{Q} : it is not a basic semialgebraic set.

equivalent to $c \in \mathcal{N}$ together with the single inequality

$$g(c) \geq -2\sqrt{(1 - c_{11}^2)(1 - c_{12}^2)(1 - c_{21}^2)(1 - c_{22}^2)}.$$

The following reformulation, due to Landau [Lan88], is not invariant under the full symmetry group of \mathcal{Q} :

$$\sqrt{(1 - c_{11}^2)(1 - c_{12}^2)} + \sqrt{(1 - c_{21}^2)(1 - c_{22}^2)} \geq |c_{11}c_{12} - c_{21}c_{22}|. \quad (5.2.6)$$

Note that these inequalities must be combined with the hypothesis $c \in \mathcal{N}$. This excludes unbounded solutions with a product of two negative factors under the square root.

Spectrahedral shadow. For any quantum correlations, given by a density operator ρ and observables A_1, A_2, B_1, B_2 , and complex numbers ξ_1, \dots, ξ_4 , we consider the operator $X = \xi_1 A_1 + \xi_2 A_2 + \xi_3 B_1 + \xi_4 B_2$. Since X^*X is positive semidefinite, we conclude that $\text{tr}(\rho X^*X) = \sum_{\nu, \mu=1}^4 \bar{\xi}_\nu C_{\nu\mu} \xi_\mu \geq 0$, where we introduced the 4×4 matrix

$$C = (C_{\nu\mu}) = \begin{pmatrix} d_1 & u & c_{11} & c_{12} \\ \bar{u} & d_2 & c_{21} & c_{22} \\ c_{11} & c_{21} & d_3 & v \\ c_{12} & c_{22} & \bar{v} & d_4 \end{pmatrix}. \quad (5.2.7)$$

The entries other than c_{ij} are

$$u = \text{tr}(\rho A_1 A_2), \quad v = \text{tr}(\rho B_1 B_2), \quad \text{and} \quad d_1 = \text{tr}(\rho A_1^2) \geq 0, \text{ etc.}$$

The positivity stated above is $C \succcurlyeq 0$, our notation for C being positive semidefinite. The existence of u, v and d_i with $d_i^2 \leq 1$ making $C \succcurlyeq 0$ is thus a necessary condition for $c \in \mathcal{Q}$. This is the bottom level of the semidefinite hierarchy [NPA08] for quantum correlations. In the case at hand, the necessary condition is also sufficient. We can further assume that u and v are real and that the diagonal entries are all 1.

Proposition 5.2.9. (\rightarrow Section 5.5.1) A point c lies in the convex body \mathcal{Q} if and only if there exist numbers $u, v \in \mathbb{R}$ such that $C \succcurlyeq 0$ in (5.2.7) with $d_1 = d_2 = d_3 = d_4 = 1$.

Hence, \mathcal{Q} is characterized by a semidefinite matrix completion problem. This is essentially the completion problem for the 4-cycle, as discussed in [MS21b, Example 12.16]. Our boundary polynomial $h(c)$ is obtained from the degree eight polynomial given there by setting the diagonal entries to be 1. The matrix inequality $C \succcurlyeq 0$ defines a spectrahedron in \mathbb{R}^6 . Eliminating the matrix entries u and v specifies a projection $\mathbb{R}^6 \rightarrow \mathbb{R}^4$. The correlation body \mathcal{Q} is the image of the spectrahedron $\{C \succcurlyeq 0\}$ under this projection. Thus, Proposition 5.2.9 furnishes an explicit realization of \mathcal{Q} as a spectrahedral shadow.

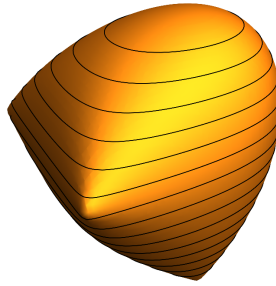


Figure 5.10: Non-uniqueness of the matrix completion problem for a family of correlations $c = tc_{\text{CHSH}} + (1-t)c_{\text{center}}$ with $c_{\text{center}} = (-1, 0, 0, 0)$, along the line segment from the center of an ellipope facet (top) to the CHSH-point (bottom). The horizontal cuts for fixed t (black meshes) represent the pairs (u, v) that make (5.2.7) positive semidefinite. The figure is a quartic spectrahedron [ORSV15].

The fiber over any interior point under our projection $\{C \succcurlyeq 0\} \rightarrow \mathcal{Q}$ is a spectrahedron in the (u, v) -plane. Figure 5.10 shows the union of these 2-dimensional fibers over a line that cuts through \mathcal{Q} . The fiber over any boundary point is a single point. In other words, the matrix completion problem has a unique solution C for $c \in \partial\mathcal{Q}$. We record the ranks of these matrices C for the various families in Proposition 5.2.4.

Proposition 5.2.10. (\rightarrow Lemma 5.5.5 and Section 5.5.3)

- (1) The matrix completion problem has a unique solution (u, v) if and only if $c \in \partial\mathcal{Q}$.
- (2) The resulting unique matrix C has rank 1 if c is of type $(\mathcal{Q}_{\text{cx}})$, it has rank 2 for types $(\mathcal{Q}_{\text{ce}})$, $(\mathcal{Q}_{\text{nx}})$ and $(\mathcal{Q}_{\text{qx}})$, and it has rank 3 for type $(\mathcal{Q}_{\text{ei}})$.
- (3) The point c is in the interior $(\mathcal{Q}_{\text{in}})$ if and only if there exists some completion with rank $C = 4$.

We close with one remark regarding item (3). It is not true that *all* the completions C of a given interior point $c \in (\mathcal{Q}_{\text{in}})$ have rank 4. For instance, the midpoint $c = 0$ clearly allows $C = \mathbf{1}$, but also the extension with $u = v = 1$, which is the direct sum of two rank 1 operators, and hence has rank 2.

Volume. The volume of \mathcal{Q} is a fundamental geometric invariant. It could be understood as the probability of quantum correlations in an ensemble, for which $c \in \mathcal{N}$ is distributed according to the Lebesgue measure. This ensemble of generalized probabilistic theories has no operational meaning, so the volume has no direct physical relevance. However, the probabilistic interpretation suggests a way to compute it stochastically: the semialgebraic description gives us a fast way to decide whether $c \in \mathcal{Q}$, for points c in a random ensemble with each c_{ij} independent and equidistributed in $[-1, 1]$. A run of 10^6 samples led to

$$\frac{V(\mathcal{Q})}{V(\mathcal{N})} \approx 0.925898.$$

On account of \sqrt{N} -fluctuations, this can be expected to be accurate to within three digits.

On the other hand, we can compute the volume exactly, by integrating the pushout over \mathcal{C} . Since the pushout acts coordinatewise, the Jacobi matrix is diagonal and the functional determinant is readily determined. The resulting trigonometric integrals can be solved, giving the overall result

$$\frac{V(\mathcal{Q})}{V(\mathcal{N})} = \frac{3\pi^2}{2} \cdot \frac{1}{16} \approx 0.9252754126.$$

For the surface area, we get the volume of the \mathcal{N} -faces as the well-known ellipope volume $\pi^2/2$ [JN98]. For the volume of the curved tetrahedra we did not find a closed expression. Testing the numerical value for being a simple fraction times a low power of π by continued fraction expansion also did not seem to give a simple expression. The (\mathcal{Q} nx) boundaries are directly expressed by the surface area of the ellipope. This area is known to be 5π , by a direct calculation found on math.stackexchange.com.

5.3. Description of the dual body

We could ask all the questions we studied so far about the three bodies $\mathcal{C} \subset \mathcal{Q} \subset \mathcal{N}$ also about their duals (see Section 1.1.2). For the duals the inclusions are reversed, so $\mathcal{N}^\circ \subset \mathcal{Q}^\circ \subset \mathcal{C}^\circ$. The big surprise, which is a rather special feature of the minimal case, is that this dual chain of inclusions is essentially *the same* as the original chain. We will spell this out in detail. For now it just means the good news that much of the work is already done.

5.3.1. The duality transform

We first noticed the duality in the polytopes $\mathcal{C} \subset \mathcal{N}$ from the observation that their f-vectors are reversals of each other. Strengthening this to an isomorphism $\mathcal{C} \cong \mathcal{N}^\circ$ goes as follows. We start from the inequalities describing \mathcal{N} . These come from the 8 vertices of \mathcal{N}° , which are

$$\pm(1, 0, 0, 0), \quad \pm(0, 1, 0, 0), \quad \pm(0, 0, 1, 0), \quad \pm(0, 0, 0, 1). \quad (5.3.1)$$

These have to be identified with the vertices of \mathcal{C} , i.e., the 8 even vertices of \mathcal{N} itself. They are

$$\pm(1, 1, 1, 1), \quad \pm(1, -1, 1, -1), \quad \pm(1, 1, -1, -1), \quad \pm(1, -1, -1, 1). \quad (5.3.2)$$

The following transformation H maps the points in (5.3.1) to those in (5.3.2). So we get $\mathcal{C} = 2H\mathcal{N}^\circ$ with

$$H = \frac{1}{2} \begin{pmatrix} 1 & 1 & 1 & 1 \\ 1 & -1 & 1 & -1 \\ 1 & 1 & -1 & -1 \\ 1 & -1 & -1 & 1 \end{pmatrix}. \quad (5.3.3)$$

Here we included the factor $1/2$ so that $H^2 = \mathbf{1}$. Since $H^* = H$, this matrix is then also unitary, i.e., a Hadamard matrix [TZ06] (note different conventions for the normalization of such matrices though). This makes it easy to write down the consequences of $\mathcal{C} = 2H\mathcal{N}^\circ$ from dualization or multiplication with H :

$$\mathcal{N}^\circ = \frac{1}{2}HC \quad \text{and} \quad \mathcal{C}^\circ = \frac{1}{2}H\mathcal{N}.$$

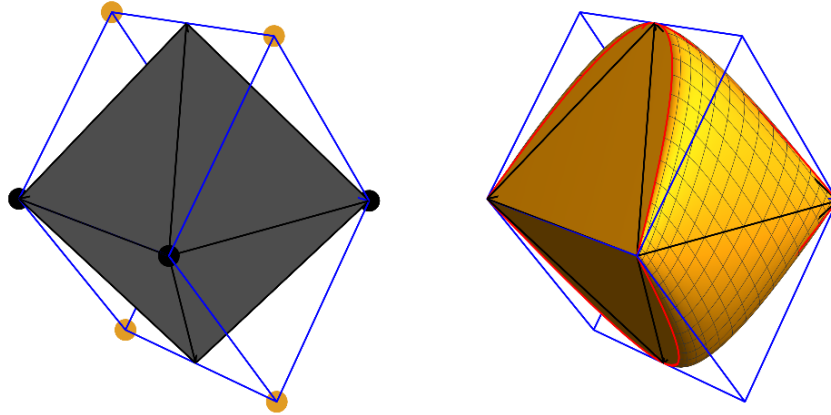


Figure 5.11: Dual bodies in the Alice-Bob symmetric sections shown in Figure 5.2. Left: \mathcal{C}° (blue cube frame) and \mathcal{N}° (black octahedron). The marked vertices of \mathcal{C}° correspond to the facets of \mathcal{C} in Figure 5.2. Right: \mathcal{Q}° , which is an affine transformation of \mathcal{Q} in Figure 5.2. This expresses the self-duality.

To visualize this duality, consider the left panel of Figure 5.11. Since the section with the hyperplane $\{c_{12} = c_{21}\}$ is also a projection, and duality swaps projection and intersection operations, this 3-dimensional picture faithfully represents the 4-dimensional duality relations. The outer blue frame represents \mathcal{C}° , the dual of the inner frame in Figure 5.2, left. It is a cube whose vertices correspond to the facets of \mathcal{C} . They can thus correspond either to a CHSH-facet (marked in yellow) or to a \mathcal{N} -facet (marked in black). Overall, the figure looks like a rotation of its counterpart in Figure 5.2. In 4 dimensions the required H is exactly an orthogonal reflection. In the 3-dimensional section it is still a submatrix of a rotation, and looks like a rotation because human 3D perception is highly capable of ignoring uneven affine stretching.

The right panel in Figure 5.11 shows the pertinent section of the dual body \mathcal{Q}° . We can draw it using the parametrized points f from Proposition 5.3.2. This mimics the right panel of Figure 5.2, by the same transformation as the one used for the polytopes. Indeed, this is true exactly, also for the full 4-dimensional body:

Proposition 5.3.1. (\rightarrow Section 5.5.2) $\mathcal{Q}^\circ = \frac{1}{2}HQ$.

This is Theorem 5.1.3, but with the matrix H spelled out. The linear transformation H is far from unique. Indeed, if S_1, S_2 are matrices representing any of the symmetries from Proposition 5.2.3, then so are their transposes. Hence $H' = S_1HS_2$, again a Hadamard

matrix, also maps the inclusion chain to its dual. Note that $S \mapsto S' = HSH^{-1}$ is an automorphism of the symmetry group which changes the semidirect product decomposition, so multiplication by an even number of signs can become a permutation and conversely.

In the terminology of axiomatic quantum mechanics, this form of self-duality of a convex set is called ‘weak self-duality’ [BGW13], as opposed to stronger forms with a canonical isomorphism between the set and its dual, that is characteristic for Jordan algebra state spaces and in particular the quantum state space. Can one strengthen Proposition 5.3.1 in that direction? Indeed, we already have a canonical mapping taking each point c of a $(\mathcal{Q}_{\text{qx}})$ patch to the unique maximizer f , via Propositions 5.2.5 and 5.3.2. By multiplying H with a symmetry of \mathcal{Q} we can achieve that it takes the patch of c to the patch of f , but can we do it for all patches simultaneously? The answer is no: a map with that property would have to commute with all symmetries. Since our representation of the group G on \mathbb{R}^4 is irreducible, we would conclude that H is a multiple of the identity. Another context of interest are normed spaces: since $-\mathcal{Q} = \mathcal{Q}$, our convex body \mathcal{Q} is the unit ball of a norm in \mathbb{R}^4 and the dual normed space has unit ball \mathcal{Q}° . So we have an example of a normed space that is isomorphic to its dual, a subject studied more generally, e.g., in [Yan11].

Parametrized extreme points of \mathcal{Q}° . The boundary patches $(\mathcal{Q}_{\text{qx}})$ of exposed extreme points have a unique maximizing functional $f \in \mathcal{Q}^\circ$. The parametrization by angles can be taken over directly.

Proposition 5.3.2. (\rightarrow Section 5.5.3) Let $\alpha, \beta, \gamma, \delta$ and c satisfy the conditions of Proposition 5.2.5. Define

$$f = (f_{11}, f_{12}, f_{21}, f_{22}) = \frac{1}{K} \left(\frac{1}{\sin \alpha}, \frac{1}{\sin \beta}, \frac{1}{\sin \gamma}, \frac{1}{\sin \delta} \right), \quad (5.3.4)$$

where $K = \cot \alpha + \cot \beta + \cot \gamma + \cot \delta$. Then $f \cdot c' \leq 1$ for all $c' \in \mathcal{Q}$ with equality if and only if $c' = c$. Moreover, the vector f is uniquely determined by this property.

Applying the duality transform to the point f in (5.3.4) gives again a point $2Hf \in \mathcal{Q}$ of type $(\mathcal{Q}_{\text{qx}})$, which in turn can be parametrized by angles. The resulting map Φ from one tetrahedron of angles to another expresses the duality of boundary points.

For a concrete computation let T be the tetrahedron defined by $\alpha, \beta, \gamma, -\delta = \alpha + \beta + \gamma \in (0, \pi)$. Write $c(\theta)$ and $f(\theta)$ for the images in Propositions 5.2.5 and 5.3.2. We obtain a self-map $\Phi : T \rightarrow T$ with the property

$$2Hf(\theta) = c(\Phi(\theta)).$$

By definition, this map will commute with the permutations of vertices of T , which extend to symmetries of \mathcal{Q} . By self-duality it is also its own inverse. This map is visualized in Figure 5.12.

By symmetry, these properties uniquely fix the map also for other $(\mathcal{Q}_{\text{qx}})$ -patches. When doing this concretely, one has to observe that whereas the association of f with the unique maximizer c is a property of \mathcal{Q} , the concrete parametrization of the tetrahedra involves a convention, and depends on the choice of self-duality operator H .

The map Φ is continuous and even analytic on the open tetrahedron. But it does not have a continuous extension to the closure of the tetrahedron. Indeed, a glance at (5.3.4) shows that when one of the angles in θ goes to zero, and the others to values not in $\{0, \pi\}$, the image $\Phi(\theta)$ approaches the opposite vertex. Hence the whole open part of the bottom face on the left panel goes to a single point. This is evident from Figure 5.12 in the form

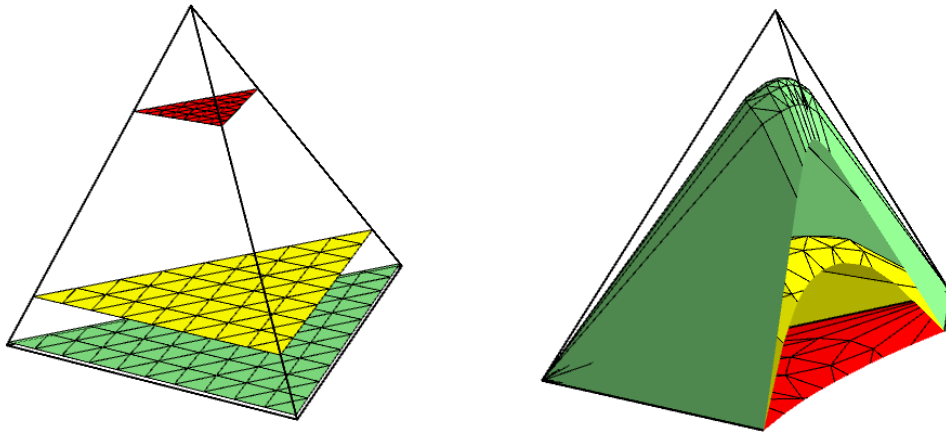


Figure 5.12: The map Φ from the tetrahedron T to itself: the triangular meshes on the left are mapped to the surfaces on the right. The figure on the right has been truncated so that the image surfaces can be seen. Since Φ^2 is the identity, the diagrams can also be read from right to left.

that most of the triangles in the evenly spaced triangulation close to the base triangle end up close to the top vertex. Similarly, when θ approaches a point on the edge, the limit of $\Phi(\theta)$ depends on the direction from which the edge is approached.

Dualized descriptions. We can now apply the duality transform to each of the previous subsections to get analogues for \mathcal{Q}° of all the statements made about \mathcal{Q} . There is no simple analogue of the pushout. The cosine parametrization of the curved tetrahedra was already given an analogue in Proposition 5.3.2 (not via duality transform).

Consider the polynomials (5.2.3) and (5.2.5) of the semialgebraic description. Since $f = (f_{11}, f_{12}, f_{21}, f_{22}) \in \mathcal{Q}^\circ$ is equivalent to $2Hf \in \mathcal{Q}$, we need to consider these polynomials after substituting $c \mapsto 2Hf$. Note that such a substitution takes polynomials which are invariant under the symmetry group to polynomials with the same property. Moreover, by linearity of the substitution, homogeneous polynomials of some degree go to homogeneous polynomials of the same degree. This constrains the number of polynomials we need to consider. The invariant polynomials of degree two are proportional to $|c|^2 = c_{11}^2 + c_{12}^2 + c_{21}^2 + c_{22}^2$, and since H is orthogonal, this goes to itself under substitution. Among the quartics we need to consider the product $p(c) = c_{11}c_{12}c_{21}c_{22}$ that already appeared in Theorem 5.1.2. Under substitution it becomes

$$q(f) = (f_{11} + f_{12} + f_{21} + f_{22})(f_{11} - f_{12} + f_{21} - f_{22})(f_{11} + f_{12} - f_{21} - f_{22})(f_{11} - f_{12} - f_{21} + f_{22}).$$

This is the quartic part in (5.2.5). The sextic part of h is the polynomial k from Theorem 5.1.2. This is self-dual in the sense that $k(2Hf) = 64k(f)$. With these building blocks, the polynomials describing \mathcal{Q} and \mathcal{Q}° are

$$\begin{aligned} h(c) &= 4k(c) - q(c), & h^\circ(f) &= \frac{1}{256} h(2Hf) = k(f) - p(f), \\ g(c) &= 2 - |c|^2 + 2p(c), & g^\circ(f) &= \frac{1}{2} g(2Hf) = 1 - 2|f|^2 + q(f). \end{aligned} \tag{5.3.5}$$

We conclude that $f \in \mathcal{Q}^\circ$ if and only if $2Hf \in \mathcal{N}$ and ($g^\circ(f) \geq 0$ or $h^\circ(f) \geq 0$).

Describing \mathcal{Q}° as a spectrahedral shadow is done in general by the dual semidefinite hierarchy [DLTW08]. Indeed, the dual of a spectrahedral shadow is again of this form [BPT12, Remark 5.43]. This holds because the operations of linear section and projection change roles under dualization, and the semidefinite cone is anyhow self-dual. In terms of matrix completion problems, where the primal matrix has unspecified entries (a subspace constraint), the dual matrix has zeros (resulting from the dual projection). In the case at hand, the unspecified entries u, v in C become zeros in the dual matrix, which we call F . The condition that the diagonal entries of C are 1 dualizes to constraint on the trace of F . This gives:

Proposition 5.3.3. (→Section 5.5.2) A point $f = (f_{11}, f_{12}, f_{21}, f_{22})$ lies in the dual body \mathcal{Q}° if and only if there exist positive real numbers p_1, p_2, p_3, p_4 with $\sum_{i=1}^4 p_i = 2$ such that

$$F = \begin{pmatrix} p_1 & 0 & -f_{11} & -f_{12} \\ 0 & p_2 & -f_{21} & -f_{22} \\ -f_{11} & -f_{12} & p_3 & 0 \\ -f_{21} & -f_{22} & 0 & p_4 \end{pmatrix} \succcurlyeq 0. \quad (5.3.6)$$

Moreover, there exists a completion satisfying the above constraints, and additionally $p_1 + p_2 = p_3 + p_4 = 1$. This condition is automatically satisfied for all boundary points.

Indeed, one checks that $\text{tr } CF = 2 - 2f \cdot c$ holds for C from (5.2.7), so $\text{tr } CF \geq 0$ is equivalent to $f \cdot c \leq 1$.

5.3.2. The normal cycle

Our goal is to describe the normal cycle $\mathbf{N}(\mathcal{Q})$ of the correlation body \mathcal{Q} and its closure $\overline{\mathbf{N}(\mathcal{Q})} \subset \mathbb{C}^8$ in the Zariski topology. We describe a stratification of $\mathbf{N}(\mathcal{Q})$ that mirrors the stratification of \mathcal{Q} in Proposition 5.2.4. The symbol $(\mathcal{Q}_{nn,mm})$ will represent the set of points (c, f) in $\mathbf{N}(\mathcal{Q})$ such that $c \in (\mathcal{Q}_{nn})$ and $f \in (\mathcal{Q}_{mm})$, for the families from Proposition 5.2.4.

Proposition 5.3.4. The normal cycle $\mathbf{N}(\mathcal{Q})$ is divided into $24 = 8 + 8 + 8$ strata of dimension 3 whose types are $(\mathcal{Q}_{qx,qx}), (\mathcal{Q}_{ei,cx}), (\mathcal{Q}_{cx,ei})$. These threefolds are separated by $88 = 32 + 32 + 24$ surfaces $(\mathcal{Q}_{nx,cx}), (\mathcal{Q}_{cx,nx}), (\mathcal{Q}_{ce,ce})$. The eight strata of type $(\mathcal{Q}_{qx,qx})$ belong to the same irreducible component of the algebraic normal cycle $\overline{\mathbf{N}(\mathcal{Q})}$, so the radical ideal of $\overline{\mathbf{N}(\mathcal{Q})}$ is the intersection of $17 = 1 + 8 + 8$ prime ideals.

All these features are made more explicit in Table 5.1. The labels refer to the strata of $\partial\mathcal{Q}$ (cf. Proposition 5.2.4).

We now briefly discuss the strata (\mathcal{Q}_{ce}) and (\mathcal{Q}_{nx}) in the fourth and fifth column of Table 5.1. These are surfaces in the threefold $\mathbf{N}(\mathcal{Q})$. Points c on the surfaces (\mathcal{Q}_{nx}) are supported only by the linear functional that supports the entire ellotope, which is $\{c\}^\circ\circ$. Hence there are 32 surfaces $(\mathcal{Q}_{nx,cx})$ in $\mathbf{N}(\mathcal{Q})$. Dually, we also get 32 surfaces of type $(\mathcal{Q}_{cx,nx})$. These do not appear in Table 5.1 because the faces of type (\mathcal{Q}_{nx}) are not exposed and thus cannot be realized as $\{f\}^\circ$. This feature is highlighted by the jump in the dimension of $\{c\}^\circ\circ$ for $c \in (\mathcal{Q}_{nx})$. All 64 surfaces arise as the intersection of the closure of $(\mathcal{Q}_{qx,qx})$ with the closure of a stratum $(\mathcal{Q}_{ei,cx})$ or $(\mathcal{Q}_{cx,ei})$. Each intersection produces four such surfaces.

The exposed edges (\mathcal{Q}_{ce}) of \mathcal{Q} are supported by one-dimensional families of normal directions. These are the exposed edges (\mathcal{Q}_{ce}) on \mathcal{Q}° . We therefore have 24 squares of type $(\mathcal{Q}_{ce,ce})$ in $\mathbf{N}(\mathcal{Q})$. Each square separates two 3-dimensional strata of type $(\mathcal{Q}_{ei,cx})$

c is a point of type	(Qqx)	(Qcx)	(Qei)	(Qce)	(Qnx)
$\{c\}^\circ$ is a face of type	$\{f\}, f \in (Qqx)$	[Qei]	(Qcx)	[Qce]	(Qcx)
$\{c\}^{\circ\circ}$ is a face of type	$\{c\}$	$\{c\}$	[Qei]	[Qce]	[Qei]
$\dim \{c\}^{\circ\circ}$	0	0	3	1	3
dim of face generated by c	0	0	3	1	0
$\dim \{c\}^\circ$	0	3	0	1	0
dim of manifold of such faces	3	0	0	0	2
sum of these dimensions	3	3	3	2	2
number of open strata in $\mathbf{N}(\mathcal{Q})$	8	8	8	24	32
irreducible components in $\overline{\mathbf{N}(\mathcal{Q})}$	1	8	8	0	0

Table 5.1: Classification of boundary points $c \in \partial \mathcal{Q}$, in the notation of Proposition 5.2.4, and what they correspond to in the normal cycle $\mathbf{N}(\mathcal{Q})$. The first three columns give the full-dimensional strata of $\mathbf{N}(\mathcal{Q})$. The last two columns are two of the three strata of dimension 2. The fact that the stratum (Qcx, nx) does not appear here reflects the non-exposed nature of (Qnx) .

and (Qcx, ei) . In addition to the 64 curved triangles of type (Qnx, cx) or (Qcx, nx) , this accounts for all 2-dimensional cells in our stratification of $\mathbf{N}(\mathcal{Q})$.

The 3-dimensional strata of $\mathbf{N}(\mathcal{Q})$ give the irreducible components of the algebraic normal cycle $\overline{\mathbf{N}(\mathcal{Q})}$. We begin with the most nonlinear stratum, denoted (Qqx, qx) . This stratum is characterized by Propositions 5.2.5 and 5.3.2. It is parametrized by angles $\alpha, \beta, \gamma, \delta$ that add up to 0 modulo 2π , and it consists of pairs (c, f) where c satisfies (5.2.2) and f satisfies (5.3.4). Its Zariski closure is an irreducible threefold in \mathbb{C}^8 . Its prime ideal is generated by 17 polynomials. The first three of these 17 generators are familiar:

$$\begin{aligned}\ell &= c_{11}f_{11} + c_{12}f_{12} + c_{21}f_{21} + c_{22}f_{22} - 1, \\ h &= 4(c_{11}c_{22} - c_{12}c_{21})(c_{11}c_{21} - c_{12}c_{22})(c_{11}c_{12} - c_{21}c_{22}) \\ &\quad - (c_{11} + c_{12} - c_{21} - c_{22})(c_{11} - c_{12} + c_{21} - c_{22})(c_{11} - c_{12} - c_{21} + c_{22})(c_{11} + c_{12} + c_{21} + c_{22}), \\ h^\circ &= f_{11}f_{12}f_{21}f_{22} - (f_{11}f_{22} - f_{12}f_{21})(f_{11}f_{21} - f_{12}f_{22})(f_{11}f_{12} - f_{21}f_{22}).\end{aligned}$$

The remaining 14 generators of our prime ideal are the following polynomials:

$$\begin{aligned}&c_{11}^2f_{11}^2 - c_{22}^2f_{22}^2 - f_{11}^2 + f_{22}^2, \\ &c_{21}f_{11}f_{12}f_{21} + c_{22}f_{11}f_{12}f_{22} + c_{11}f_{11}f_{21}f_{22} + c_{12}f_{12}f_{21}f_{22}, \\ &c_{11}^2f_{11}f_{12} - c_{21}^2f_{21}f_{22} - c_{12}c_{21}f_{12}f_{22} + c_{11}c_{22}f_{12}f_{22} - f_{11}f_{12} + f_{21}f_{22}, \\ &c_{11}^2f_{11}f_{21} - c_{12}^2f_{12}f_{22} - c_{12}c_{21}f_{21}f_{22} + c_{11}c_{22}f_{21}f_{22} - f_{11}f_{21} + f_{12}f_{22}, \\ &c_{12}^2f_{11}f_{12} - c_{21}^2f_{21}f_{22} - c_{11}c_{21}f_{11}f_{22} + c_{12}c_{22}f_{11}f_{22} - f_{11}f_{12} + f_{21}f_{22}, \\ &c_{12}^2f_{12}f_{21} - c_{11}^2f_{11}f_{22} - c_{11}c_{21}f_{21}f_{22} + c_{12}c_{22}f_{21}f_{22} - f_{12}f_{21} + f_{11}f_{22}, \\ &c_{21}^2f_{11}f_{21} - c_{12}^2f_{12}f_{22} - c_{11}c_{12}f_{11}f_{22} + c_{21}c_{22}f_{11}f_{22} - f_{11}f_{21} + f_{12}f_{22}, \\ &c_{21}^2f_{12}f_{21} - c_{11}^2f_{11}f_{22} - c_{11}c_{12}f_{12}f_{22} + c_{21}c_{22}f_{12}f_{22} - f_{12}f_{21} + f_{11}f_{22}, \\ &(c_{11}c_{12}^2 + c_{11}c_{21}^2 + c_{11}c_{22}^2 - 2c_{12}c_{21}c_{22})f_{11} + c_{12}^3f_{12} + c_{21}^3f_{21} + c_{22}^3f_{22} - 1, \\ &c_{11}c_{12}f_{12}f_{21} - c_{21}c_{22}f_{12}f_{21} + c_{12}c_{21}f_{21}f_{22} - c_{11}c_{22}f_{21}f_{22} + c_{12}^2f_{12}f_{22} - c_{22}^2f_{12}f_{22}, \\ &c_{12}c_{21}f_{11}f_{21} - c_{11}c_{22}f_{11}f_{21} + c_{11}c_{21}f_{11}f_{22} - c_{12}c_{22}f_{11}f_{22} + c_{21}^2f_{21}f_{22} - c_{22}^2f_{21}f_{22}, \\ &c_{12}c_{21}f_{11}f_{12} - c_{11}c_{22}f_{11}f_{12} + c_{11}c_{12}f_{11}f_{22} - c_{21}c_{22}f_{11}f_{22} + c_{12}^2f_{12}f_{22} - c_{22}^2f_{12}f_{22}, \\ &(c_{12}^3 - c_{11}^2c_{12} - c_{12}c_{21}^2 - c_{12}c_{22}^2 + 2c_{11}c_{21}c_{22})f_{12} - (c_{22}^3 - c_{11}^2c_{22} - c_{12}^2c_{22} - c_{21}^2c_{22} + 2c_{11}c_{12}c_{21})f_{22}, \\ &(c_{21}^3 - c_{11}^2c_{21} - c_{12}^2c_{21} - c_{21}c_{22}^2 + 2c_{11}c_{12}c_{22})f_{21} - (c_{22}^3 - c_{11}^2c_{22} - c_{12}^2c_{22} - c_{21}^2c_{22} + 2c_{11}c_{12}c_{21})f_{22}.\end{aligned}$$

This list was generated by computer algebra as follows. We start from a list of polynomials that cuts out $\overline{\mathbf{N}(\mathcal{Q})}$ as a subset of \mathbb{C}^8 . That list consists of ℓ, h, h° and the twelve 2×2

minors of the two matrices

$$\begin{pmatrix} c_{11} & c_{12} & c_{21} & c_{22} \\ \partial h^\circ / \partial f_{11} & \partial h^\circ / \partial f_{11} & \partial h^\circ / \partial f_{21} & \partial h^\circ / \partial f_{21} \end{pmatrix}, \begin{pmatrix} f_{11} & f_{12} & f_{21} & f_{22} \\ \partial h / \partial c_{11} & \partial h / \partial c_{11} & \partial h / \partial c_{21} & \partial h / \partial c_{21} \end{pmatrix}.$$

The respective rows are linearly dependent for any pair (c, f) of supporting linear functions. The resulting ideal has the desired prime ideal as its radical, by Hilbert's Nullstellensatz. We computed that radical.

We now describe the other components of the variety $\overline{\mathbf{N}(\mathcal{Q})}$. The eight strata $(\mathcal{Q}_{ei,cx})$ consist of points (c, f) where one of the entries of f is ± 1 and the others are 0. This linear functional f exposes one of the ellipotes in $\partial \mathcal{Q}$. For example, consider $f = (1, 0, 0, 0)$. The prime ideal of this component is

$$\langle f_{11} - 1, f_{12}, f_{21}, f_{22}, c_{11} - 1 \rangle.$$

The corresponding stratum in the semialgebraic set $\mathbf{N}(\mathcal{Q})$ satisfies the additional cubic inequality

$$c_{12}^2 + c_{21}^2 + c_{22}^2 - 2c_{12}c_{21}c_{22} \leq 1. \quad (5.3.7)$$

The boundary of the ellipote, seen inside $\mathbf{N}(\mathcal{Q})$, separates $(\mathcal{Q}_{ei,cx})$ from the nonlinear stratum $(\mathcal{Q}_{qx,qx})$.

By duality, there are also eight strata $(\mathcal{Q}_{cx,ei})$ in the normal cycle $\mathbf{N}(\mathcal{Q})$. Now, the ellipotes appear in the f -coordinates and c is one of the 8 classical extreme points (\mathcal{Q}_{cx}) . These are obtained by exchanging the roles of f and c , using the linear transformation H . The ideal of one of the components $(\mathcal{Q}_{cx,ei})$ is

$$\langle c_{11} - 1, c_{12} - 1, c_{21} - 1, c_{22} - 1, f_{11} + f_{12} + f_{21} + f_{22} - 1 \rangle.$$

The semialgebraic description of this stratum is obtained by setting $c = 2Hf$ in the cubic inequality (5.3.7).

5.3.3. Support function

In the sequel we study the support function $\phi_{\mathcal{Q}}$. Notice that by self-duality, it is closely related to the radial function of \mathcal{Q}° (cf. Section 1.1.3). Since the set \mathcal{Q} has two markedly different kinds of boundary points, the support function requires a binary distinction concerning a functional f : will $\max_{c \in \mathcal{Q}} f \cdot c$ be attained at a classical point or at an exposed extreme point? The answer is the same for all multiples of f , including $-f$, so we are really asking about the projective geometry of the boundary points of \mathcal{Q}° . Once we know the nature of the maximizer, however, the computation of ϕ is straightforward. In the first case, it is the maximum of an affine functional over the 8 vertices of \mathcal{C} . Namely, $\phi_{\mathcal{Q}}(f) = \phi_{\mathcal{C}}(f)$ with

$$\begin{aligned} \phi_{\mathcal{C}}(f) &= \max\{f \cdot c \mid c \in \partial_e \mathcal{C}\} \\ &= \max\{|f_{11} + f_{12} + f_{21} + f_{22}|, |f_{11} + f_{12} - f_{21} - f_{22}|, \\ &\quad |f_{11} - f_{12} + f_{21} - f_{22}|, |f_{11} - f_{12} - f_{21} + f_{22}|\} \\ &= \|2Hf\|_\infty, \end{aligned} \quad (5.3.8)$$

In the second line, we grouped the maxima over a pair of antipodal classical extreme points by writing an absolute value. In the third equality, $\|\cdot\|_\infty$ denotes the maximum

norm on \mathbb{R}^4 . This case applies exactly when the ray $\mathbb{R}f$ intersects the boundary of \mathcal{Q}° in an \mathcal{N} -facet.

The other possibility is that the ray intersects the boundary in a curved tetrahedron. In this case we think of $\phi_{\mathcal{Q}}$ as the inverse of the radial function of \mathcal{Q}° . We need to determine the intersection point of the ray spanned by $\{f\}$ with $\partial\mathcal{Q}^\circ$. This point is in the zero set of h° . The equation $h^\circ(\lambda f) = 0$ in (5.3.5) is readily solved for λ , using the splitting of h° into homogeneous parts. We get $\lambda^6 k(f) - \lambda^4 p(f) = 0$, so in this case λ equals

$$\tilde{\phi}(f) = \sqrt{\frac{k(f)}{p(f)}}. \quad (5.3.9)$$

This function is homogeneous of degree 1, as required. The above heuristics is made precise in the following proposition, which extends Theorem 5.1.2:

Proposition 5.3.5. (\rightarrow Section 5.5.3) For any $f \in \mathbb{R}^4 \setminus \{0\}$, the following conditions are equivalent:

- (1) The ray $\{\lambda f\}$ intersects the boundary of \mathcal{Q}° in a point of type $(\mathcal{Q}\text{qx})$.
- (2) Some point $c \in \mathcal{Q}$ maximizing $f \cdot c$ is of type $(\mathcal{Q}\text{qx})$.
- (3) We have $p(f) < 0$ and

$$m(f) = \min_{i,j=1,2} |f_{ij}| \left(\sum_{i,j=1,2} |f_{ij}|^{-1} \right) > 2.$$

- (4) We have $p(f) < 0$ and $\tilde{m}(f) < 0$, where

$$\tilde{m}(f) = \left(\frac{1}{f_{11}} + \frac{1}{f_{12}} + \frac{1}{f_{21}} + \frac{1}{f_{22}} \right) \left(\frac{1}{f_{11}} + \frac{1}{f_{12}} - \frac{1}{f_{21}} - \frac{1}{f_{22}} \right) \left(\frac{1}{f_{11}} - \frac{1}{f_{12}} + \frac{1}{f_{21}} - \frac{1}{f_{22}} \right) \left(\frac{1}{f_{11}} - \frac{1}{f_{12}} - \frac{1}{f_{21}} + \frac{1}{f_{22}} \right)$$

- (5) Perform a symmetry transformation (even number of sign changes) so that the maximum in (5.3.8) of $f \cdot c$ over \mathcal{C} is attained at the extreme point $c = (1, 1, 1, 1)$, i.e., $\phi_{\mathcal{C}}(f) = f_{11} + f_{12} + f_{21} + f_{22}$. Then

$$f_{11}f_{12}f_{21} + f_{11}f_{12}f_{22} + f_{11}f_{21}f_{22} + f_{12}f_{21}f_{22} < 0. \quad (5.3.10)$$

In this case the support function of \mathcal{Q} is $\phi_{\mathcal{Q}}(f) = \tilde{\phi}(f)$ from (5.3.9), otherwise $\phi_{\mathcal{Q}}(f) = \phi_{\mathcal{C}}(f)$ from (5.3.8).

In the domain described by Proposition 5.3.5, the maximizer of $\phi_{\mathcal{Q}}(f)$ is a unique exposed point $c^* \in \mathcal{Q}$. An explicit formula $f \mapsto c^*$ would correspond to solving for c given f in the system of 17 polynomials defining the stratum $(\mathcal{Q}\text{qx}, \text{qx})$ in $\overline{\mathbf{N}(\mathcal{Q})}$. In terms of the angle parametrization of boundary pieces, it is essentially the self-dual counterpart of the map Φ sketched in Figure 5.12.

5.4. Geometric aspects of quantum key distribution

Quantum key distribution (QKD) is an important task in quantum information technology [BB14]. It furnishes the main practical reason for studying the body \mathcal{Q} . Here we discuss geometric features that are fundamental for that task. The goal of QKD is for two distant parties, Alice and Bob, to utilize quantum correlations for generating a key which is

guaranteed to be secret from any eavesdropper, here called Eve. Eve is only assumed to be constrained by the laws of quantum mechanics, but otherwise enjoys every possible freedom. In particular, she is allowed to manipulate the correlated systems on which the scheme is based, the quantum channels by which they are transmitted, and even the measurement devices. She also gets a copy of the communications exchanged between Alice and Bob. However, she can only read these but not change them. One must also assume that once the data collection starts, Eve cannot reach into Alice's and Bob's lab and access their measurement settings or outcomes. Indeed, if Eve could do that, she would not even need to bother with the whole quantum setup, or she could play a trivial woman-in-the-middle attack, and secrecy would be obviously impossible. So the rules of the game force her to gain at least some information from the quantum systems. According to the laws of quantum mechanics, this introduces a disturbance detectable by Alice and Bob. When they do detect such deviations from the expected statistics the key distribution has failed. Eve can always achieve that, but this is counted as a failure for her, because she will also not learn any secrets.

We want to show here that the minimal setup in this paper is already sufficient to support QKD. Moreover, the main security argument is based directly on the geometry of \mathcal{Q} . In undisturbed operation the setup leads to some correlations $c \in \mathcal{Q}$. Alice and Bob will use a random sample of their particles to verify this via the public classical channel, and will abort the process if they find significant deviations from c . We claim that QKD is possible whenever c is a *non-classical extreme point* (cf. [FFW11]).

Suppose Alice and Bob test their correlations and find them to be such a point $c \in \partial_e \mathcal{Q}$. What could Eve know about their measurement results? Let ε be a random variable that summarizes her findings. The conditional correlation c_ε is the 2×2 matrix that pertains to those cases where Eve found ε . We have $c_\varepsilon \in \mathcal{Q}$ since Eve is constrained by quantum mechanics. Combining the data with the probabilities p_ε for observing ε , we get $c = \sum_\varepsilon p_\varepsilon c_\varepsilon$. But since c is extremal, all c_ε that appear with nonzero probability must be equal to c . That is the same as saying that ε is statistically independent of Alice's and Bob's information. So while Eve knows ε , she learns nothing about c .

Note, however, that the argument applies equally to classical extreme points. Only, in that case the extreme points are completely deterministic. In the case of deterministic agreement probabilities indeed factorize, say $c_{ij} = a_i b_j$. With $c_{ij} \in \{0, 1\}$ and $a_i, b_j \in \{0, 1\}$, this factorization would be $1 \cdot 1 = 1$ or $0 \cdot 0 = 0$. Of course, this is utterly useless for drawing a secret key. So what Alice and Bob use to generate the key are the non-trivial correlations that may be present in *non-classical* extreme points. Any non-classical correlation is fine for that purpose, since this may be further distilled into perfect agreement.

The full analysis of QKD takes not only error correction into account, but also the overhead of statistically verifying that the given source is really described by c . This necessarily involves errors, and the experimental implementation will have additional errors of its own. The analysis, done carefully also for c sufficiently close to $\partial_e \mathcal{Q}$, results not in a blanket statement that Eve will know ‘nothing’, but in a quantitative bound on how much she might know in the worst case. So, in addition to error correction (getting the keys to be really the same) one needs ‘privacy amplification’, a process that had already been studied in purely classical settings [BBCM95] prior to the advent of QKD. The traditional information theoretic view focuses on rates in the asymptotic regime, i.e., for a large number of exchanged raw key bits. This systematically neglects the overhead of reliably estimating c . This can be considerable in real, and therefore finite, runs. A usable QKD security proof always has to include the finite key analysis, and all imperfections. This is far beyond the current work, and we refer to [SBV⁺20, TSB⁺20]. To connect

with the literature, we emphasize that here we have described ‘device independent’ QKD, for which the experimental entrance ticket is a ‘loophole free’ Bell test, which has been achieved only recently [G⁺15, HH⁺15, S⁺15]. The quality of these experiments is still not in the range where the data collection could be done in the lifetime of a lab. Nevertheless, recent advances on the theoretical side [SBV⁺20, TSG⁺20, TSB⁺20] have brought this into feasible range. On the other hand, systems not realizing the ideal of device independence are already commercially available (see [Wik21, Section 3.2]).

5.5. Proofs

In this section we prove all theorems and propositions seen so far. Since many results in our paper have appeared previously in the literature, we could give many proofs by citation. However, we aim to make our text self-contained. Where the pedestrian argument, tailored to the case at hand, can be understood as an example of a more general theory, we provide this background as well. As a help for monitoring the logical flow we included some summaries of what has been shown up to some point. These are formatted like the definitions and propositions throughout the paper, and numbered consecutively with these.

There are, of course, many ways to organize the proofs. We now briefly describe our overall strategy and the structure of Section 5.5. We begin in Section 5.5.1 with the equivalences of Theorem 5.1.1, centered around the matrix completion problem. Self-duality (Theorem 5.1.3) follows in Section 5.5.2. On this path we already gain some information about the boundary, which is extended to the detailed classification of boundary points in Section 5.5.3. The study of boundary points is perhaps a bit more detailed than necessary, since it uses a local criterion for excluding certain points from the extreme boundary of the convex hull of a variety. This technique might be helpful more generally. We conclude the section with the computation of the support function (Proposition 5.3.5), which proved to be more subtle than expected, even with a full understanding of the boundary.

5.5.1. Proof of Theorem 1

For the sake of this proof let us denote by $\mathcal{Q}_{(x)} \subset \mathbb{R}^4$ the set characterized by item (x) in Theorem 5.1.1. We have to show that these are all equal. The backbone of the proof is the chain

$$\mathcal{Q}_{(a)} \subset \mathcal{Q}_{(e)} = \mathcal{Q}_{(d)} = \mathcal{Q}_{(b)} \subset \mathcal{Q}_{(a)}$$

and separate arguments for $\mathcal{Q}_{(e)} = \mathcal{Q}_{(f)}$ and $\mathcal{Q}_{(b)} = \mathcal{Q}_{(c)}$. The main work will be getting the solution set $\mathcal{Q}_{(e)}$ of the matrix completion problem in great detail. The boundary information coming out of that, in particular for rank $C = 2$, will then be used to get the further equivalences and finally go back to $\mathcal{Q}_{(a)}$.

Making matrix completion real. The inclusion $\mathcal{Q}_{(a)} \subset \mathcal{Q}_{(e)}$ is an important step, because the definition of $\mathcal{Q}_{(a)}$ admits infinite Hilbert space dimension, while $\mathcal{Q}_{(e)}$ only allows finite dimension. This reduction step works for more parties, settings, and outcomes, as well, which is the whole point of the semidefinite hierarchies [DLTW08, NPA08]. But outside the minimal scenario the inclusion is strict.

We saw the inclusion $\mathcal{Q}_{(a)} \subset \mathcal{Q}_{(e)}$ in Section 5.2.2. From the quantum model we

naturally get a positive definite matrix with some unknown complex entries, and diagonal not equal to 1. These assumptions are part of the description of $\mathcal{Q}_{(e)}$, however. In order to prove $\mathcal{Q}_{(a)} \subset \mathcal{Q}_{(e)}$, we thus have to make sure that the additional assumptions do not make $\mathcal{Q}_{(e)}$ smaller. This is the content of Proposition 5.2.9.

Proof of 5.2.9. Consider a matrix $C \succcurlyeq 0$ of the form (5.2.7) with diagonal entries $d_i \leq 1$. We also fix the matrix $C' = \Re C$, the entrywise real part of C . Then since the complex conjugate of a positive semidefinite matrix is again semidefinite, $C' \succcurlyeq 0$. Add to this the matrix with diagonal entries $1 - d_i$ to get C'' . Then $C'' \succcurlyeq C' \succcurlyeq 0$ is a matrix with the same off-diagonal c_{ij} , but in the standard form with u, v real and $d_i = 1$. \square

Solving the real completion problem. In this and the following two paragraphs, we proceed to actually solve the matrix completion problem defining $\mathcal{Q}_{(e)}$, i.e., decide which c 's permit real values u, v that make the following matrix positive semidefinite:

$$C = \begin{pmatrix} 1 & u & c_{11} & c_{12} \\ u & 1 & c_{21} & c_{22} \\ c_{11} & c_{21} & 1 & v \\ c_{12} & c_{22} & v & 1 \end{pmatrix}. \quad (5.5.1)$$

The solution uses Sylvester's criterion. We use the standard notation C_I for the principal submatrix selecting the rows and the columns specified by the indices in I , and $m_I = \det C_I$ for the corresponding principal minor. Sylvester's necessary and sufficient criterion for $C \succcurlyeq 0$ is that $m_I \geq 0$ for all $2^n - 1$ index sets I . For $C \succ 0$ it suffices to have $m_1, m_{12}, m_{123}, m_{1234} > 0$. The positivity of principal 2×2 -minors gives $c_{ij}^2 \leq 1$ or equivalently $\mathcal{Q}_{(e)} \subseteq \mathcal{N}$ as a necessary condition. Consider next the principal 3×3 -minors

$$C_{123} = \begin{pmatrix} 1 & u & c_{11} \\ u & 1 & c_{21} \\ c_{11} & c_{21} & 1 \end{pmatrix} \succcurlyeq 0 \quad \text{and} \quad C_{124} = \begin{pmatrix} 1 & u & c_{12} \\ u & 1 & c_{22} \\ c_{12} & c_{22} & 1 \end{pmatrix} \succcurlyeq 0. \quad (5.5.2)$$

These do not involve v , and they give a condition for u . We show that (5.5.2) is all we need to consider:

Lemma 5.5.1. Suppose that, for some $u \in \mathbb{R}$, the matrices in (5.5.2) are positive semidefinite. Then one can find v such that in (5.5.1) we have $C \succcurlyeq 0$, i.e., $c \in \mathcal{Q}_{(e)}$.

Proof. We invoke a general result on semidefinite matrix completion [GJSW84, Theorem 7]. Consider the graph G whose edges represent the given entries of a partial matrix

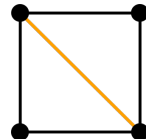


Figure 5.13: The black graph is the 4-cycle associated to $\mathcal{Q}_{(e)}$ with vertices 1, 3, 2, 4 starting from the upper-left corner. It is not chordal. On the other hand, adding the orange edge, which corresponds to assuming the existence of u satisfying (5.5.2), makes it chordal.

whose completion we seek. The necessary conditions for completable are that for those subsets of vertices, where all matrix entries are specified (called ‘cliques’ of G), the corresponding submatrices are positive semidefinite. Then, if the graph is *chordal* (meaning

any cycle of length ≥ 4 allows a shortcut), this condition is also sufficient. Moreover, this holds for both strict positive definiteness and semidefiniteness. In the case at hand, the graph given for $\mathcal{Q}_{(e)}$ is a 4-cycle shown in Figure 5.13. Assuming the existence of u with $C_{123}, C_{124} \succcurlyeq 0$ adds a diagonal, making the graph chordal. Hence no further condition needs to be considered. \square

Lemma 5.5.1 eliminates v and leaves us with the nonnegativity of the following three principal minors:

$$\begin{aligned} m_{12} &= 1 - u^2 & (A) \\ m_{123} &= 1 - c_{11}^2 - c_{21}^2 + 2c_{11}c_{21}u - u^2 & (B) \\ m_{124} &= 1 - c_{12}^2 - c_{22}^2 + 2c_{12}c_{22}u - u^2 & (C) \end{aligned} \quad (5.5.3)$$

We have $c \in \mathcal{Q}_{(e)}$ if and only if these are simultaneously satisfied for the same u . By Helly's Theorem in \mathbb{R}^1 , the three positivity intervals have a common point if and only if they intersect pairwise. Hence we can consider pairwise intersections. The maximum of (B) is

$$\max_u m_{123} = (1 - c_{11}^2)(1 - c_{21}^2) = m_{13}m_{23} \geq 0,$$

attained at $u = c_{11}c_{21} \in [-1, 1]$, so its positivity interval intersects that of (A) , and similarly for the pair (A, C) . Hence only the pair (B, C) needs to be considered. We conclude:

Summary 5.5.2. If $c \in \mathcal{N}$, then $c \in \mathcal{Q}_{(e)}$ if and only if (B) and (C) are both non-negative for some $u \in \mathbb{R}$.

Joint positivity of two parabolas. We next examine the criterion in Summary 5.5.2 independently of the specific context. We do the quantifier elimination carefully, because the structure of the solution explains the disjunction in Theorem 5.1.1 (d). Thus at the end of this paragraph we will achieve the equality $\mathcal{Q}_{(e)} = \mathcal{Q}_{(d)}$.

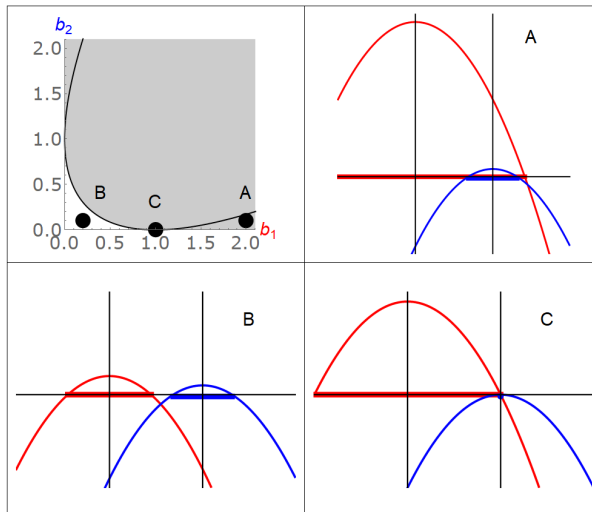


Figure 5.14: The configurations of two parabolas $f_i(x) = b_i - (x - a_i)^2$ with $a_1 = 0$ and $a_2 = 1$. Top Left: parameter plane for (b_1, b_2) . Shaded: region where the intersection of the positivity ranges is non-empty. Points A,B,C: parameters for the other panels. Black parabola: line at which the intersection of the parabolas lies on the x -axis.

The configurations of two parabolas in the following lemma are shown in Figure 5.14. Both are given by quadratic polynomials $f(x) = b - (x - a)^2$ with the same negative quadratic term. The parameters are chosen so that $(x, y) = (a, b)$ is the location of the maximum. This function is positive in the interval $[a - \sqrt{b}, a + \sqrt{b}]$. The question is when for two such parabolas the positivity intervals overlap. It is clear that the problem is invariant under shifts (adding a constant to both a_1 and a_2), and $(a_1 - a_2)^2$ just sets a scale for the b 's. Hence we could choose $a_1 = 0$ and $a_2 = 1$. Figure 5.14 is drawn with this choice.

Lemma 5.5.3. Given two quadratic polynomials $f_i(x) = b_i - (x - a_i)^2$, $i = 1, 2$, the following are equivalent:

- (1) There exists a point $u \in \mathbb{R}$ such that $f_1(u) \geq 0$ and $f_2(u) \geq 0$.
- (2) $b_1 \geq 0 \wedge b_2 \geq 0 \wedge [b_1 + b_2 - (a_1 - a_2)^2 \geq 0 \vee 4b_1b_2 - (b_1 + b_2 - (a_1 - a_2)^2)^2 \geq 0]$.

If one demands strict inequality then the following are also equivalent:

- (1') There exists a point $u \in \mathbb{R}$ such that $f_1(u) > 0$ and $f_2(u) > 0$.
- (2') $b_1 > 0 \wedge b_2 > 0 \wedge [b_1 + b_2 - (a_1 - a_2)^2 \geq 0 \vee 4b_1b_2 - (b_1 + b_2 - (a_1 - a_2)^2)^2 > 0]$.

Proof. This is based on Figure 5.14. Clearly, both positivity ranges must be non-empty. So, unless $b_1, b_2 \geq 0$, there is nothing to prove. We can also trivially take care of the cases with $a_1 = a_2$, because then the positivity intervals are contained in each other. The maximum of each parabola is in the positivity interval. So if $b_1 \geq (a_1 - a_2)^2$ the maximum of the second parabola is in the positivity range of the first, and so there is a non-empty intersection. Symmetrically, this holds for $b_2 \geq (a_1 - a_2)^2$. This gives two closed rectangles in the (b_1, b_2) -plane with non-empty intersection.

Next consider the intersection of the two parabolas. Their unique intersection point is

$$(x_s, f_i(x_s)) = \left(\frac{a_1 + a_2}{2} - \frac{b_1 - b_2}{2(a_1 - a_2)}, \frac{4b_1b_2 - (b_1 + b_2 - (a_1 - a_2)^2)^2}{4(a_1 - a_2)^2} \right). \quad (5.5.4)$$

Now suppose $f_i(x_s) \geq 0$. Then x_s is in the intersection of the positivity ranges. The corresponding region, defined by the positivity of the numerator of $f_i(x_s)$ in (5.5.4) is the closed parabola in Figure 5.14. Hence we have non-zero intersection for the union of the two rectangles and the parabola in Figure 5.14. This can be simplified as the union of just two regions, namely the parabola and the region $\{b_1 + b_2 \geq (a_1 - a_2)^2\}$, which contains the two rectangles plus a triangle, which is contained in the parabola.

To complete the proof of the first part, we need to show that, for any point outside this region, the positivity ranges have empty intersection. This complement is defined by the conditions $0 \leq b_i < (a_1 - a_2)^2$ and $f_i(x_s) < 0$. Now the first condition implies $|b_1 - b_2| < (a_1 - a_2)^2$. Hence the second term for x_s in (5.5.4) is bounded by $|a_1 - a_2|/2$, so x_s lies between a_1 and a_2 . Therefore one of the maxima lies to the right of x_s and the other one lies on its left, and therefore the same holds for the positivity ranges of the parabolas. Since $x_s < 0$ the ranges do not intersect. This completes the proof of the first part. The primed statements characterize the interior of the parameter set, i.e., the region just described without the boundary points, for which $b_1 = 0$, or $b_2 = 0$ or $f_i(x_s) = 0$. \square

We now apply Lemma 5.5.3 to the quadratic polynomials (B),(C) in (5.5.3). The parameters are

$$\begin{aligned} a_1 &= c_{11}c_{21}, & a_2 &= c_{12}c_{22}, \\ b_1 &= (1 - c_{11}^2)(1 - c_{21}^2), & b_2 &= (1 - c_{12}^2)(1 - c_{22}^2). \end{aligned} \quad (5.5.5)$$

With this, the two polynomials in Lemma 5.5.3 (2) are g in (5.2.3) and h in (5.2.5). The combination of Summary 5.5.2 and Lemma 5.5.3 now establishes the equivalence of (d) and (e) in Theorem 5.1.1. We record this as follows:

Summary 5.5.4. $\mathcal{Q}_{(e)} = \mathcal{Q}_{(d)}$: for $c \in \mathbb{R}^4$, we have $c \in \mathcal{Q}_{(e)}$ if and only if $c \in \mathcal{N}$ and $(g(c) \geq 0 \text{ or } h(c) \geq 0)$. Furthermore, we have $c \in \text{int}(\mathcal{Q}_{(e)})$ if and only if $c \in \text{int}(\mathcal{N})$ and $(g(c) > 0 \text{ or } h(c) > 0)$.

Properties of the boundary and extreme points. Summary 5.5.4 characterizes membership in the spectrahedral shadow $\mathcal{Q}_{(e)}$. We now come to its boundary, beginning with an extended version of the first statement in Proposition 5.2.10.

Lemma 5.5.5. Given any point $c \in \mathcal{Q}_{(e)}$, the following three conditions are equivalent:

- (1) $c \in \partial\mathcal{Q}_{(e)}$.
- (2) The matrix completion problem for c has a unique solution (u, v) .
- (3) Either $(c \in \partial\mathcal{N} \text{ and } g(c) \geq 0)$ or $(g(c) < 0 \text{ and } \text{rank}(C) \leq 2 \text{ for every completion } C \text{ of } c)$.

Proof. Suppose that c is in the interior of $\mathcal{Q}_{(e)}$. Then the fiber over c of the projection from the 6-dimensional spectrahedron $\{C \succcurlyeq 0\}$ onto the 4-dimensional body $\mathcal{Q}_{(e)}$ is two-dimensional. Hence (2) is false. Also, both conditions in (3) are false. The first condition fails because $\text{int}(\mathcal{Q}_{(e)}) \subseteq \text{int}(\mathcal{N})$ and the second condition fails because c has a preimage C that is positive definite and hence has rank 4.

It remains to show that (1) implies both (2) and (3). Let $c \in \partial\mathcal{Q}_{(e)}$. We have $g(c) \geq 0$ or $h(c) \geq 0$, by Lemma 5.5.3 (2) applied to (5.5.5). We distinguish two cases, namely $c \in \partial\mathcal{N}$ and $c \notin \partial\mathcal{N}$. If $c \in \partial\mathcal{N}$ then $c_{ij} = \pm 1$ for some i, j . Up to symmetry we may assume $c_{11} = -1$. From (5.2.4) we see that $h(c) = -g(c)^2$ and hence $g(c) \geq 0$, so (3) holds. For (2) we note that $m_{123}(u) = -(u + c_{21})^2$ and $m_{134}(v) = -(v + c_{12})^2$. Nonnegativity of principal minors requires $u = -c_{21}$ and $v = -c_{12}$, so the matrix completion is unique.

Now assume $c \notin \partial\mathcal{N}$. Then we have $h(c) = 0$, and this implies $g(c) < 0$, so that the parabolas from Lemma 5.5.3 have a unique point of intersection at level 0. This point is given either by $u = a_1 - \sqrt{b_1} = a_2 + \sqrt{b_2}$, or $u = a_2 - \sqrt{b_2} = a_1 + \sqrt{b_1}$. Analogously there is also a unique v . These unique choices u, v make all third order principal minors $m_{123}, m_{124}, m_{234}, m_{134}$ vanish. This means $\text{rank}(C) \leq 2$. Hence (2) and (3) hold in this case as well. \square

The next lemma shows how the trigonometric functions arise in the parametrization of the boundaries.

Lemma 5.5.6. Suppose that c is extremal in $\mathcal{Q}_{(e)}$, then

- (1) It must have a unique matrix completion with $\text{rank } C \leq 2$.
- (2) It must be of the form $c_{ij} = a_i \cdot b_j$ for unit vectors $a_1, a_2, b_1, b_2 \in \mathbb{R}^2$,
- (3) It can be written as $c_{ij} = \cos(\alpha_i - \beta_j)$ for some $\alpha_1, \alpha_2, \beta_1, \beta_2 \in \mathbb{R}$.

Proof. (1) Extreme points are always part of the boundary, hence the previous lemma applies. So by part (3) of the previous lemma, they either have $\text{rank } C \leq 2$ anyway, or else belong to a face of the cube \mathcal{N} . In the latter case, up to symmetry, we have $c_{22} = 1$. Then $C_{124} \succcurlyeq 0$ forces $u = c_{12}$, so the extendability is just the ellotope condition

$\det C_{123} = 1 - c_{12}^2 c_{23}^2 c_{31}^2 - 2c_{12}c_{23}c_{31} \geq 0$. Since we are not just assuming c to be on the boundary, but even extremal, this inequality must be tight, and so we also get $\text{rank } C \leq 2$.

(2) By the spectral theorem, every positive semidefinite $d \times d$ matrix can be written as a Gram matrix, i.e., $C_{\alpha\beta} = w_\alpha \cdot w_\beta$ for vectors w_1, \dots, w_d in some Euclidean space \mathbb{R}^r . Here $r = \text{rank } C$ is the number of non-zero eigenvalues. In our case the diagonal matrix entries are 1, so these vectors are unit vectors. Moreover, the c_{ij} are themselves matrix elements of C , so we just need to rename the vectors according to whether the dimension belongs to Alice or to Bob, i.e., $a_1 = w_1$, $a_2 = w_2$, $b_1 = w_3$, and $b_2 = w_4$.

(3) Unit vectors in \mathbb{R}^2 lie on the unit circle, parameterized by angles. Scalar products between such vectors are the cosines of the enclosed angle. Setting $w_i = (\cos \alpha_i, \sin \alpha_i)$ for some $\alpha_i \in \mathbb{R}$, we thus have

$$C = \begin{pmatrix} 1 & \cos(\alpha_1 - \alpha_2) & \cos(\alpha_1 - \alpha_3) & \cos(\alpha_1 - \alpha_4) \\ \cos(\alpha_1 - \alpha_2) & 1 & \cos(\alpha_2 - \alpha_3) & \cos(\alpha_2 - \alpha_4) \\ \cos(\alpha_1 - \alpha_3) & \cos(\alpha_2 - \alpha_3) & 1 & \cos(\alpha_3 - \alpha_4) \\ \cos(\alpha_1 - \alpha_4) & \cos(\alpha_2 - \alpha_4) & \cos(\alpha_3 - \alpha_4) & 1 \end{pmatrix}. \quad (5.5.6)$$

Renaming according to the Alice/Bob distinction, i.e. $\alpha_3 = \beta_1$ and $\alpha_4 = \beta_2$, we obtain the claim. \square

Part (2) of Lemma 5.5.6 says that $\partial_e \mathcal{Q}_{(e)} \subset \mathcal{Q}_{(f)}$, and part (3) that $\partial_e \mathcal{Q}_{(e)} \subset \mathcal{Q}_{(b)}$. Since $\mathcal{Q}_{(f)}$ is convex by a direct sum construction, and $\mathcal{Q}_{(b)}$ is anyhow defined to be convex, this also means that $\mathcal{Q}_{(e)} \subset \mathcal{Q}_{(f)}$ and $\mathcal{Q}_{(e)} \subset \mathcal{Q}_{(b)}$. The first of these inclusions can be inverted trivially, because we can just set $u = a_1 \cdot a_2$ and $v = b_1 \cdot b_2$ to get a matrix completion from the unit vectors a_i, b_j . To revert the second inclusion, we have to combine Summary 5.5.4, the inclusion $\mathcal{Q}_{(a)} \subset \mathcal{Q}_{(e)}$ proved above, and the concrete quantum model from Remark 5.2.7, which realizes all cosine parametrized c , and thus shows $\mathcal{Q}_{(b)} \subset \mathcal{Q}_{(a)}$. Altogether this gives

Summary 5.5.7. $\mathcal{Q}_{(e)} = \mathcal{Q}_{(f)}$, $\mathcal{Q}_{(e)} = \mathcal{Q}_{(d)}$, and $\mathcal{Q}_{(a)} \subset \mathcal{Q}_{(e)} \subset \mathcal{Q}_{(b)} \subset \mathcal{Q}_{(a)}$, i.e., all these sets are equal.

This leaves only one part of Theorem 5.1.1, namely the equality with $\mathcal{Q}_{(c)}$. This will be shown in the next paragraph. Also, we have established one part of Proposition 5.2.5, the cosine parametrization, in a slightly different parametrization. The one used in Propositions 5.2.5 and 5.2.6 follows from the form (5.5.6) by setting

$$\alpha = \alpha_1 - \alpha_3, \quad \beta = \alpha_4 - \alpha_1, \quad \gamma = \alpha_3 - \alpha_2, \quad \delta = \alpha_2 - \alpha_4.$$

Note that the signs were chosen (not changing the respective cosine) such that $\alpha + \beta + \gamma + \delta = 0$. This constraint reflects the fact that only differences $\alpha_i - \alpha_j$ matter. What we have not shown yet, however, is the criterion $\Delta < 0$ for a tuple of angles to give an extreme point. This will be done in Section 5.5.3.

The pushout characterization. The continuous map $t \mapsto \sin(\pi t/2)$ takes the interval $[-1, 1]$ to itself, and it has a continuous inverse. By applying this map coordinate-wise, we conclude that the pushout map in (5.2.1) is a homeomorphism from the cube $\mathcal{N} = [-1, 1]^4$ to itself. Here we shall establish Proposition 5.2.2, which states that $\mathcal{Q} = \sin(\mathcal{C})$. Note that in the literature of matrix completion, this is often presented as $\mathcal{Q} = \cos(\pi \text{MET}(K_{2,2}))$ which is obvious if one realizes that the metric polytope $\text{MET}(K_{2,2})$ of the complete

bipartite graph $K_{2,2}$ is isomorphic to the classical polytope \mathcal{C} . See [Lau97] and references therein.

Our strategy is to show this for the boundaries, i.e., $\mathbf{sin}(\partial\mathcal{C}) = \partial\mathcal{Q}$. Suppose that we know this, then notice that \mathbf{sin} maps connected components of $\mathcal{N} \setminus \partial\mathcal{C}$ to connected components of $\mathcal{N} \setminus \partial\mathcal{Q}$. Since 0 is in both the classical polytope and the quantum set, and $\mathbf{sin}(0) = 0$ we get that \mathcal{C} is precisely mapped to \mathcal{Q} . Hence equality of the boundaries is sufficient.

We examine the boundary of the demicube \mathcal{C} facet by facet. This task is greatly reduced by symmetry, given that \mathbf{sin} commutes with all symmetry operations explained in Proposition 5.2.3. Only one CHSH face and one \mathcal{N} -face need to be considered. Consider first the CHSH facet $\{(x, y, z, w) \in [-1, 1]^4 : x + y + z - w = 2\}$. The images of the points on this facet under the pushout map \mathbf{sin} are

$$\mathbf{sin}(x, y, z, w) = \left(\sin\left(\frac{\pi}{2}x\right), \sin\left(\frac{\pi}{2}y\right), \sin\left(\frac{\pi}{2}z\right), \sin\left(\frac{\pi}{2}w\right) \right) = (\cos\alpha, \cos\beta, \cos\gamma, \cos\delta),$$

where $\alpha = \pi(1-x)/2$, $\beta = \pi(1-y)/2$, $\gamma = \pi(1-z)/2$, $\delta = \pi(w-1)/2$. This gives $\alpha + \beta + \gamma + \delta = \pi - (x + y + z - w)\pi/2 = 0$. Moreover, $x, y, z, w \in [-1, 1]$ implies $\alpha, \beta, \gamma \in [0, \pi]$ and $\delta \in [-\pi, 0]$. These inequalities imply $\Delta = \sin\alpha \sin\beta \sin\gamma \sin\delta \leq 0$. Hence we get exactly those parametrized patches (\mathcal{Q}_{qx}) from Proposition 5.2.5, for which $\alpha, \beta, \gamma > 0 > \delta$. The other seven patches (\mathcal{Q}_{qx}) are obtained by symmetry.

Next consider an \mathcal{N} -face of \mathcal{C} , say that defined by $w = 1$. The pushout map preserves this equation. We can now go through the same considerations as above, but in one dimension lower. The geometric statement is that the pushout of the tetrahedron equals the ellipope (see Figure 5.7). This also follows from the fact that \mathbf{sin} identifies their boundaries. We know this from the above discussion of the CHSH facets.

Together with Summary 5.5.7 this completes the proof of Theorem 5.1.1.

5.5.2. Self-duality

Self-duality is a special feature of the pair $\mathcal{Q}, \mathcal{Q}^\circ$. With the boundary information obtained so far one could try to derive self-duality extreme point by extreme point. Another possibility is to obtain it from the support and radial function. Here we use an approach based on the duality of the semidefinite matrices C and F , and their representations as Gram matrices. We begin with the characterization of the F matrices.

Proof of Proposition 5.3.3. The primal/dual characterization of spectrahedral shadows described briefly before the statement of Proposition 5.3.3 is a standard result, so we omit its proof and are left with the additional property $p_1 + p_2 = p_3 + p_4$. We can take $p_1 + p_2$ and $p_3 + p_4$ both non-zero, since otherwise we have the trivial case $f = 0$, $F = \frac{1}{2}\mathbb{1}$.

Now observe that the matrix $F' = \Lambda F \Lambda$, where Λ is the diagonal matrix with diagonal $(\lambda, \lambda, \lambda^{-1}, \lambda^{-1})$, is also positive semidefinite and has the same off-diagonal block f_{ij} . The diagonal is changed to $(p'_1, p'_2, p'_3, p'_4) = (\lambda^2 p_1, \lambda^2 p_2, \lambda^{-2} p_3, \lambda^{-2} p_4)$. In order to satisfy the sum constraint we need $\lambda^2 = (p_3 + p_4)/(p_1 + p_2)$. Then $(F + F')/2$ is the desired extension with $p_1 + p_2 = p_3 + p_4$. This is different from F , if $\lambda^2 \neq 1$.

Finally, using a similar argument, we show that if the point f has a completion F for which the condition $p_1 + p_2 = p_3 + p_4 = 1$ does not hold, then f is not extreme. Using the diagonal matrix with $(\lambda_A, \lambda_A, \lambda_B, \lambda_B)$, and assuming, without loss of generality that $x = p_1 + p_2 - 1 > 0$, the normalization condition becomes $\lambda_A^2(1+x) + \lambda_B^2(1-x) = 2$.

Then choosing both terms equal to 1 maximizes $\lambda_A \lambda_B = (1 - x^2)^{-1/2} > 1$. We conclude that $f'_{ij} = \lambda_A \lambda_B f_{ij}$ is again in \mathcal{Q}° , so f is not a boundary point. \square

We now consider matrices C and F as Gram matrices of suitable vectors in a real Euclidean space. That is, we choose a_1, a_2, b_1, b_2 from the characterization (f) in Theorem 5.1.1, and similarly four vectors x_1, x_2, y_1, y_2 whose scalar products give F , and $-f_{ij} = x_i \cdot y_j$. The conditions on these vectors for C to be of the form (5.5.1) and F to be of the form (5.3.6) with $p_1 + p_2 = 1$ are

$$\|a_1\| = \|a_2\| = 1 \quad \text{and} \quad x_1 \perp x_2, \quad \|x_1\|^2 + \|x_2\|^2 = 1,$$

and analogous conditions for b_j and y_j . The sets of vectors can be mapped to each other by

$$a_1 = x_1 + x_2, \quad a_2 = x_1 - x_2 \quad \text{and} \quad x_1 = (a_1 + a_2)/2, \quad x_2 = (a_1 - a_2)/2.$$

With the analogous relations for the b_j and y_j , we get a bijective correspondence between the allowed vectors. Expressing the relation by the Hadamard matrix $H_2 = 2^{-1/2} \begin{pmatrix} 1 & 1 \\ 1 & -1 \end{pmatrix}$ and inserting them into $c_{ij} = a_i \cdot b_j$, one relates the 4-vector $c = (c_{11}, c_{12}, c_{21}, c_{22})$ to the corresponding $f \in \mathbb{R}^4$ by $H = H_2 \otimes H_2$, i.e., (5.3.3). This proves Proposition 5.3.1 and Theorem 5.1.3.

5.5.3. Further boundary properties

The pushout characterization makes the disjoint union structure of Proposition 5.2.4 obvious, but we need to verify various geometric properties of strata mentioned in that proposition.

Classification of boundary points by rank. We now show the remainder of Proposition 5.2.9, the rank statements in Proposition 5.2.10, and the parametrization of boundary points in Proposition 5.2.6. Each of these propositions has items referring to different parts of the boundary. The proofs will be not be organized by these, but by the classification of 5.2.4. The ordering of these items was modified to give a better flow of the arguments. C will be a matrix completion for c .

(Qin) \Leftrightarrow $\text{rank } C$ may be 4.

Any interior point c can be written as a convex combination in which the origin $c = 0$ has positive weight. There exists a matrix completion C in which $\mathbf{1}$ has a positive weight, so C has full rank. Conversely, if C has rank 4, a small change of c translates to a small change of C , leaving the other matrix entries unchanged. As full rank positive matrices are open, this will not lead out of \mathcal{Q} . Hence c is an interior point.

(Qei) $\Leftrightarrow c \in \partial \mathcal{Q}$ and $\text{rank } C = 3$.

From now on all c will be in the boundary, and so by Lemma 5.5.5 c has a unique completion C . Whenever $|c_{ij}| = 1$ for a pair $\{i, j\}$, the i^{th} and the $(j+2)^{\text{th}}$ rows/columns are equal up to sign, so the rank is reduced by 1. Deleting one of these row/column pairs leaves a 3×3 correlation matrix, whose semidefiniteness describes the ellipse. This has full rank precisely in the interior.

(Qnx), (Qce) $\Leftrightarrow c \in \partial \mathcal{Q}$ exactly one, resp. two $|c_{ij}| = 1$.

From now on, we have $\text{rank } C \leq 2$, and so by Lemma 5.5.6 (3), the matrix C lies in the

cosine-parametrized family shown in (5.5.6). If at least one $|c_{ij}|$ equals 1 then the point is in the boundary case of an ellipope. It is clear from the embedding of the ellipope into the cube that the non-classical points are exactly the ones that are not in another cube face. The edges lie in exactly 2 cube faces. This directly translates to the corresponding angles in the parametrization being multiples of π , as claimed in Proposition 5.2.5.

$$(\mathcal{Q}_{\text{cx}}) \Leftrightarrow c \in \partial \mathcal{Q} \text{ rank } C = 1$$

If three $|c_{ij}| = 1$, it must actually be four, and hence we have a classical extreme point. It is easy to see that this implies rank 1: up to symmetry this is the case $c_{ij} = 1$ for all $i, j = 1, 2$, which clearly has the rank 1 matrix $C_{ij} \equiv 1$ as a completion. For the converse, note that $\text{rank } C = 1$ and $C \succcurlyeq 0$ imply $C_{ij} = x_i x_j$ for some vector x , and $c_{ij} = x_i x_{j+2}$. If we now insist on the special form of C from Proposition 5.2.9, i.e., unit diagonal, we must have an extreme point just from the rank condition. However, we get even many interior rank 1 points, and $c \in \partial \mathcal{Q}$ needs to be imposed as well.

$$(\mathcal{Q}_{\text{qx}}) \Leftrightarrow c \in \partial \mathcal{Q} \cap (\text{int } \mathcal{N}) \Leftrightarrow \Delta < 0 \text{ in Proposition 5.2.5}$$

From the semialgebraic description of \mathcal{Q} in Proposition 5.2.8 this type consists of the points $c \in \mathcal{N}$ with $h(c) = 0$ and $g(c) < 0$. But for the cosine parametrized correlations with $\delta = -(\alpha + \beta + \gamma)$ we get the identity

$$g(\cos \alpha, \cos \beta, \cos \gamma, \cos \delta) = 2\Delta.$$

This completes the proofs of Propositions 5.2.9, 5.2.10 and 5.2.6.

Exposing functionals.

Proof of Proposition 5.3.2. Since c is a boundary point, we have $c \cdot f = \max\{c \cdot f' | f' \in \mathcal{Q}^\circ\} = 1$ for some $f \in \mathcal{Q}^\circ$; we fix such f . Thus $c' \cdot f$ has a global maximum at $c' = c$, and therefore a local maximum on the surface $c_{ij} = \cos \theta_{ij}$ with $\sum_{ij} \theta_{ij} = 0$ where the θ_{ij} are the given angles.

We analyze this extremum problem by introducing a Lagrange multiplier λ . The critical equations are

$$0 = d\left(\sum_{ij} f_{ij} \cos(\theta_{ij}) + \lambda \theta_{ij}\right) = \sum_{ij} (-f_{ij} \sin(\theta_{ij}) + \lambda) d\theta_{ij}.$$

Because $\Delta < 0$, all $\sin(\theta_{ij}) \neq 0$, and $f_{ij} = \lambda / \sin(\theta_{ij})$. The multiplier is determined from $c \cdot f = 1$ to be $\lambda^{-1} = \sum_{ij} \cot \theta_{ij} \equiv K$. Hence a maximizing f is unique, and given by the formula. \square

This proof utilizes our knowledge from other sources that such c are extremal. When computing the convex hull of a parametrized surface (as in [CKLS19b]) this is the tricky part. We can compute the tangent hyperplane at every point of such a surface, but is the local extremum a global maximum? It is then natural to look first at the local criterion and to rule out saddle points. That is, by looking at the parametrization in second order Taylor approximation, we can determine whether the surface is locally on one side of the tangent plane. If not, the point can be omitted from the list of potential extreme points. We carried this out for the case at hand, and found that *all* points with $\Delta > 0$ are saddles.

From the self-duality of the convex body we deduce that $\{h = 0\}$ is a self-dual variety. For the study of \mathcal{Q} this is not only modified by intersecting with the cube, but also by eliminating the branch of the variety in the interior of \mathcal{Q} . Under dualization these

operations are connected, i.e., the duals of the normalized tangents of interior points end up outside the dual body.

Unique CHSH violation. It is clear that each curved tetrahedron, being the pushout of a CHSH-face, violates exactly that CHSH inequality. That this is true for all non-classical correlations is an elementary fact that we have not used otherwise. Its self-dual version has likewise nothing to do with \mathcal{Q} , but only with the enclosing polytopes \mathcal{C} and \mathcal{N} . It states that for any non-trivial Bell inequality, i.e., for any affine inequality valid for all classical correlations ($f \in \mathcal{C}^\circ$), which is not true by virtue of positivity constraints alone ($f \notin \mathcal{N}^\circ$) there is a unique non-local box ($c \in \partial_e \mathcal{N}$) making this evident ($c \cdot f > 1$).

Proof of Proposition 5.2.1. The 8 CHSH inequalities are $\pm c_{11} \pm c_{12} \pm c_{21} \pm c_{22} \leq 2$, where the product of the signs is -1 . Given two distinct inequalities of this sort, the signs cannot be equal in all four places (then the inequalities would be the same), and also not in three places (because this would imply equality on the fourth place). Adding two violated inequalities thus gives $\pm 2c_{ij} \pm 2c_{kl} > 4$, which contradicts the inequality $|c_{ij}| \leq 1$ following from non-signalling. Hence at most one such inequality is violated for $c \in \mathcal{N}$. On the other hand, for $c \notin \mathcal{C}$ at least one is violated. \square

Face duality. We now consider the normal cycle and the duality relations of faces. Some claims about exposedness are already made in Proposition 5.2.4. These and the entries in Table 5.1 will now be treated in detail. As in Section 5.5.3, statements are grouped by boundary types. For points $\{c\}$ of each type we must identify the functionals $f \in \mathcal{Q}^\circ$ attaining the maximal value 1 at c , i.e., the face $\{c\}^\circ$. Note that the dual face operation

$$S^\circ = \{f \in \mathcal{Q}^\circ \mid \forall c \in S \subset \mathcal{Q}, c \cdot f = 1\}$$

also depends on the whole convex body in which this is taken (here: \mathcal{Q}). We will write S°_c} and S°_N} when we take orthogonal complements with regards to \mathcal{C} and \mathcal{N} respectively. Obviously, the operation is monotone in the sense that for $S \subset \mathcal{C}$ we have $S^{\circ_N} \subset S^\circ \subset S^{\circ_c}$.

$$(\mathcal{Q}_{\text{cx}})^\circ = [\mathcal{Q}_{\text{ei}}] = (\mathcal{Q}_{\text{ei}}) \cup (\mathcal{Q}_{\text{nx}}) \cup (\mathcal{Q}_{\text{ce}}) \cup (\mathcal{Q}_{\text{cx}}):$$

Consider a classical extreme point in $(\mathcal{Q}_{\text{cx}})$; without loss of generality $c = (1, 1, 1, 1)$. Then $\{c\}^\circ \subset \{c\}^{\circ_c}$, i.e., $\{c\}^\circ$ is a face contained in a facet of the cube \mathcal{C}° . This was our definition of an \mathcal{N} -face. Since these characterizations are taken over by self-duality, let us look at $2Hf$ for $f \in \{c\}^\circ$. The first component $(2Hf)_{11}$ is just $c \cdot f = 1$; the others (with maybe a sign added) are the scalar products of f with all the other classical points, which need to be ≤ 1 for $f \in \mathcal{Q}^\circ$. Hence $2Hf$ is indeed in the standard cube, with $(2Hf)_{11} = 1$. The condition $2Hf \in \mathcal{Q}$ singles out an ellipope satisfying the third order inequality, which in terms of f is the elementary symmetric polynomial appearing in (5.3.10), albeit with the opposite inequality. Note that $\{c\}^\circ$ is thus the closed ellipope $[\mathcal{Q}_{\text{ei}}]$, which also contains boundary points of type $(\mathcal{Q}_{\text{cx}}), (\mathcal{Q}_{\text{ce}}), (\mathcal{Q}_{\text{nx}})$. Computing their complements, as we will do presently, will give faces including c .

$$(\mathcal{Q}_{\text{ei}})^\circ = (\mathcal{Q}_{\text{cx}}):$$

Starting from an interior ellipope point c , self-duality gives us essentially the dual of the previous paragraph. More explicitly, set $c = (1, x, y, z)$ with $1 - x^2 - y^2 - z^2 + 2xyz \geq 0$, and $x^2, y^2, z^2 < 1$, to avoid edges and classical extreme points. For an interior point, the equality $c \cdot f = 1$ clearly extends from c to the face generated by this. Hence f must be

$(1, 0, 0, 0)$, and $2Hf = (1, 1, 1, 1)$ is the classical extreme point considered in the previous paragraph.

$(Qnx)^\circ = (Qcx)$:

More care is needed for ellipope boundary points, because, in principle, this could allow more freedom for f . We will use the local extremality in the sense of Proposition 5.3.2, with angles $\theta_{11} = 0$, and $\sin(\theta_{ij}) \neq 0$ for the other $(i, j) \neq (1, 1)$. Then the equation $f_{ij} \sin(\theta_{ij}) = \lambda$ implies $\lambda = 0 \cdot f_{11} = 0$; since the other sines are $\neq 0$, then once again the only possibility is $f = (1, 0, 0, 0)$. This shows that the (Qnx) -points are indeed non-exposed extreme points as claimed in Proposition 5.2.4.

$(Qce)^\circ = [Qce] = (Qce) \cup (Qcx)$:

Now consider a point c on an edge, but not a vertex. This forces exactly two angles, say $\theta_{11} = \theta_{12}$, to be zero (cf. Proposition 5.2.6) and by the same reasoning used in the previous point, $\lambda = 0$, and $f_{21} = f_{22} = 0$. However, f_{11} and f_{12} remain unconstrained and merely have to add up to 1. Remarkable here is that we get a drop of expected dimension from \mathcal{C} , where the complement of an edge is a 2-dimensional face:

$$\{(1, 1, 0, 0)\}^{\circ c} = \left\{ ((1+x)/2, (1-x)/2, y/2, -y/2) \mid |x| + |y| \leq 1 \right\}.$$

Geometrically, 3-dimensional faces of \mathcal{C} containing this edge meet at an angle, whereas the corresponding ellipopes are tangent.

$(Qqx)^\circ = (Qqx)$:

Here points go to points, as discussed in detail in Section 5.5.2.

Table 5.1 also gives the manifold dimensions of each boundary type. We only have one continuous family of type (Qqx) , of dimension 3. All other types occur only in discrete instances, i.e., with dimension zero.

Support function. As described in Section 5.3.3, we seek the criteria for a ray to hit the boundary of \mathcal{Q}° either in an exposed extreme point or in an \mathcal{N} -face. The problem becomes almost trivial, however, if we already know by which face the ray leaves the surrounding cube: then we just have to check whether the boundary point is inside or outside the ellipope, for which we have a convenient third order criterion. The following proof is based on the case distinction by cube faces. Since these are all connected by symmetries, it boils down to just considering one case.

Proof of Proposition 5.3.5. (1) \Leftrightarrow (2): We use the normal cycle: the set of pairs $(c, f) \in \mathbf{N}(\mathcal{Q})$ such that both c and f are uniquely determined when the other is fixed is just the stratum (Qqx, qx) . Hence, if f is of type (Qqx) , so is c .

Reduction by symmetry:

Applying a symmetry to f , i.e., a permutation of the components or an even number of sign changes, clearly does not change the validity of (1), (2), (3), or (4), while (5) respects the symmetry by requiring the necessary transformation to be made first. Hence it suffices prove for f in a standard form achievable by symmetry transformation. Since all extreme points of \mathcal{C} are connected by symmetry we can assume, as required in (5) that a maximizer for $c \cdot f$ in $\partial_e \mathcal{C}$ is $c = (1, 1, 1, 1)$. Now suppose that two or more coordinates $f_{ij} < 0$. Then, by applying an even sign change to c we could increase $c \cdot f$. So our assumption actually

rules out more than one negative sign. By the same argument, if there is a negative sign, this must be on an f_{ij} which minimizes $|f_{ij}|$. By a permutation we may assume that this element is f_{22} .

We can quickly handle the case that all $f_{ij} \geq 0$. In that case, $\max\{c \cdot f | c \in \mathcal{C}\} = \sum_{ij} f_{ij} = \sum_{ij} |f_{ij}| = \max\{c \cdot f | c \in \mathcal{N}\}$. So the maximum over \mathcal{Q} is attained at a classical point, $p(f) \geq 0$ and the product in (5.3.10) cannot be < 0 , so all conditions evaluate to false. So we may assume that there is just one negative sign and sort the remaining f_{ij} . That is, from now on we take

$$f_{11} \geq f_{12} \geq f_{21} \geq |f_{22}| > 0 > f_{22}. \quad (5.5.7)$$

(1) \Leftrightarrow (5): We use the same classification of boundary points for \mathcal{Q} and \mathcal{Q}° via duality transform. So (1) means that $c = 2Hf$ is a multiple of a $(\mathcal{Q}\text{qx})$ point. We know that the component with the largest absolute value is the first, $c_{11} = \sum_{ij} f_{ij}$. Thus the point where the ray $\mathbb{R}c$ intersects the boundary of \mathcal{N} is $(1, c_{12}/c_{11}, c_{21}/c_{11}, c_{22}/c_{11}) = (1, x, y, z)$. This is in an \mathcal{N} -facet of \mathcal{Q} if and only if $1 - x^2 - y^2 - z^2 + 2xyz \geq 0$. Otherwise, this intersection is already outside of \mathcal{Q} , and hence the ray intersects $\partial\mathcal{Q}$ at a $(\mathcal{Q}\text{qx})$ point. So the necessary and sufficient condition for (1) is that the cubic is < 0 . Multiplying by c_{11}^3 , which we know to be positive, and rearranging the resulting homogeneous polynomial in the f_{ij} 's, gives condition (5).

(5) \Leftrightarrow (3): Under the above symmetry reduction we have

$$m(f) = (-f_{22}) \left(\frac{1}{f_{11}} + \frac{1}{f_{12}} + \frac{1}{f_{21}} - \frac{1}{f_{22}} \right) = 1 - \frac{f_{22}}{f_{11}} - \frac{f_{22}}{f_{12}} - \frac{f_{22}}{f_{21}}.$$

Subtracting 1 from both sides of the inequality $m(f) > 2$, and multiplying by $f_{11}f_{12}f_{21}$, gives (5).

(4) \Leftrightarrow (5): The first factor in $\tilde{m}(f)$ is the polynomial in (5.3.10), divided by $p(f)$. So while $p(f) < 0$, the positivity of this factor is equivalent to (4). We complete the proof by showing that under the symmetry reduction (5.5.7) the other three factors are always, respectively, positive, negative and positive. Indeed, in the second factor the f_{11} and f_{22} -terms together are positive, and so are the f_{12} and f_{21} -terms. Similarly, in the third factor we group the f_{11}, f_{12} and the f_{21}, f_{22} -terms (both negative), and use the same grouping in the forth factor, giving two positive terms. \square

It is interesting to see what a purely algebraic approach as in [BPT12, Section 5.3] would say about the situation. First of all, the support function asks us to compute a maximum of a linear functional over a variety. Evaluating just the first order conditions, we get an expression for the maximum for each patch of $\partial\mathcal{Q}$. For the curved $(\mathcal{Q}\text{qx})$ patches this will be just $\tilde{\phi}$. So we get little progress over the simple story told in Section 5.3.3. In many well-known problems of duality, we can simply take the maximum of the different branches of the algebraic function, i.e., the maximum of $\tilde{\phi}$ and $\phi_{\mathcal{C}}$. Suffice it to say that this fails, and one easily finds points where $\tilde{\phi}(f) > \phi_{\mathcal{C}}(f) = \phi_{\mathcal{Q}}(f)$. To get this to work, one must ensure that the associated maximizers are contained in the quantum set.

5.6. Conclusions

On one hand, there are some geometric aspects of \mathcal{Q} we did not discuss. On the other hand, many techniques might be useful for studying higher-dimensional correlation bodies. Let us briefly comment on possible research directions.

- *Constrained Hilbert space dimension*

In the 222|0 case, it happens to be sufficient to use a 4-dimensional Hilbert space to get all the extreme points of \mathcal{Q} , but no assumption like this is made in the definition of \mathcal{Q} . However, one can ask how such an assumption would change \mathcal{Q} . Let us denote by \mathcal{Q}_m the (warning: nonconvex!) set of quantum correlations that are obtainable by models as in Section 5.1.1 under the additional assumption $\dim \mathcal{H} = m$. We also write $\mathcal{C}_m \subset \mathcal{Q}_m$ for the corresponding set of classical correlations realized in a sample space of m points. We know that extreme points of the full bodies can be realized in fixed dimensions, so $\partial_e \mathcal{C} \subset \mathcal{C}_1$ and $\partial_e \mathcal{Q} \subset \mathcal{Q}_4$. Thus Carathéodory's Theorem allows us to put a bound on the required m : since in an n -dimensional convex body every point is the convex combination of at most $n + 1$ extreme points, and $n = 4$, we conclude that $\mathcal{C} \subset \mathcal{C}_5$ and $\mathcal{Q} \subset \mathcal{Q}_{20}$. The Carathéodory bound is typically tight only for polytopes, where most points require $n + 1$ of the vertices for a convex representations. When there is a continuum of extreme points, that *Carathéodory number* is usually smaller. It can be proved that $\mathcal{Q}_m \subset \mathcal{C} \neq \mathcal{Q}$ for $m \leq 3$, and $\mathcal{Q}_m = \mathcal{Q}$ for $m \geq 4$. The analogous set \mathcal{C}_m for the cross polytope \mathcal{C} is also interesting and worth further study: for instance, \mathcal{C}_1 is the subset of rank 1 matrices $c \in \mathbb{R}^{2 \times 2}$.

- *The full 222 case, and the C^* -algebra generated by two projections*

In the 222 case, without the zero marginals condition, the correlation body \mathcal{Q} is a convex body in \mathbb{R}^8 . Here we can parametrize its extreme points by the product of spheres $\mathbb{S}^1 \times \mathbb{S}^1 \times \mathbb{S}^3$, analogous to Proposition 5.2.5. A Macaulay2 computation reveals that this variety has degree 40 and its prime ideal is generated by 28 polynomials whose degrees are 5, 6, 7 and 8. This may be a starting point for the analysis of the 222 case.

- *Duality*

The duality in Theorem 5.1.3 depends on the minimality assumption. Already the duality of just \mathcal{N} and \mathcal{C} requires at least the dimensions of these sets to coincide, which fails for $MK > 4$.

- *Algebra*

Algebraic methods are expected to apply once a reduction to finite dimension has been achieved by other means. We found them directly useful in the full 222 case, but there are also applications to the N22 and 2M2 cases. However, the complexity of algebraic characterizations can be expected to increase very rapidly.

- *Algebraic statistics*

Consider the ± 1 -valued random variables A_1, A_2, B_1, B_2 satisfying (5.1.1). Their statistical model is the graphical model whose graph G is the 4-cycle with edges $A_1 - B_1, B_1 - A_2, A_2 - B_2, B_2 - A_1$. This is [GMS⁺06, Example 4] up to relabelling. The sufficient statistics of this model are obtained by applying the linear map $A(G)$ in [GMS⁺06, Example 4]. The image of this map is our classical polytope \mathcal{C} . In particular this map is a bijection between the model and \mathcal{C} and inverting it is called *maximum likelihood estimation* (MLE). We can recover also \mathcal{N} from this construction, and more in general such polytopes can be defined for any toric model. For an undirected graphical model G we have that $\mathcal{C} = \mathcal{N}$ if and only if the graph is decomposable; the four-cycle model is the smallest non-decomposable model so we can deduce also from this argument that the inclusion is strict. It would be particularly interesting to examine the general 222 case through the lens of algebraic statistics.

Bibliography

- [ABN22] Gianira N. Alfarano, Martino Borello, and Alessandro Neri. A geometric characterization of minimal codes and their asymptotic performance. *Advances in Mathematics of Communications*, 16(1):115–133, 2022.
- [ACGH85] E. Arbarello, M. Cornalba, P. A. Griffiths, and J. Harris. *Geometry of Algebraic Curves. Vol. I*, volume 267 of *Grundlehren der Mathematischen Wissenschaften*. Springer-Verlag, New York, 1985.
- [ADRS00] Christos A. Athanasiadis, Jesús A. De Loera, Victor Reiner, and Francisco Santos. Fiber polytopes for the projections between cyclic polytopes. *European Journal of Combinatorics*, 21(1):19–47, 2000.
- [AS16] Karim A. Adiprasito and Raman Sanyal. Whitney numbers of arrangements via measure concentration of intrinsic volumes. *arXiv:1606.09412*, 2016.
- [Aum65] Robert J. Aumann. Integrals of set-valued functions. *Journal of Mathematical Analysis and Applications*, 12(1):1–12, 1965.
- [Bar02] Alexander Barvinok. *A course in convexity*, volume 54 of *Graduate Studies in Mathematics*. American Mathematical Society, 2002.
- [BB14] Charles H. Bennett and Gilles Brassard. Quantum cryptography: Public key distribution and coin tossing. *Theoretical Computer Science*, 560:7–11, 2014.
- [BBCM95] C. H. Bennett, G. Brassard, C. Crepeau, and U. M. Maurer. Generalized privacy amplification. *IEEE Transactions on Information Theory*, 41:1915–1923, 1995.
- [BBLM22] Paul Breiding, Peter Bürgisser, Antonio Lerario, and Léo Mathis. The zonoid algebra, generalized mixed volumes, and random determinants. *Advances in Mathematics*, 402:108361, 2022.
- [BBMS22] Katalin Berlow, Marie-Charlotte Brandenburg, Chiara Meroni, and Isabelle Shankar. Intersection bodies of polytopes. *Beiträge zur Algebra und Geometrie / Contributions to Algebra and Geometry*, January 2022.
- [BCP⁺14] Nicolas Brunner, Daniel Cavalcanti, Stefano Pironio, Valerio Scarani, and Stephanie Wehner. Bell nonlocality. *Rev. Mod. Phys.*, 86:419–478, 2014.
- [BCR13] Jacek Bochnak, Michel Coste, and Marie-Françoise Roy. *Real algebraic geometry*, volume 36. Springer Science & Business Media, 2013.

- [BGW13] H. Barnum, C.P. Gaebler, and A. Wilce. Ensemble steering, weak self-duality, and the structure of probabilistic theories. *Found Phys*, 43:1411–1427, 2013.
- [BJ17] I. Belegradek and Z. Jiang. Smoothness of Minkowski sum and generic rotations. *J. Math. An. Appl.*, 450(2):1229–1244, 2017.
- [BL16] Peter Bürgisser and Antonio Lerario. Probabilistic schubert calculus. *Journal für die reine und angewandte Mathematik (Crelles Journal)*, 2020:1 – 58, 2016.
- [BL21] Alexander Black and Jesús De Loera. Monotone paths on cross-polytopes. *arXiv:2102.01237*, 2021.
- [Bla23] W. Blaschke. *Vorlesungen über Differentialgeometrie. II*. Springer-Verlag, Berlin, 1923.
- [Bol69] E. D. Bolker. A class of convex bodies. *Trans. Amer. Math. Soc.*, 145:323–345, 1969.
- [Bol71] E. D. Bolker. The zonoid problem. *Amer. Math. Monthly*, 78(5):529–531, 1971.
- [BPT12] Grigoriy Blekherman, Pablo Parrilo, and Rekha Thomas. *Semidefinite Optimization and Convex Algebraic Geometry*. MOS-SIAM Series on Optimization 13. SIAM, Philadelphia, 2012.
- [Brä14] Petter Brändén. Hyperbolicity cones of elementary symmetric polynomials are spectrahedral. *Optimization Letters*, 8(5):1773–1782, 2014.
- [BS92] Louis J. Billera and Bernd Sturmfels. Fiber polytopes. *Annals of Mathematics*, 135(3):527–549, 1992.
- [Cam99] Stefano Campi. Convex intersection bodies in three and four dimensions. *Mathematika*, 46(1):15–27, 1999.
- [CKLS19a] Daniel Ciripoi, Nidhi Kaihsa, Andreas Löhne, and Bernd Sturmfels. Computing convex hulls of trajectories. *Rev. Un. Mat. Argentina*, 60(2):637–662, 2019.
- [CKLS19b] Daniel Ciripoi, Nidhi Kaihsa, Andreas Löhne, and Bernd Sturmfels. Computing convex hulls of trajectories. *Rev. Un. Mat. Argentina*, 60:637–662, 2019.
- [CLO15] David A. Cox, John Little, and Donal O’Shea. *Ideals, varieties, and algorithms*. Undergraduate Texts in Mathematics. Springer, fourth edition, 2015.
- [CSM03] David Cohen-Steiner and Jean-Marie Morvan. Restricted Delaunay triangulations and normal cycle. In *Proceedings of the nineteenth annual symposium on Computational geometry*, pages 312–321, 2003.
- [DGMP11] Alexander A. Davydov, Massimo Giulietti, Stefano Marcugini, and Fernanda Pambianco. Linear nonbinary covering codes and saturating sets in projective spaces. *Advances in Mathematics of Communications*, 5(1):119–147, 2011.
- [DLTW08] Andrew C Doherty, Yeong-Cherng Liang, Ben Toner, and Stephanie Wehner. The quantum moment problem and bounds on entangled multi-prover games. In *23rd Annual IEEE Conference on Computational Complexity*, pages 199–210. IEEE, 2008.

- [EH16] D. Eisenbud and J. Harris. *3264 and All That - A Second Course in Algebraic Geometry*. Cambridge University Press, Cambridge, 2016.
- [Eis88] D. Eisenbud. Linear sections of determinantal varieties. *Amer. J. Math.*, 110(3):541–575, 1988.
- [Eis05] D. Eisenbud. *The geometry of syzygies*, volume 229 of *Graduate Texts in Mathematics*. Springer-Verlag, New York, 2005.
- [EK08] Alexander Esterov and Askold Khovanskii. Elimination theory and newton polytopes. *Functional Analysis and Other Mathematics*, 2(1):45–71, 2008.
- [Est08] Aleksandr Esterov. On the existence of mixed fiber bodies. *Moscow Mathematical Journal*, 8(3):433–442, 2008.
- [Fed59] Herbert Federer. Curvature measures. *Trans. Amer. Math. Soc.*, 93:418–491, 1959.
- [FFW11] T. Franz, F. Furrer, and R. F. Werner. Extremal quantum correlations and cryptographic security. *Phys. Rev. Lett.*, 106:250502, 2011.
- [FOV99] H. Flenner, L. O’Carroll, and W. Vogel. *Joins and intersections*. Springer, 1999.
- [Fri12] Tobias Fritz. Tsirelson’s problem and Kirchberg’s conjecture. *Rev. Math. Phys.*, 24:1250012, 2012.
- [FS14] Szabolcs Fancsali and Péter Sziklai. Lines in higgledy-piggledy arrangement. *Electron. J. Comb.*, 21, 2014.
- [Fu14] Joseph HG Fu. Algebraic integral geometry. In E. Gallego and G. Solanes, editors, *Integral geometry and valuations*, pages 47–112. Springer, 2014.
- [G⁺15] Marissa Giustina et al. Significant-loophole-free test of bell’s theorem with entangled photons. *Phys. Rev. Lett.*, 115:250401, 2015.
- [Gar94a] Richard J. Gardner. Intersection bodies and the Busemann-Petty problem. *Trans. Amer. Math. Soc.*, 342(1):435–445, 1994.
- [Gar94b] Richard J. Gardner. A positive answer to the Busemann-Petty problem in three dimensions. *Ann. of Math. (2)*, 140(2):435–447, 1994.
- [Gar06] Richard J. Gardner. *Geometric Tomography*, volume 58 of *Encyclopedia of Mathematics and its Applications*. Cambridge University Press, New York, second edition, 2006.
- [GJSW84] R. Grone, C.R. Johnson, E.M. Sá, and H. Wolkowicz. Positive definite completions of partial hermitian matrices. *Lin. Alg. Appl.*, 58:109–124, 1984.
- [GKS99] Richard J. Gardner, Alexander Koldobsky, and Thomas Schlumprecht. An analytic solution to the Busemann-Petty problem on sections of convex bodies. *Ann. of Math. (2)*, 149(2):691–703, 1999.
- [GKW⁺18] Koon Tong Goh, Jędrzej Kaniewski, Elie Wolfe, Tamás Vértesi, Xingyao Wu, Yu Cai, Yeong-Cherng Liang, and Valerio Scarani. Geometry of the set of quantum correlations. *Phys. Rev. A*, 97:022104, 2018.

- [GM21] F. Gesmundo and C. Meroni. The geometry of discotopes. *arXiv:2111.01241*, 2021. to appear in Le Matematiche.
- [GMS⁺06] Dan Geiger, Christopher Meek, Bernd Sturmfels, et al. On the toric algebra of graphical models. *Ann. Statist.*, 34:1463–1492, 2006.
- [GS] D. R. Grayson and M. E. Stillman. Macaulay2, a software system for research in algebraic geometry (v.1.17). Available at <http://www.math.uiuc.edu/Macaulay2/>.
- [GW93] P. Goodey and W. Weil. Zonoids and generalisations. In *Handbook of convex geometry*, pages 1297–1326. Elsevier, 1993.
- [Har92] J. Harris. *Algebraic geometry. A first course*, volume 133 of *Graduate Texts in Mathematics*. Springer-Verlag, New York, 1992.
- [HH⁺15] B. Hensen, R. Hanson, et al. Loophole-free Bell inequality violation using electron spins separated by 1.3 kilometres. *Nature*, 526:682 EP –, 2015.
- [HHMM20] Guillermo Hansen, Irmina Herburt, Horst Martini, and Maria Moszyńska. Starshaped sets. *Aequationes Mathematicae*, 94(6):1001–1092, 2020.
- [HN10] J. W. Helton and J. Nie. Semidefinite representation of convex sets. *Mathematical Programming*, 122(1):21–64, 2010.
- [JN98] C. R. Johnson and G. Nævdal. The probability that a (partial) matrix is positive semidefinite. In I. Gohberg, R. Mennicken, and C. Tretter, editors, *Recent Progress in Operator Theory*, pages 171–182, Basel, 1998. Birkhäuser Basel.
- [JNP⁺11] M. Junge, M. Navascues, C. Palazuelos, D. Perez-Garcia, V. B. Scholz, and R. F. Werner. Connes’ embedding problem and Tsirelson’s problem. *J. Math. Phys.*, 52:012102, 2011.
- [JNV⁺20] Zhengfeng Ji, Anand Natarajan, Thomas Vidick, John Wright, and Henry Yuen. MIP*=RE, 2020.
- [Jou80] J.-P. Jouanolou. *Théoremes de Bertini et applications*, volume 37. Université Louis Pasteur, 1980.
- [JP98] Vaughan F. R. Jones and J. H. Przytycki. Lissajous knots and billiard knots. *Banach Cent. Pub.*, 42:145–163, 1998.
- [Kho12] Askold Khovanskii. Completions of convex families of convex bodies. *Mathematical Notes*, 91, 2012.
- [KM40] M. G. Kreĭn and D P Milman. On extreme points of regular convex sets. *Studia Mathematica*, 9:133–138, 1940.
- [Kol98] Alexander Koldobsky. Intersection bodies, positive definite distributions, and the Busemann-Petty problem. *Amer. J. Math.*, 120(4):827–840, 1998.
- [KPS17] Kaie Kubjas, Pablo A Parrilo, and Bernd Sturmfels. How to flatten a soccer ball. In *Homological and Computational Methods in Commutative Algebra*, volume 20 of *INdAM Ser.*, pages 141–162. Springer, 2017.

- [KW10] Jukka Kiukas and Reinhard F. Werner. Maximal violation of Bell inequalities by position measurements. *J. Math. Phys.*, 51:072105, 2010.
- [Lan88] Lawrence J. Landau. Empirical two-point correlation functions. *Found. Phys.*, 18:449–460, 1988.
- [Lau97] Monique Laurent. The real positive semidefinite completion problem for series-parallel graphs. *Linear Algebra and its Applications*, 252:347–366, 1997.
- [LM22] Antonio Lerario and Léo Mathis. On tameness of zonoids. *Journal of Functional Analysis*, 282(4):109341, 2022.
- [LMS⁺21] T. P. Le, C. Meroni, B. Sturmfels, R. F. Werner, and T. Ziegler. Quantum correlations in the minimal scenario. *arXiv:2111.06270*, 2021.
- [LP95] Monique Laurent and Svatopluk Poljak. On a positive semidefinite relaxation of the cut polytope. *Linear Algebra and its Applications*, 223:439–461, 1995.
- [LRS10] Jesus De Loera, Joerg Rambau, and Francisco Santos. *Triangulations*. Springer-Verlag GmbH, August 2010.
- [Lud06] Monika Ludwig. Intersection bodies and valuations. *Amer. J. Math.*, 128(6):1409–1428, 2006.
- [Lut88] Erwin Lutwak. Intersection bodies and dual mixed volumes. *Adv. in Math.*, 71(2):232–261, 1988.
- [Mar94] Horst Martini. Cross-sectional measures. In *Intuitive Geometry (Szeged, 1991)*, volume 63 of *Colloq. Math. Soc. János Bolyai*, pages 269–310. North-Holland, Amsterdam, 1994.
- [Mas03] L Masanes. Necessary and sufficient condition for quantum-generated correlations, 2003.
- [Mas05] L Masanes. Extremal quantum correlations for n parties with two dichotomic observables per site, 2005.
- [MM21] L. Mathis and C. Meroni. Fiber Convex Bodies. *arXiv:2105.12406*, 2021.
- [MS21a] Mateusz Michałek and Bernd Sturmfels. *Invitation to Nonlinear Algebra*, volume 211 of *Graduate Studies in Mathematics*. AMS, 2021. available from personal website.
- [MS21b] Mateusz Michałek and Bernd Sturmfels. *Invitation to Nonlinear Algebra*, volume 211 of *Graduate Studies in Mathematics*. AMS, 2021. available from personal website.
- [Mum95] D. Mumford. *Algebraic geometry. I: Complex projective varieties*. Classics in Mathematics. Springer-Verlag, Berlin, 1995. Reprint of the 1976 edition in Grundlehren der mathematischen Wissenschaften, vol. 221.
- [NPA08] Miguel Navascués, Stefano Pironio, and Antonio Acín. A convergent hierarchy of semidefinite programs characterizing the set of quantum correlations. *New J. Phys.*, 10:073013, 2008.

- [NW⁺] Miguel Navascues, R. F. Werner, et al. Open quantum problems. Website at IQOQI, Vienna.
- [ORSV15] John Ottem, Kristian Ranestad, Bernd Sturmfels, and Cynthia Vinzant. Quartic spectrahedra. *Mathematical Programming, Ser. B*, 151:585–612, 2015.
- [OSC22] Oscar – open source computer algebra research system, version 0.8.1-dev, 2022.
- [PSW21] Daniel Plaumann, Rainer Sinn, and Jannik Lennart Wesner. Families of faces and the normal cycle of a convex semi-algebraic set. *arXiv:2104.13306*, 2021.
- [Ren06] James Renegar. Hyperbolic programs, and their derivative relaxations. *Foundations of Computational Mathematics*, 6:59–79, 02 2006.
- [RG17] Pierre Roussillon and Joan Alexis Glaunès. Surface matching using normal cycles. In *International Conference on Geometric Science of Information*, pages 73–80. Springer, 2017.
- [RS10] Philipp Rostalski and Bernd Sturmfels. Dualities in convex algebraic geometry. *Rendiconti di Mathematica*, 30:285–327, 2010.
- [Rus16] F. Russo. *On the geometry of some special projective varieties*. Lecture Notes of the Un. Mat. Ital. Springer, 2016.
- [S⁺15] Lynden K. Shalm et al. Strong loophole-free test of local realism. *Phys. Rev. Lett.*, 115:250402, 2015.
- [Sag21] The Sage Developers. *SageMath, the Sage Mathematics Software System (Version 9.2)*, 2021. <https://www.sagemath.org>.
- [San13] Raman Sanyal. On the derivative cones of polyhedral cones. *Advances in Geometry*, 13(2):315–321, 2013.
- [ŠB20] Ivan Šupić and Joseph Bowles. Self-testing of quantum systems: a review. *Quantum*, 4:337, 2020.
- [SBV⁺20] P. Sekatski, J. D. Bancal, X. Valcarce, E. Y. Z. Tan, R. Renner, and N. San-gouard. Device-independent quantum key distribution from generalized CHSH inequalities, 2020.
- [Sch70] R. Schneider. Über eine Integralgleichung in der Theorie der konvexen Körper. *Math. Nach.*, 44(1-6):55–75, 1970.
- [Sch13] Rolf Schneider. *Convex Bodies: The Brunn–Minkowski Theory*. Encyclopedia of Mathematics and its Applications. Cambridge University Press, 2 edition, 2013.
- [Sch18a] C. Scheiderer. Semidefinite representation for convex hulls of real algebraic curves. *SIAM Journal on Applied Algebra and Geometry*, 2(1):1–25, 2018.
- [Sch18b] C. Scheiderer. Spectrahedral shadows. *SIAM J. Appl. Alg. Geom.*, 2(1):26–44, 2018.
- [Sch18c] Claus Scheiderer. Spectrahedral shadows. *SIAM J. Appl. Algebra Geometry*, 2:26–44, 2018.

- [SGP⁺20] Rene Schwonnek, Koon Tong Goh, Ignatius W. Primaatmaja, Ernest Y. Z. Tan, Ramona Wolf, Valerio Scarani, and Charles C. W. Lim. Robust device-independent quantum key distribution, 2020.
- [Sin14] Rainer Sinn. *Algebraic Boundaries of Convex Semi-Algebraic Sets*. PhD thesis, Universität Konstanz, Konstanz, 2014.
- [Sin15] R. Sinn. Algebraic Boundaries of Convex Semi-Algebraic Sets. *Research in the Mathematical Sciences*, 2(1), 2015.
- [SLC⁺19] Kehua Su, Na Lei, Wei Chen, Li Cui, Hang Si, Shikui Chen, and Xianfeng Gu. Curvature adaptive surface remeshing by sampling normal cycle. *Computer-Aided Design*, 111:1–12, 2019.
- [Slo19] William Slofstra. The set of quantum correlations is not closed. *Forum of Mathematics, Pi*, 7:e1, 2019.
- [SS19] Anna-Laura Sattelberger and Bernd Sturmfels. D-modules and holonomic functions. *arXiv:1910.01395*, 2019.
- [Sta07] Richard Stanley. An introduction to hyperplane arrangements. In *Geometric Combinatorics*, pages 389–496. American Mathematical Society, October 2007.
- [Stu21] B. Sturmfels. Twenty Facets of Convex Bodies. Available at https://www.mis.mpg.de/fileadmin/pdf/exercises_congeo21_5016.pdf, 2021.
- [SW83] R. Schneider and W. Weil. Zonoids and related topics. *Convexity and its Applications*, pages 296–317, 1983.
- [SY08] Bernd Sturmfels and Josephine Yu. Tropical implicitization and mixed fiber polytopes. In *Software for algebraic geometry*, pages 111–131. Springer, 2008.
- [TSB⁺20] Ernest Y. Z. Tan, Pavel Sekatski, Jean-Daniel Bancal, René Schwonnek, Renato Renner, Nicolas Sangouard, and Charles C. W. Lim. Improved DIQKD protocols with finite-size analysis, 2020.
- [TSG⁺20] Ernest Y. Z. Tan, René Schwonnek, Koon Tong Goh, Ignatius William Primaatmaja, and Charles C. W. Lim. Computing secure key rates for quantum key distribution with untrusted devices, 2020.
- [Tsi80] B. S. Tsirelson. Quantum generalizations of Bell’s inequality. *Letters in Mathematical Physics*, 4:93–100, 1980.
- [Tsi87] Boris S. Tsirelson. Quantum analogues of the Bell inequalities. the case of two spatially separated domains. *J. Soviet Math.*, 36:557–570, 1987.
- [TVC19] Le Phuc Thinh, Antonios Varvitsiotis, and Yu Cai. Geometric structure of quantum correlators via semidefinite programming. *Phys. Rev. A*, 99:052108, 2019.
- [TZ06] Wojciech Tadej and Karol Życzkowski. A concise guide to complex Hadamard matrices. *Open Systems & Information Dynamics*, 13:133–177, 2006.
- [Vit91] R. A. Vitale. Expected absolute random determinants and zonoids. *Ann. Appl. Prob.*, 1(2):293–300, 1991.

- [VW01] K. G. H. Vollbrecht and R. F. Werner. Entanglement measures under symmetry. *Phys. Rev. A*, 64:062307, 2001.
- [Wei77] W. Weil. Blaschkes Problem der lokalen Charakterisierung von Zonoiden. *Arch. Math.*, 29(1):655–659, 1977.
- [Wei82] W. Weil. Zonoide und verwandte Klassen konvexer Körper. *Monatsh. Math.*, 94(1):73–84, 1982.
- [Wik21] Wikipedia contributors. Quantum key distribution — Wikipedia, the free encyclopedia. https://en.wikipedia.org/w/index.php?title=Quantum_key_distribution&oldid=1049733050, 2021. [Online; accessed 25-October-2021].
- [Win82] Peter Wintgen. Normal cycle and integral curvature for polyhedra in Riemannian manifolds. In Gy. Soos and J. Szenthe, editors, *Differential Geometry*, volume 21. North-Holland, Amsterdam, 1982.
- [WW01] R. F. Werner and M. M. Wolf. All multipartite Bell correlation inequalities for two dichotomic observables per site. *Phys. Rev. A*, 64:032112, 2001.
- [WWS16] Yukun Wang, Xingyao Wu, and Valerio Scarani. All the self-testings of the singlet for two binary measurements. *New J. Phys.*, 18:025021, 2016.
- [Yan11] Nikos Yannakakis. Stampacchia’s property, self-duality and orthogonality relations. *Set-Valued and Variational Analysis*, 19:555–567, 2011.
- [Zäh86] Martina Zähle. Integral and current representation of Federer’s curvature measures. *Arch. Math.*, 46:557–567, 1986.
- [Zei90] Doron Zeilberger. A holonomic systems approach to special functions identities. *Journal of Computational and Applied Mathematics*, 32(3):321–368, 1990.
- [Zha99a] Gaoyong Zhang. Intersection bodies and polytopes. *Mathematika*, 46(1):29–34, 1999.
- [Zha99b] Gaoyong Zhang. A positive solution to the Busemann-Petty problem in \mathbb{R}^4 . *Ann. of Math. (2)*, 149(2):535–543, 1999.
- [Zie95] Günther M. Ziegler. *Lectures on Polytopes*. Springer, Berlin, 1995.
- [Zie12] Günter M Ziegler. *Lectures on polytopes*, volume 152. Springer Science & Business Media, 2012.

Bibliographische Daten

Semialgebraic Convex Bodies
(Semialgebraische konvexe Körper)
Meroni, Chiara
Universität Leipzig, Dissertation, 2022
121 Seiten, 33 Abbildungen, 130 Referenzen

Selbstständigkeitserklärung

Hiermit erkläre ich, die vorliegende Dissertation selbstständig und ohne unzulässige fremde Hilfe angefertigt zu haben. Ich habe keine anderen als die angeführten Quellen und Hilfsmittel benutzt und sämtliche Textstellen, die wörtlich oder sinngemäß aus veröffentlichten oder unveröffentlichten Schriften entnommen wurden, und alle Angaben, die auf mündlichen Auskünften beruhen, als solche kenntlich gemacht. Ebenfalls sind alle von anderen Personen bereitgestellten Materialien oder erbrachten Dienstleistungen als solche gekennzeichnet.

Leipzig, den April 26, 2022

.....
(Chiara Meroni)

Daten zum Autor

Name: Chiara Meroni
Geburtsdatum: 22.01.1996 in Gorizia (Italien)

10/2015 - 7/2018 B.Sc. in Mathematik
Universität Trieste

10/2018 - 7/2020 M.Sc. in Mathematik
Universität Trieste

seit 10/2020 Doktorandin der Mathematik